COMPOSITION AND EVOLUTION OF THE PROTEROZOIC VIOOLSDRIF BATHOLITH (INCLUDING THE ORANGE RIVER GROUP), NORTHERN CAPE PROVINCE, SOUTH AFRICA

Hendrik Minnaar

Submitted for the degree of
philosophiae doctor
in the Department of Geology
University of the Free State

December 2011

Supervisor: Prof. A.E. Schoch

CONTENTS

Abstract

The Vioolsdrif Suite and Orange River Group represent genetically related calcalkaline plutonic and volcano-sedimentary assemblages of Palaeoproterozoic age formed during the Orange River orogeny. Together they occupy the largest part of the Richtersveld Subprovince – a unique tectono-stratigraphic terrane. Radiometric data indicate the period of formation roughly between 2.0-1.73 Ga. The subprovince has been vastly eroded and isolated from its original tectonic environment by subsequent tectonic processes, leaving a relatively small portion of its original extent for investigation. Previous studies have dealt with limited parts of the subprovince and although informal subdivisions of the Orange River Group and Vioolsdrif Suite are generally in use, some correlations and further subdivisions remained controversial. This study has two main aims, viz., to propose formal subdivisions of the two units and to investigate the magmatic processes and original tectonic environment of their formation. Geochemical evidence is presented here to support the proposed subdivisions, which were previously based entirely on field evidence. The subdivisions largely follow that of previous studies.

The Orange River Group is subdivided into the Haib and De Hoop Subgroups. Geochemical evidence show that these two subgroups differ in the magmatic processes that led to their formation. The Haib Subgroup shows a genetic gradational relationship with the Vuurdood Subsuite, which is regarded as remnants of the primary magmas. The De Hoop Subgroup does not display this relationship with the Vuurdood Subsuite.

The Vioolsdrif Suite is subdivided into the Vuurdood, Goodhouse and Ramansdrif Subsuites. Mafic-ultramafic bodies of the Vuurdood Subsuite are regarded as remnants of the primary magmas. This is based on multi-element variation diagram patterns and comparison to source magmas in modern island arcs (MORB). Previous studies have also shown that initial isotope ratios for the Vuurdood Subsuite are similar to those of the Goodhouse Subsuite and Orange River Group, relating them to a similar source. Dark mineral cumulate material are contained in the mafic-ultramafic bodies.

The Goodhouse Subsuite is subdivided into the Khoromus Tonalite, Blockwerf Migmatite, Xaminxaip River Granodiorite, Gaarseep Granodiorite and Hoogoor Granite. The Khoromus Tonalite is identified as the oldest unit within the subsuite based on contact relationships as well as radiometric data, which continuously render older ages for the Khoromus Tonalite compared to the other units within the subsuite. Certain field and petrological observations in this unit may be interpreted as products of magma mixing processes. The Blockwerf Migmatite is distinguished from the other units by its migmatitic character and anomalous La/Yb ratios. The unit is identified as a possible remnant volcanic centre. The Xaminxaip River Granodiorite is interpreted as a subvolcanic unit and is characterised by the development of migmatite in places. This migmatite is attributed to metamorphic conditions which locally reached high grade in an orogenic geothermal regime. The Gaarseep Granodiorite represents the main phase of the Vioolsdrif Suite. Its compositional range includes all those represented by the other units individually from gabbro through diorite, tonalite and granodiorite to granite. Its development spans almost the entire evolutionary history of the Richtersveld Subprovince as a whole. The Hoogoor Granite is included in the Goodhouse Subsuite based on the geochemical variation patterns and available radiometric evidence.

The Ramansdrif Subsuite is subdivided into the Ghaams and Sout Granites based on grain size variation and petrological evidence. The subsuite could have been formed by partial melting of the older plutonic phases of the Vioolsdrif Suite. The deformation associated with this partial melting event has not been identified.

Previous studies have related the evolution of the Richtersveld Subprovince to modern subduction zone magmatism similar to that of the Andean volcanic arc. This is largely supported by the current study, however, a change in magmatic processes and the tectonic environment can be observed in the geochemical variation patterns. Multi-element diagrams show patterns typical of subduction zone magmatism for both the Orange River Group and Vioolsdrif Suite. During the initial stages, primary magmas, now represented by the Vuurdood Subsuite, were derived from a depleted mantle reservoir. The first volcanic eruptions – those of the Haib Subgroup – represent

fractional crystallization products off the primary magmas. With progressive development of the arc, newly formed crust was continuously recycled back into the mantle and crustal partial melting led to a change in magmatic processes with magma mixing and contamination becoming increasingly important. Tectonic discrimination diagrams suggest that the initial stages of the batholith development may be compared to a primitive continental arc, while the later stages may be be compared to a typical continental arc.

Samevatting

Die Vioolsdrif Suite en Oranjerivier Groep verteenwoordig Palaeoproterosoïese kalkalkaliese plutoniese en vulkanies-sedimentêre opeenvolgings wat gevorm is tydens die Oranjerivier orogenese. Tesame beslaan hulle die grootste deel van die Richtersveld Subprovinsie – 'n unieke tektonies-stratigrafiese terrein. Volgens radiometriese data was die tydperk van ontwikkeling tussen ongeveer 2.0-1.73 Ga. Die subprovinsie is grootliks verweer en latere tektoniese prosesse het dit van die oorspronklike tektoniese terrein geïsoleer sodat 'n relatiewe klein gedeelte vir bestudering oorgebly het. Vorige studies het slegs oor beperkte gedeeltes van die subprovinsie gehandel. Alhoewel informele onderverdelings van die Oranjerivier Groep en Vioolsdrif Suite algemeen in gebruik is, is sekere korrelasies en verdere onderverdelings nog kontroversieël. Die doel van die huidige studie is veral tweërlei nl., om algemeen-aanvaarde onderverdelings van die twee eenhede voor te stel en om die tektonies-magmatiese prosesse waardeur hulle ontwikkel het te ondersoek. Geochemiese data word hier aangebied om die onderverdeling, wat voorheen geheel en al op veldverwantskappe berus het, te steun. Die voorgestelde onderverdeling wyk nie noemenswaardig af van dié in vorige studies nie.

Die Oranjerivier Groep word onderverdeel in die Haib en De Hoop Subgroepe. Geochemiese data dui daarop dat dié twee subgroepe deur verskillende magmatiese prosesse ontstaan het en dat die tektoniese terreine waarin hulle ontstaan het nie heeltemal dieselfde was nie.

Die Vioolsdrif Suite word onderverdeel in die Vuurdood, Goodhouse en Ramansdrif Subsuites. Die mafies-ultramafiese liggame van die Vuurdood Subsuite word beskou as oorblyfsels van die primêre magmas en dit bevat ook kumulate van donkerminerale. Die Vuurdood Subsuite toon 'n genetiese verwantskap met die Haib Subgroep maar nie met die De Hoop Subgroep nie. Die verwantskap tussen die Vuurdood Subsuite en die Haib Subgroep kan moontlik die gevolg van fraksionele kristallisasie wees.

Die Goodhouse Subsuite word onderverdeel in die Khoromus Tonaliet, Blockwerf Migmatiet, Xaminxaiprivier Granodioriet, Gaarseep Granodioriet en Hoogoor Graniet. Die Khoromus Tonaliet word beskou as die oudste eenheid in die subsuite op grond van kontakverwantskappe sowel as radiometriese data. Daar is veld- en petrografiese getuienisse wat daarop dui dat magma vermengingsprosesse 'n rol gespeel het in die vorming van hierdie eenheid. Die Blockwerf Migmatiet word van die ander eenhede onderskei deur sy migmatitiese karakter en anomale La/Yb verhoudings. Die eenheid word geïdentifiseer as 'n moontlike vulkaankeël-oofblyfsel. Die Xaminxaiprivier Granodioriet word geïnterpreteer as 'n subvulkaniese eenheid en word gekenmerk deur die ontwikkeling van migmatiet op plekke. Hierdie migmatiet word geïnterpreteer as die produk van lokale hoëgraadse metamorfe toestande wat geheers het in die orogene subduksieregime. Die Gaarseep Granodioriet is die hooffase van ontwikkeling van die Vioolsdrif Suite. Dit oorheers in volume en oorvleuel met feitlik die hele vormingsgeskiedenis van die Richtersveld Subprovinsie. Dit bevat die volledige samestellingsreeks wat in die ander plutoniese eenhede individueel verteenwoordig word van gabbro deur dioriet, tonaliet en granodioriet tot graniet. Die Hoogoor Graniet word in die Goodhouse Subsuite ingesluit op grond van geochemiese variasiepatrone en beskikbare radiometriese data.

Die Ramansdrif Subsuite word onderverdeel in die Ghaams en Sout Graniete op grond van korrelgroottevariasies en petrologiese getuienis. Die subsuite is skynbaar gevorm deur gedeeltelike insmelting van die ouer Goodhouse Subsuite plutoniese eenhede. Die vervormingsepsiode wat met hierdie gedeeltelike insmelting gepaard sou gaan, is nie geïdentifiseer nie.

Vorige studies vergelyk die ontwikkeling van die Richtersveld Subprovinsie met tektonies-magmatiese prosesse wat werksaam is in moderne vulkaanboë soos die Andesboog. Hierdie vergelyking word grootliks deur die huidige studie ondersteun maar 'n verandering in die magmatiese prosesse en die tektoniese omgewing gedurende die ontwikkelingsgeskiedenis is waarneembaar in die geochemiese data. Multi-element diagramme vertoon tipiese subduksiesone variasiepatrone vir beide die

Oranjeriviergroep en die Vioolsdrif Suite. Gedurende die aanvangstadium is primêre magmas gegenereer in die mantel, wat 'n verarmde samestelling gehad het. Die Vuurdood Subsuite verteenwoordig oorblyfsels van die primêre magmas. Die eerste vulkaniese lawas – dié van die Haib Subgroep – was produkte van fraksionele kristallisasie vanaf die primêre magmas. Met die geleidelike ontwikkeling van die vulkaanboog is nuwe kors in groter-wordende volumes geproduseer. Hierdie kors is voortdurend in die mantel herwin en gedeeltelike insmelting het daartoe gelei dat prosesse soos magma vermenging en kontaminasie belangriker geword het as fraksionele kristallisasie in die bepaling van die magmasamestellings. Tektoniese diskriminasiediagramme dui daarop dat die aanvangstadiums van die batoliet se ontwikkeling moontlik plaasgevind het in 'n primitiewe kontinentale boog, terwyl die latere stadiums in 'n gewone kontinentale boog plaasgevind het.

1. INTRODUCTION

The Richtersveld Subprovince is largely occupied by the Vioolsdrif Suite and Orange River Group. Together these two units record Palaeoproterozoic juvenile crust formation processes. At the current level of erosion, the Vioolsdrif Suite (in particular the Goodhouse Subsuite) volumetrically predominates with the Orange River Group occurring as rafts within the plutonic suite. The term Vioolsdrif Batholith in the title is meant to include the Orange River Group (with which it is genetically related), which is not mentioned repeatedly.

1.1 MOTIVATION, AIMS AND LIMITATIONS

During 2002, the statutory mapping program of the Council for Geoscience came to include the extreme northwestern parts of the country, including the current study area. At the time, there were still some unresolved controversies concerning the Orange River Group and Vioolsdrif Suite and it was decided that the field mapping should be concentrated on some of these issues. The fact that these two units are genetically related and occupy a distinct tectonic subprovince has long been recognized. The recognition of individual units, their stratigraphic positions and the formalization of nomenclature are important aims of statutory mapping programs and no recent compilation in which the two units are studied as a whole, are available. Individual studies were previously concentrated on parts of it. The statutory project presented the opportunity to accumulate a large number of samples, field data and new observations, so that a comprehensive academic study became possible. Field mapping commenced from 2002 to 2005 and 1:50 000 scale field maps were produced in consultation with maps produced during previous studies. Aerial photographs of 1:60 000 scale were used in the field. The statutory mapping of 1:50 000 scale is used to compile 1:250 000 scale maps for publishing.

Although Joubert *et al*. (1986) included the Vioolsdrif Suite and Orange River Group in a single compilation, some important subdivisions were added in later studies. The distinction between the Khoromus Tonalite and Gaarseep Granodiorite was recognized by Prinsloo (1987) and first published by Marais *et al*. (2001). Although Ritter (1980) recognized the Xaminxaip River Granodiorite, controversies remained concerning the unit's genesis and stratigraphic position (De Villiers and Söhnge, 1959; Ritter, 1980; Minnaar *et al*., 2011). New radiometric age data (U-Pb zircon by LA-ICPMS) is presented here as additional evidence as to its stratigraphic position (see 2.4.2.2 Xaminxaip River Granodiorite). Controversy also reigns over the inclusion of the Hoogoor Granite in the Vioolsdrif Suite (Strydom *et al*., 1987; Moen and Toogood, 2007). This originates from the fact that the Hoogoor Granite is pervasively overprinted by Namaqua foliation and metamorphism, which has obliterated evidence and contact relationships in the field. Colliston and Schoch (2006; Fig. 5) addressed the effects of high strain deformation on the rocks of the Vioolsdrif Suite.

Field observations are the foundation of any geological study, as will also become apparent for this investigation. However, in igneous terranes, geochemical and isotopic studies have become indispensable additions for arriving at meaningful conclusions as to the evolutionary history and original tectonic setting of the rock units. The recognition of the results of processes such as fractional crystallization, magma mixing, wall rock assimilation, homogenization in a magma chamber, partial melting, mantle wedge metasomatism, and basaltic underplating, is vastly aided by these studies. Indeed, the modeling of modern plate tectonic processes relies heavily, in some cases entirely, on geochemical and isotopic evidence.

The evolutionary history of the Richtersveld Subprovince also has consequences for the understanding of the surrounding Namaqua Metamorphic Province. Current theories suggest that this tectono-metamorphic province was formed by accretion of a number of individual, previously separated, terranes of which the Richtersveld Subprovince is one. The terrane accretion model has gained wide acceptance in recent literature but controversies concerning the exact configuration and terrane boundaries persist. This study aims to make a positive contribution to the insight into the geological evolution of the entire Namaqua Metamorphic Province.

The aims of the current study are:

a) To present acceptable subdivisions of the Orange River Group and Vioolsdrif Suite in South Africa. Geochemical data available from the Namibian side for the two units from previous studies were also included for the geochemical investigation (see Appendix 1: Analyses, sample localities, data treatment and processing).

b) To recognize and study the igneous and tectonic processes involved during the formation of the Orange River Group and Vioolsdrif Suite.

The study suffers from two limitations, viz., incomplete sampling coverage and limited isotopic analyses, which were the result of budget constraints. The Namibian portion of the Richtersveld Subprovince (representing about half of it) was not included in this study. For the geochemical study, the analyses of Reid (1977) on the Namibian side in the Haib area are included. However, due to the lack of field data the subdivisions and resulting map does not include the Namibian side. Radiometric age determinations were obtained for only four samples (U-Pb by LA-ICPMS on zircons). Two of these determinations are owed to collaboration with colleagues at the University of Gothenburg, Sweden (see 6. Acknowledgements).

1.2 LOCATION

The Richtersveld Subprovince is located in northwestern South Africa and southwestern Namibia, straddling the Orange River from the Richtersveld eastwards into the Bushmanland of South Africa (Figure 1.1).

For the most part it is a rugged, mountainous terrain set in an arid climate with a very low population density and sparse vegetation and animal life. The Orange River is the only perennial river in the area. The natural scenery is dominated by outcrops, especially in the Haib area (east of the Neint Nababeep plateau). Access is relatively good with a well developed network of field tracks, in places only accessible by four-wheel drive vehicle.

The tarred road leading south from Vioolsdrif into the Namaqualand interior is the main access route and runs through the batholith type area south of Vioolsdrif.

There are two important geographic features in the study area, which also represent geological boundaries. In the Richtersveld, the Rosyntjieberg mountain range includes the highest mountain peaks in the area (Vandersterrberg is the highest point at 1 400 m). This mountain range forms an almost inaccessible southern boundary to the Richtersveld National Park (Figure 1.2).

Figure 1.2: Part of the Rosyntjieberg mountain range which represents the southern boundary of the Richtersveld National Park. Photo taken in a southerly direction from Tatasberg in the eastern part of the park (17.2650°E; 28.3251°S). Distance to horizon approximately 15 km. The highest mountain peak in this photo is represented by Rosyntjieberg (1 329 mamsl).

Stretching in an east-west direction, it was also used by Ritter (1980) as a geological division, including all the volcanic rocks of the Orange River Group to the south thereof in the Windvlakte Formation. Between the settlements of Vioolsdrif and Eksteenfontein, the Neint Nababeep Plateau represents the sedimentary succession of the Nama Group

(Germs, 1972; Gresse and Germs, 1993) in the study area. It divides the Vioolsdrif Batholith into two distinct parts namely the Haib area to the east, and the Richtersveld area to the west. This represents a historical subdivision, the basis of which will be discussed in detail later (2.2 Current subdivision).

1.3 PREVIOUS WORK

The first comprehensive description of rocks of the Vioolsdrif Batholith is to be found in the survey mapping of Rogers (1916) in the Richtersveld area. In those early years, the volcanic rocks of the current Orange River Group were correlated with similar rocks of the "Kheis System" (Rogers, 1911) in the Upington-Prieska area (Gevers *et al*., 1937; Gevers, 1941; Von Backström, 1953; De Villiers and Söhnge,1959; Von Backström and De Villiers, 1972). This correlation was largely based on the similar stratigraphic succession and the assumption that the "grey gneissic granite" (current Goodhouse Subsuite) was part of the Archean magmatic cycle. De Villiers and Burger (1967) obtained an U-Pb zircon age of 1 850 Ma for these granites, showing that they could not belong to the Archean magmatic cycle.

Early in the nineteen-seventies, the Precambrian Research Unit of the University of Cape Town, started studies on the rocks in the current study area. The radiometric age of De Villiers and Burger (1967), along with the lack of rigorous evidence for the correlation of the rocks over the large distance between the Richtersveld and the Upington-Prieska area, inspired Blignault (1974) to propose a new subdivision for the volcanic pile in the Richtersveld. He included them in the Orange River Group and distinguished between the Haib Subgroup in the Haib area (to the east of the Neint Nababeep Plateau), which is largely similar to the "Wilgenhout Drift Series" of the "Kheis System", and the De Hoop Subgroup in the Richtersveld area (to the west of the Neint Nababeep Plateau), which is largely similar to the "Marydale Series" of the "Kheis System". The predominantly quartzitic unit of the current Rosyntjieberg Formation was termed the Rosynebos Formation. This was changed to the Rosyntjieberg Formation by Kröner and Blignault (1976) after the name of the mountain range. Blignault (1977) subdivided the Haib

Subgroup into the predominantly felsic Tsams, and predominantly mafic Nous, Formations. Ritter (1980), on the basis of textural differences and the recognition of protoliths for the metavolcanic rocks, subdivided the De Hoop Subgroup into the Paradys River, Abiekwa River, Klipneus, Kook River and Kuams River Formations. He included all the volcanic rocks of the Orange River Group to the south of the Rosyntjieberg mountain range in the Windvlakte Formation and stated that the original textures in this formation have been obliterated by deformation and metamorphism.

Gevers *et al*. (1937) and Gevers (1941) regarded the rocks of the current Vioolsdrif Suite as a genetically related group; the latter author identified the more basic phases as the oldest. Coetzee (1941) recognized the older age of the Vioolsdrif Suite relative to the Namaqualand gneisses and referred to it as the “basement granite”. De Villiers and Söhnge (1959) mapped large areas of the “grey gneissic granite” (current Goodhouse Subsuite) and regarded the type area to be south of Vioolsdrif. Von Backström and De Villiers (1972) referred to the leucogranites of the Vioolsdrif Suite (current Ramansdrif Subsuite) in the unfoliated Richtersveld domain as “red granites”, and correlated them with the “pink gneisses” in the foliated Namaqua domain to the east. De Villiers and Burger (1967) proposed that the “grey gneissic granite” be renamed the “Vioolsdrif Granite”.

Blignault (1977, p. 13) defined the current Vioolsdrif Suite on the basis of spatial association and evidence that the various compositional intrusive types constitute an igneous rock series. The subdivisions of Blignault (1977) and Ritter (1980) were accepted and formalized by SACS (1980). Strydom *et al*. (1987) assigned this rock association suite status and subdivided it into the Vuurdood, Goodhouse and Ramansdrif Subsuites. Within the Goodhouse Subsuite, Marais *et al*. (2001) were the first to recognise the distinction between the Khoromus and Gaarseep “Gneisses”. Minnaar *et al*. (2011) suggested a distinction between the Ghaams and Sout Granites within the Ramansdrif Subsuite.

Reid (1974, 1977, 1979, 1982, 1997) made a great contribution to the understanding of the magmatic evolution of the Vioolsdrif Batholith and provided excellent radiometric data (Rb-Sr and U-Pb) for the Haib area. Reid (1974) established the chronological order within the batholith, which is in accordance with available field evidence. The eruption of the Orange River volcanics (1 996±15 Ma) was followed by the intrusion of the Vuurdood Subsuite (<1 996 Ma) and then the intrusion of the Goodhouse Subsuite (1 900±30 Ma). After a 170 m.y. period of igneous quiescence, the Ramansdrif Subsuite was intruded around 1 730 Ma.

Reid (1977) geochemically identified the environment of formation of the batholith as that of an island arc. The study furthermore showed that a model of fractional crystallization can account for the magmatic evolution of most of the various igneous rock types, although not for the batholith as a whole. The isotopic evidence presented in the study indicated that the members of the Goodhouse Subsuite as well as that of the Orange River Group are linked to the same parental magma. A model of fractional crystallization from a high-Mg basaltic magma under the influence of high water pressure, was proposed for the magmatic evolution of the Vioolsdrif Suite. A similar model but under low water pressure, is also appropriate for the Orange River Group.

Reid (1982) showed that the mafic-ultramafic bodies of the Vuurdood Subsuite are also linked to the same parental magma as the Goodhouse Subsuite and Orange River Group and that the bodies may represent cumulate material within the early magmas. The study furthermore suggested that the granites of the Ramansdrif Subsuite were probably derived by partial melting from the earlier tonalites and granodiorites.

Reid (1997) put forward strong evidence from Sm-Nd isotope ratios, that the Vioolsdrif Batholith represents juvenile crust formation from a bulk earth-like mantle. He stated that the isotope signatures excluded the possibility of recycling of older crust into the Vioolsdrif Batholith source material. Nordin (2009), on the other hand, considered the source material to be that of a depleted mantle based on Lu-Hf isotope evidence from a single sample from the Haib Subgroup. A single inherited zircon age of 2.7 Ga also suggested the presence of pre-existing Archean crust.

Various previous studies investigated the relationship between the largely undeformed, low metamorphic terrane which is the Vioolsdrif Batholith type area, and the surrounding Namaqua Metamorphic Province. On regional scale, the contrast between these two terranes is rather obvious. Gevers *et al*. (1937) established, on field evidence, that the "Namaqualand Granite and Gneiss" were younger than what is currently termed the Vioolsdrif Suite. Beukes (1973) and Blignault *et al*. (1974) mapped the position of isograds in southern Namibia, indicating the metamorphic transition from the low-grade Vioolsdrif Batholith type area, to the surrounding medium-grade Namaqua Province. Based on this, Beukes (1973) indicated the "Namaqua Front" as the boundary between his Richtersveld and Namaqualand "Provinces" (see Figure 2.1). Kröner and Blignault (1976) distinguished the two areas as two separate tectono-stratigraphic terranes, each with its own unique stratigraphic, structural and metamorphic imprints.

During the first half of the nineteen-eighties, the Bushmanland Project (University of the Orange Free State) led to extensive field mapping which included part of the current study area. By this time, a tectonic model of plate accretion was suggested by all the available evidence. The wedge-shaped terrane occupied by the Vioolsdrif Suite and Orange River Group (Richtersveld Subprovince) was interpreted as a terrane which was thrusted upon the Namaqua Province, being preserved from the Namaqua deformation and metamorphism (Blignault *et al*., 1983; Joubert, 1986; Van der Merwe, 1986). Ritter (1980) did not agree with this model, claiming that the differences in deformation, metamorphism and age could be explained by differences in crustal level. Blignault *et al*. (1983), by field mapping, extended the Vioolsdrif Suite eastward from the type area across Beukes's (1973) Namaqua Front, into the Namaqua Province as far as the vicinity of Onseepkans (Colliston and Schoch, 2006; see Figure 2.1). They identified the Lower Fish River thrust as the northern boundary while the Groothoek thrust (Van der Merwe, 1986) was identified as the southern boundary (see Figure 2.1). The eastward extension of the Vioolsdrif Suite was not accepted by Moen and Toogood (2007), claiming that their "Hoogoor Suite" could be distinguished from the Vioolsdrif Suite on the basis of field evidence (this will be discussed in more detail under 3.2.3.2.4 Hoogoor Granite). This controversy was largely the result of the pervasive overprint of the Namaqua deformation and metamorphism on the proposed Hoogoor Suite.

In a global context, following various studies such as those by Stowe *et al*. (1984), Hartnady *et al*. (1985), Joubert *et al*. (1986) and Piper (2000), the Richtersveld Subprovince is currently interpreted by most researchers to represent a Kheisian (2.0-1.73 Ga) tectono-stratigraphic terrane which is surrounded along tectonic boundaries by the 1.3-1.0 Ga Namaqua Metamorphic Province. Igneous rocks of the Vioolsdrif Suite and Orange River Group occupy most of the Richtersveld Subprovince and record a major juvenile crust-formation event, while the Namaqua Province correlates with the global Grenville and Kibaran orogenies of North America and Central Africa respectively. The latter orogenies record the assembly of the supercontinent Rodinia.

On the evolutionary history of the Vioolsdrif Suite and Orange River Group, it has always been generally agreed that the environment of formation was that of an island arc, as evidenced by the calcalkaline bulk composition and the stratigraphy. Ritter (1983) compared it specifically to a Cordilleran-type setting, such as typified by the modern Andes. However, some controversy still prevails. Reid (1977, 1997) propose the igneous rocks of the Richtersveld Subprovince to represent a period of juvenile crust formation from a bulk earth-model mantle in an area where no crust existed before. Nordin (2009), however (as noted before; p.8), on evidence of a single relict Archean zircon, as well as Lu-Hf model ages, claims that previous crust must have been present. Noteworthy is the fact that no basement to the Orange River Group has been identified as yet. Miller (2008) suggests the volcanics might have been deposited on an ocean floor.

Isotopic and radiometric age data are available from various previous studies including Reid (1975, 1977, 1982, 1997), Allsopp *et al*. (1979), Barton (1983) and Kröner *et al*. (1983).

The Vioolsdrif Batholith is host to numerous deposits of economic important minerals. A thorough investigation of the tungsten deposits (which were exploited in earlier days) has been made by Bowles (1988). Some of the more promising porphyry-type copper deposits have been investigated (e.g., Minnitt 1979).

1.4 THE RICHTERSVELD SUBPROVINCE IN GLOBAL CONTEXT

Various previous studies (e.g., Blignault, 1977; Reid, 1977; Ritter, 1980; Barton, 1983) have identified the Vioolsdrif Batholith as a calcalkaline batholith formed in a volcanic arc environment. On the current globe, two types of subduction-related arcs are recognized, viz., the intra-ocean island arc (e.g., Kermadec, Tonga, Marianas, Izu-Bonin and Kurile arcs) and the continental arc, where oceanic crust is subducted beneath continental crust (e.g., Lesser Antilles, Cascades and Andes arcs). A third orogenic arc – the continent-continent collision arc (e.g., the Himalayas) – represents an area where the ocean separating the two continents has been destroyed, subduction has ended and tectonism is dominated by metamorphic processes leading to the production of S-type dominated magmatism.

When the Richtersveld Subprovince is considered in its regional setting within the Namaqua Metamorphic Province, formation of the Vioolsdrif Batholith itself coincides with a global era of Late Archean-early Proterozoic crust formation events around 2.0-1.9 Ga, while the Namaqua Metamorphic Province coincides with the Grenville orogeny (1.3-1.0 Ga) during which the supercontinent Rodinia was assembled (Condie, 2005b). According to Condie (*op cit.*), it is recognized that continental crust was already present on the globe by 4.0 Ga, probably even 4.4 Ga. Evidence indicate that crust formation processes during the Archean were much more active in the northern hemisphere than in the south (where the Vioolsdrif Batholith was formed). In North America, about five provinces are recognized which were assembled during the same time in which only a part of the Vioolsdrif Batholith was developing (1.95-1.75 Ga). They include the Rae and Hearne provinces (both Archean), the Trans-Hudson province (up to 500 km wide) and the Penokean and Yavapai provinces (Condie, *op cit.*). Suturing of the latter two provinces occurred at 1.90 and 1.75 Ga respectively (Condie, 2005b). It seems therefore that much less older crust, if any, was present in the study area compared to the northern hemisphere, during the time of formation of the Vioolsdrif Batholith. Reconstructions of Rodinia also support this as the continental crust in the northern hemisphere already occupied a much larger area than in the south; Laurentia already dominated the crustal configuration at that time.

Hamilton (1998) put forward strong evidence that modern plate tectonic processes (rifting and subduction) could not have been active in the Archean, but that they were operating by about 2.0 Ga, which is the time of onset of the evolution of the Vioolsdrif Batholith. Therefore, subduction-related tectonic and magmatic theories would be realistic to account for the development of the Vioolsdrif Batholith. According to Miyashiro (1974) the main rocks in island arc settings are usually basalts and basaltic andesites of the tholeiite series while those in continental arc settings are andesites and dacites of the tholeiite and calcalkaline series. The main volcanic rocks in continental margins are andesites, dacites and rhyolites of the calcalkaline series and the proportion of calcalkaline rocks among all the volcanic rocks tends to increase with advancing development of continental crust. Therefore, based on the absence of basaltic volcanic rocks and the proportion of calcalkaline rocks of between 60-95% (Miyashiro, 1974), the bulk of the Vioolsdrif Batholith can be compared to modern continental arcs such as typified by the Andean arc, as suggested by previous studies. This is as opposed to the island arc settings where basaltic compositions are important and the proportion of calcalkaline rocks does not exceed 50% (commonly 0-10%).

Reid (1997), however, concluded that Sm-Nd isotopic signatures preclude the possibility of incorporation of previously existing continental crust. Initial $^{87}Sr/^{86}Sr$ values from Reid (1977) support this with values for all of the Vuurdood Subsuite, the Orange River Group and the Goodhouse Subsuite being low (~0.703). Values for the Ramansdrif Subsuite does suggest crustal reworking (~0.707). Reid (1997) concluded that the best interpretation of the isotopic signatures involves slight enrichment in radiogenic Pb and Sr by subduction zone metasomatism of a mantle wedge with an undifferentiated bulk earth signature. He proposed that the evolution of the Vioolsdrif Batholith involved juvenile crust formation from the mantle with subsequent reworking of newly-formed crust to produce felsic magmatism.

The Vioolsdrif Batholith provides evidence on two important issues relating to Proterozoic tectonic and magmatic processes. Firstly, there is the question of whether pre-existing crust was present in the study area prior to the development of the batholith. No evidence of such pre-existing crust and basement to the Orange River Group has as yet been identified in the field. A single inherited zircon age of 2.7 Ga in a lava sample from the Haib Subgroup (Nordin, 2009) currently bears the only testimony to the possibility of Archean crust in the study area. Sm-Nd isotope signatures, however, strongly argue against the presence of pre-existing crust in the area (Reid, 1997).

Secondly, the Vioolsdrif Batholith provides evidence as to the tectonic and magmatic processes which were active during a time when the earth's crust-formation processes apparently changed dramatically. Various lines of evidence show a distinction between the Archean processes which produced mainly TTG (adakitic) magmas, and modern processes which produce mainly calcalkaline magmas. These changes, in global context, approximately spans the evolutionary history of the Vioolsdrif Batholith.

2. FIELD DESCRIPTIONS

A map of the Vioolsdrif Suite and Orange River Group in South Africa, with the subdivisions as motivated for in this study, is presented in a folder at the back of this thesis. Comprehensive field descriptions are given in previous studies and recent reviews of such descriptions can be found in Moen and Toogood (2007), Miller (2008) and Minnaar *et al*. (2011). Only observations which are considered relevant to the current study (including those from previous work and from the current study), will be discussed here.

2.1 EXTENT, SHAPE AND FORM

Consensus has not been reached concerning the boundaries of the Vioolsdrif Batholith. Although most current researchers agree that the batholith is tectonically bounded within the Richtersveld Subprovince between the Lower Fish River thrust in the north (Namibia) and Groothoek thrust in the south (RSA), observations from various studies suggest that it might in fact extend into the Namaqua Province. This is not, however, a major concern of the present study. The extent of the batholith (including the Orange River Group) according to most current literature, is presented in Figure 2.1.

The type area of the batholith is defined as the relatively undeformed and low-metamorphic-grade part of the batholith. Along the boundaries of the batholith, it has been subjected to deformation and metamorphism of the Namaqua orogeny, the foliation varying from weak to intense. The batholith is surrounded to the north, east and south by the Namaqua Metamorphic Province in which the rocks are pervasively overprinted by intense, predominantly east-west trending foliation and medium-grade metamorphism.

The batholith type area can be referred to in tectonic terms as the Vioolsdrif Terrane of the Richtersveld Subprovince (after Joubert *et al.*,1986). It is delineated to the east by the Namaqua Front of Beukes (1973) who defined this boundary as a tectonic transition and described it as “well defined north of Goodhouse but becoming vague eastward”. At

Ramansdrif 135 it is said to be tentative by Van der Merwe and Botha (1989). North of the Orange River it corresponds to the sillimanite-in isograd, as such representing a metamorphic transition. Blignault (1977) defined a similar line further towards the northwest in the Ais-ais area, marking the position where the generally non-penetrative fabric of his “Richtersveld Domain” becomes regional and penetrative, and called it the Southern Front. This represents the western extension of Beukes’s Namaqua Front. Both these authors stated that these lines merely mark the position where the intensity of foliation changes markedly, and do not represent terrane boundaries. In Namibia, Blignault included the “grey gneisses” to the north of the Southern Front in the Vioolsdrif Suite, correlating it with the rocks of the Goodhouse Subsuite. Moen and Toogood (2007) omitted all indications of a sharp boundary between the unfoliated Vioolsdrif and foliated Namaqua rocks in the Goodhouse area, stating that the transition is entirely gradational.

The Lower Fish River thrust (Blignault *et al*., 1983) and Groothoek thrust (Van der Merwe, 1986) were identified during the Bushmanland Project (1981-1986; see 1.3 Previous work). They represent the northern and southern boundary of the Vioolsdrif Batholith respectively. To the west, the batholith is overlain by the Gariep Supergroup (780-520 Ma; Von Veh, 1993). To the east, the Groothoek thrust combines with the Onseepkans thrust (Moen and Toogood, 2007), which is the extension of the Lower Fish River thrust (Namibia) in South Africa. As such, the Richtersveld Subprovince (after Joubert 1986) is enclosed within these boundaries. In its eastern parts, the Richtersveld Subprovince includes rock groups other than the Vioolsdrif Batholith, however, this study is only concerned with the batholith and then mainly the type area. The only unit which is investigated beyond the type area, is the Hoogoor Granite (Hoogoor Suite of Moen and Toogood, 2007). Contributing to solving the controversy regarding its inclusion or non-inclusion in the Vioolsdrif Suite, was one of the initial aims of this study.

The Vioolsdrif Batholith (in the current tectonic framework) covers an area of approximately 220 km in length and with an average width of 110 km. Evidence show that most of the original batholith has been eroded. Blignault (1977) proposed that the current level of erosion (in the Haib area) represents the root zone of the Orange River Group at a depth of 6-10 km. This interpretation is based on the recognition of features indicating a position in the transitional epizone-mesozone of the crust (after Buddington, 1959).

2.2 DISTINCTION BETWEEN THE HAIB AND RICHTERSVELD AREAS

In the batholith type area, the Orange River Group is separated into two parts by an area of no outcrop (the Nein Nababeep plateau) with the De Hoop Subgroup occurring to the west thereof, and the Haib Subgroup to the east. This distinction is a historical one and is primarily based on the fact that the Haib Subgroup is overwhelmingly volcanic in composition, while the De Hoop Subgroup is relatively rich in interlayered metasedimentary rock types, the Rosyntjieberg Formation representing an unique, rather thick and mature (arenitic), metasedimentary unit within the subgroup. During early regional mapping programs, the current Orange River Group was correlated with the "Kheis System" of Rogers (1911) in the Upington-Prieska area (e.g., Rogers, 1916; De Villiers and Söhnge, 1959; Von Backström and De Villiers, 1972). In this three-fold subdivision, most of the current Haib Subgroup resembles the "Wilgenhout Drift Series", most of the De Hoop Subgroup the "Marydale Series" and most of the Rosyntjieberg Formation the "Kaaien Series", of the Kheis System. Blignault (1974) did not support this correlation over such a large distance and introduced the Orange River Group as a separate unit from the Kheis System. However, in his subdivision he retained the distinction between the Haib and De Hoop Subgroups.

The possible correlation of the Haib and De Hoop Subgroups has been considered by a number of previous investigators (e.g., Minnitt, 1979; Ritter, 1980). Reid (1979) stated that this possible correlation cannot be ruled out on petrological grounds. Minnaar *et al.* (2011) considered the available evidence at the time and came to the conclusion that there is enough evidence to retain the subdivision. They highlighted the most important differences between the two areas, not only in the Orange River Group but also in the Vioolsdrif Suite, as follow:

a) The Pan African deformation is absent in the Haib area, while it is pervasively developed in the Richtersveld. This suggests that the boundary between the two areas (currently concealed by the Nama Group) may represent an important tectonic feature.

b) A large proportion of sedimentary rocks (greywacke, conglomerate and quartzite) are interbedded in the volcanics in the Richtersveld area but are relatively scarce in the Haib area.

c) The absence of a thick, relatively mature, quartzitic unit (Rosyntjieberg Formation) overlying the volcanic pile in the Haib area.

d) The Haib Subgroup is on average much more mafic than the De Hoop Subgroup.

e) The Goodhouse Subsuite has an overall more felsic nature in the Richtersveld than in the Haib area. Both the Vuurdood Subsuite and Khoromus Tonalite (the two most mafic units in the Vioolsdrif Suite) are absent in the Richtersveld.

2.3 ORANGE RIVER GROUP

The stratigraphic sequence within the Orange River Group has been a matter of controversy but this comes as no surprise if the degree of deformation and dismemberment of the unit, largely due to the intrusion of the plutonic suite, is taken into account. The uncertain relationship between the Haib and De Hoop Subgroups, the deformed contact relationships within the De Hoop Subgroup, and the isolated occurrences of individual fragments are the main complicating factors in deciphering the stratigraphic sequence.

Within the Haib Subgroup, Blignault (1977) found a single location where he considered that the relationship between the Tsams (underlying) and Nous Formations could be established with certainty. This stratigraphic sequence within the Haib Subgroup is substantiated by the Rb-Sr radiometric age results of Reid (1977), which show the Tsams Formation to be 2 020±70 Ma (dacites-rhyolites) and the Nous Formation 1 970±70 Ma (basaltic andesites-andesites).

Within the De Hoop Subgroup, Ritter (1980) based the stratigraphic sequence on a model of deposition from a common volcanic centre situated in the northeast of the Richtersveld, and the recognition of proximal and distal facies. He considered the Rosyntjieberg Formation to be interlayered between the underlying rocks to the north thereof and the overlying Windvlakte Formation. This contradicts De Villiers and Söhnge (1959), who considered it to occur between the underlying Haib and overlying De Hoop Subgroups. Blignault (1977), again, thought that the Rosyntjieberg Formation overlies all the volcanic rocks, forming the top of the succession along a discordant contact. Minnaar *et al*. (2011) is in agreement with Blignault (*op cit.*) but consider the contact to be gradational (over a few meters).

Radiometric data for the De Hoop Subgroup is very limited with available results including only one sample from the volcanic Paradys River Formation and one from the quartzitic Rosyntjieberg Formation. Both these samples are from the current study and single zircon U-Pb ages were determined by LA-ICPMS (the analyses are included in Appendix 2). The volcanic (dacite) sample rendered an age of 1 883±7.4 Ma, which is notably younger than the ages of Reid (1977) for the Haib Subgroup. The quartzite sample rendered detrital zircon ages which support the inferred stratigraphic position of the formation, overlying the volcanic pile. The probability distribution curve of 42 analyses shows a major peak between 1 850-1 800 Ma with single grains showing ages of 1 760 Ma, 1 920 Ma and 2 050 Ma. This also confirms a Vioolsdrif Batholith provenance to the formation.

Although deformation has rendered primary textures difficult to recognize and even obliterated in some areas, it is possible to identify a protolith for the rocks in almost the whole of the group. Aphanitic lavas are very fine- to fine-grained and often the minerals cannot be discerned under the microscope. However, overall the grain size of the volcanic rocks in the Orange River Group is such that the individual minerals can be discerned under the microscope (if not pervasively altered, which is often the case). The feldspar porphyroblasts of porphyritic lavas commonly exhibit a milky white or greenish colour owing to alteration. The quartz porphyroblasts are mostly rounded but may be subhedral. Some andesitic lavas display quartz-containing vesicles, such as those in the Nous and Klipneus Formations.

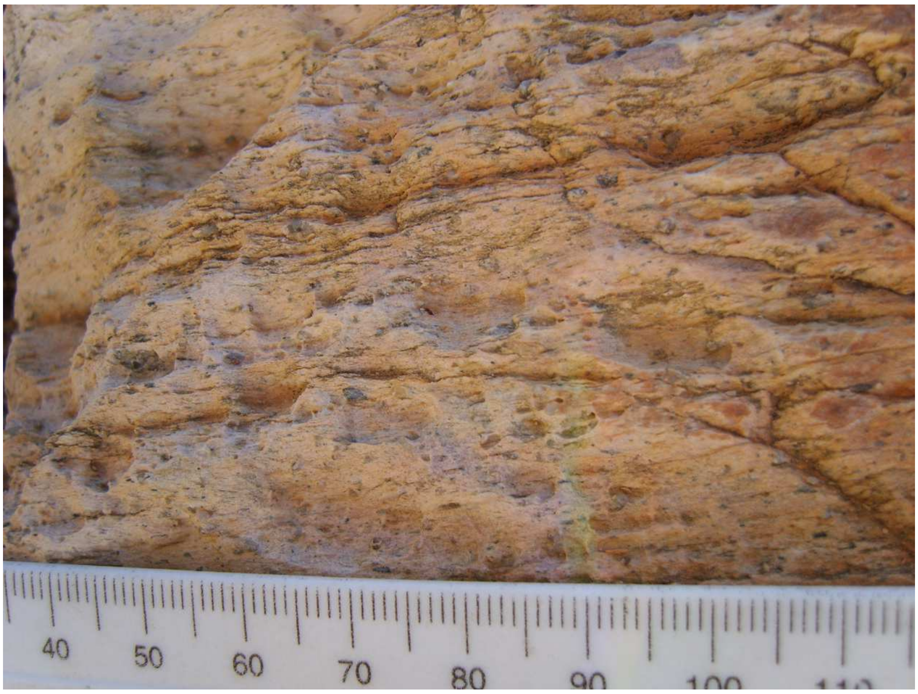

Figure 2.2: Foliated leucocratic tuff (Pan African deformation) of the Paradys River Formation. Location: 16.9883°E; 28.2912°S.

Tuffs are recognized by the presence of rock fragments smaller than 2 cm in the matrix (e.g., Figure 2.2). Rock fragments, glass shards and pumice fragments occur along with phenocrysts and are elongated and flattened parallel to the foliation. Agglomerates are recognized by the presence of fragments larger than 2 cm in the matrix (e.g., Figure 2.3). These fragments vary greatly in size, commonly between 1-20 cm but they grade into millimeter sizes at the one end and rare sizes of up to half a meter have been encountered. They comprise mostly lava and chert and are invariably locally derived, correlating with the rocks of the same or at least associated, formations. Agglomerates are rather abundant throughout the Orange River Group and especially in certain parts, e.g., in the Klipneus Formation in the Richtersveld National Park and the Windvlakte Formation in its northeastern parts.

Figure 2.3: Foliated leucocratic agglomerate (Pan-African deformation) from the Windvlakte Formation, east of Eksteenfontein (17.2817°E; 28.7383°S). Large fragments comprise lava and chert.

2.3.1 Haib Subgroup

The stratigraphy of the Haib Subgroup may be summarized as in Table 1.

Table 1: Subdivision and descriptions of the Haib Subgroup.

Formation	**Description**
Nous	Melanocratic volcanics (aphanitic lava, vesicular lava, tuff, volcanic breccia).
Tsams	Leucocratic to mesocratic aphanitic and porphyrytiv lava.

2.3.1.1 Tsams Formation

In volume, the Tsams Formation is subordinate to the Nous Formation and predominantly leucocratic. Thyolite is the predominating composition. Minor melanocratic lenses and discontinuous layers occur sporadically. Aphanitic lava, quartz-porphyry and tuff predominates while volcanic breccia has been described from a number of localities.

Rare interlayered quartzites have been reported from the formation (Minnaar *et al*., 2011). At one locality in the course of the Oernoep River, where the track from Nous enters the river, leucocratic volcanics of the Tsams Formation are overlain by a thin (approximately 1 m thick) layer of quartzite which is persistent over a distance of approximately 1 km. The contact relationship is gradational, with interlayered quartzite lenses making their appearance in the felsic lava near the contact and becoming increasingly abundant upward towards the contact. Eastward, the Tsams Formation undergoes facies changes with metasedimentary rocks becoming more abundant untill they predominate over the volcanic rocks in the formation (Colliston and Schoch, 1996; Moen and Toogood, 2007).

At a point approximately 2,5 km northeast of Ghaams, to the west of the track leading from Ghaams to Kamgab, the leucocratic volcanics contain spherical leucocratic nodules (Figure 2.4). These nodules comprise mainly quartz, K-feldspar and muscovite with accessory plagioclase. Biotite and ore are the dark constituents and are concentrated in the centre of the nodules. The nodules are on average 2 x 3 x 7 cm in diameter. In the same vicinity these nodules may also occur in the form of veins approximately 5 cm wide and 50 cm long.

Figure 2.4: Leucocratic nodules in leucocratic volcanics of the Tsams Formation east of Ghaams. Location: 17.933083°E, 28.978832°S.

2.3.1.2 Nous Formation

The Nous Formation dominates the Haib Subgroup. It is overwhelmingly melanocratic with interlayered leucocratic lavas which are conspicuous in outcrop from a distance. Aphanitic lava and tuff are the most common rock types while vesicular lava and volcanic breccia also occur. Agglomerate and volcanic conglomerate (lava containing pebbles of dacite) have been described and attest to reworking in the formation (Figure 2.5). Xenoliths of older volcanics are quite common in the Nous lavas. Xenoliths of granitoids (tonalite, granodiorite and granite) were also found in melanocratic Nous lavas at one locality (Figure 2.6). No radiometric age has been obtained for these xenoliths but they present rare evidence of pre-existing crust which is older than the lava in which they are contained. They may also represent reworked material of earlier phases of the Vioolsdrif Suite (not Archean crust).

Figure 2.5: Conglomerate from the Nous Formation coprising a matrix of melanocratic metalava (amphibolite-biotite schist) containing rounded fragments of dacite (location: 17.9822°E; 28.8344°S).

Figure 2.6: Well rounded xenoliths of granitoids in melanocratic Nous lava at a hill south of Vioolsdrif (17.6859°E; 28.823°S).

The occurrence of locally developed linear, cross-cutting veins (Figure 2.7) is a common phenomenon in the melanocratic aphanitic lavas of the Nous Formation. These veins vary in thickness but are usually not thicker than 5 mm. They can be densely concentrated and cut each other in all directions. They could have been caused by contraction during cooling in a particularly homogeneous aphanitic lava. Another characteristic feature of the mafic lavas of the Nous Formation (although not occurring frequently), is the occurrence of quartz vesicles, tubes and veinlets.

Figure 2.7: Linear cross-cutting veins in melanocratic lava of the Nous Formation east of the Nougaseb River. Location: 17.7476°E; -28.8043°S.

A speckled appearance is often induced in the melanocratic volcanics, especially the tuffs, by the clustering of dark minerals in aggregates which are on average 5 mm in diameter. Where such aggregates are weathered out, the rock is left with a pitted surface. Growth of secondary minerals also often leads to an increase in the grain size to medium-grained.

The Nous Formation is often highly foliated, the less competent lavas often being altered to schist. This foliation is near-vertical and weathering patterns such as flaggy, bladed, columnar, rod-shaped or needle-shaped, are characteristic of the formation in highly deformed areas such as in the vicinity of Nous. Parallel layering, on average 5 mm thick, can be discerned in places and represents a primary flow texture. Interlayering and interfingering between lava and tuff can be observed at certain localities (Figure 2.8).

Figure 2.8: Interfingering relationship between lava (fine-grained) and tuff in the Nous Formation near Ghaams, Nous area. Location: 18.000179°E; 28.954834°S.

2.3.2 De Hoop Subgroup

The Richtersveld area (between the Neint Nababeep Plateau and the Gariep Supergroup) is pervasively overprinted by roughly north-south trending, low metamorphic-grade Pan African (720-550 Ma) foliation (see Figures 2.1 and 2.9).

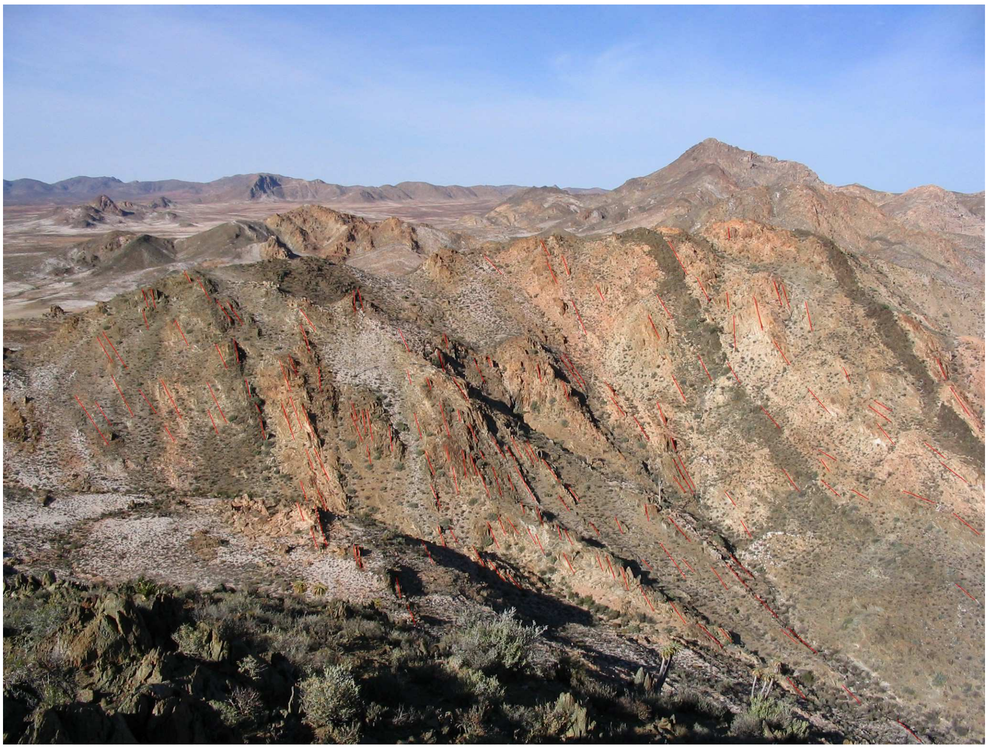

Figure 2.9: North-south trending Pan-African foliation imprinted on rocks of the Vioolsdrif Batholith within the Devil's Castle shear zone (Ritter 1980), east of Eksteenfontein. Looking south from 17.3111°E; 28.7923°S. Foliation is indicated with red trend lines.

In the Richtersveld National Park, north of the Rosyntjieberg mountain range, the De Hoop Subgroup consists of two distinct successions, i.e., in the northeast along the Orange River, and in the southwest underlying the Rosyntjieberg Formation. These two entities are nowhere in contact with each other and therefore age relationships are difficult to establish. Ritter (1980) considered them to form the limbs of a regional anticline of which the core is occupied by granitoids of the Vioolsdrif Suite. According to Ritter (*op cit.*), the northeastern succession represents a centre of volcanism which was active throughout its development, while the southern succession can be seen as a recipient of sediments derived from this volcanic terrane. Based on this interpretation, the Abiekwa River, Kook River and Kuams River Formations are interpreted as distal facies in which volcanic rocks predominate, while the Paradys River and Klipneus Formations are interpreted as proximal facies in which a relatively large proportion of reworked material occur.

Due to the fact that the Windvlakte Formation is nowhere in contact with the other volcanic units of the De Hoop Subgroup, being separated from them by the Rosyntjieberg Formation, it is not possible to determine its stratigraphic position within the subgroup.

The stratigraphy of the De Hoop Subgroup may be summarized as in Table 2.

Table 2: Subdivision and descriptions of the De Hoop Subgroup.

Formation	**Description**
Rosyntjieberg	Massive and feldspathic quartzite with interlayered metapelite and black, iron-rich quartzite and overlying conglomerate. Discontinuous conglomerate bed at the base.
Kuams River	Melanocratic and mesocratic aphanitic and porphyrytic lava with interlayered leucocratic lava and metasediments (quartz, conglomerate).
Kook River	Mesocratic and melanocratic quartz-feldspar porphyry.
Klipneus	Mesocratic and melanocratic tuff, lava and agglomerate with interlayered metasediments (conglomerate, quartzite, chert)
Abiekwa River	Leucocratic, mesocratic and melanocratic welded tuff and lava with interlayered metasediments in places.
Paradys River	Leucocratic, mesocratic and minor melanocratic tuff.
Windvlakte	Undifferentiated leucocratic, mesocratic and melanocratic volcanics; partly recrystallized with primary textures often obliterated.

2.3.2.1 Windvlakte Formation

This formation is extensively intruded by the granitoids of the Vioolsdrif Suite which led to its dismemberment into isolated occurrences. The rocks are highly deformed and recrystallized and primary textures are difficult to recognize or have been obliterated.

The Windvlakte Formation is a heterogeneous unit comprising undifferentiated leucocratic, mesocratic and melanocratic volcanic rocks with interlayered metasedimentary rocks. There is a compositional gradation in the formation from southwest to northeast with leucocratic volcanics predominating in the areas to the south of Eksteenfontein, mesocratic volcanics predominating in the central parts of the outcrop area, and melanocratic volcanics predominating in the areas bordering the Orange River. Porphyrytic lava, agglomerate and agglomeratic tuff predominate in localities where original textures can be identified.

Contact relationships among the volcanic rocks in the formation are sharp in places and gradational in others. Lenses and discontinuous layers of the one occur in the other. Contacts between the volcanics and the Xaminxaip River Granite are mostly gradational, locally over narrow (> 0.5 m) zones. Sharp contacts between these two rock types have been observed but are rare and not convincingly intrusive (not cross-cutting). Contacts between the volcanics and the Gaarseep granitoids leave no doubt that the latter are intrusive (sharp, cross-cutting contacts and abundant xenoliths of volcanics in the granites). [The Xaminxaip River Granite is also intruded by Gaarseep granitoids.]

The presence of metasedimentary rock types associated with the felsic volcanic unit in the area between Jenkinskop and Eksteenfontein, is suggested by several occurrences of sillimanite in the rocks. In this highly sheared environment the rocks are schistose and the occurrence of quartz-sericite-sillimanite schist points to an originally sedimantary assemblage. It is however, also possible that the schist represents an original acid volcanic. In areas immediately to the west and close to the contact with the Gariep Supergroup, the schist commonly contains chlorite, hornblende and haematite, pointing to a volcanic origin. Sillimanite is especially plentiful at Jenkinskop itself.

Porphyritic felsic lava was found in a number of places in the Windvlakte Formation. Approximately 8 km south of Eksteenfontein, the lava occurs within a strongly foliated zone (Figure 2.10). The foliation trends N-S and is related to Pan-African deformation. The quartz porphyroblasts are milky white, elongated parallel to the foliation and are on average 5 mm in diameter (long axes). The foliation anastomises around the porphyroblasts.

Figure 2.10: Foliated felsic porphyritic lava approximately 8 km south of Eksteenfontein. Location: 17.25894°E, 28.901451°S.

The geographically northeastern part of the formation, closest to the Orange River, is especially rich in agglomerate (see figure 2.3). This agglomerate zone can be traced along strike up to an area just south of the Rosyntjieberg Formation, where extensive development of the Xaminxaip River Granodiorite terminates its extension along strike. To the north of the Rosyntjieberg mountain range, the agglomerates of the Klipneus Formation are situated along strike of these, suggesting that the Klipneus Formation may represent the continuation of at least part of the Windvlakte Formation, north of the Rosyntjieberg mountain range.

2.3.2.2 Paradys River Formation

The basement of the Paradys River Formation has not been identified. It is intruded by the Vioolsdrif Suite and overlain by the Rosyntjieberg Formation. The contact with the overlying Rosyntjieberg Formation is mostly obscured by deformation but can, in some places, be observed to be gradational (see 2.3.2.7 Rosyntjieberg Formation). Along strike to the northwest, the Rosyntjieberg Formation pinches out and the Paradys River Formation is overlain by the Abiekwa River Formation, the contact being gradational.

Figure 2.11: Intensely foliated leucocratic porphyrytic dacite of the Paradys River Formation at the foot of the Rosyntjieberg mountain range, Richtersveld National Park. Lenses of the overlying Rosyntjieberg Formation quartzite occur in the dacite. Location: 17.0617°E; 28.3475°S.

The largest part of the Paradys River Formation comprises leucocratic volcanic rocks, mostly tuff (see Figure 2.2), while lava and agglomerate occur interlayered. Along strike to the southeast, the rocks become mesocratic while at the foot of Rosyntjieberg, minor melanocratic volcanics occur in the formation. Intense northwest-trending foliation is developed throughout the Paradys River Formation (Figure 2.11). This is thought to be the result of sinistral shear associated with Pan African deformation, during which the overlying quartzite unit acted as a more competent unit relative to the underlying volcanic unit.

A dacite sample which was dated during this study from the Paradys River Formation rendered an U-Pb zircon age (LA-ICPMS) of 1 883±7.4 Ma (Appendix 2).

2.3.2.3 Abiekwa River Formation

The Abiekwa River Formation was the main locus of intrusion by the Vioolsdrif granitoids in the Richtersveld National Park. Not only was most of the formation engulfed by the granites, but the intrusion also caused thinning and uplifting of the supracrustal succession on both sides of the intrusive body, to compensate for the lack of space.

In the northern parts of the Richtersveld National Park, the Abiekwa River Formation is overlain by both the Kook River Formation and Kuams River Formation, the boundary represented by a thrust with the Abiekwa River Formation overriding the latter two formations. In the eastern parts of the park, the Abiekwa River Formation grades upwards into the Kuams River Formation.

The Abiekwa River Formation comprises approximately equal volumes of mesocratic and leucocratic volcanics, mostly represented by tuff and interlayered lava. Agglomerates are also fairly common and comprise of locally derived material (Figure 2.12).

Figure 2.12: Agglomeratic leucocratic porphyrytic lava of the Abiekwa River Formation, Richtersveld National Park. Location: 17.1081°E; 28.2239°S.

2.3.2.4 Klipneus Formation

The Klipneus Formation occurs along strike with the Paradys River Formation but is separated from it on lithological grounds, a prominent shear zone between the two being interpreted as an important tectonic boundary (the Kwaggarug shear, Ritter 1980). It is nowhere in contact with the other volcanic units but it is thought to be associated with the Kook and Kuams River Formations because of its predominantly melanocratic character. It contains interlayered meso- and leucocratic rocks and is the most heterogeneous unit of the Orange River Group comprising mainly tuff, lava (including vesicular lava) and agglomerate but also sedimentary rock types such as conglomerate and chert. Well developed agglomerate can be observed along the road in the eastern part of the Richtersveld National Park north of the Oudinnisiep River course. Here the contact between the steeply foliated Orange River Group and the weakly deformed, near-horizontal Karoo Supergroup, can also be observed (Figure 2.13).

Figure 2.13: Contact (largely concealed by tallus) between foliated (Pan-African foliation) schist of the Klipneus Formation and undeformed strata of the Karoo Supergroup, Richtersveld National Park. Location: 17.3590°E; 28.3467°S.

Figure 2.14: Contact between mesocratic (bottom) and melanocratic quartz-feldspar porphyry of the Kook River Formation in the Richtersveld National Park. The contrats is not well defined in the photo but follows the horizontal joint. Location: 17.2599°E; 28.2420°S.

2.3.2.5 Kook River Formation

The upper contact of the Kook River Formation with the overlying Kuams River Formation is gradational. The Kook River Formation consists entirely of quartz-feldspar porphyry, the lower part being mesocratic and the upper part melanocratic. The contrast between these two compositional varieties is conspicuous and the contact is sharp (Figure 2.14). The contrast can be observed from the road leading down the course of the Kook River immediately to the west of De Hoop in the Richtersveld National Park. In hand specimen, the phenocrysts are represented by both plagioclase and quartz.

2.3.2.6 Kuams River Formation

The Kuams River Formation consists predominantly of porphyritic lava, but contains intercalated tuff layers. Mafic enclaves are sporadically contained in the lava (Figure 2.15).

Figure 2.15: Mafic enclave in porphyrytic melanocratic lava of the Kuams River Formation north of De Hoop, Richtersveld National Park. Location: 17.1848°E; 28.1631°S.

Two types of enclaves were recognized, viz. xenoliths of other lava, and restites composed of dark minerals. The lavas are predominantly melanocratic, with subordinate interlayered leucocratic units. Epiclastic metasediments are present in places in the form of quartzite, cross-bedded biotite-muscovite gneiss and conglomerate. To the northeast, the unit is intruded by granitoids of the Vioolsdrif Suite. Xenoliths (of various sizes) of the Kuams River Formation occur within the plutonic units of the Vioolsdrif Suite.

2.3.2.7 Rosyntjieberg Formation

The Rosyntjieberg Formation is a quartzite-dominated unit that gives rise to the Rosyntjieberg mountain range. The formation gradually thins out along strike in a northwesterly direction. Duplication in the formation due to isoclinal folding and thrusting is apparent where the formation is at its thickest.

The contact relationship with the underlying volcanic pile is, for the most part, sharp, giving the impression that the metasediments overlie the volcanics unconformably. However, this sharp contact relationship results from Pan African deformation, which led to displacement between the volcanic and quartzitic units. In places, the original contact relationship is preserved and can be observed to be gradational with lenses and discontinuous layers of quartzite becoming more plentiful in the underlying volcanics until the quartzite predominate, which in turn contains lenses of the underlying volcanics (Figure 2.16). These lenses of volcanic rocks eventually disappear completely higher up in the succession.

In Paradyskloof in the Richtersveld National Park, intrusive contact relationships can be observed between the Quartzites of the Rosyntjieberg Formation and granites of the Gaarseep Granodiorite unit (Figure 2.17).

Figure 2.16: Interlayered quartzite in intensely foliated, leucocratic porphyrytic lava of the Paradys River Formation near the base of the Rosyntjieberg Formation (the stratigraphic bottom-to-top in the photo is from right to left, location: 17.0618°E; 28.3471°S, Rosyntjiewater, Richtersveld National Park).

Figure 2.17: Xenolith of Rosyntjieberg quartzite in granite of the Goodhouse Subsuite (Gaarseep Granodiorite) in Paradyskloof, Richtersveld National Park (17.0247°E; 28.3141°S). Length of measuring-stick in the photo is 50 cm.

The bulk of the formation comprises quartzite, varying in composition between brown feldspathic and white, fine- to very fine-grained arenitic quartzite, with the latter predominating. A variety of sedimentary structures are preserved in the unit including cross- and parallel bedding, ball-and-pillow structures (Figure 2.18), and ripple marks.

Figure 2.18: Parallel- and cross-bedding as well as ball-and-pillow structures in the Rosyntjieberg Formation, Richtersveld National Park (17.0052°E; 28.3284°S). Head of hammer on cross-bedding.

At the base of the formation, a conglomeratic layer is sporadically developed. A persistent argillaceous unit approximately 50 m thick occurs interlayered in the quartzitic sequence and can be traced along the entire strike of the formation (Figure 2.19). Seen from the north, the unit forms a conspicuous dark-coloured band within the white quartzites. On close inspection it is seen to be very heterogeneous, being dominated by black, iron-rich quartzite and further comprising metapelite, mudstone, siltstone and arkose. At the summit of Oemsberg and the surrounding area, a quartzitic conglomerate constitutes the top of the Rosyntjieberg Formation. The matrix as well as the pebbles are quartzitic. Both the bottom and top conglomerate beds comprise only locally derived pebbles.

Figure 2.19: Dark-weathering argillaceous unit near the base of the Rosyntjieberg Formation, Richtersveld National Park. Location: 17.0647°E; 28.3936°S.

Detrital zircon ages (U-Pb by LA-ICPMS) from one sample of quartzite from the Rosyntjieberg Formation rendered a probability distribution curve with a major peak between 1 850-1 800 Ma and single grains showing ages of 1 760 Ma, 1 920 Ma and 2 050 Ma (n=42; see Appendix 2)

2.4 VIOOLSDRIF SUITE

Contrary to the Orange River Group, the Vioolsdrif Suite shows little deformation in the batholith type area. Clear contact relationships among the various units of the Vioolsdrif Suite, as well as between the suite and the volcanic group, are common within the type area, with the exception of the Vuurdood Subsuite.

Compositional references in the names of the units (Khoromus "Tonalite", Gaarseep "Granodiorite", Xaminxaip River "Granodiorite" and Hoogoor "Granite"), are based on that unit's average composition as indicated on the chemical classification diagram of De le Roche *et al*. (1980; see Figure 4.2).

The stratigraphy of the Vioolsdrif Suite may be summarized as in Table 3.

Table 3: Subdivision and description of the Vioolsdrif Suite.

Subsuite	**Unit**	**Description**
Ramansdrif	Sout Granite	Medium- to coarse-grained leucocratic granite.
	Ghaams Granite	Fine- to medium-grained leucocratic granite.
Goodhouse	Hoogoor Granite	Light-brown weathering floiated granitoids (granite, granodiorite, tonalite).
	Gaarseep Granodiorite	Homogeneous brown-weathering, coarse-grained granitic and mafic intrusives (granodiorite, granite, tonalite, diorite, gabbro).
	Blockwerf Migmatite	Heterogeneous migmatitic mafic and granitic plutonic rocks (diorite, tonalite, granodiorite).
	Xaminxaip River Granodiorite	Orange-brown weathering, even-grained (medium-grained) granodiorite.
	Khoromus Tonalite	Dark-brown to black weathering, grey, medium-grained granitic and mafic intrusives (tonalite, granodiorite, diorite, gabbro).
Vuurdood		Mafic-ultramafic bodies of limited extent. Composites of gabbro, pyroxenite, peridotite, minor troctolite.

2.4.1 Vuurdood Subsuite

The Vuurdood Subsuite is mainly developed in the Haib area to the south of Vioolsdrif and is conspicuously absent in both the Richtersveld area and within the Hoogoor

Granite. Mafic-ultramafic bodies which are present in the Richtersveld area to the east and southeast of Eksteenfontein (De Villiers and Söhnge, 1959; Middlemost, 1965; Minnaar *et* al., 2011) is not included in the Vuurdood Subsuite because field evidence suggest that they were emplaced during post-Vioolsdrif times (reliable radiometric dating is needed to confirm this). But even if they do correlate with the Vuurdood Subsuite, then they are still volumetrically vastly inferior to those in the Haib area. In the Hoogoor Granite, sporadic bodies of amphibolite are encountered which may represent metamorphosed bodies of the Vuurdood Subsuite but again, even if that is the case, they cannot volumetrically be compared to those in the Haib area.

The Vuurdood Subsuite comprises composite bodies, containing various proportions of gabbro, amphibolite, peridotite and pyroxenite. Reid (1977) distinguished troctolite in the Swartkop body. The bodies vary in size and shape, ranging from about 100 m to about 2 km across and are invariably enclosed within the Goodhouse Subsuite. Contact relationships between the bodies and the rocks of the Goodhouse Subsuite are either obscured due to shearing, or covered by talus fans. This has previously led to some controversy as to the nature of these bodies. Some regarded them as earlier phases of the Vioolsdrif Suite (e.g., Blignault, 1977), some as cumulate material within the Goodhouse Subsuite (e.g., Reid, 1982), while others regarded them as intrusive bodies in the Goodhouse Subsuite (e.g., Beukes, 1973). Radiometric age determinations and isotopic studies by Reid (1977, 1982) have established beyond reasonable doubt that they are among the oldest in the batholith (overlapping in age with the early volcanics) and that they originate from similar parent magmas as both the Orange River Group and Goodhouse Subsuite. During the current study, xenoliths of gabbro, closely resembling those of the Vuurdood Subsuite, were found in Goodhouse Subsuite granites (Figure 2.20).

Figure 2.20: Xenoliths of gabbro, probably from the Vuurdood Subsuite, in granitoids of the Khoromus Tonalite at a locality southeast of Vioolsdrif (17.9411°E; 28.8420°S).

Figure 2.21: Gabbro of the Vuurdood Subsuite at a locality southeast of Vioolsdrif (17.9431°E; 28.8878°S).

The bodies of the Vuurdood Subsuite are melanocratic and the gabbros often show a speckled surface appearance with white (average 5 mm) feldspar porphyroblasts in the melanocratic matrix (Figure 2.21). Original rock textures are invariably destroyed by the growth of large secondary minerals, leading to a massive texture and the production of boulder-sized rubble. Zoning was recognized during the current mapping in some of the bodies where the ultramafic rocks (pyroxenite and peridotite) form a marginal zone around a central core of gabbro. The contact between rim and core is gradational. Ultramafic compositions also occur within the central gabbroic part, probably as cumulates.

2.4.2 Goodhouse Subsuite

The Goodhouse Subsuite is volumetrically dominant in the Vioolsdrif Suite. The Gaarseep Granodiorite unit can be considered to typify the suite and its type area is along the national Namibian-South African highway south of Vioolsdrif (see map). The subsuite as a whole comprises a range of compositions from gabbro, diorite, tonalite and granodiorite to monzo- and syenogranite. However, four units can be distinguished within the subsuite within which mineralogical and geochemical variation is limited.

The exact proportions of tonalite, granodiorite and granite within the subsuite is difficult to determine as they resemble each other closely in the field in physical character. Diorite and gabbro show a gradation, making them difficult to distinguish from each other but can, however, be distinguished from the granitoids fairly easily by an overall darker weathering colour. They represent about 10% of the total volume within the Goodhouse Subsuite.

In the Haib area, contacts between the Goodhouse Subsuite and Orange River Group are sharp and cross-cutting with numerous xenoliths of the latter contained in the former (Figure 2.22). In the Richtersveld area, the contacts between these two units are typically concordant, with xenoliths of the volcanics still abundant in the intrusives.

Figure 2.22: Typical contact relationship between the volcanics of the Orange River Group and granitoids of the Vioolsdrif Suite in the Haib area as seen at a locality southeast of Vioolsdrif (17.9617°E; 28.8850°S).

Figure 2.23: Heterogeneous enclave swarm in the Khoromus Tonalite at a locality in the Oernoep River course, southeast of Vioolsdrif (17.9457°E; 28.9339°S). They consit of xenoliths of the Orange River Group and older phases of the Vioolsdrif Suite as well as dark mineral cumulates.

A characteristic feature of the Goodhouse Subsuite is the widespread occurrence of dark mafic enclaves in the granitoids. These enclaves are of various types and include xenoliths of the Orange River Group and restites or cumulates of dark minerals which formed within the unconsolidated magmas. There are also enclaves that were deformed, occurring as flattened and elongated dark mineral cumulates, the origin of which is uncertain. In places, enclave swarms, some homogeneous and some heterogeneous (e.g., Figure 2.23), occur. The xenoliths of Orange River Group volcanics are the most abundant. They vary in shape from angular to rounded and in size from a few millimeters to tens of meters or even hundreds of meters in diameter. A detailed investigation of the enclaves was not done for this study.

2.4.2.1 Khoromus Tonalite

The Khoromus Tonalite is the oldest unit within the Goodhouse Subsuite, as can be deduced from contact relationships, and is extensively developed only in the Haib area. In the field, the Khoromus Tonalite can be distinguished from the Gaarseep Granodiorite from a distance by an overall darker weathering colour that can be recognised even on aerial photographs. A characteristic feature of a landscape built by the Khoromus Tonalite, is the presence of conspicuous hills capped by black-weathering bodies with dark debris along the slopes (Figure 2.24).

This is in contrast with the areas underlain by Gaarseep Granodiorite, which display homogeneous brown colours (Figure 2.35). Contacts between the Khoromus Tonalite and Gaarseep Granodiorite are sharp and cross-cutting with xenoliths of the former occurring in the latter (Figure 2.25).

Figure 2.24: Typical view over an area underlain by the Khoromus Tonalite unit. Locality near the Nougaseb River course (17.9619°E; 28.8649°S). Direction of view is to the east.

Figure 2.25: Xenoliths of Khoromus Tonalite (dark) in Gaarseep Granodiorite (17.9253°E; 28.9191°S).

Figure 2.26: Typical Khoromus Tonalite granitoid in outcrop. Course of the Oernoep River, southeast of Vioolsdrif (17.9417°E; 28.9286°S). The well-rounded xenoliths probably represent mafic volcanic rocks of the Orange River Group.

In outcrop, granitoids of the Khoromus Tonalite are typically medium-grained with a speckled grey colour (Figure 2.26). The speckles are due to aggregates (average 5 mm) of dark minerals (biotite and hornblende). Such aggregates may be up to 2 cm across and are sometimes weathered out, leaving a pitted surface. Feldspar phenocrysts, on average 5 mm in diameter, are often discernible in outcrop.

The black-weathering rocks which are so conspicuous from a distance (see Figure 2.24), occur as numerous isolated patches of a few meters to tenths of meters across. The black weathering is due to a coat of desert varnish on the surface of the rocks. They typically produce a metallic clang when hit with a hammer. The fresh rock is blue-grey and medium-grained, while grey quartz and green plagioclase crystals can be discerned. Dark minerals (biotite and hornblende) sometimes also cause a speckled appearance to this melanocratic rock. Contacts between these black-weathering rocks and the brown-weathering varieties are gradational over a few meters (Figure 2.27). Leucocratic varieties of the Khoromus Tonalite rocks also occur but are scarce and limited in extent. The unit is predominantly medium-grained but coarse-grained variations occur. The presence of mafic enclaves is a characteristic feature of both the Khoromus Tonalite and the Gaarseep Granodiorite.

Figure 2.27: Gradational contact relationship between melanocratic and mesocratic varieties within the Khoromus Tonalite at a locality north of Ghaams. Location: 18.0008°E; 28.8936°S.

The rocks of the Khoromus Tonalite unit commonly display textures in outcrop which may be interpreted as products of magma mixing (after studies like, e.g., Perugini *et* al. 2002; Perugini and Poli 2004). These include banding and "streaky" textures (Figure 2.28), which conform with descriptions of "filament" and "globular" regions in rocks which have been shown to represent products of magma mixing.

Figure 2.28: Banding and "streaky" textures commonly displayed in the Khoromus Tonalite unit which may be interpreted as "filament" (leucocratic areas) and "globular" (melanocratic areas) areas as defined in Perugini *et al*. (2002) and interpreted as the result of chaotic mixing dynamics during magma mixing processes. Southeast of Vioolsdrif (17.9253°E; 28.9191°S).

2.4.2.2 Xaminxaip River Granodiorite

The Xaminxaip River Granodiorite is best developed in the area to the east of Eksteenfontein and is named after a dry river bed in that area (see map). It was first mapped as an independent unit by Ritter (1980), who referred to it as "even-grained granodiorite". Minnaar *et al*. (2011) named it the Xaminxaip River Granodiorite. Unfortunately this name is uncommon in the English language but was chosen for reference purposes on published maps. Being a deserted area, such references are few and far between on the relevant maps. The name "Xaminxaip" should be pronounced "kaminkaip" (refer to the international phonetic alphabet) as it originates from a Nama word in which a clicking sound (with the tongue) is replaced by "x" (after De Villiers and Söhnge, 1959). As there is no such clicking sound in the English alphabet, "k" is the closest to it.

U-Pb zircon (LA-ICPMS) ages were obtained for a sample from the unit (see Appendix 2). A crystallization age of 1 892.5±4.8 Ma is very similar to that of the Gaarseep granitoids as determined by Reid (1977) in the Haib area. It is chronologically placed older than the Gaarseep Granodiorite since contact relationships attest to it being intruded by the Gaarseep Granodiorite (Figure 2.29). In some cases, the relationship is unclear with the contact being gradational, however, the interpretation is supported by previous studies of De Villiers and Söhnge (1959) and Ritter (1980), who came to the same conclusion.

Figure 2.29: Xenolith of Xaminxaip River Granodiorite in granite of the Gaarseep Granodiorite (17.4406°E; 28.8035°S).

The Xaminxaip River Granodiorite is spatially associated with the volcanic rocks of the Windvlakte Formation. Contact relationships between the two units are mostly gradational and it is often possible to identify volcanic textures, such as tuffaceous fragments, in the granitoids (Figure 2.30). Ritter (1980) considered the Xaminxaip River Granodiorite to represent a subvolcanic unit between the Vioolsdrif Suite and the overlying volcanics.

Figure 2.30: One of the textures often found in the Xaminxaip River Granodiorite unit which is interpreted to represent an original volcanic character (mesocratic tuff in this case) from the Windvlakte Formation after recrystallization (location: 17.3203°E; 28.7466°S, east of Eksteenfontein).

The Xaminxaip River Granodiorite as a whole is very homogeneous in composition and grain size (medium-grained, average 1 mm) although, transitions to fine- and coarse-grained varieties do occur. It displays a characteristic grey colour and weathers light-brown. Xenoliths of Orange River Group volcanics as well as other types of enclaves occur in places, although much less frequent than in the Khoromus Tonalite and Gaarseep Granodiorite.

The development of metamorphic banding, plastic deformation and, locally, fully developed migmatite (Figure 2.31), may be considered characteristic of the Xaminxaip River Granodiorite. De Villiers and Söhnge (1959) considered the migmatite to be a direct result of the intrusion of the Gaarseep Granodiorite into the Xaminxaip River Granodiorite (thus, by contact metamorphism). Ritter (1980) regarded the migmatite in Helskloof to the east of Eksteenfontein, as a product of metamorphism at a deeper crustal level. Contacts between the migmatite and the homogeneous granodiorite within the unit are entirely gradational. Areas of migmatite development are commonly a few metres in extent.

Figure 2.31: Migmatite developed in the Xaminxaip River Granodiorite at Helskloof, east of Eksteenfontein (17.4398°E; 28.8037°S).

2.4.2.3 Blockwerf Migmatite

The Blockwerf Migmatite was originally termed the Blockwerf Migmatite Complex by Ritter (1980). It is situated on the bank of the Orange Riverin the northeastern part of the Richtersveld National Park in South Africa. It intrudes the Kuams River Formation and is itself intruded by the Gaarseep Granodiorite. These relationships are indicated by cross-cutting contacts between the migmatites and the Gaarseep Granodiorite (Figure 2.32), xenoliths of the Kuams River Formation volcanics found within the granitoids of the Blockwerf Migmatite, and xenoliths of the Blockwerf Migmatite in the granitoids of the Gaarseep Granodiorite.

Figure 2.32: Contact between granodiorite of the Gaarseep Granodiorite unit (top) and migmatite of the Blockwerf Migmatite at Blockwerf, Richtersveld National Park. Location: 17.1221°E; 28.0798°S.

Figure 2.33: Migmatite of the Blockwerf Migmatite, the migmatitic character is owed to a large number and high concentration of mafic enclaves in the intruding granitoids. Location: 17.1525°E; 28.1074°S.

The migmatitic character of the Blockwerf Migmatite is a direct result of the large number and high concentration of mafic enclaves in the intruding granitoids. In other words the mafic enclaves (which vary in size and are densely and randomly distributed) cause a deformation of the granitoid's matrix in such a way that the impression of plastic deformation is created, which is being termed migmatite (Figure 2.33). The majority of the enclaves closely resemble the volcanic rocks of the Kuams River Formation, while others are represented by cumulates of mafic minerals.

Two phases of migmatite can be distinguished within he Blockwerf Migmatite, based on how well the migmatitic character is developed (which is directly related to the density of enclaves in the granitic matrix). The first phase is represented by those parts where the density of mafic enclaves is high and the migmatitic character is well developed. In this phase, the dark mineral contents is also high and the granitoids are melanocratic. The second phase is represented by those parts in which the density of enclaves are low and the granotoids are not migmatitic. This phase has a lower dark mineral contents and is mesocratic. This relative difference in composition between the two phases can also be observed on a TAS classification diagram (Figure 4.19; 4.2.7 Blockwerf Migmatite). The two phases may be referred to as phase 1 and phase 2 (as in Figure 4.19). There is a complete gradation between the two phases.

There is a large variation in the sizes of the enclaves from a few centimetres to bodies of about 3 km in length and 1 km wide. Patches of granite occurring within such large bodies, are melanocratic. For the most part, the matrices of the Blockwerf Migmatite are coarse-grained (average 4 mm) and the dark minerals cause a speckled appearance in the fresh rock. In phase 1, the matrix is often fine-grained. Gradational contact relationships between the enclaves and the granitoid matrix in phase 1, suggest that the granitoid may be a hybrid rock (i.e., formed by the complete assimilation of the country rock which it intruded; Figure 2.34).

The intruding granites of the Gaarseep Granodiorite are characterised by homogeneity in all of composition, grain size and weathering colour. In these characteristics they closely resemble phase 2 of the Blockwerf Migmatite where the enclave densities are low. The Gaarseep granitoids have, compared to the granitoids of the Blockwerf Migmatite, much fewer enclaves and their concentration is very low in the unit. They are evenly distributed, well-rounded and their sizes are even, varying only between 2 – 5 cm. In addition to the enclave types found in the Blockwerf Migmatite, the Gaarseep granitoids also contain xenoliths of the Blockwerf Migmatite itself. The composition of the Gaarseep granitoids do not seem to be influenced by the engulfment of the migmatites, nor by the engulfment of the Kuams River volcanics (from observations elsewhere).

Figure 2.34: Hybrid rock of the Blockwerf Migmatite. Location: 17.1373°E; -28.1002°S. Blockwerf, Richersveld National Park.

2.4.2.4 Gaarseep Granodiorite

The Gaarseep Granodiorite has by far the most extensive distribution in the Vioolsdrif Suite and is very homogeneous. It is coarse-grained and invariably exhibits a brown weathering colour and a woolsack weathering pattern (Figure 2.35). The type area for the unit has historically been considered to be the area south of Vioolsdrif (see map). The occurrence of mafic enclaves is a characteristic feature, as for the Khoromus unit. These enclaves are relatively homogeneous in size and shape, being mostly very well rounded and on average 5 cm in diameter. In the fringe areas of the batholith, where the Gaarseep Granodiorite is overprinted by Namaqua foliation, large (up to 3 cm) idiomorphic secondary hornblende crystals are commonly developed in the granotoids (see Figure 3.9).

Figure 2.35: Typical view over an area underlain by the Gaarseep Granodiorite. Dark-weathering outcrop of the Khoromus Tonalite are visible in the background. Locality near the Oudanisiep River course (17.9619°E; 28.8649°S). Direction of view is to the south.

Based on field evidence and contact relationships, it can be said that the timespan of development of the Gaarseep Granodiorite unit overlaps that of the entire Vioolsdrif Batholith,from the earliest phases overlapping with the Orange River Group, through to the final stages, even as young as Ramansdrif Subsuite. Xenoliths of it are found in some of the earliest volcanics (see 2.3.1.2 Nous Formation), and it can be observed to intrude all of the Orange River Group, Khoromus Tonalite, Xaminxaip River Granodiorite, Blockwerf Migmatite and Rosyntjieberg Formation, the latter of which render some of the youngest radiometric ages in the batholith (see 2.3.2.7 Rosyntjieberg Formation). Contact relationships with the Hoogoor Granite could not be established in the field. The Gaarseep Granodiorite is on average more felsic in the Richtersveld than in the Haib area. In the southern parts of the Richtersveld National Park, the granites commonly display green and pink alteration of the feldspars in outcrop.

A sample from the Gaarseep Granodiorite in the Richtersveld, which is found to intrude the Rosyntjieberg Formation, rendered U-Pb zircon (LA-ICPMS) ages of 1896±12 Ma (see Appendix 2). This age is problematic because it contradicts the field evidence. According to contact relationships it should be younger than all of the Paradys River Formation (1 883±7 Ma), Rosyntjieberg Formation (<1 800-1 850 Ma), and Xaminxaip River Granodiorite (1 892±5 Ma). Given the relatively wide time span of development of the Gaarseep Granodiorite, it is possible that the wrong outcrop was sampled for the age determination. According to field mapping, the sample is from the same pluton that intrudes the Rosyntjieberg Formation (see map in folder). However, the sample is not from the actual locality where the two units are found in contact (Paradyskloof, Richtersveld National Park).

2.4.2.5 Hoogoor Granite

The Hoogoor Granite is located within the areas surrounding the batholith type area where it is pervasively overprinted by foliation and metamorphism of the 1.3-1.0 Ga Namaqua orogeny (Figure 2.36), which has led to the obliteration of original textures and contact relationships.

This has been the cause of controversies regarding the correlation of the unit with the Vioolsdrif Suite (Gaarseep Granodiorite). Blignault *et al.* (1983) extended the Vioolsdrif Suite through field mapping out of its relatively undeformed type area eastward up to the vicinity of Onseepkans, thus correlating what is termed the Hoogoor Granite in this study, with the Gaarseep Granodiorite. Following this, Strydom *et al.* (1987) included the unit in the Goodhouse Subsuite. However, this correlation was not followed by Moen and Toogood (2007) who, in agreement with Von Backström (1953), distinguished the unit separately as the Hoogoor Suite. They based this subdivision on the following field evidence:

Figure 2.36: Intense foliation associated with the Namaqua (1.3-1.0 Ga) orogeny, which is attained in places within the Hoogoor Granite unit. Location: 18.5039°E; 28.9236°S.

a) the overall more felsic nature of the Hoogoor Granite compared to the Gaarseep Granodiorite in the Haib area,

b) the general absence of the Vuurdood Subsuite mafic-ultramafic bodies, which is typically associated with the Goodhouse Subsuite in its type area,

c) the common association of the Hoogoor Granite with metasedimentary rocks, as opposed to the Goodhouse Subsuite's general association with metavolcanic rocks,

d) the virtual absence of mafic enclaves in the Hoogoor Granite, which is considered characteristic of the Goodhouse Subsuite.

Moen and Toogood (2007) furthermore report field evidence which suggest that parts of the Hoogoor Granite actually belong with the metasedimentary supracrustal units. Such evidence include gradational contacts with metapelites and quartzites, horizontal facies changes and the occurrence of abundant sillimanite in the gneiss in places. Colliston and Schoch (2006), on the other hand, demonstrated that many of the textural differences between the Gaarseep Granodiorite and Hoogoor Granite, may be accounted for by differences in strain intensity between the Orange River orogeny and Namaqua orogeny, thereby maintaining the correlation between the two units. This correlation is supported by a U-Pb zircon (SHRIMP) age of 1 890 Ma, which is reported by Moen and Toogood (2007; pers. comm. R. Armstrong). This age agrees well with the intermediate members of the Gaarseep Granodiorite unit, as well as with the Xaminxaip River Granodiorite.

The fact that the Gaarseep Granodiorite and Hoogoor Granite are time equivalents does not necessarily imply that they are genetically related. This study investigates the geochemical relationship between them. Some of the geochemical characteristics, especially those involving trace and rare earth elements, are regarded to reflect primary igneous processes. Moen and Toogood (2007) suggested further investigations into the age relationship between the Hoogoor Granite and the metasedimentary units which are typically associated with them, especially the Guadom Formation of Strydom *et al.* (1987). Indeed, in the eastern extension of the unit and in Namibia, it becomes part of much more complicated correlation issues involving a number of supracrustal units. Such investigations are not within the scope of the current study.

In outcrop, the Hoogoor Granite displays light-brown weathering colours. The Namaqua foliation is pervasively developed, varying in intensity, and the rocks display a granoblastic texture with a relatively wide variation in grain size. Moen and Toogood (2007) recognized an association between coarse-grained (>4 mm) varieties and the development of an augen texture. The augen may be composed of alkali feldspar or intergrowths of quartz and feldspar.

2.4.3 Ramansdrif Subsuite

The Ramansdrif Subsuite includes the leucocratic endmembers of the suite. It is found intrusive into the Gaarseep Granodiorite (Figure 2.37) and represents the final stage of the batholith evolution (Reid 1977).

The granites of the Ramansdrif Subsuite weather to light-brown colours, similar to other units in the Namaqua Metamorphic Province which are commonly referred to as "pink gneisses". Two distinct grain size variations can be distinguished in outcrop and Minnaar *et* al. (2011) proposed the subdivision of the unit into the Ghaams (fine- to medium-grained) and Sout (medium- to coarse-grained) Granites, named after wells in the study area (see map). Contacts with the rocks of the Goodhouse Subsuite are sharp and discordant.

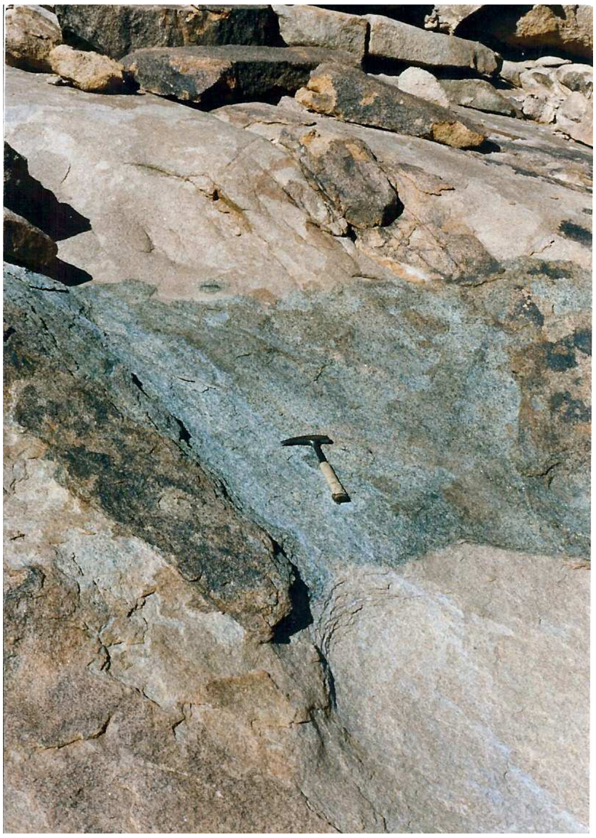

Figure 2.37: Intrusive relationship between the Sout Granite and Gaarseep Granodiorite at a locality southeast of Vioolsdrif (17.9419°E; 28.8878°S).

2.4.3.1 <u>Ghaams Granite</u>

The Ghaams Granite is fine- to medium-grained and commonly displays a gneissic texture. In the southern part of the Haib area within the foliated fringe areas of the batholith, the Ghaams Granite’s characteristic leucocratic nature contrasts sharply with the granodioritic rocks of the Goodhouse Subsuite (Figure 2.38). Also in these foliated areas, the gneiss is exceptionally rich in muscovite and commonly associated with the development of pegmatite and greissen.

Figure 2.38: Conatact between the leucocratic Ghaams Granite (right) and mesocratic granitoids of the Goodhouse Subsuite in the southern, foliated parts of the batholith south of Ghaams (17.8850°E; 28.9659°S). Direction of view is to the east.

Figure 2.39: Leucocratic nodules and lenses in the Ghaams granite at a localtion south of Ghaams. Location: 17.9227°E; -28.9647°S.

Occurrences of leucocratic nodules, lenses and discontinuous veins is a characteristic feature in certain parts of the Ghaams Granite (Figure 2.39). They comprise quartz, K-feldspar, subordinate plagioclase and muscovite with biotite and opaque minerals being concentrated along the centres. They are similar to those described for the Tsams Formation and are thought to originate during deformation and metamorphism through migration of felsic melts which originate by partial melting of the granites.

2.4.3.2 Sout Granite

The Sout Granite is medium- to coarse-grained, leucocratic and typically void of dark minerals. The K-feldspar typically displays a reddish alteration (Figure 2.40). Very coarse-grained varieties are also found. It commonly weathers to a woolsack weathering pattern.

Figure 2.40: Reddish alteration of K-feldspar in coarse-grained Sout Granite at a locality south of Kamgab. Location: 18.0154°E; -28.8657°S.

3. PETROGRAPHY

3.1 ORANGE RIVER GROUP

Within the Orange River Group, the matrix of aphanitic lavas are sometimes too fine-grained to recognize individual minerals under the microscope. Commonly however, even though fine-grained, the matrices of the Orange River Group volcanics lend itself to microscopic investigation. The porphyrytic lavas mostly contain both quartz and feldspar phenocrysts. The latter phenocrysts are typically euhedral to subhedral and the degree of alteration varies from entirely altered to unaltered (e.g., Figure 3.1). Alteration of the feldspars may be related to metamorphism during the Orange River Orogeny or to the presence of fluids during the late stages of crystallization of the volcanics. Sericite, soussurite and epidote are common alteration products leading to the formation of a cloudy mass within the crystals.

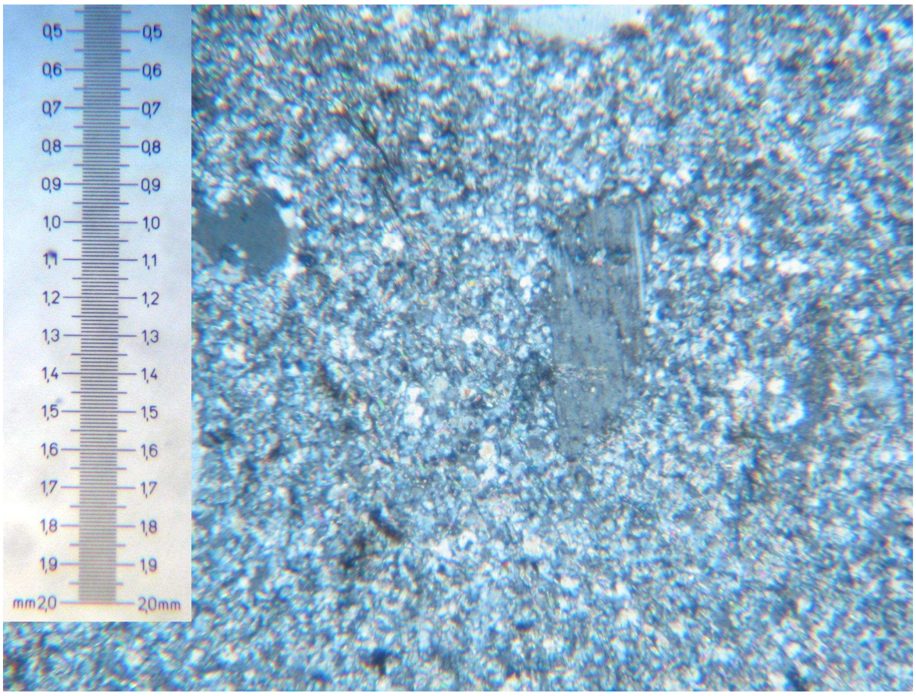

Figure 3.1: Thin section of leucocratic porphyrytic lava of the Tsams Formation showing a fine-grained matrix and euhedral, relatively unaltered plagioclase phenocrysts. location of sample: 17.6632°E; 28.8044°S.

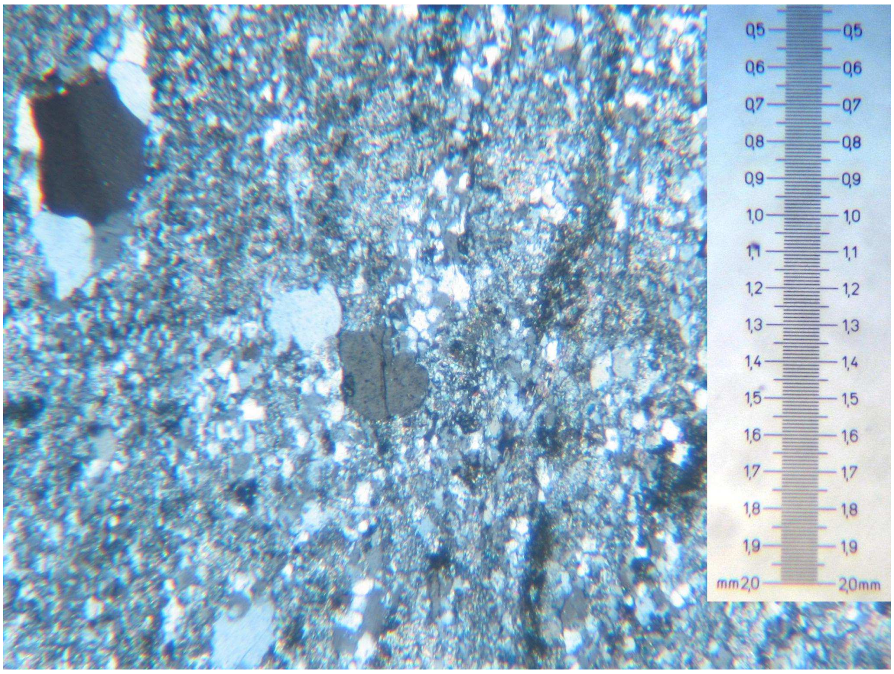

Figure 3.2: Thin section of quartz-feldspar porphyry of the Kook River Formation showing porphyroblasts comprising quartz aggregate (flattened along the foliation) and unaltered, subhedral feldspar. Location of sample: 17.1771°E; 28.1833°S.

The quartz porphyroblasts are rounded to subhedral. They may also be comprised of aggregates and may be flattened along the foliation, as is commonly seen in the Paradys River Formation, which was greatly affected by Pan African deformation (Figure 3.2). Tuffs throughout the Orange River Group contain fragments of very fine-grained lava and chert.

The dark mineral constituents in the Orange River Group include hornblende, biotite, chlorite, epidote and opaque minerals and muscovite occurs as an additional phase. Sphene occurs in accessory amounts. The proportion of dark minerals in the rock varies depending on the composition. The basaltic andesites of the Nous Formation are dominated by plagioclase in which the alteration varies between completely altered to unaltered. Hornblende, biotite and epidote are the predominating dark minerals. Epidote occur mostly as alteration products but may also represent primary crystals. Andesites throughout the Orange River Group also contain hornblende but to a lesser extent than in the Nous basaltic andesites. Muscovite becomes a significant phase in the andesites. The dark mineral contents is low in the dacites. Hornblende is still present as a minor phase. Rhyolites do not contain hornblende while muscovite is a common phase. Hornblende, biotite and muscovite may occur either as primary phases or alteration products, while chlorite and epidote are alteration products throughout.

Regarding the metamorphic grade, the greenschist-facies conditions inferred for the Orange River Group and Vuurdood Subsuite in various previous studies (e.g., Beukes, 1973; Blignault, 1977; Reid, 1977) is confirmed by the mineral assemblages studied. The green amphibole actinolite is a common constituent especially in the Vuurdood Subsuite and both hornblende and biotite display well-defined pleochroism. The rocks of the Haib Subgroup are commonly altered to schist in areas of high strain deformation. In thin section, the foliation in these schists is defined by dark minerals orientated in a parallel array and varying in proportion in accordance with the composition. Hornblende often occurs as large, secondary crystals overgrowing the primary phases. A speckled appearance in hand-specimen may be caused either by dark mineral aggregates or large, poikilitic hornblende or biotite flakes. In the De Hoop Subgroup, foliation related to the Pan African orogeny is pervasively present and imparts a schistose texture in the rocks. Mainly the Paradys River Formation has been subjected to intense strain.

Two generations of feldspar are present. One generation comprises unaltered crystals while the other comprises cloudy, altered crystals. The degree of alteration within the latter generation varies among individual crystals (e.g., Figure 3.3). This is mainly true for the Windvlakte and Abiekwa River Formations, both of which were intensely subjected to recrystallization, as seen in the field. As such, alteration of the first feldspar generation in these rocks could possibly be related to metamorphism during which fluids were liberated.

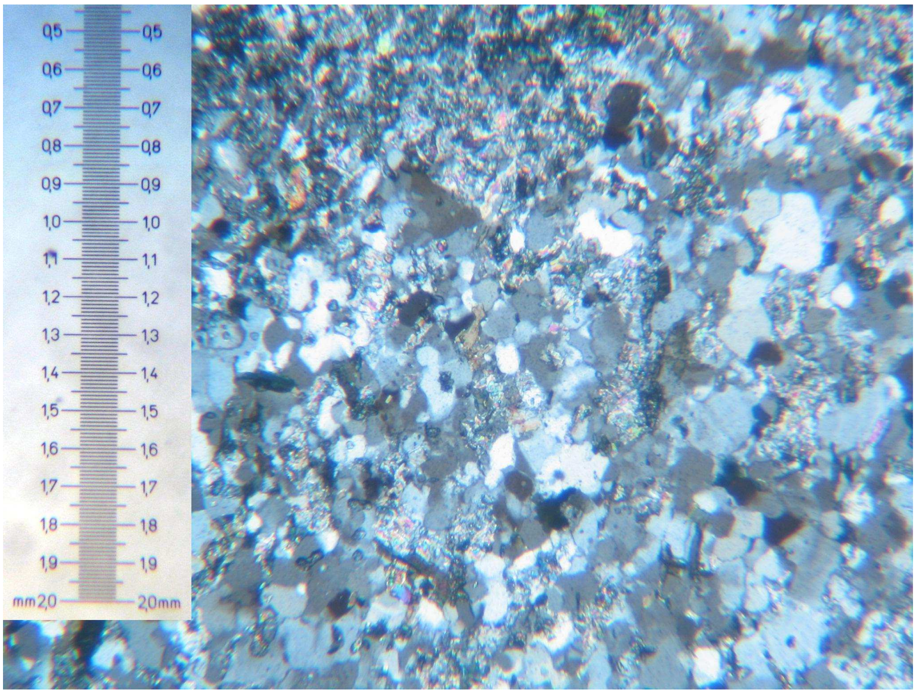

Figure 3.3: Thin section of dacite from the Windvlakte Formation. Two generations of feldspar can be distinguished namely an altered and unaltered phase. Location of sample: 17.3549°E; 28.9432°S.

3.2 VIOOLSDRIF SUITE

3.2.1 Vuurdood Subsuite

In the Vuurdood Subsuite, only remnants of the original minerals can be recognized in the altered phases. In some cases, the rock may still be unaltered (e.g., Figure 3.4). The gabbros comprise plagioclase, orthopyroxene, clinopyroxene, olivine and hornblende. Biotite, muscovite, chlorite, epidote, zoisite, and opaque minerals occur in varying amounts. Actinolite is a common alteration product while K-feldspar, quartz, apatite and allanite represent accessory phases. The peridotites and pyroxenites are commonly highly altered to serpentinite. Orthopyroxene (hypersthene), olivine, phlogopite and opaque minerals comprise the other constituents in addition to serpentine. The amphibolites consist of actinolite, hornblende and subordinate epidote. Limited occurrences of troctolite at Swartberg comprise olivine and plagioclase as major components and clinopyroxene and hornblende as subordinate constituents.

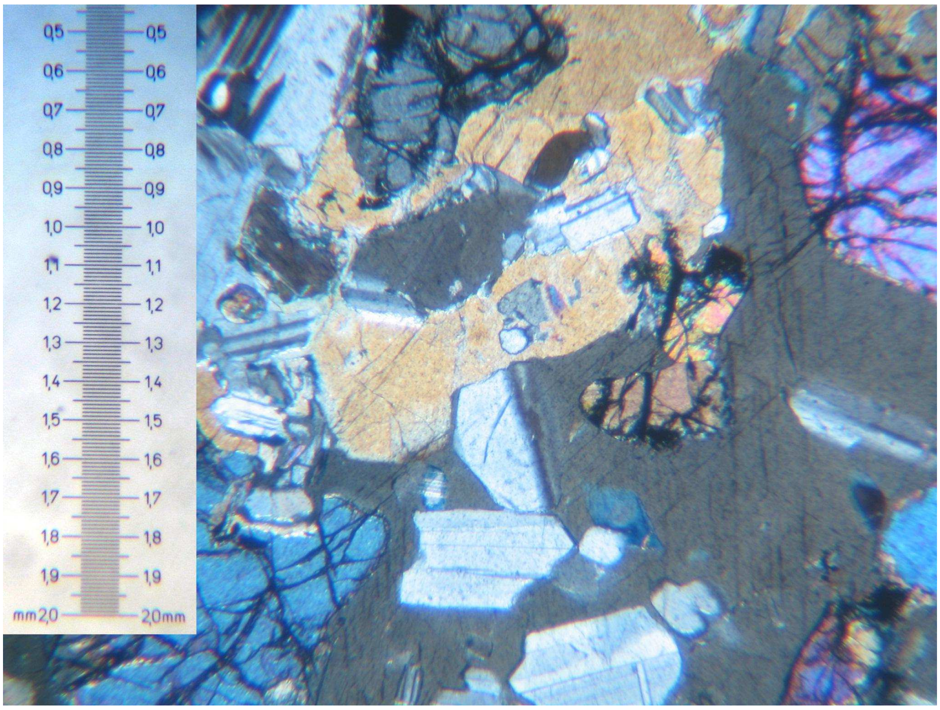

Figure 3.4: Thin section of olivine gabbro from the Vuurdood Subsuite showing relatively unaltered mineralogy comprising plagioclase, hornblende, clinopyroxene and olivine. Location of sample: 18.1197°E; 28.9086°S.

In the Vuurdood Subsuite as a whole, green amphibole constitutes the major phase – an estimated 41%. It is difficult to determine how much of this amphibole is primary. REE patterns with positive Eu anomalies in some samples of the Vuurdood Subsuite (Figure 4.12), suggest that a substantial amount may be primary, since positive Eu anomalies are commonly thought to indicate large-scale amphibole fractionation or amphibole retention in the source (Rollinson, 1993). However, the alteration process from pyroxene to amphibole is very commonly observed (almost throughout), suggesting that a large proportion of the amphibole represents alteration products from pyroxene. The alteration is thought to be related to greenschist facies metamorphic conditions. This is based on the fact that the Vuurdood Subsuite and Orange River Group are of similar age and as such, probably underwent the same deformational and metamorphic processes. Greenschist facies metamorphism is common in the Orange River Group.

3.2.2 Goodhouse Subsuite

In the Goodhouse Subsuite, alteration of the feldspars varies between completely altered and unaltered. In partly altered crystals, alteration may be concentrated along the rim or in the centre. Epidote and sericite are common alteration products of the feldspars. Epidote alteration may be associated with a cloudy mass or may occur as single flakes which are distributed randomly throughout the feldspar crystal. In situations where the plagioclase composition could be estimated by the Michél-Levy method (using the extinction angle), an andesine composition prevailed. One occurrence revealed an oligoclase composition (Hoogoor Granite).

The dark mineral contents in the Goodhouse Subsuite resembles that of the Orange River Group. Biotite is found both as alteration product of amphibole and as a primary phase. Amphibole often occurs as a primary and secondary phase. Most commonly, the amphibole crystals will display a poikilitic character (Figure 3.5). Such phases can be identified as secondary in some samples where it is found in contact with the primary phase. The primary phase is altered to biotite and does not show a poikilitic character.

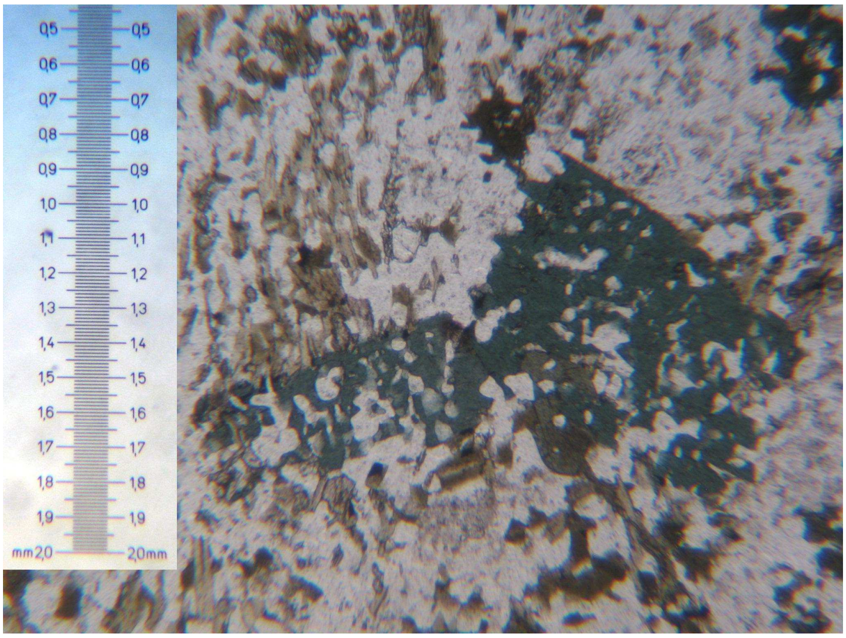

Figure 3.5: Typical poikilitic character of primary hornblende in granitoids of the Khoromus Tonalite. Location of sample: 17.9259°E; 28.9200°S.

Epidote most commonly represents an alteration product of feldspar but also occurs as a primary phase in the form of idiomorphic matrix crystals. It is also often seen to develop in the centre of biotite flakes. Muscovite too, is most commonly associated with alteration but also occur as primary crystals. Chlorite is an alteration product throughout, either of hornblende or biotite. Ortho- and clinopyroxene are limited to the mafic endmembers in which they occur in accessory amounts.

Estimated modal persentages in the Goodhouse Subsuite are as follow (number of samples studied in brackets):

Unit	Qtz	Fsp	Bt	Hbl	Ep	Chl	Ttn	Op	Ms	Cpx	Opx	Act
Khoromus Tonalite (61)	33	38	13	3	7	2	2	2	acc	acc	acc	
Xaminxaip River Granodiorite (21)	34	49	5		5	3	acc	1	2			
Gaarseep Granodiorite (106)	29	39	12	5	8	1	2	1	2		acc	
Hoogoor Granite (28)	37	38	11	4	3	1	2	2	acc			2

In the Khoromus Tonalite, contacts between so-called “filament” and “globular” areas as identified in the field (see Figure 2.28), are well defined in thin section (Figure 3.6). The “filament area” is represented by a relatively coarse felsic matrix, the feldspar being generally unaltered and the dark mineral content low. The “globular area” is represented by a mafic matrix, rich in dark minerals and highly altered feldspar. These textures may be interpreted as possible products of magma mixing processes (Perugini *et al*., 2002). They may however, also represent products of partial melting during migmatite-forming processes.

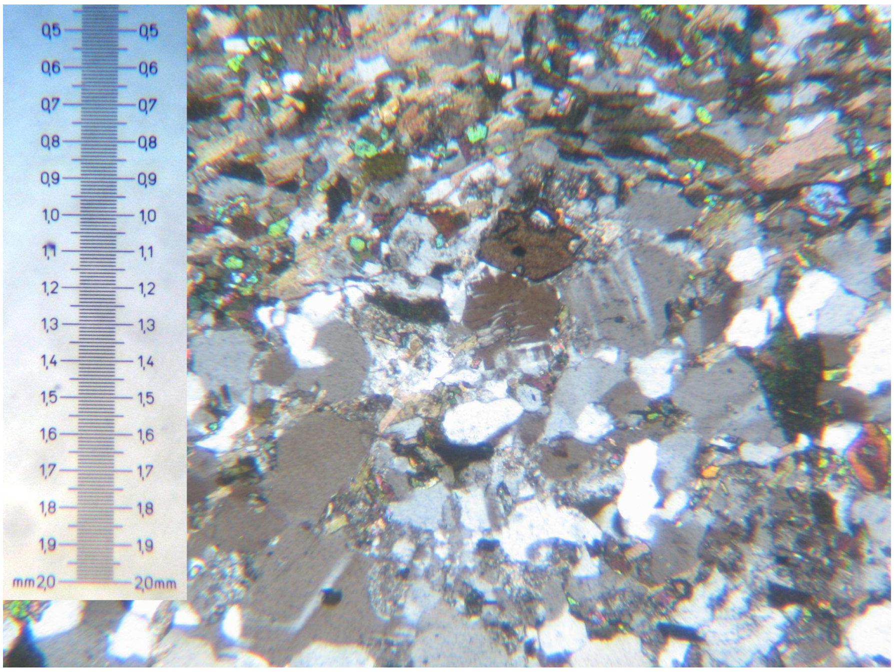

Figure 3.6: Thin section of granite from the Khoromus Tonalite showing a well-defined contact between a mafic (top of photo) and a felsic matrix (the contact transects the scale bar at approximately 1.35 mm). These two matrices may be interpreted as “globular” and “filament” areas respectively in terms of magma mixing models (Perugini *et al*., 2002). Location of sample: 17.9260°E; 28.9187°S.

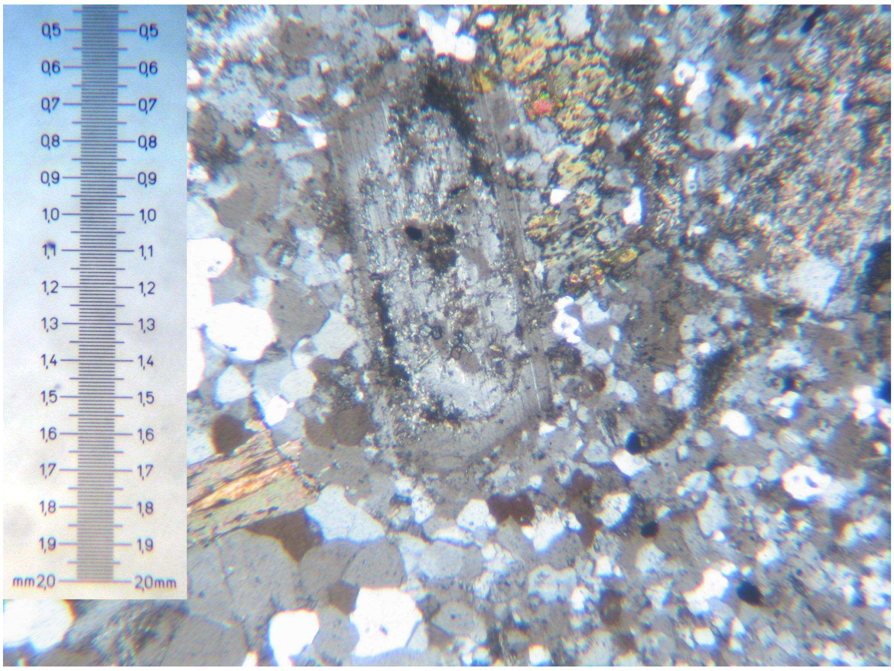

Figure 3.7: Thin section showing a normally zoned plagioclase crystal in granite from the Khoromus Tonalite. Location of sample: 17.9260°E; 28.9187°S.

Another observation speaking in favour of magma mixing processes in the Khoromus Tonalite, is the frequent occurrence of zoned feldspar crystals (Figure 3.7).

This zonation is found to be both normal and reversed. Although less common, zoned hornblende crystals can also be found in the Khoromus Tonalite. Zoned crystals may also be explained in terms of normal fractional crystallization processes during which they were in disequilibrium with the melt when they crystallized. However, zoned crystals were not noted for any of the other units. The Gaarseep Granodiorite, with which the Khoromus Tonalite is closely associated, lacks any evidence of magma mixing processes, both in the field and in thin section. More detailed studies are needed to confirm a magma mixing model for the Khoromus Tonalite.

In the coarse-grained granitoids of the Gaarseep Granodiorite, coarse, unaltered microcline crystals often contain inclusions of older phases such as altered feldspar, quartz and dark minerals (Figure 3.8).

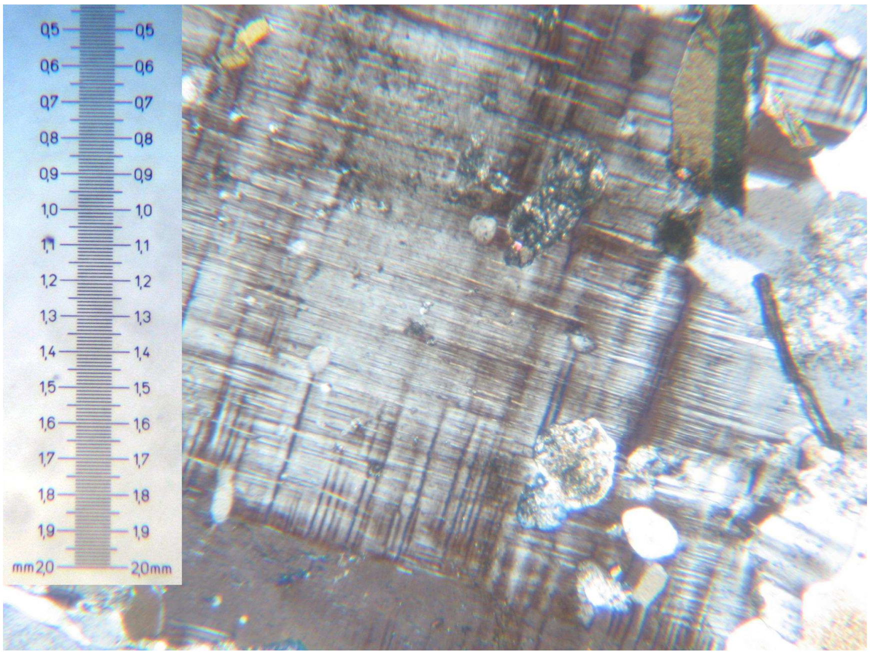

Figure 3.8: Thin section of Gaarseep Granodiorite showing inclusions of well rounded, pervasively altered feldspar and quartz within an euhedral and relatively unaltered microcline phenocryst. Location of sample: 17.0152°E; 29.0294°S.

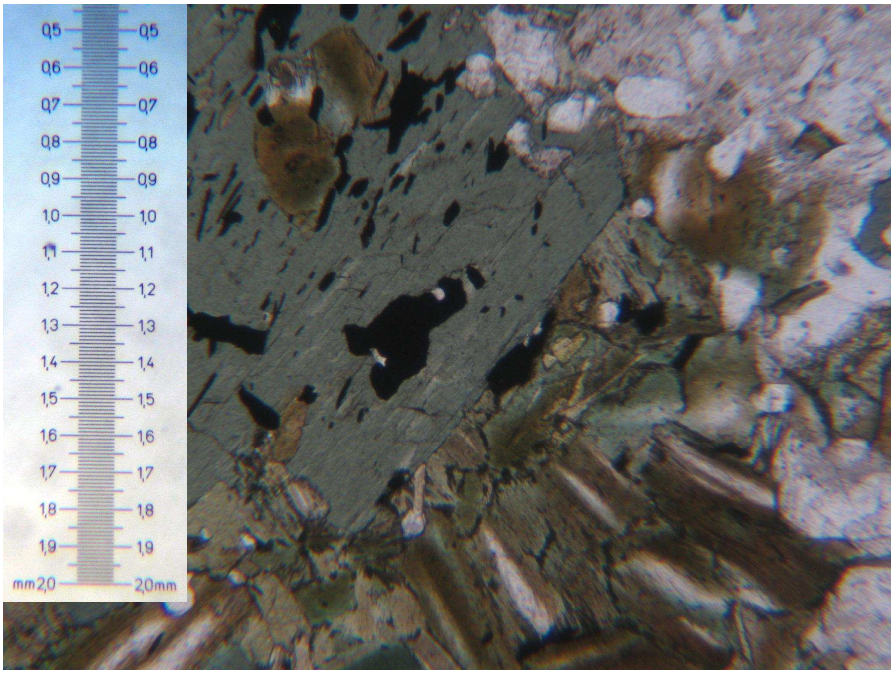

Figure 3.9: Thin section showing euhedral, unaltered secondary hornblende containing inclusions of opaque minerals and altered primary dark minerals, overgrowing the primary, altered mineralogy in the Gaarseep Granodiorite. Location of sample: 17.9664°E; 28.9919°S.

The altered feldspar generation may occur interstitially in the form of pods, veins and stringers, or disseminated within a matrix of unaltered feldspar and quartz. In areas affected by the Namaqua deformation, hornblende and biotite often also occur as two generations, the second being due to metamorphic effects. These second generation crystals are occasionally seen in contact with the older altered phases and may contain inclusions of them, attesting to their secondary nature (Figure 3.9). Both the hornblende and biotite are orientated in a preferred orientation, imparting a foliation on the rock.

The Hoogoor Granite is entirely overprinted by Namaqua foliation. The typical Hoogoor Granite has a common granitic composition with coarse alkali feldspar and a low dark mineral content. Microcline dominates the alkali feldspar compositions but orthoclase also occur. Plagioclase also forms part of the unaltered matrix. Hornblende and biotite represent the dark mineral constituents and are mostly idiomorphic, unaltered and strongly pleochroic.

The degree of metamorphism of the minerals in the Hoogoor Granite increases from west to east. In the western parts around Goodhouse, original amphibole-rich rocks may be altered to actinolite-epidote gneiss, after greenschist-facies metamorphism. The feldspars are extremely altered and the original characteristics can be recognized only in rare cases. Hornblende is associated with alteration and flattened along the foliation (Figure 3.10). In places, the rock is porphyroblastic with the porphyroblasts consisting of quartz aggregates which also encloses certain altered feldspar masses. Further to the east, altered feldspars are rarely observed and the rock is dominated by coarse, unaltered and undeformed alkali feldspar, Here, altered feldspar phases occur only as small, rounded inclusions in the coarse and porphyrytic, unaltered alkali feldspars, or as interstitial stringers.

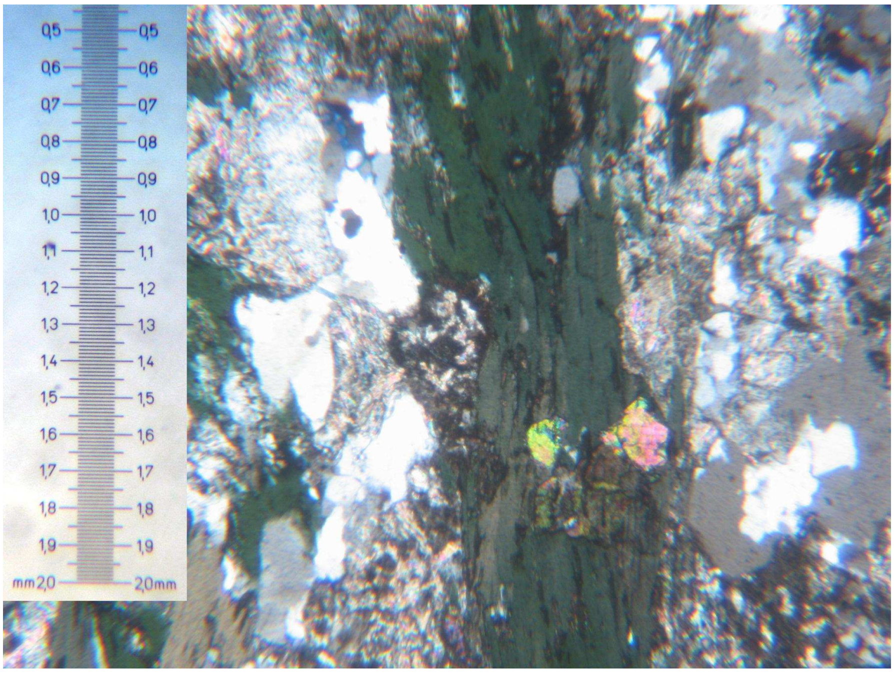

Figure 3.10: Thin section of foliated Hoogoor Granite displaying pervasively altered feldspar, quartz, green amphibole altered to epidote in places and biotite, from the western part of the unit. Location of sample: 18.3817°E; 28.9235°S.

3.3.3 RAMANSDRIF SUBSUITE

In the Ramansdrif Subsuite, estimated modal compositions are as follow:

a) Ghaams Granite: (24 samples studied) quartz - 43%, feldspar - 38%, muscovite - 9%, biotite - 5%, chlorite - 1%, epidote - 1%, opaque minerals - 1%. The muscovite contents is exceptionally high in the southern fringe areas of the batholith where the rocks are affected by the Namaqua foliation. Also in these southern fringe areas, the gneiss occasionally contain leucosome nodules with garnet developed in their cores.

b) Sout Granite: (12 samples studied) quartz - 50%, alkali feldspar - 39%, plagioclase - 5%, muscovite - 2%, biotite - 1%, chlorite - 1%, opaque minerals - 2%.

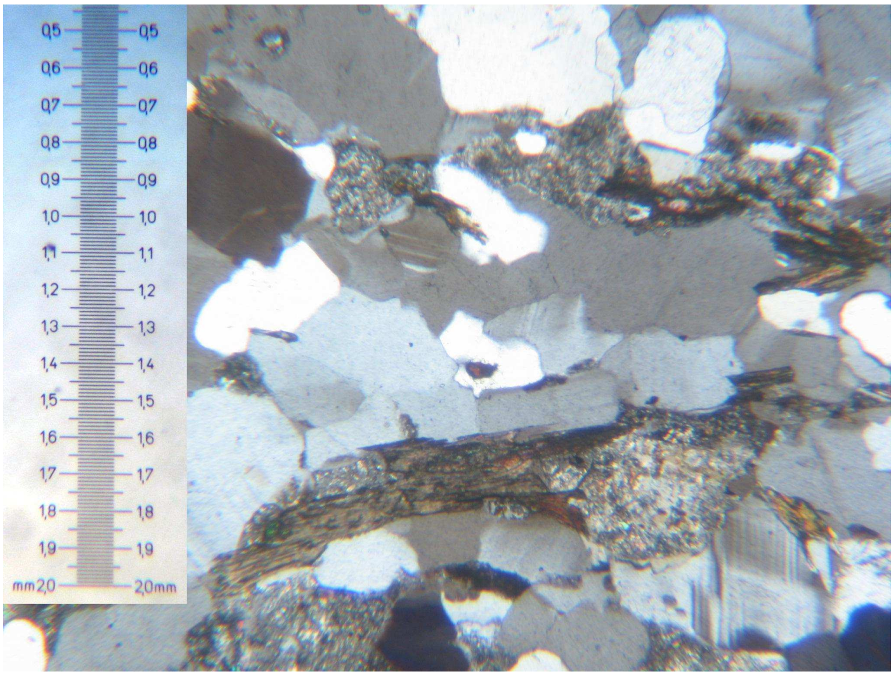

Figure 3.11: Thin section of Ghaams Granite with a foliation caused by the linear distribution of flattened pervasively altered feldspar and biotite occurring interstitially among undeformed and unaltered feldspar and quartz. Location of sample: 17.9573°E; 28.9947°S.

Muscovite is a common constituent in the Ramansdrif Subsuite, mostly associated with sericite as alteration products of the feldspars. However, secondary muscovite also occur as unaltered, idiomorphic flakes. The Ghaams Granite is confined to the areas affected by the Namaqua foliation and here, idiomorphic second generation biotite flakes typically display strong pleochroism varying between light-brown and dark-green. The foliation in the Ghaams Granite in these areas is imparted by orientated biotite and/or muscovite. It may also be the result of pervasively altered feldspar and biotite being aligned and flattened in parallel layers, occurring interstitially among the unaltered second phase (Figure 3.11). Based on petrographic correlations, all the occurrences of the Ramansdrif Subsuite which are located within the Hoogoor Granite, correlate with the Ghaams Granite.

In the Sout Granite, the feldspars are predominantly coarse- to very coarse-grained, unaltered and void of inclusions. Where limited alteration do occur, sericite is almost exclusively the alteration product. A finer-grained matrix is typically developed interstitially among the coarse phenocrysts. This interstitial matrix occur in the form of pods and veins. As in the case of the phenocrysts, the interstitial feldspars do not show any appreciable alteration or deformation (e.g., Figure 3.12). It is interpreted to represent the late stages in a normal crystallization history.

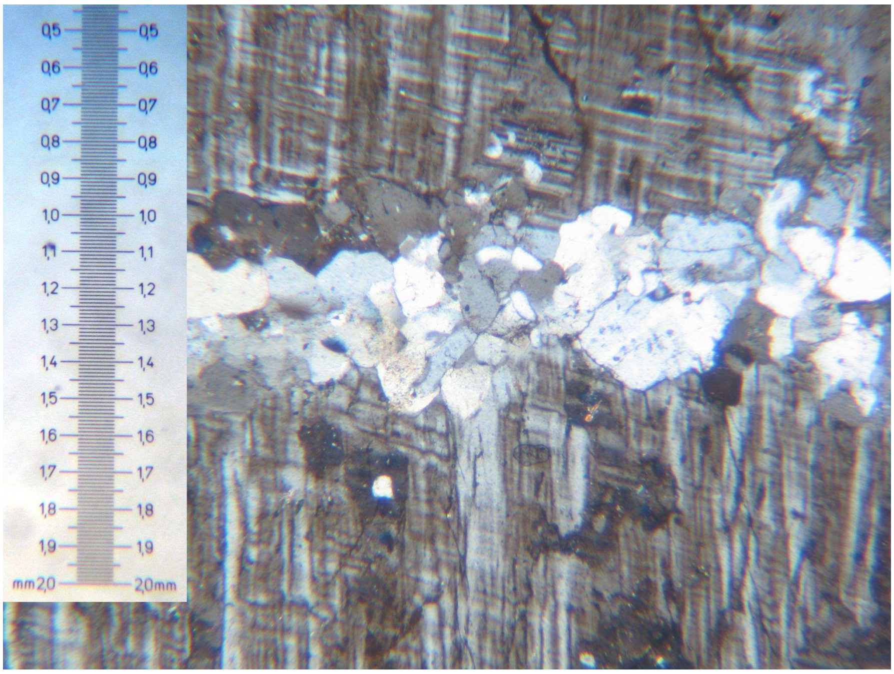

Figure 3.12: Thin section of Sout Granite showing two alkali feldspar phenocrysts with interstitial fine-grained matrix occurring in the form of a vein. location of sample: 17.8901°E; 28.8774°S.

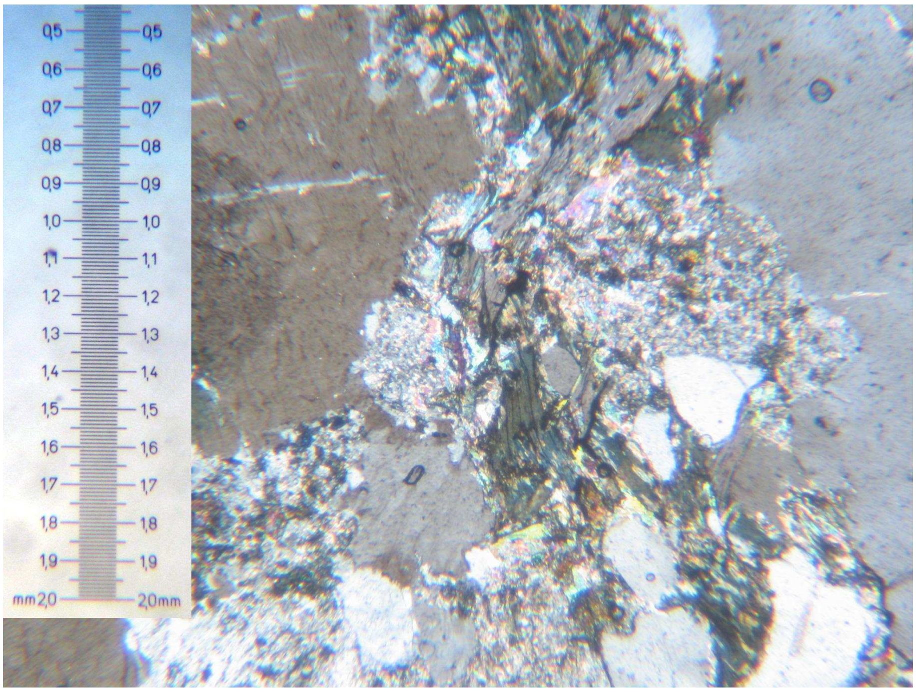

Figure 3.13: Thin section showing first phase altered feldspar and dark minerals being deformed along the margins of a second phase feldspar in granodiorite of the Xaminxaip River unit. Location of sample: 17.4437°E; 28.7747°S.

Two generations of coarse feldspar may therefore be recognized in the Vioolsdrif Batholith namely phenocrysts (magmatic in origin) and porphyroblasts (metamorphic in origin). In porphyrytic samples of the Sout Granite, interstitial feldspars are nowhere found to be deformed along the rims of the phenocrysts, attesting to a magmatic origin (Figure 3.12). Evidence attesting to feldspar blasthesis is found where the interstitial matrix is seen to be deformed along the rims of feldspar porphyroblasts, e.g. as in Figure 3.13. In such cases, minerals in the deformed matrix may sometimes be seen to be broken or cracked.

Exsolution textures are very rarely observed and only on small scale, in feldspars of the Goodhouse Subsuite as well as the Ghaams Granite, (e.g., Figure 3.14).

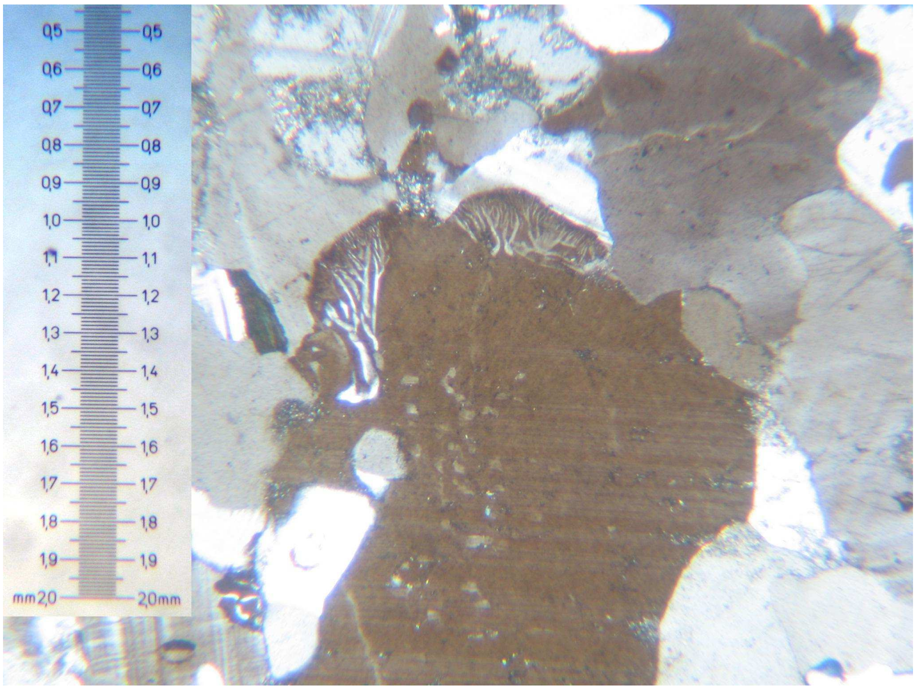

Figure 3.14: Thin section showing rare myrmekite developed along the edge of a quartz crystal in Hoogoor Granite. Location of sample: 18.5467°E; 28.8793°S.

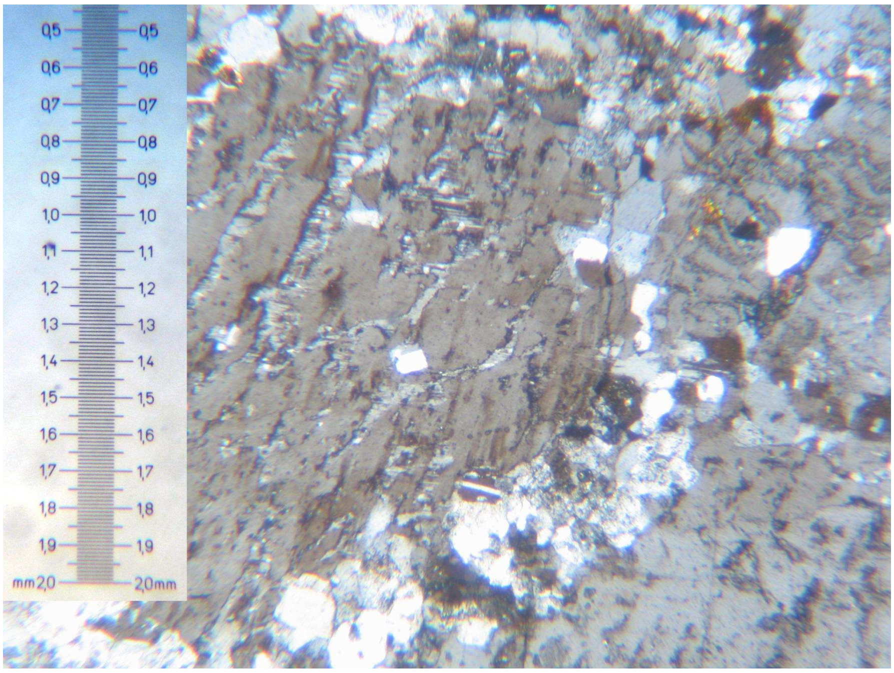

Figure 3.15: Thin section showing perthite which is commonly developed in the Sout Granite in its type area south of Nous. Location of sample: 17.8785°E; 28.8703°S.

However, these textures are very common in the feldspar of the Sout Granite. In the Sout Granite type area around Nous, as well as in the Richtersveld National Park to the east of Sendelingsdrif, perthite represents the prevailing exsolution type (Figure 3.15). In the occurrences in the Haib area to the east of Kamgab, exsolution is less well developed, appearing only in the larger phenocrysts. The phenocrysts at this locality are notably unaltered.

4. GEOCHEMISTRY

4.1 GEOCHEMICAL VARIATIONS

A number of classification and variation diagrams will be presented here for the Vioolsdrif Batholith with two aims in mind:

a) To geochemically compare the various units in the batholith with each other.
b) To identify the tectonic environment and associated magmatic processes.

Some of the evidence presented here have already been presented in previous studies. However, a repeat of such evidence is justified in the light of significant additional data as well as some advances in classification systems since the last published previous study. Furthermore, no previous study presented a geochemical comparison of the various units based on the current subdivision.

4.1.1 Classification diagrams

A diversity of classification systems for igneous rocks are in use, reflecting the fact that they may be produced by a variety of processes in a variety of tectonic settings.

The total alkalis-silica (TAS) diagram is one of the most useful variation diagrams and has been shown by Cox *et* al. (1979) to present a sound theoretical basis for the classification of volcanic rocks. The current version of the diagram was constructed by Le Maitre *et* al. (1989) from a large database of volcanic rocks. Figure 4.1 shows the Orange River Group plotted on this diagram.

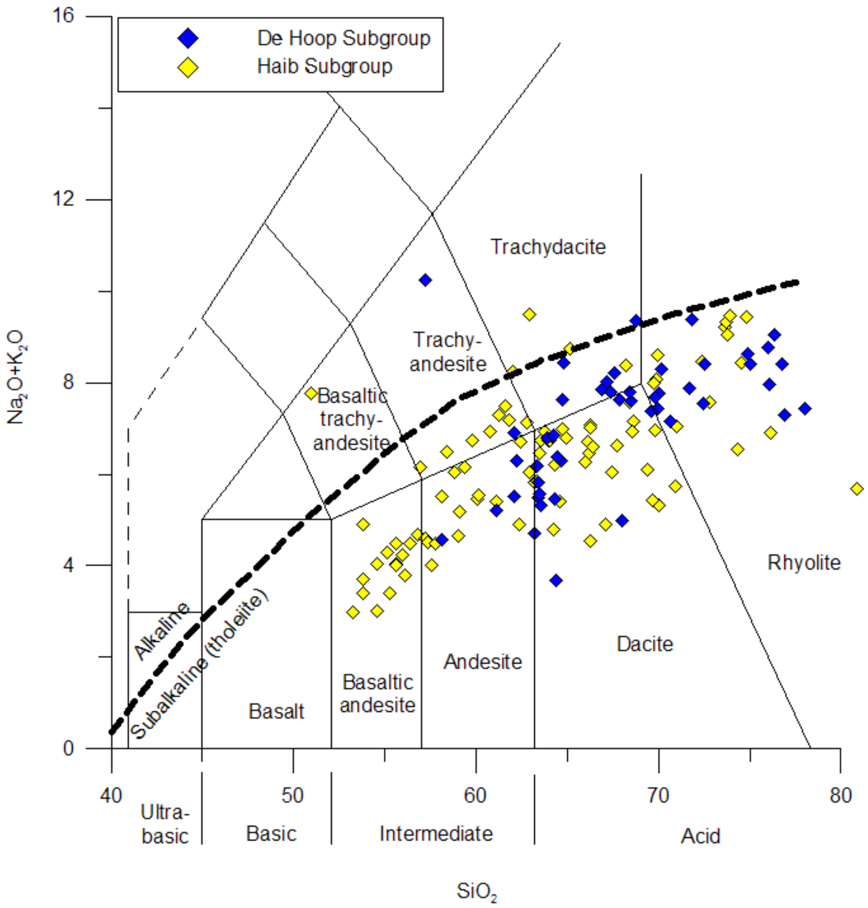

Figure 4.1: The two subgroups of the Orange River Group on the total alkali-silica diagram of Le Maitre *et al* (1989). Alkaline-subalkaline boundary is that of of Irvine and Baragar (1971).

The boundary dividing the alkaline from the subalkaline (tholeiite) series after Irvine and Baragar (1971) is also shown. The Orange River Group represents a well defined subalkaline series. The average composition is granitic with SiO_2>63%. Deviations into high alkali contents may be caused either by primary feldspar phenocrysts or later feldspar blasthesis (as suggested in thin section), which lead to a high feldspar:quartz ratio in the rock. Deviations into low-alkali areas may be caused by alkali depletion during metamorphism. A distinction can be observed between the Haib and De Hoop Subgroups in that the latter subgroup has no equivalent compositions to the basaltic andesites of the former.

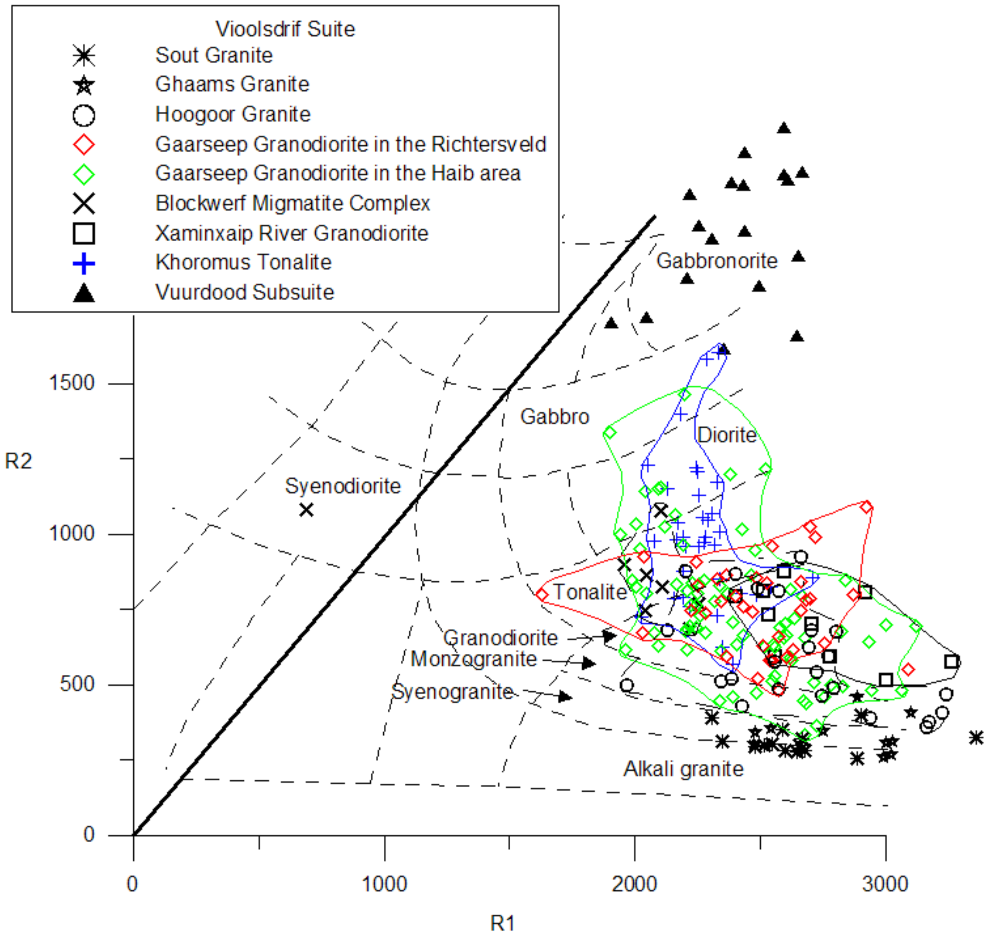

Figure 4.2: The Vioolsdrif Suite on the classification diagram of De la Roche *et al*. (1980). R1 = [4Si – 11(Na + K) – 2(Fe + Ti)]; R2 = Al + 2Mg + 6Ca.

The R1-R2 classification diagram of De la Roche *et al*. (1980) is used here (Figure 4.2) to distinguish between the individual units within the Vioolsdrif Suite. The names of these units are based on their average compositions. Although the diagram has the disadvantage that the data range plots in a small area of the diagram, it incorporates the more commonly used granite nomenclature. Furthermore, it takes into account all the more abundant major elements and depicts the variation of SiO_2 as well as the changes in Fe/(Fe+Mg) ratio and plagioclase composition.

The Khoromus Tonalite and Gaarseep Granodiorite have endmembers sharing the gabbro field with the Vuurdood Subsuite, thus coinciding with the basaltic andesites of the Haib

Subgroup. In the Gaarseep Granodiorite, these mafic endmembers are all from the Haib area.

The sample from the Blockwerf Migmatite which plots in the syenodiorite field is porphyrytic and seen in thin section to be highly altered. This suggests that its anomalous plot is the result of alkali loss during metamorphism. The Xaminxaip River Granodiorite may be distinguished on the diagram based on its limited compositional variation within the granodiorite field. Although the Khoromus Tonalite and Gaarseep Granodiorite largely overlap, the two units can be distinguished on their average compositions. The Gaarseep Granodiorite also extends across the entire compositional range defined by the two units, while the Khoromus Tonalite does not extend into the granite field. The Gaarseep Granodiorite in the Richtersveld area may be distinguished from that in the Haib area based on the fact that it shows a distinctly narrower and more felsic range, being almost limited to the granodiorite field. The Hoogoor Granite can be distinguished from the Gaarseep Granodiorite being more limited in composition, as well as more felsic.

Although the Ramansdrif Subsuite overlaps with the felsic endmembers of both the Gaarseep and Hoogoor units, it does define a distinct average composition. The Ghaams and Sout Granites both occupy the range monzogranite-syenogranite-alkali granite. However, the Ghaams Granite average composition is shifted to the right along the R1 axis, compared to the Sout Granite. This can be attributed to the higher dark mineral contents of the Ghaams Granite (see 3. Petrography), leading to elevated Fe and Ti contents.

Norm calculations have been executed on all the available samples from the Vioolsdrif Batholith. In Figure 4.3, the Vioolsdrif Suite and Orange River Group are plotted on the classification diagrams of Streckeisen (1976) for plutonic and volcanic rocks. This classification scheme is currently the most widely used for igneous rocks. The calcalkaline trend is clearly defined for both assemblages.

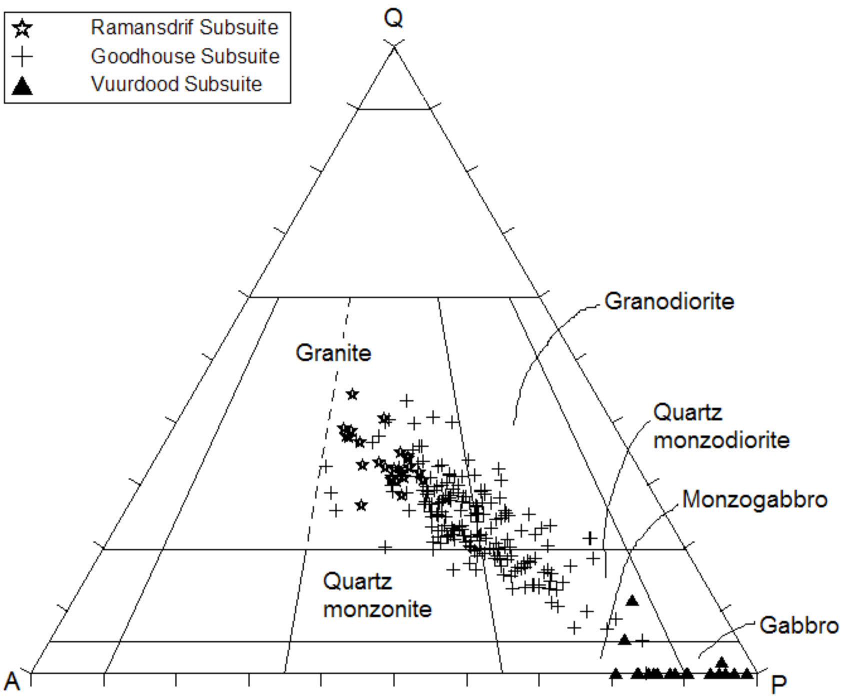

Figure 4.3(a): The Vioolsdrif Suite (after norm calculations) plotted on the classification diagram of Streckeisen (1976) for plutonic rocks.

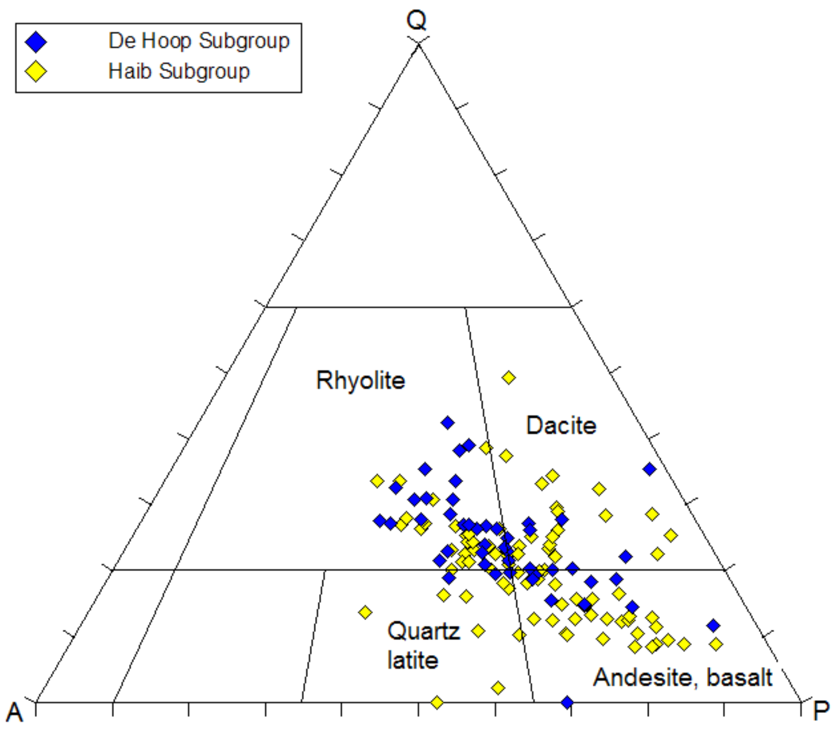

Figure 4.3(b): The Orange River Group (after norm calculations) plotted on the classification diagram of Streckeisen (1976) for volcanic rocks.

4.1.2 Harker diagrams

Figure 4.4 shows Harker diagrams for selected elements in the Vioolsdrif Batholith. For the La/Yb ratio, chondrite normalized values after Boynton (1984) are used.

On Harker diagrams, the trend of an igneous rock suite will typically follow what Bowen (1928) defined as the "liquid line of descent", which can be directly related to the fractional crystallization process. However, other magmatic processes, specifically partial melting, will produce the same trend. Numerous studies show that only rarely will a suite of volcanic rocks, showing a progressive chemical change, erupt as a time sequence (Rollinson, 1993). This is also true for the Orange River Group in which the oldest volcanics have felsic compositions (the Tsams Formation; Reid, 1977). Therefore, Harker diagrams do not go a long way in distinguishing magmatic processes. They are however, useful in comparing geochemical variations among the various units within the same igneous suite. They are also useful in identifying the influence of metamorphism and alteration.

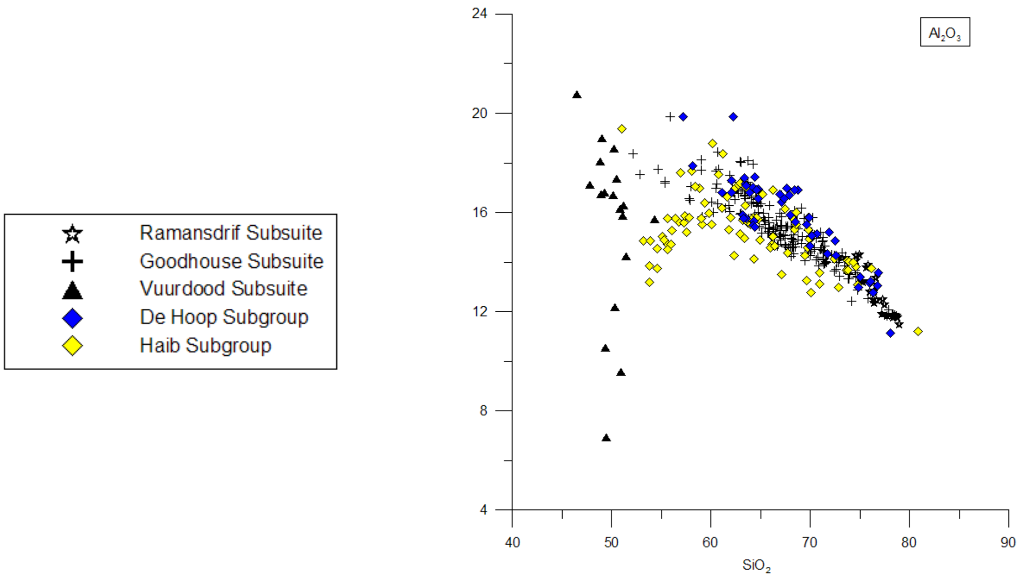

Figure 4.4: Harker diagrams for selected elements in the Vioolsdrif Batholith.

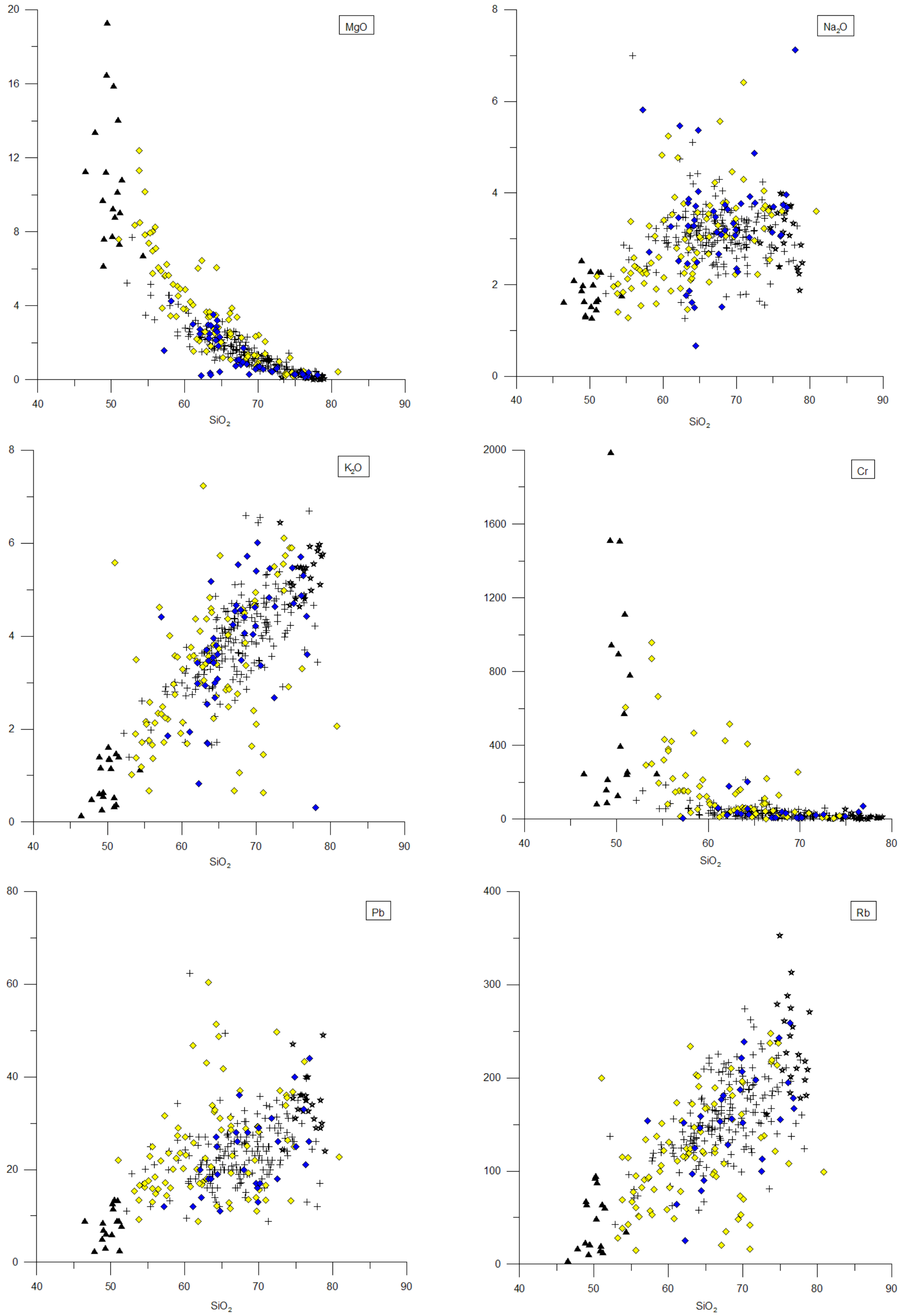

Figure 4.4: (Continue).

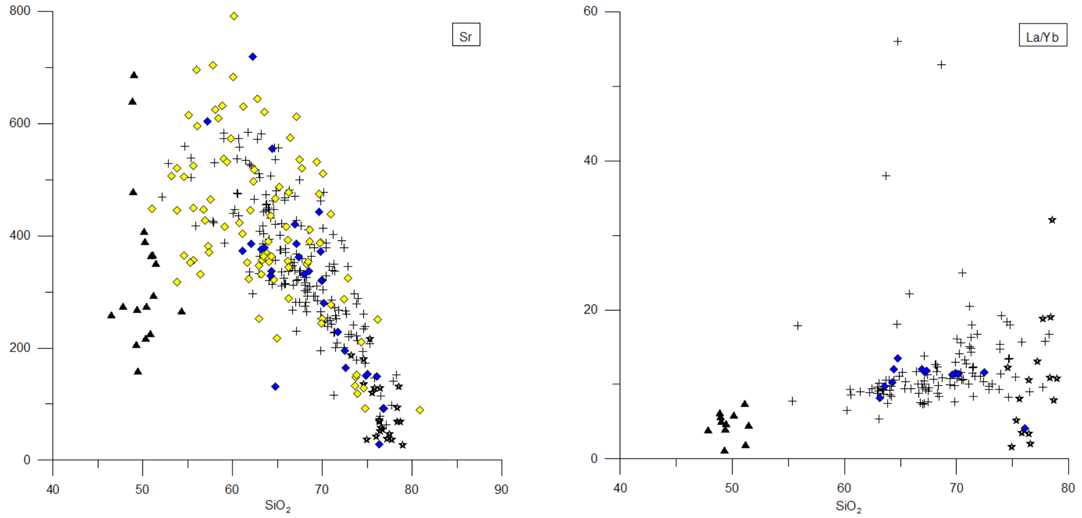

Figure 4.4: (Continue).

Metamorphic alteration in the Hoogoor Granite is to be expected given the pervasive overprint of the Namaqua orogeny. The elements K_2O, Na_2O, Pb and Rb all show a linear increase from mafic to felsic and relatively high values are to be expected in the felsic Hoogoor granites. However, some samples of this unit show significant depletion in these elements. This can be ascribed to element mobility during metamorphism since these elements are classified as incompatible mobile elements (e.g., Rollinson, 1993). The depletion in Rb and Pb specifically, has implications for age determinations by the Rb-Sr and U-Th-Pb systems. However, for the purpose of the current study, the deviation of these samples from the average trend is not considered a major factor. When correlation among units is considered, multi-element and REE patterns carry more weight as evidence since an array of elements are used in multi-element diagrams and not single ones, and the REE are notoriously resistant to influence from metamorphism.

Alteration is also evident in the Windvlakte and Abiekwa River Formations of the De Hoop Subgroup, which is in accordance with field and petrological evidence suggesting large-scale recrystallization in these formations. A number of samples from these two formations are depleted in K_2O and Rb, both of which are classified as mobile elements (e.g., Rollinson, 1993). The rest of the De Hoop Subgroup coincide closely with the average trend.

The Vuurdood Subsuite is unique in its mafic-ultramafic composition and represents a clearly defined group at the mafic end of the trend on all the diagrams. Despite this, it displays a definite association with the rest of the batholith, always falling on the extension of the trend defined by the rest of the batholith. For some elements, the trend defined by the rest of the batholith continues linearly into the Vuurdood Subsuite, e.g., MgO, K_2O, Rb and Pb. For others, (e.g., Al_2O_3, Cr and Sr), the trend defined by the rest of the batholith widens and curves at the mafic end so as to coincide with the field defined by the Vuurdood Subsuite. The Sr diagram displays this especially well.

Within the Goodhouse Subsuite (in all of the diagrams in Figure 4.4), there is a broad overlap between the Khoromus Tonalite, Gaarseep Granodiorite and Hoogoor Granite. The Gaarseep Granodiorite extends across the entire field occupied by these three units while the Khoromus Tonalite is concentrated at the mafic end and the Hoogoor Granite at the felsic end. The latter two units do not overlap. The Xaminxaip River Granodiorite is distinguished by its limited variation, which coincides with equivalent compositions in the Gaarseep Granodiorite. (Although the Xaminxaip River Granodiorite samples are few, they do represent the entire compositional range within the unit, based on field evidence.) The Blockwerf Migmatite is distinguished on the Harker diagram (Figure 4.4) for the La/Yb ratio, on which it shows values above the average trend. This elevated La/Yb ratios is the single most characteristic geochemical feature of this unit.

The Ramansdrif Subsuite coincides with the felsic members of the Goodhouse Subsuite in Figure 4.4 (in all the elements) and trends within the two subsuites are similar for individual elements. Within the Ramansdrif Subsuite, the Ghaams Granite is on average slightly less felsic than the Sout granite.

The Harker diagram (Figure 4.4) for the La/Yb ratio highlights three distinguishing features in the Vioolsdrif Batholith when comparing geochemical variations among the units:

a) It distinguishes the three subsuites of the Vioolsdrif Suite. The Vuurdood Subsuite does not show a linear trend, while the trend for the Ramansdrif Subsuite is steeply positive. In the Goodhouse Subsuite, the trend is flat-lying linear (if the anomalous samples of the Blockwerf Migmatite is ignored) with a moderate positive slope.

b) It shows a good correlation between the Goodhouse Subsuite and the Orange River Group, suggesting that they share similar magmatic processes during their evolution, which are not shared by the Vuurdood and Ramansdrif Subsuites. Note that only the De Hoop Subgroup is represented on this diagram for the Orange River Group, as no REE analyses are available for the Haib Subgroup.

c) It distinguishes the Blockwerf Migmatite in its elevated La/Yb ratios compared to the rest of the batholith.

There is a notable association between the Vuurdood Subsuite and the Haib Subgroup in the elements Al_2O_3 and Cr (also for TiO_2, P_2O_5 and Ni, which are not shown). At the mafic end, the trend for the Haib Subgroup deviates from the main trend defined by the other units, curving into lower values of the Vuurdood Subsuite. This association is not displayed by the De Hoop Subgroup, nor by the Goodhouse Subsuite, both of which continue linearly into the higher values of the Vuurdood Subsuite. On all the other diagrams, the Haib Subgroup also represents, for the most part, the range of values intermediate between the Vuurdood Subsuite and the rest of the batholith, between which there is typically a notable gap. The De Hoop Subgroup displays a striking association with the Goodhouse Subsuite throughout.

The association between the Vuurdood Subsuite and Haib Subgroup as described above, can be shown to be a genetic one, and not influenced by later metamorphic or alteration processes. The fact that both Cr and Ni follow this trend supports a primary origin since both these elements are highly compatible and immobile (e.g., Rollinson, 1993). Furthermore, deviations from the average trend to higher and lower values for the Haib

Subgroup in a wide range of elements (TiO_2, Al_2O_3, CaO, K_2O, MgO, P_2O_5, Cr, Ni, Rb, Sr, V and Zn), are distributed evenly and not concentrated below the average trend. If these deviations were caused by alteration, the majority would fall below the average trend, as is the case for the Hoogoor Granite and the Windvlakte and Abiekwa River Formations.

4.1.3 Eigenvectors and eigenvalues

Le Maitre (1976) used eigenvectors and eigenvalues to study in more detail the geochemical variability within diferent igneous rock types. Eigenvectors represent the comparison of straight lines in a multidimensional space in the direction of maximum variation. Most commonly, the first two or three eigenvalues represent between 80-90% of the chemical variation within a rock and as such, it is possible to construct a two dimensional projection representative of the maximum variation. In Figure 4.5(a), the Vioolsdrif Batholith is plotted along eigenvectors which were calculated for all igneous rocks (Le Maitre, 1976). On this diagram, the three vectors represent 92.1% of the total chemical variation in the rocks. No clear distinction can be made between the units. Since the average composition of the Vioolsdrif Batholith is granodioritic, eigenvectors calculated for this composition may be able to discriminate among the various units. This is shown in Figure 4.5(b) with the accumulatetive eigenvalue representing 90.3% of the chemical variation in the rocks. Again, no distinction can be made among any of the units.

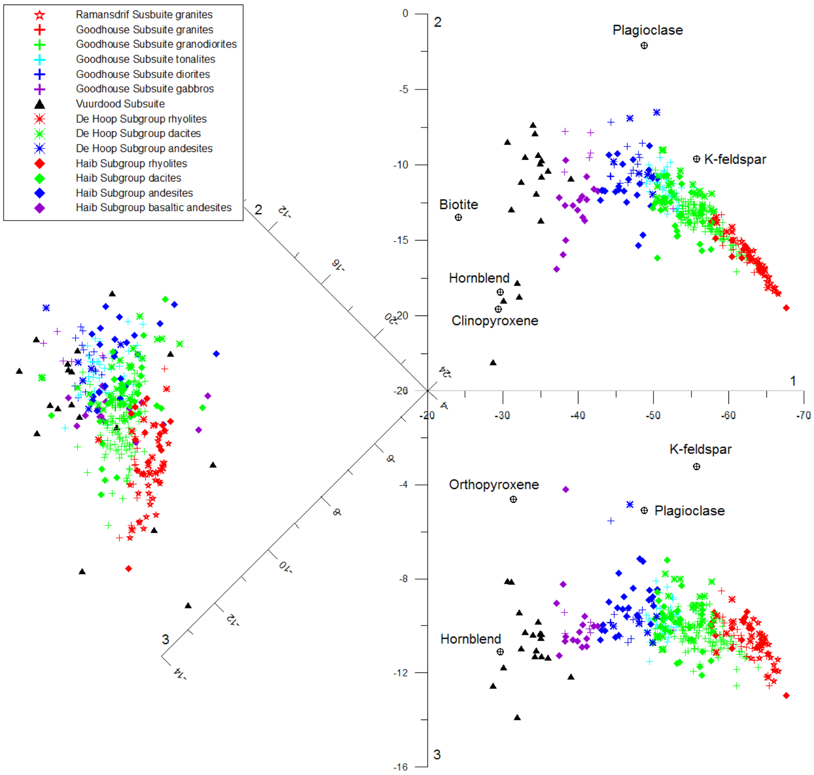

Figure 4.5(a): The Vioolsdrif Batholith plotted along eigenvectors calculated for all igneous rocks (Le Maitre, 1976).

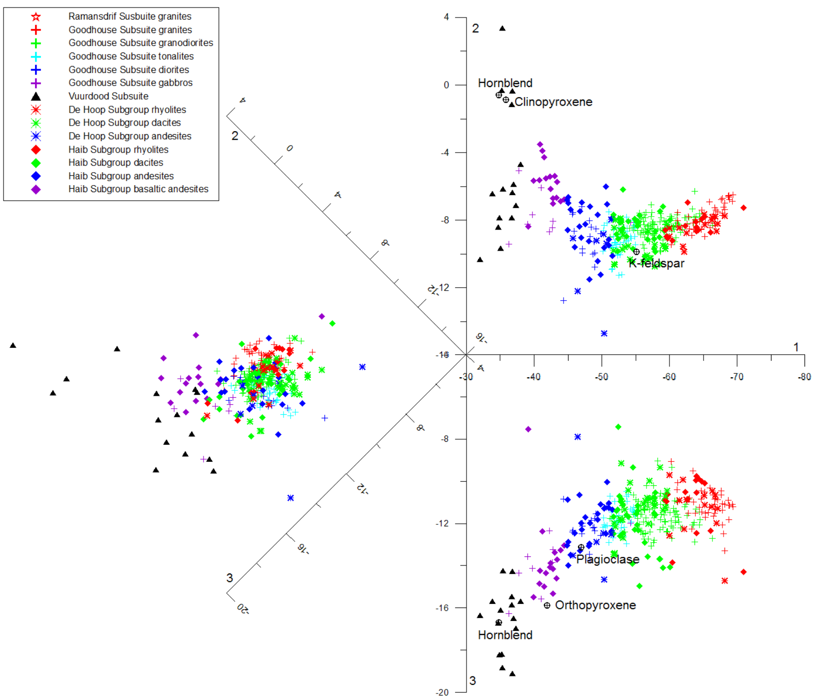

Figure 4.5(b): The Vioolsdrif Batholith plotted along eigenvectors calculated for granodiorites (Le Maitre, 1976).

The fact that the eigen diagrams do not distinguish among the various units of the batholith means that field evidence must be regarded as the most important indicator for subdividing the batholith into its composite units. The reason why the geochemical composition of similar rock types among the various units of the batholith coincide so closely, must be related to primary igneous processes, since variation diagrams (in agreement with field evidence) show that metamorphic mobilization of the elements did not play a very sigificant role. The gradational relationship between the Vuurdood Subsuite and Haib Subgroup as displayed on Harker diagrams is also evident on the eigen diagrams. This indicates that this relationship is indeed the result of chemical properties and is not due to projections.

4.1.4 Multi-element diagrams

Multi-element diagrams compare trace element variations in rocks relative to a standard. Since trace element fractionation is more sensitive than major elements, and since it is primarily controlled by magmatic processes, multi-element diagrams are useful to provide evidence on the nature of these processes, as well as in the correlation among various rock units.

In this study, a chondrite model with normalizing values of Thompson (1982) is used. A selection of incompatible trace elements are arranged from left to right in order of decreasing mobility (LILE to the left, HFSE to the right).

For evidence on the magmatic processes involved in the formation of the Vioolsdrif Batholith, as well as for initial correlation among the main units, multi-element diagrams are constructed for average concentrations of elements in the Orange River Group and the three subsuites of the Vioolsdrif Suite (Figure 4.6).

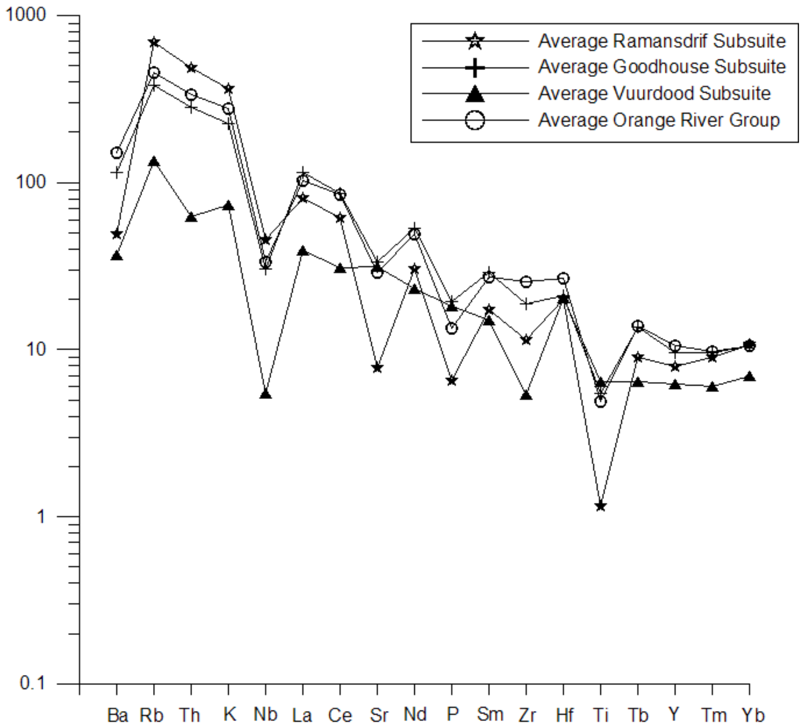

Figure 4.6: Comparison of the multi-element variation patterns for the three subsuites of the Vioolsdrif Suite and the Orange River Group, including REE.

The Vioolsdrif Batholith as a whole displays characteristics which are considered distinct of the subduction zone environment. They include the following:

a) High LILE:HFSE ratios (decoupling of the LILE from the HFSE). This is considered to be the result of metasomatism in the mantle wedge by hydrothermal fluids originating from the dehydration of the subducting basaltic slab which underlies it (e.g., Pearce and Parkinson, 1993; Pearce and Peate, 1995, Dhuime *et al.*, 2007). These fluids also act as a flux which promotes melting in the mantle wedge, leading to the extraction of the LILE to be carried upward and concentrated in the evolving overlying crust. Dry peridotite solidus is too high for melting to take place in the mantle wedge. The high LILE:HFSE ratios of arc magmas show that water plays a significant role in arc magmatism. This subduction of volatile components to provide fluxing materials for the melting of the overlying material, is what distinguishes convergent plate boundaries from all other tectonic settings (Wyllie, 1983).

b) Prominent troughs of especially Nb and Ta but most often also Ti, Zr and Hf. This is a characteristic feature of modern arc volcanics and is often referred to as "the subduction component" (e.g., Condie, 2005b; Castillo, 2006). The mechanism of how it is acquired is still unclear as it implies decoupling of these elements from the LILE and REE. Depletion of Nb and Ta is thought to be caused by the retention of rutile in the source.

The patterns in Figure 4.6 for average values in the Goodhouse Subsuite and Orange River Group correlate very well. Patterns for the Vuurdood and Ramansdrif Subsuites are each unique. Troughs at Zr in the Vuurdood and Ramansdrif Subsuites are not developed in the Goodhouse Subsuite, nor the Orange River Group. The Vuurdood Subsuite is furthermore distinguished by small Sr and P troughs.

For more detailed comparison of trace element variations among the various units of the batholith, individual rock compositions have to be considered. Due to limited ICPMS analyses (specifically insufficient REE data for the Orange River Group), the REE, Hf and Th are omitted from the diagrams that follow. Figure 4.7 shows multi-element diagrams for average trace element concentrations in the various rock types within the various units of the Vioolsdrif Suite. Also shown are the variations in the series from mafic to felsic (gabbro-diorite-tonalite-granodiorite-granite) in the Goodhouse Subsuite.

For the Vuurdood Subsuite, patterns for the ultramafic rocks and gabbronorites are also shown, however, gabbro is the only rock type with equivalent compositions in the rest of the batholith. The patterns of the individual rock types in the Vuurdood Subsuite are variable both in total concentrations and in shape. However, it is important to note that this subsuite, like the other units, displays all the characteristics of the subduction zone environment. This implies that it was formed by the same processes as the other units. The lowest concentrations of both Nb and Zr are found in the Vuurdood Subsuite.

The pattern of gabbro in the Vuurdood Subsuite does not correlate with the gabbros in the Khoromus Tonalite and the Gaarseep Granodiorite. Both the LILE and Nb concentrations increase systematically from the Vuurdood Subsuite to the Khoromus Tonalite to the Gaarseep Granodiorite. The HFSE of the Khoromus Tonalite and Gaarseep Granodiorite are very similar. Since the gabbroic composition is shared by the three units, the increase in LILE concentrations cannot be attributed to fractional crystallization. It may be a function of progressing metasomatism in the mantle wedge. This is in agreement with their relative ages, decreasing from the Vuurdood Subsuite to the Khoromus Tonalite to the Gaarseep Granodiorite. Both Nb and Zr show a sudden large increase between the Vuurdood Subsuite and the two units of the Goodhouse Subsuite. While Nb still displays a trough in the gabbros of the latter subsuite, Zr does not. This implies the fusion of zircon and partial fusion of rutile during the formation of the Goodhouse Subsuite, which was not the case during the formation of the Vuurdood Subsuite. This must be the result of an increase in fusion temperatures and a possible explanation would be that the zone where melting occurs above the subducting slab, increased in depth possibly due to an increase in the thickness of the overlying continental crust.

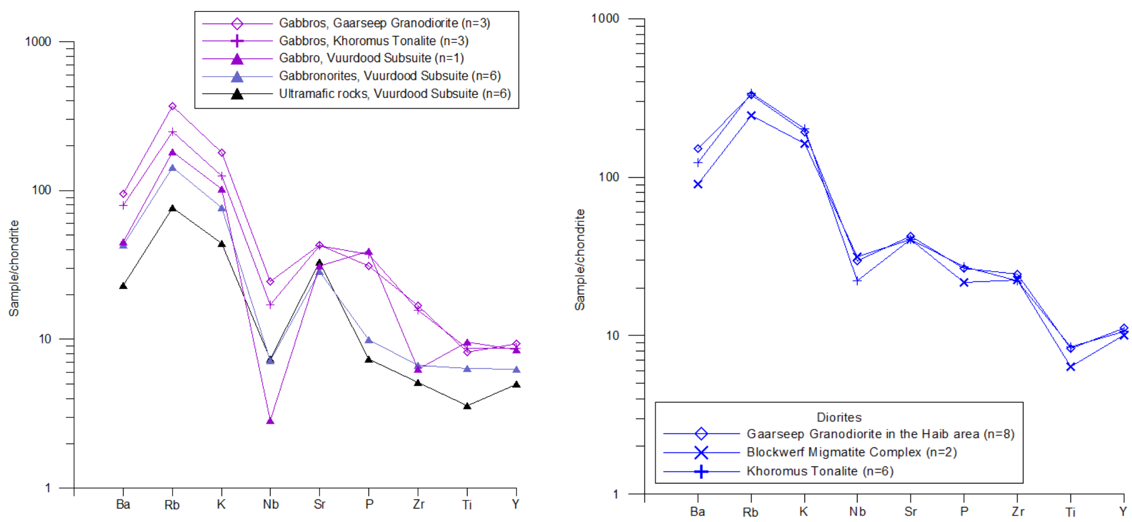

Figure 4.7: Multi-element diagrams for average concentrations in the various rock types and units of the Vioolsdrif Suite.

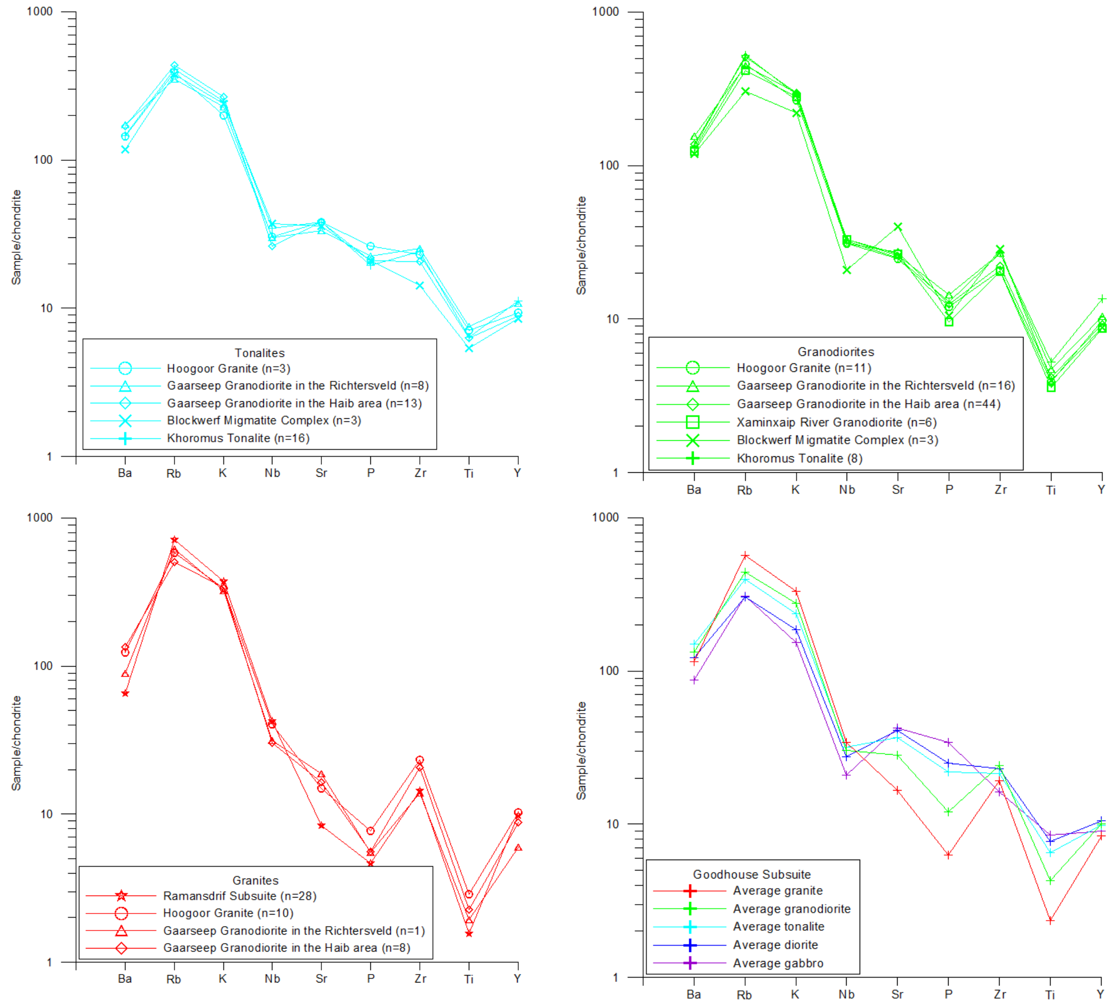

Figure 4.7: (Continue).

Within the Goodhouse Subsuite, a good degree of correlation is displayed when the various rock types are compared. Diorites occur in the Khoromus Tonalite, Blockwerf Migmatite and Gaarseep Granodiorite and their patterns fit very closely. Tonalites occur in the Khoromus Tonalite, Blockwerf Migmatite, Gaarseep Granodiorite and Hoogoor Granite and again their patterns also correlate well. The fact that the Blockwerf Migmatite is not distinguished from the other units on these multi-element diagrams where the REE are not considered, is noteworthy. Granodiorites occur in the Khoromus Tonalite, Xaminxaip River Granodiorite, Blockwerf Migmatite, Gaarseep Granodiorite and Hoogoor Granite, their patterns being almost indistinguishable. Granites occur in the Gaarseep Granodiorite, Hoogoor Granite and Ramansdrif Subsuite. Their patterns show some variation in Sr, P and Ti, however, there is large variation among the patterns in each unit individually (not shown) and therefore, variation in their average patterns is to be expected. The variations do not distinguish any of the units as unique among the others. When the Gaarseep Granodiorite is considered independently, no distinction can be made in any of the rock types between the Haib and Richtersveld areas. The variation pattern in the series from mafic to felsic (gabbro-diorite-tonalite-granodiorite-granite) in the Goodhouse Subsuite shows systematic increase in LILE and Nb concentrations and systematic decrease in Sr, P and Ti concentrations. All these are inaccordance with variations on Harker diagrams and in accordance with a fractional crystallization model.

Figure 4.8 shows multi-element diagrams for average trace element concentrations in the various rock types within the various units of the Orange River Group. Also shown is the variation in the series from mafic to felsic (basaltic andesite-andesite-dacite-rhyolite). Anomalous samples were omitted from the calculation of these average trends.

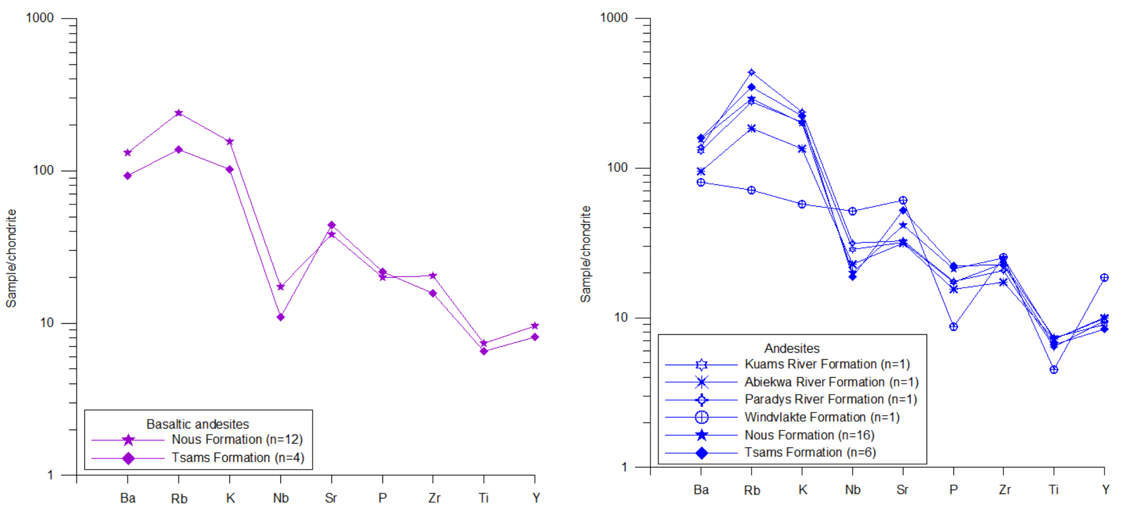

Figure 4.8: Multi-element diagrams for average concentrations in the various rock types and units of the Orange River Group.

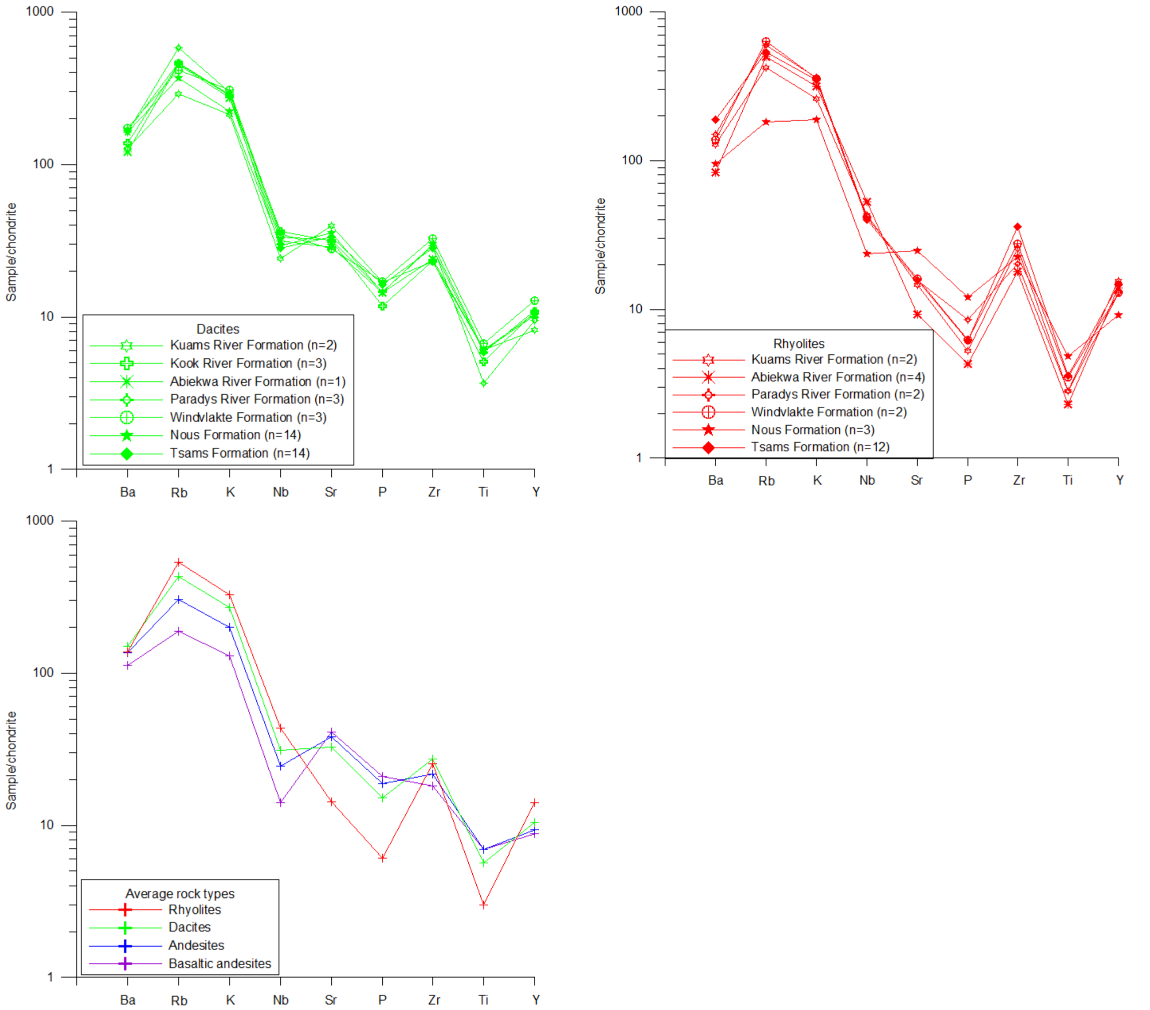

Figure 4.8: (Continue).

The basaltic andesites in the Tsams Formation show notably lower LILE concentrations than those in the Nous Formation. Andesites of the Abiekwa River Formation show on average lower LILE values than those of the other formations, which in turn show good correlation. Based on field and petrographic evidence as well as evidence from Harker diagrams, lower LILE contents of the Abiekwa River Formation can be attributed to element mobility during metamorphism. The dacite patterns of all the formations coincide very well. The Rb and K concentrations in the pattern for the Windvlakte Formation andesite are anomalous compared to similar rocks in the rest of the Orange River Group. However, this pattern represents an average which was calculated off only one sample which may not be representative. As for the Abiekwa River Formation, all the evidence points to element mobility during metamorphism as the cause of the low Rb and K values. The average patterns for dacite and rhyolite in the Windvlakte Formation are not anomalous in relation to the other units. Therefore there is no reason to believe that the anomalous pattern in the single andesite sample is related to magmatic processes.

As in the Goodhouses Subsuite, there is a systematic increase in LILE concentrations and an associated decrease in Sr, P and Ti, in the variation from mafic to felsic. Again this is in agreement with variations on Harker diagrams and may be related to a fractional crystallization process.

In Figure 4.9, the Vioolsdrif Suite and Orange River Group are compared through average multi-element diagrams.

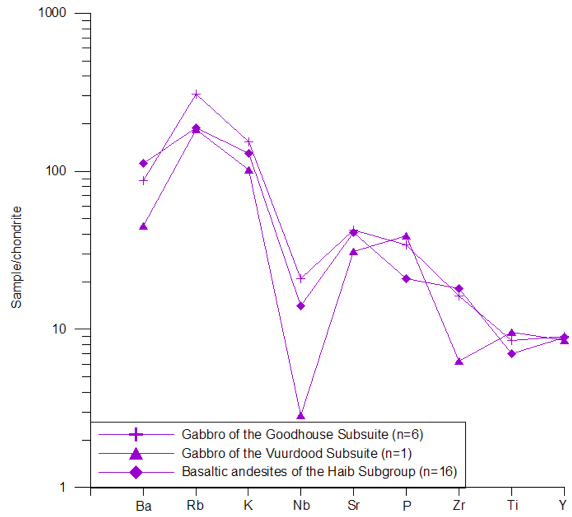

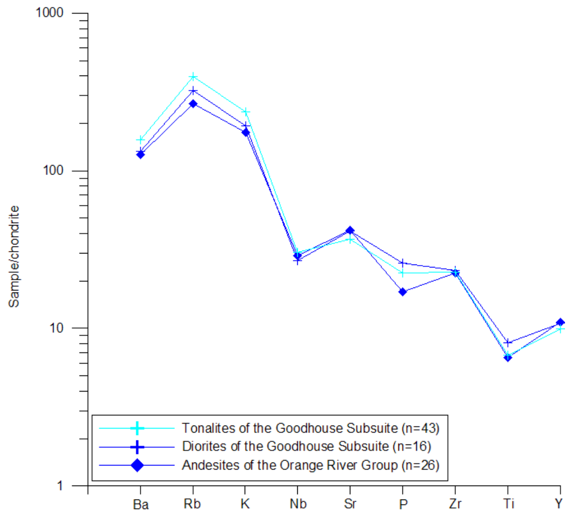

Figure 4.9: A comparison of the multi-element variation patterns between rock types of the Vioolsdrif Suite and Orange River Group.

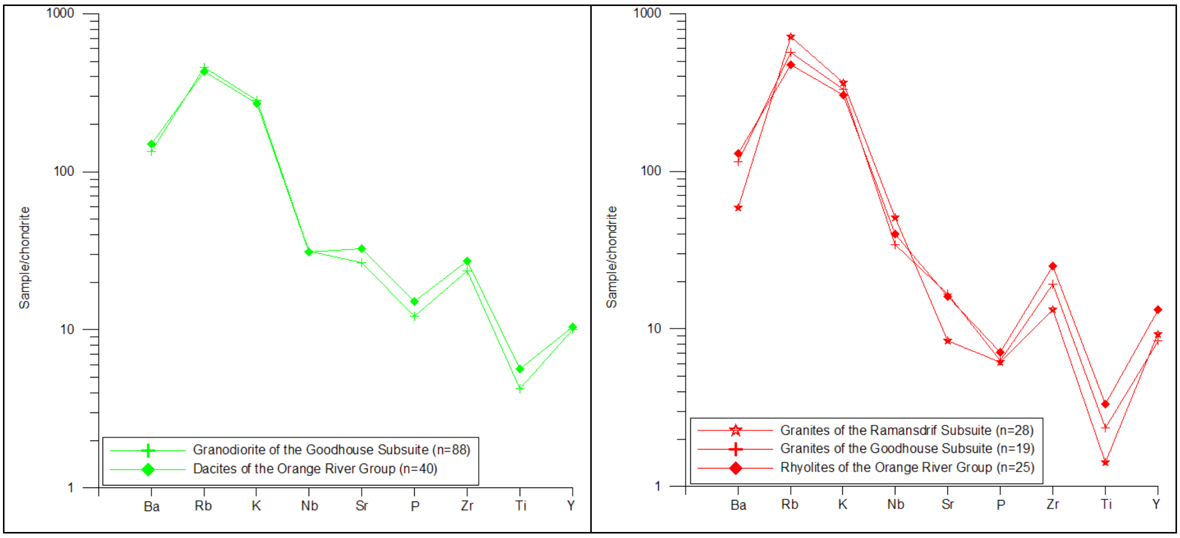

Figure 4.9: (Continue)

For the Vuurdood Subsuite, only the pattern for gabbro is shown as it is the only rock type in the subsuite which is comparable to the rest of the batholith. It displays the largest Nb trough in the batholith while it is also the only one which displays a Zr trough. The pattern for the basaltic andesites of the Haib Subgroup is distinct in its LILE and Nb concentrations and falls between that of the Vuurdood Subsuite and the gabbros of the Goodhouse Subsuite. In most of the HFSE (except P), it coincides very closely with the gabbros of the Goodhouse Subsuite. Since the basaltic andesite composition is comparable to that of gabbro, the increasing LILE and Nb trend from the Vuurdood Subsuite to the De Hoop Subgroup to the Goodhouse Subsuite, cannot be attributed to fractional crystallization. Again (as previously postulated for a similar pattern between the Vuurdood Subsuite, Khoromus tonalite and Gaarseep Granodiorite) it may be the function of progressing metasomatism in the mantle wedge with progressing subduction. However, according to radiometric data, the Haib Subgroup is either contemporaneous with the Vuurdood Subsuite, or predates it. Another possible explanation of the elevated LILE and Nb concentrations in the Haib Subgroup compared to the Vuurdood Subsuite, is contamination of the Haib magmas with these elements as they rise to surface. But if this was the only mechanism leading to the higher values, then the Haib Subgroup's values should also be higher than that of the Goodhouse Subsuite, which is not the case. As such, the two processes probably both played a role.

There is no equivalent composition to the Haib Subgroup's basaltic andesites in the De Hoop Subgroup. For the other rock types, the patterns for diorites in the plutonic suite and andesites in the volcanic group coincide closely, the granodiorites and dacites correspond as well as the granites and rhyolites.

4.1.5 REE patterns

A limited number of REE analyses were done for the Orange River Group during this study and none are available from previous studies. Of those that were done during this study, all are for the De Hoop Subgroup. Therefore, an REE investigation of the volcanic group extended only as far as the construction of an average pattern (Figure 4.10), which, as such, is representative only of the De Hoop Subgroup.

Like multi-element diagrams, REE patterns are useful in the correlation among various rock units of the same suite, since their fractionation is even more sensitive than the other trace elements, and also primarily controlled by magmatic processes. They are especially useful in testing the process of fractional crystallization because theoretically, their behaviour during this process can be accurately predicted, based on their distribution coefficients (e.g., Rollinson, 1993). According to such predictions, both the size of the Eu-anomaly and the La/Yb ratio, should increase in the range from mafic to felsic in a rock unit which is the product of this process (given the mineral composition of the Vioolsdrif Batholith).

Figure 4.10 shows REE patterns of average concentrations in the Orange River Group and the three subsuites of the Vioolsdrif Suite. The Blockwerf Migmatite is shown here independantly as its slope is different in relation to the rest of the batholith to such an extent that it distorts the pattern for the Goodhouse Subsuite if it is included in it.

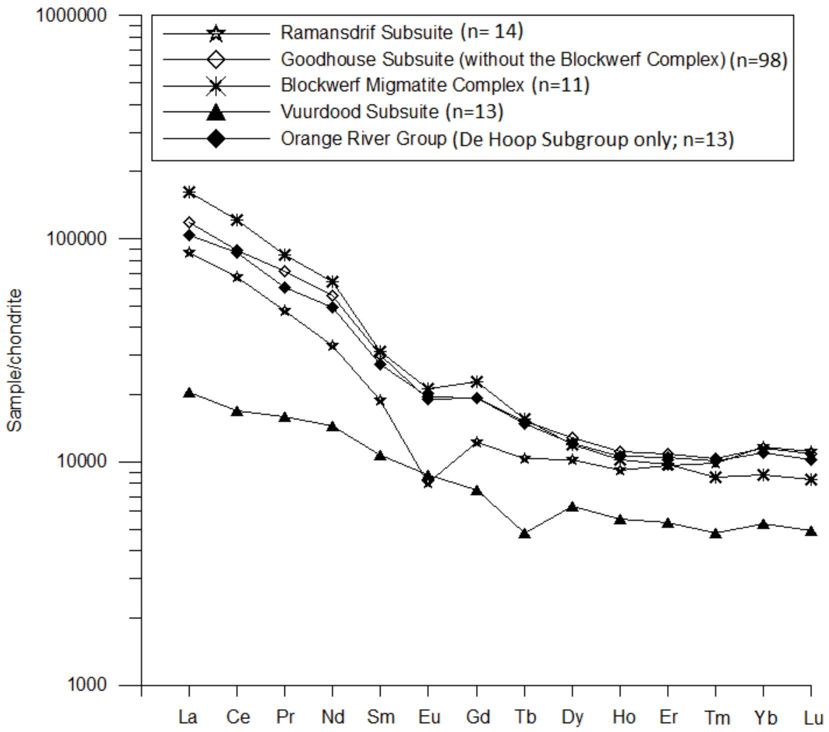

Figure 4.10: Patterns for average REE abundances in the three subsuites of the Vioolsdrif Suite and the Orange River

There is very good correlation between the patterns of the De Hoop Subgroup and Goodhouse Subsuite, while the Vuurdood and Ramansdrif Subsuites each defines a distinct pattern. Although the Vuurdood Subsuite pattern has lower overall concentrations than those of the Goodhouse Subsuite and Orange River Group, its shape is nearly parallel to these two units. This speaks in favour of a similar source for the three units. The pattern for the average Ramansdrif Subsuite shows lower overall concentrations and a flatter slope than that of the Goodhouse Subsuite. This would not have been the case if the Ramansdrif Subsuite represented the final stages of crystallization in a continuous fractional crystallization process for the suite as a whole.

The pattern for the Vuurdood Subsuite in Figure 4.10 shows a negative Tb anomaly. In mafic melts, the MREE are controlled by amphibole and clinopyroxene with their distribution coefficients the highest in hornblende (e.g., Rollinson, 1993). Therefore, the development of negative Tb anomalies in the Vuurdood Subsuite may be regarded to indicate an amphibolitic source composition. When REE patterns for the different rock types in the Vuurdood Subsuite are considered (Figures 4.11 and 4.12), it can be seen that the Tb anomalies are characteristic of the ultramafic rocks and not of the gabbro. This may indicate that some of the ultramafic samples represent cumulates of amphibolite and pyroxene.

For a more detailed investigation of the Vioolsdrif Suite, REE patterns for average concentrations in the various rock types within the various units of the suite are shown in Figure 4.11. Due to insufficient REE data for the Orange River Group, the unit is excluded from these investigations.

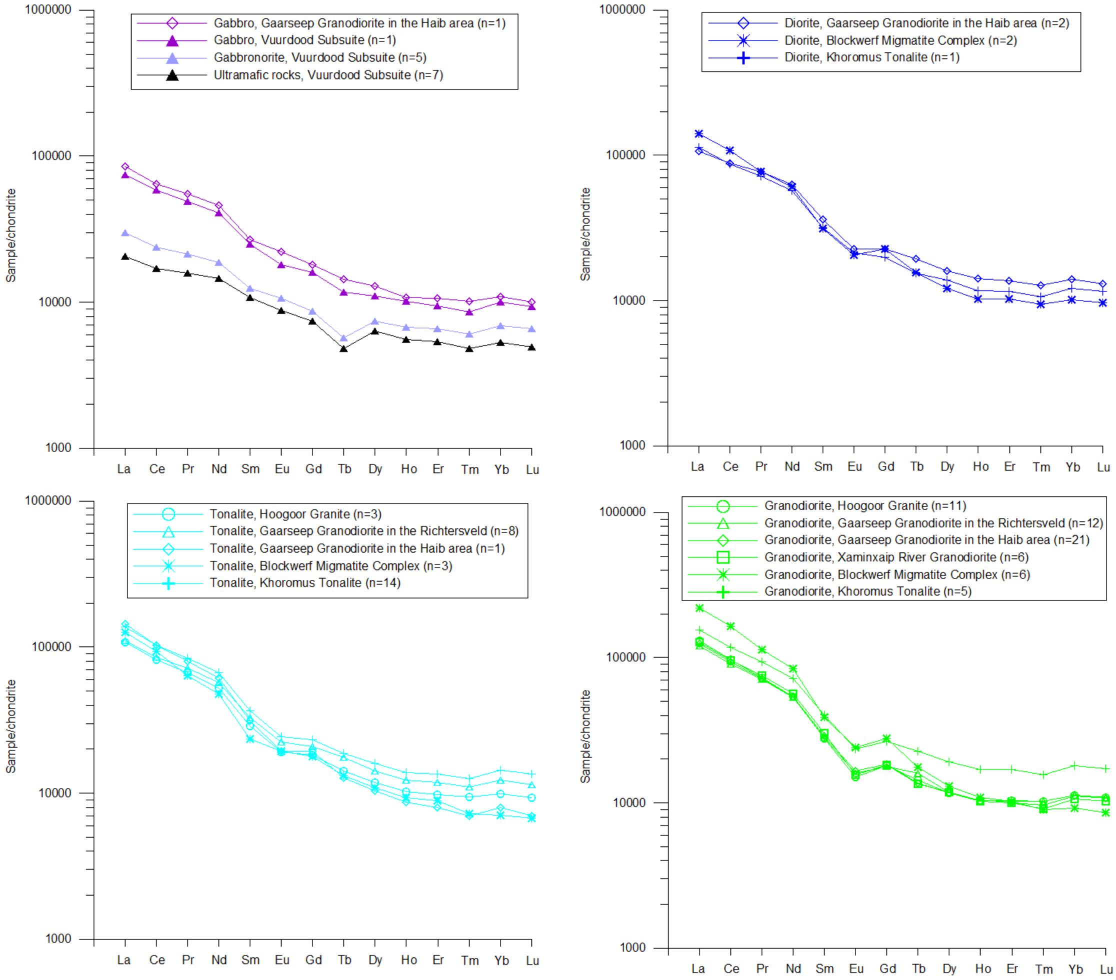

Figure 4.11: Patterns for average REE concentrations in the various rock types within the various units of the Vioolsdrif Batholith. Chondrite normalized values of Boynton (1984).

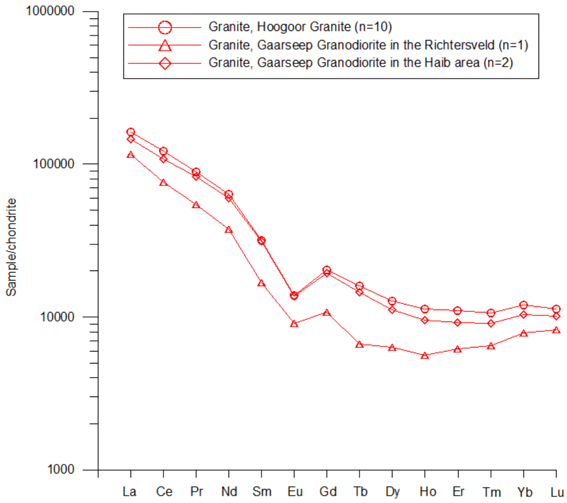

Figure 4.11: (Continue).

Within the Vuurdood Subsuite, the ultramafic rocks have much lower overall concentrations than the gabbro, but similar slope (except the Tb anomaly). The gabbro in the Vuurdood Subsuite shows good correlation with that in the Gaarseep Granodiorite, both in slope and overall concentrations.

The Blockwerf Migmatite is distinguished in its steeper slope (higher La/Yb ratios) compared to similar compositions in other units. Diorite patterns in the Khoromus Tonalite and Gaarseep Granodiorite show good correlation. Patterns for tonalite among the various units show variation mainly in the HREE concentrations, while the LREE concentrations show better correlation. Patterns for granodiorite among the various units in which it occurs, show very good correlation except the pattern for the Khoromus Tonalite, which shows higher overall concentrations. Granite patterns for the Gaarseep Granodiorite and Hoogoor Granite show very good correlation, while the granites of the Ramansdrif Subsuite can be distinguished by a flatter slope. The Gaarseep Granodiorite occurs in both the Haib and Richtersveld areas. Granodiorites of this unit from the two areas cannot be distinguished in the REE patterns but in the patterns for granite, there is a distinction with those in the Richtersveld showing lower overall concentrations than those in the Haib area. However, this pattern is of only one sample and may not be representative.

In Figure 4.12, the variation in REE patterns for average concentrations is shown for the range from mafic to felsic compositions, in units which comprise a compositional series. These units include the Vuurdood Subsuite (ultramafic-gabbronorite-gabbro), Khoromus Tonalite (diorite-tonalite-granodiorite), Blockwerf Migmatite (diorite-tonalite-granodiorite), Gaarseep Granodiorite in the Haib area (gabbro-diorite-tonalite-granodiorite-granite), Gaarseep Granodiorite in the Richtersveld (tonalite-granodiorite-granite) and the Hoogoor Granite (tonalite-granodiorite-granite).

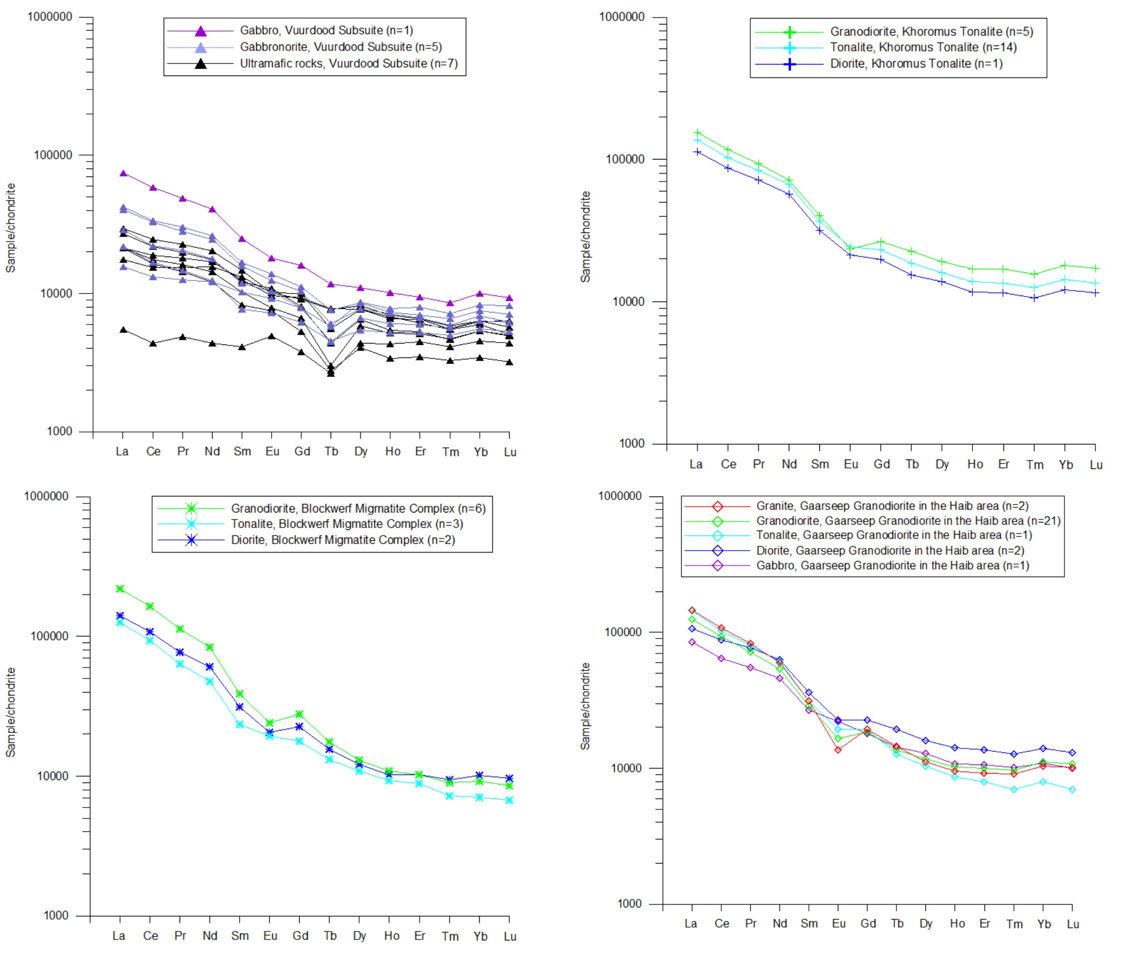

Figure 4.12: Variation of REE patterns within the units of the Vioolsdrif Batholith. Chondrite normalizing values after Boynton (1984).

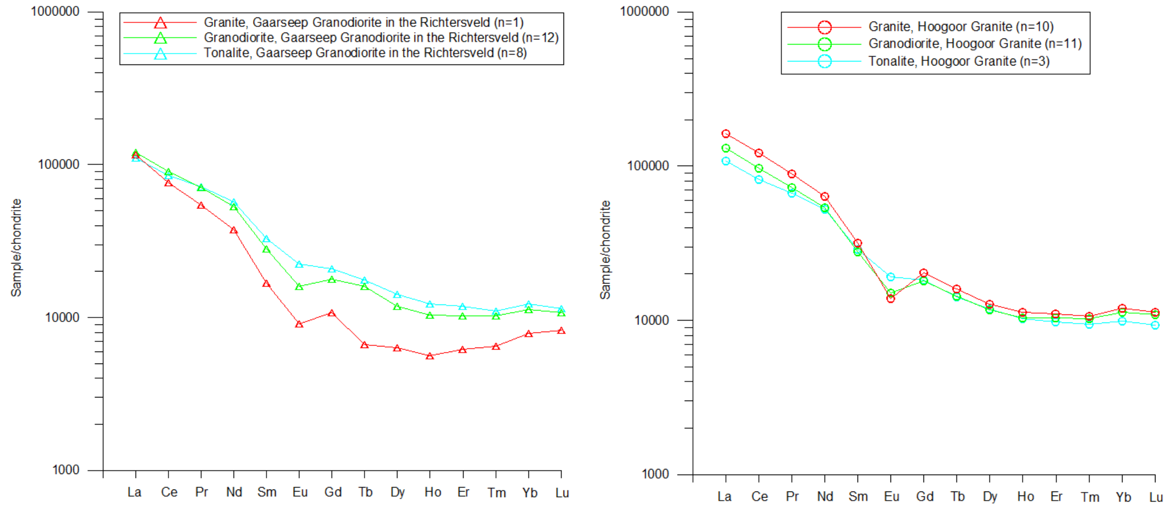

Figure 4.12: (Continue).

For the Vuurdood Subsuite, the patterns of individual samples are shown because of the large degree of variation displayed. Patterns of average concentrations would not be representative, especially of the ultramafic rocks. In the ultramafic samples, patterns show variation in overall concentration, slope as well as the extent of the Tb anomaly. The patterns for gabbronorite are more consistent in slope. There is a gradual decrease in the size of the Tb anomaly with increasing overall concentrations. The single gabbro sample shows the highest overall concentrations with no Tb anomaly. As such, the influence of fractional crystallization can be recognized in the range from gabbronorite to gabbro. However, among the ultramafic samples the variability in the patterns suggest the influence of alternative or additional processes. The suggestion made earlier that some of these samples may represent cumulate material, is supported by this observation, as there is no systematic process involved in the formation of cumulates.

Within the Khoromus Tonalite there is a gradual increase in overall concentrations. The Eu anomaly in the granodiorite is larger than in the diorite and tonalite, however, no clear systematic increase in the size of the anomaly is discernable from diorite to tonalite to granodiorite. These observations do not support a model of fractional crystallization as a single process in the development of the Khoromus Tonalite.

Patterns for the Blockwerf Migmatite (individual samples) are characterized by variation in overall concentration, slope and the Eu-anomaly. One granodiorite samples shows a large positive Eu anomaly, which is commonly attributed to hornblende fractionation (e.g., Rollinson, 1993). The large degree of variation in all the aspects of the patterns rules out fractional crystallization as the dominant process in the formation of this unit.

A distinction is made between the Gaarseep Granodiorite in the Haib and Richtersveld areas. Within the Gaarseep Granodiorite in the Haib area, no systematic trend can be observed. The gabbros and diorites show flatter-lying slopes than the more felsic rocks, with the gabbros having lower overall concentrations than the diorites. There is a sudden and large increase in slope between the diorites and tonalites with the latter showing the steepest slope of all the rocks in this unit. There is a decrease in the slope from tonalite to granodiorite and granite, the latter two patterns coinciding almost exactly. The Eu-anomaly systematically increases in size from mafic to felsic compositions. Most of these observations also speaks against a single model of fractional crystallization for the development of the Gaarseep Granodiorite in the Haib area.

The Gaarseep Granodiorite in the Richtersveld area displays an increase in slope from mafic to felsic compositions, along with a gradual increase in the size of the Eu anomaly. The increase in slope, however, is not the result of a more rapid increase in LREE concentrations compared to HREE concentrations. As such, it does not support a model of fractional crystallization for its development. The increase in slope from mafic to felsic compositions is contrary to the trends in the Gaarseep Granodiorite in the Haib area. But again, the single granite sample from the Richtersveld may not be representative.

Patterns in the Hoogoor Granite show a systematic increase in slope as well as the size of the Eu anomaly from mafic to felsic compositions. This speaks in favour of a fractional crystallization model for the development of the unit.

As such, within the Goodhouse Subsuite, when individual units are considered, the evidence presented suggest that various magmatic processes may have been involved during its evolution. Except for the Hoogoor Granite, the influence of contamination processes in addition to fractional crystallization, is indicated.

4.2 MAGMATIC PROCESSES

4.2.1 Vuurdood Subsuite in relation to the rest of the batholith

Due to unclear contact relationships in the field, the exact nature of the Vuurdood Subsuite and its relationship with the rest of the batholith, has been controversial among previous investigators. Possibilities as to its nature included remnants of the mantle sources, xenoliths of earlier plutonic phases, cumulate material in the primary magmas, and later intrusions in the Goodhouse Subsuite. At present, enough evidence have amassed to rule out the possibility that the Vuurdood Subsuite (i.e., the bodies occurring in the Haib area) may represent post-Goodhouse intrusions.

Radiometric data (Reid, 1977, 1982) show that the Vuurdood Subsuite is the oldest unit in the Vioolsdrif Suite and overlaps in age with the Orange River Group. Initial isotope data (Reid, 1982) show that the Vuurdood Subsuite share similar parental sources with the Goodhouse Subsuite and Orange River Group. Multi-element diagrams indicate that the Vuurdood Subsuite experienced similar magmatic processes as the Goodhouse Subsuite and Orange River Group in having similar patterns (Figures 4.6, 4.7, 4.9). REE patterns support the initial isotope data in showing that the Vuurdood Subsuite share similar sources with the Goodhouse Subsuite, since their slopes are nearly parallel. Overall REE concentrations in gabbros (the only rock type which the two units have in common) also closely coincide (Figure 4.12). All this evidence taken into account, it would be realistic to postulate that the Vuurdood Subsuite may represent remnant bodies of the primary source magmas.

The REE patterns also suggest that the process of fractional crystallization can be recognized as one of the magmatic processes which was active during the evolution of the Vuurdood Subsuite, but that other factors must have played a role in producing the observed variations among the trends. Based on the large negative Tb anomalies and large variation in slopes of some of the ultramafic samples, these samples may represent cumulates of amphibole and pyroxene.

Evidence from Harker diagrams (4.1.3 Harker diagrams) suggest a genetic link between the Vuurdood Subsuite and Haib Subgroup which is not observed between the Vuurdood Subsuite and the De Hoop Subgroup, nor the Goodhouse Subsuite. A progressive increase in LILE concentrations from the Vuurdood Subsuite, through the Haib Subgroup, to the Goodhouse Subsuite in rocks of similar composition, is observed on multi-element diagrams (4.1.4 Multi-element diagrams, Figure 4.9). Increases in LILE concentrations in subduction zone magmatism is commonly attributed to metasomatic processes in the mantle wedge (e.g., Pearce and Parkinson, 1993). This suggests that the observed systematic increases in LILE concentrations may be the result of progressing metasomatic processes from the formation of the Haib Subgroup to that of the De Hoop Subgroup and Goodhouse Subsuite, from a common Vuurdood-like source.

The Jensen cation plot (Jensen, 1976) is a classification scheme for subalkaline rocks. It has the advantage that it distinguishes tholeiitic and komatiitic rocks from basalts and calcalkaline rocks. In Figure 4.13, the Vioolsdrif Batholith is plotted on this diagram.

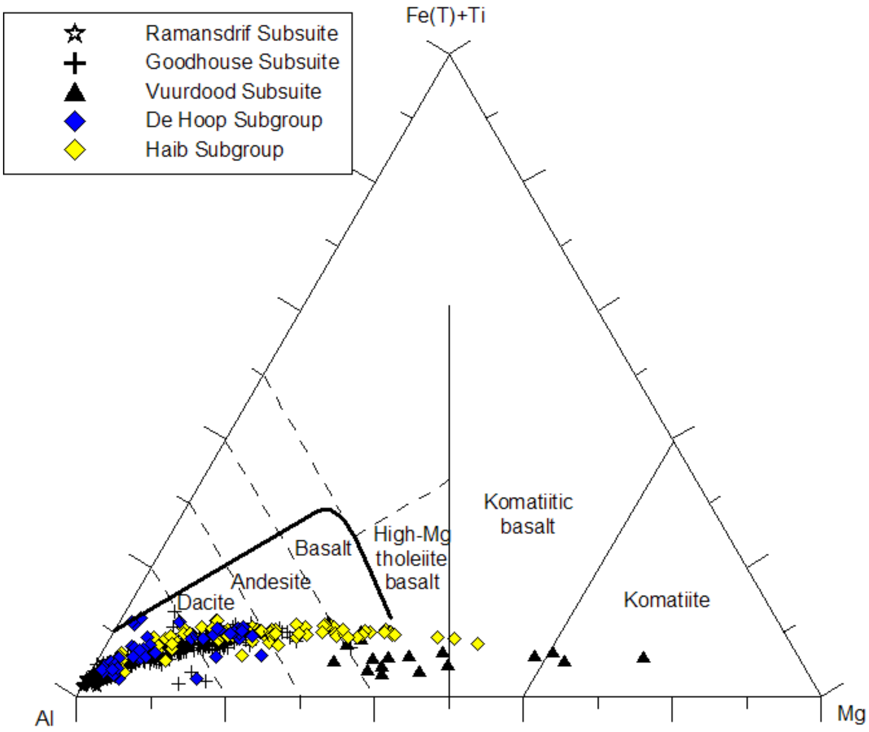

Figure 4.13: The Vioolsdrif Batholith on the Jensen cation plot (Jensen 1976).

Most of the Vuurdood Subsuite samples show resemblance to high-Mg tholeiite basalt. These are the primary magmas which are produced in modern volcanic arcs from a MORB-like source (e.g., Condie, 2005b). Some of the ultramafic samples plot in the komatiite field with a space separating them from the other samples of the subsuite. This plot in the komatiite field is related to elevated Mg contents and may be explained in terms of cumulate material which is rich in pyroxene and olivine. While the other units of the batholith are clearly parted from the Vuurdood Subsuite on this diagram, the Haib Subgroup represents a continuous range towards the Vuurdood Subsuite.

Evidence can furthermore be provided that the magmatic processes which were active during the formation of the Haib Subgroup, differed from those which were active during the formation of the De Hoop Subgroup and Goodhouse Subsuite. Kostitsyn *et al*. (2007) used diagrams of compatible vs. incompatible trace elements to study the crystallization history of an igneous rock unit. If two igneous rock units originate from the same source, the distribution of any two elements within them will depend on the distribution coefficient of the elements and the magmatic processes that were active during their formation.

Figure 4.14 shows a plot of Rb vs. Cr (compatible vs. incompatible element) for rocks of similar composition in the Vioolsdrif Batholith. These include gabbros, diorites and basaltic andesites, which can be shown on both multi-element and REE diagrams to overlap closely in composition.

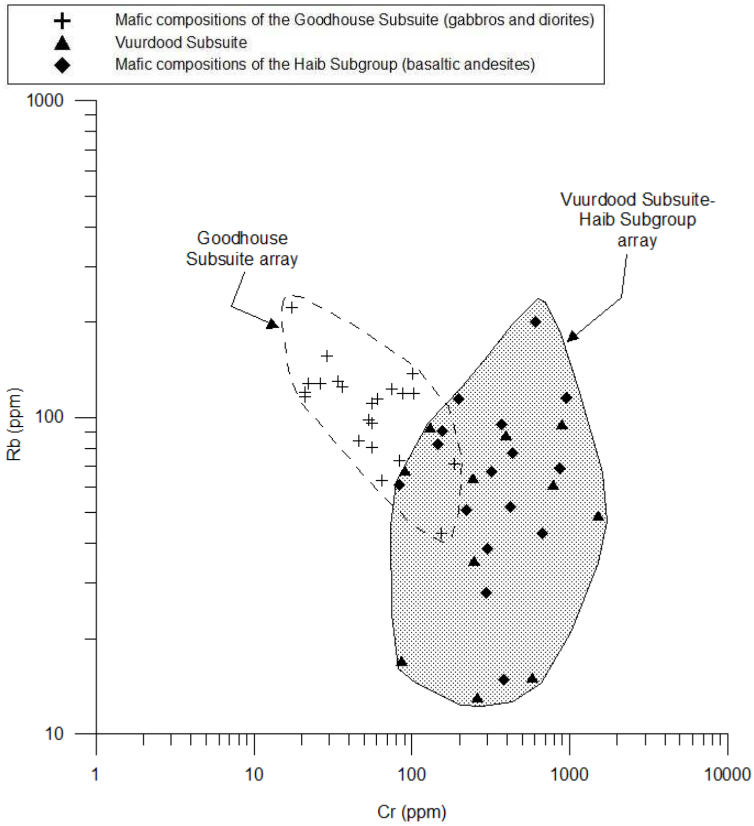

Figures 4.14: Variations of Rb vs. Cr in mafic rocks of the Vioolsdrif Batholith (gabbros, diorites and basaltic andesites).

The Vuurdood Subsuite and Haib Subgroup are associated in a single linear trend, while the Goodhouse Subsuite defines a linear trend which is oriented at an angle to the former. (There are no equivalent rock compositions in the De Hoop Subgroup.) Since these units in Figure 4.14 originated from a similar source (Reid, 1977; 1982), it can be assumed that the magmatic processes which led to the formation of the two trends, differed. As such, the Vuurdood Subsuite and Haib Subgroup are genetically linked, while the Goodhouse Subsuite is not genetically linked to the Vuurdood Subsuite. All classification and variation diagrams show a close association between the Goodhouse Subsuite and the De Hoop Subgroup. Therefore, it can be assumed that the De Hoop Subgroup is also not genetically linked to the Vuurdood Subsuite.

The use of compatible vs. incompatible element diagrams can be extended to include all the rock compositions in the batholith. Kostitsyn *et al*. (2007) showed that rocks produced by fractional crystallization from a common parent, must display linear trends on logarithmic variation diagrams of compatible vs. incompatible elements. The variation of Rb vs. Cr among the various rock types and within various units of the Vioolsdrif Batholith, is displayed on logarithmic diagrams in Figure 4.15.

Within the Haib Subgroup, there is a transition observed from the basaltic andesites to the rest of the compositions. The trend of the basaltic andesites is steep and positive and coincides with that of the Vuurdood Subsuite. It grades into the trend for andesites, which is flat-lying and negative, and continues linearly into those for the dacites and rhyolites. Since Rb is a highly mobile element, the single values on the diagram which plot below the average trends, are considered to be the result of later metamorphism.

None of the Goodhouse Subsuite, nor the De Hoop Subgroup trends show a linear association with the Vuurdood Subsuite, such as that of the Haib basaltic andesites. Compositions in the Goodhouse Subsuite which overlap with the Vuurdood Subsuite coincide with the negative trend defined by the rest of the rock types. The trends of individual rock types within the Goodhouse Subsuite are curved, as is the combined trend from mafic to felsic. This curved nature distinguishes it from the linear trend defined by the Haib Subgroup. The De Hoop Subgroup also defines a linear trend as does the Haib Subgroup, however, the trend for the De Hoop Subgroup is slightly positive, which distinguishes it from the slightly negative Haib Subgroup trend.

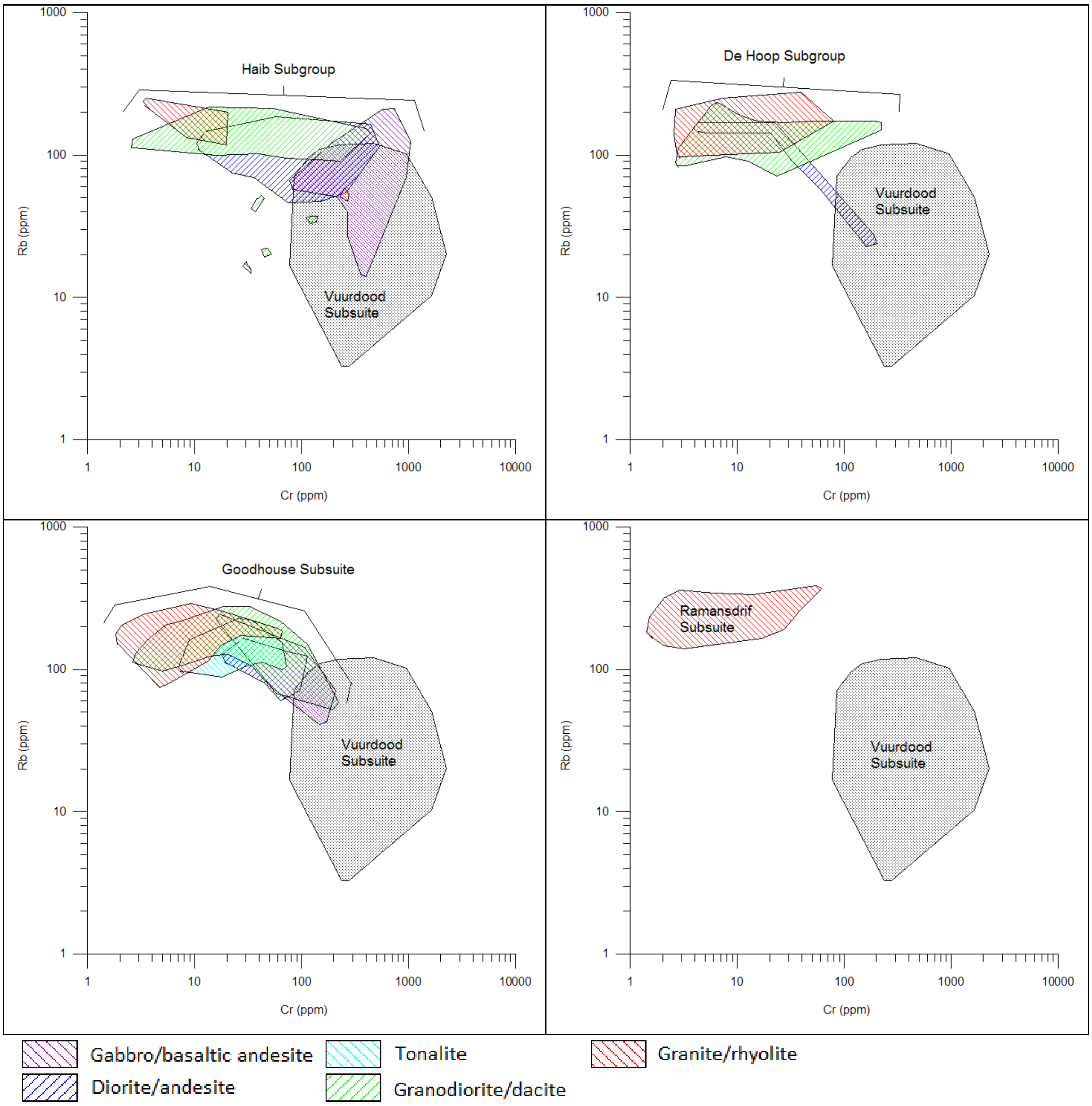

Figure 4.15: Variations in Cr vs. Rb for the various units of the Vioolsdrif Batholith.

The linear trends in the Haib and De Hoop Subgroups suggest that fractional crystallization played the dominant role in the development of the volcanic rocks. The curved trends in the Goodhouse Subsuite, however, suggest major influence from alternative processes in the development of the plutonic suite. Through major and trace element modeling, Reid (1977) found that a simple fractional crystallization model could not account for the production of the whole continuous range from diorite through tonalite and granodiorite to granite in the Goodhouse Subsuite. Reid (*op cit*., p. 278) proposed that models of contamination and magma mixing may explain some of these discrepancies. Von Backström and De Villiers (1972, p. 40), as well as Beukes (1973, p. 68) noticed an influence on the composition of the granitoids through processes of contamination. During field work for the current study, it was often noticed that the granotoids have a more mafic composition in the vicinity of mafic and ultramafic bodies. This is attributed to processes of magma mixing since the contacts were found to be gradational and since the granitoids and the mafic and ultramafic bodies are so closely related in time.

4.2.2 Vuurdood Subsuite as remnants of the primary magmas

The features displayed by the Vuurdood Subsuite on multi-element diagrams (Figure 4.6) are typical of subduction zone magmatism (e.g., Pearce and Parkinson, 1993). In Figure 4.16, the Vuurdood Subsuite is compared to similar rocks in modern volcanic arcs. Also shown is the pattern for MORB and the modeled depleted mantle.

Modern island arc volcanics originate from MORB. Based on the fact that the pattern of the Vuurdood Subsuite closely parallels that of modern island arc volcanics, it can be assumed that the processes which led to their formation, were similar. The concentration of Ba, K, La, Ce and Sr in the Vuurdood Subsuite furthermore closely match their concentrations in modern arc volcanics. According to Pearce and Parkinson (1993), these are elements which originate in the mantle source due to metasomatic processes. Therefore, it can also be assumed that the source of the Vuurdood Subsuite was similar to that of modern arc volcanics. Pearce and Parkinson (*op cit.*) furthermore considered the concentrations of Nb, Zr, Ti, Y and the HREE, to represent that in the source before subduction started. Based on these assumptions, a pattern can be projected for the mantle source from which the Vuurdood Subsuite originated (indicated on Figure 4.16).

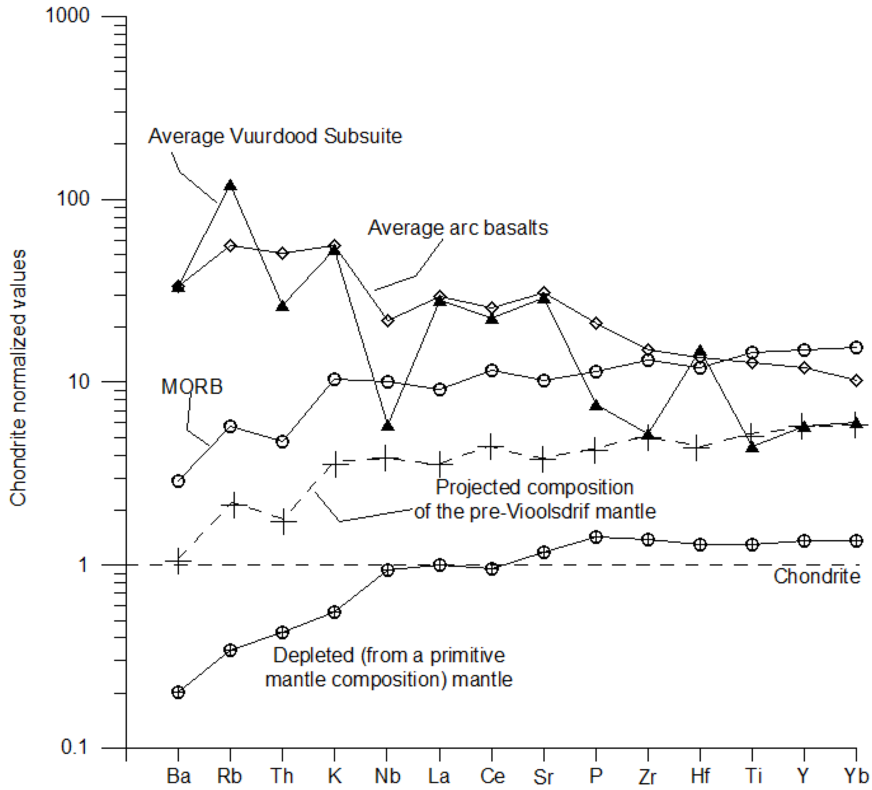

Figure 4.16: Multi-element diagrams of average values for the Vuurdood Subsuite compared to that of modern volcanic arcs (including the Kermadec, Tonga, Marianas, Izu-Bonin, Kurile, Lesser Antilles, Cascades and Central Volcanic Zone of the Andes arcs) and MORB (values of Pearce, 1983). Values for the volcanic arcs were obtained from the internet georoc database (http://georoc.mpch-mainz.gwdg.de/georoc/). Chondrite normalizing values are from Thompson (1982).

The modeled depleted mantle in Figure 4.16 represents that of the mantle residue after continental crust extraction around 2 Ga (Patchett, 1989). This time coincides with the onset of formation of the Vioolsdrif Batholith. The difference in overall concentrations between the modeled depleted mantle and the projected source of the Vioolsdrif Batholith, indicates that the Vioolsdrif Batholith did not originate from the model depleted mantle, but from a mantle which was higher in overall concentrations. Various previous studies point out the fact that the mantle is not continuously being depleted through time (e.g., Polat *et al*., 2011). This is again shown in Figure 4.16 for both the Vioolsdrif Batholith source as well as MORB. One way in which such elevated concentrations can be achieved, is through the recycling of continental crust into the mantle (e.g., Griffin *et al*., 2009). This speaks in favour of pre-existing crust in the study area before the evolution of the Vioolsdrif Batholith. If this is indeed the case, this pre-existing crust must have been completely recycled, since no trace of it is currently found. However, recycling of pre-existing crust contradicts the Sm-Nd isotope evidence presented by Reid (1997). Another way in which the element concentrations in the mantle can be elevated, is through continuous refertalization from the asthenosphere (Griffin *et al.*, 2009). However, since the time of onset of the evolution of the Vioolsdrif Batholith coincides with the time the depleted mantle was formed (2 Ga), this mechanism cannot be invoked for the Vioolsdrif Batholith.

Nordin's (2009) model T_{DM} ages suggest that crust formation in the area already started at 2 300 Ma, which favours the presence of pre-existing crust. This was supported by the presence of a single inherited zircon of about 2 700 Ma, indicating the presence of Archean material. T_{CHUR} ages from the same study do not allow time for the formation of pre-existing crust, however, some of these ages are negative, which suggest that this model is not applicable. Reid (1997), however, agrees with the latter model, especially based on the initial isotope signatures, which preclude the possibility of incorporation of pre-existing crust. He suggested a juvenile crust-producing episode at around 2 000 Ma from a bulk earth mantle, followed by the rapid recycling of young crust that generated granitic and rhyolitic components.

The deeper troughs at Nb, P and Zr and the lower values of Ti, Y and Yb in the Vuurdood pattern compared to that of modern arcs, suggest either that the processes which create these troughs were more efficient in the Proterozoic than they are today, or that they were different processes all together. In modern arcs, they are associated with metasomatism of the mantle wedge by dehydration of the subducting slab and there are currently no alternative models. The mechanism by which the pre-Vioolsdrif mantle became enriched relative to the model depleted mantle is not resolved here if the presence and complete recycling of pre-existing continental crust is denied. Most of the evidence presented here support this theory.

4.2.3 Radiometric evidence reviewed

Reid (1977) determined initial $^{87}Sr/^{86}Sr$ ratios for the Vuurdood Subsuite (0.7031), Nous Formation (0.7035), Tsams Formation (0.7028), Khoromus Tonalite (0.7029) and Gaarseep Granodiorite (0.7030). This means that the Vuurdood Subsuite, Orange River Group and Goodhouse Subsuite originate from a similar source.

The available radiometric data for the Richtersveld area is not sufficient to indicate the chronological order for all the units in the Vioolsdrif Batholith. In the Haib area, the whole rock Rb-Sr results of Reid (1977) are in accordance with field evidence. It shows the dacite-rhyolite compositions of the Tsams Formation to be 2 020±70 Ma and the basaltic andesite-andesite compositions of the Nous Formation to be 1 970±70 Ma. This means that the felsic volcanics in the Haib Subgroup are not only older than their mafic counterparts, but that they are indeed the oldest of all the rocks in the batholith, including the Vuurdood Subsuite. This is another piece of evidence arguing for the presence of pre-existing crust in the area (which was completely recycled) as felsic magma simply cannot be produced as a primary melt from a mantle source (e.g., Leake, 1983).

Although the study of Reid (1977) did not recognize the current subdivision of the Goodhouse Subsuite, his sample localities and sample descriptions offer reliable indications as to which of the current units they belong to. Gabbros and diorites (chemical classification) from the Khoromus Tonalite rendered an age of 1 975 Ma±55 Ma. Of the remaining thirty samples representing the tonalites, granodiorites and granites in the Goodhouse Subsuite, 28 are from the Gaarseep Granodiorite. The tonalites dated at 1 965±80 Ma, the granodiorites at 1 925±45 Ma and the adamellites at 1 800±40 Ma. As such, there is a clear relationship between the chronological sequence and the compositional range within the Goodhouse Subsuite in the Haib area, the units becoming progressively younger from mafic to felsic. However, as stated before, the study concluded through major and trace element modelling that fractional crystallization cannot account for the formation of the entire series from diorite to adamellite.

A single age determination on the Xaminxaip River Granodiorite (U-Pb zircon by LA-ICPMS; Appendix 2) of 1 892±4.8 Ma coincides with similar compositions in the Gaarseep Granodiorite. Field evidence indicate that the Gaarseep Granodiorite intrude the Xaminxaip River Granodiorite. An age of about 1 890 Ma (SHRIMP U-Pb zircon) is reported by Moen and Toogood (2007) for the Hoogoor Granite which is also more or less similar in age to the granodiorites in the subsuite.

In the Richtersveld, the Paradys River Formation has been dated at 1 883±7.4 Ma (U-Pb zircon by LA-ICPMS; Appendix 2). This age is significantly younger than any of the ages obtained by Reid (1977) for the Haib Subgroup. The Rosyntjieberg Formation rendered detrital zircon ages which indicate a Vioolsdrif Batholith provenance with one as young as 1 760 Ma (Appendix 2). The latter age agrees well with the crystallization age of the Ramansdrif Subsuite and no deformation related to this age has been identified. Therefore, metamorphic overprint is not a likely explanation to the 1 760 Ma detrital zircon age. Rather it is thought to reflect the presence of Ramansdrif-age rocks in the Rosyntjieberg Formation provenance. The fact that the Rosyntjieberg Formation is intruded by granites of the Gaarseep Granodiorite (see 2.3.2.7 Rosyntjieberg Formation), suggests that the Gaarseep Granodiorte in the Richtersveld may be significantly younger than that in the Haib area. However, a U-Pb zircon age (LA-ICPMS) of 1896±12 Ma for this granite (Appendix 2) coincides with the ages obtained by Reid (1977) for those in the Haib area and also predates most of the detrital ages in the Rosyntjieberg Formation. As stated before, it is possible that the sample which was taken for dating was taken from the wrong outcrop. Even though the map suggests that it is from the same pluton that intrudes the quartzites, it is not from the actual location where the two units are found in contact (Paradyskloof, Richtersveld National Park; see map).

4.2.4 Unique signatures of the subduction environment

In the subduction zone environment, the elements Nb, Ta, Zr, Hf, Ti, Y and the REE in calcalkaline basalts, are derived almost entirely from the mantle wedge while Rb, Ba, Th and K are among those which include a significant contribution from the subducting slab

(Pearce and Parkinson, 1993). Therefore, a ratio such as Ba/Nb would indicate the involvement of hydrothermal fluid from the subducting slab, while a ratio such as La/Nb would indicate the involvement of arc-like processes (e.g., Kay, 2005; Kay and Mpodozis, 2002). Furthermore, the influence of the subducting slab can be divided into two processes, i.e., the influence of hydrothermal fluid and the influence of melt generated through the partial melting of the slab (this represents the adakitic component). These two processes can be distinguished from each other on a plot of Ba/Nb (fluid component) vs. Sr/Y (melt component) (e.g., Kaur *et al*., 2009).

Figure 4.17 shows the Vioolsdrif Suite plotted on a diagram of Ba/Nb vs. La/Nb (the Orange River Group is not included due to lack of La analyses), as well as both the Vioolsdrif Suite and Orange River Group on a diagram of Ba/Nb vs. Sr/Y. The positive linear trend on both diagrams suggest that the three processes envisaged to be operating in subduction zones (fluid-induced metasomatism, melting of a subducting slab and processes leading to the production of a “subduction component” on multi-element diagrams), are applicable to the Vioolsdrif Batholith. The fact that values for the various units overlap suggests that these processes were active during the entire evolutionary history of the batholith and that they remained constant throughout its evolutionary history.

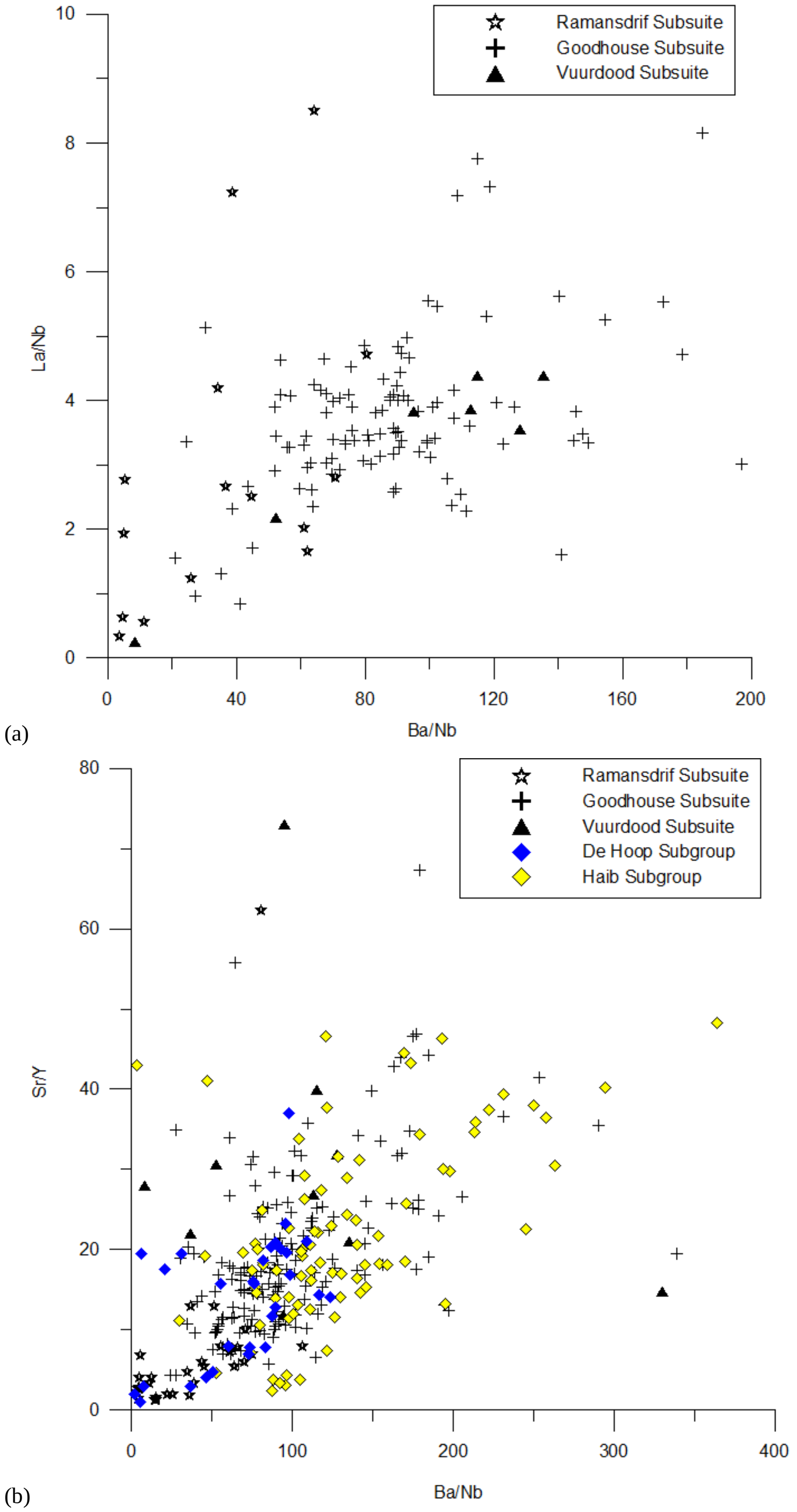

Figure 4.17: Plots of (a) Ba/Nb vs. La/Nb (based on Kay, 2005 and Kay and Mpdozis, 2002) for the Vioolsdrif Suite, and (b) Ba/Nb vs. Sr/Y (based on Kaur *et al*., 2009) for both the Vioolsdrif Suite and Orange River Group.

The temperature in the mantle wedge in a subduction zone tectonic setting is most likely controlled by heat exchange with the cooler subducting slab (Pearce and Parkinson, 1993). Temperature control in the source region will determine which mineral assemblages will fuse, as such controlling the distribution of specific elements between the source and the magma. The elements Nb and Zr are among those which Pearce and Parkinson (*op cit.*) considered to originate almost entirely from the mantle wedge in the subduction zone environment. They are also both very highly incompatible elements and their fractionation from each other is dependant on low degrees of melting since, with higher degrees of melting, the distinction between them is progressively smoothed out (Pearce and Parkinson , *op cit.*). In Figure 4.18, these two elements are plotted against each other for various units in the Vioolsdrif Batholith.

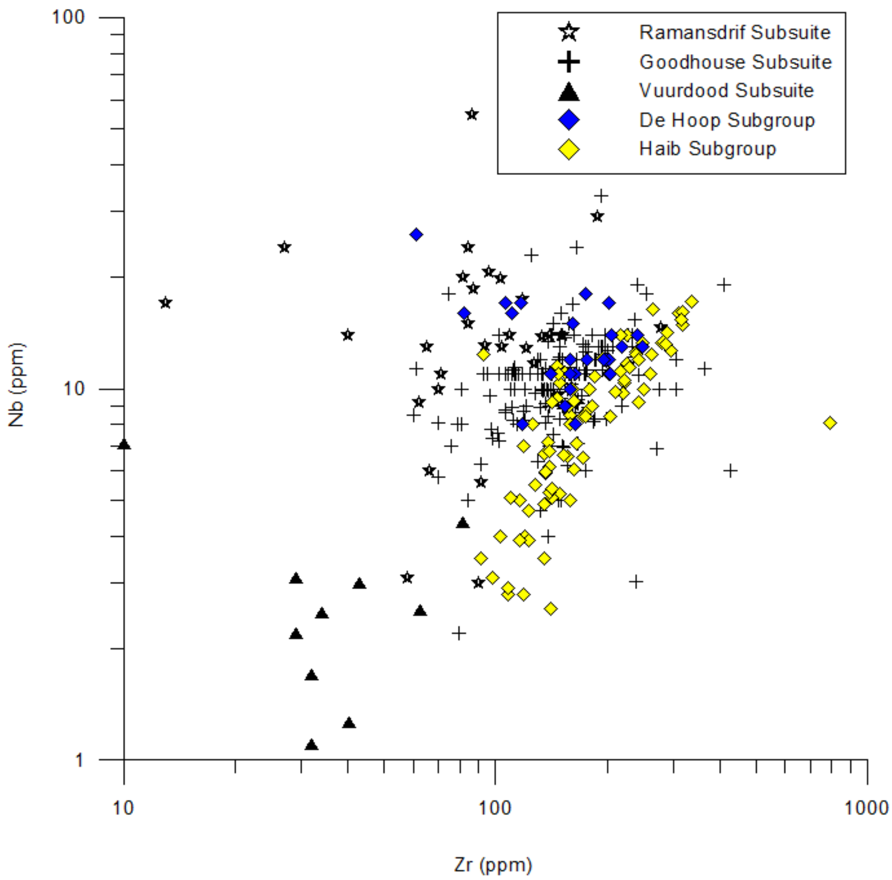

Figure 4.18: Zr-Nb variations in the various units of the Vioolsdrif Batholith.

Variation within the Haib Subgroup follows a positive linear trend while, in the rest of the batholith, there is no systematic relationship. As such, these two elements behaved as a unity during the development of the Haib Subgroup, but became decoupled from each other during the rest of the batholith's development. Concentrations for the rest of the batholith cluster around the maximum values attained in the Haib Subgroup.

4.2.5 Origin of the Blockwerf Migmatite

The two phases within the Blockwerf Migmatite, as identified in the field (2.4.2.3 Blockwerf Migmatite), is also clearly distinguished on the total alkali-silica classification diagram (Figure 4.19). Phase 1 (high concentration of mafic enclaves and well developed migmatitic character) is on average more mafic than phase 2 (low concentration of mafic enclaves and granitic texture). Phase 2 is also compositionally similar to the granitoids of the Gaarseep Granodiorite which intrudes it.

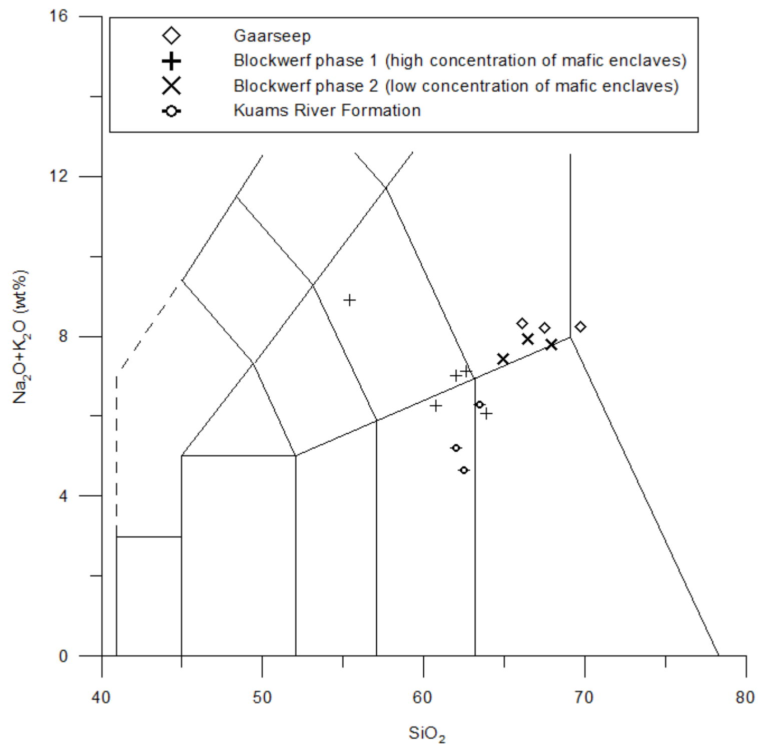

Figure 4.19: Plots of the Blockwerf Migmatite, Gaarseep Granodiorite which intrudes it and Kuams River Formation volcanics which are intruded by it, on a TAS classification diagram.

REE patterns for the Blockwerf Migmatite have been discussed earlier (4.1.5 REE patterns; Figure 4.12). The large variations in their overall concentrations, slopes and Eu-anomalies rule out fractional crystallization as the dominant magmatic process in the development of the unit. Figure 4.20 shows the REE patterns for the Gaarseep Granodiorite and Kuams River Formation volcanics which are found in contact with the Blockwerf Migmatite.

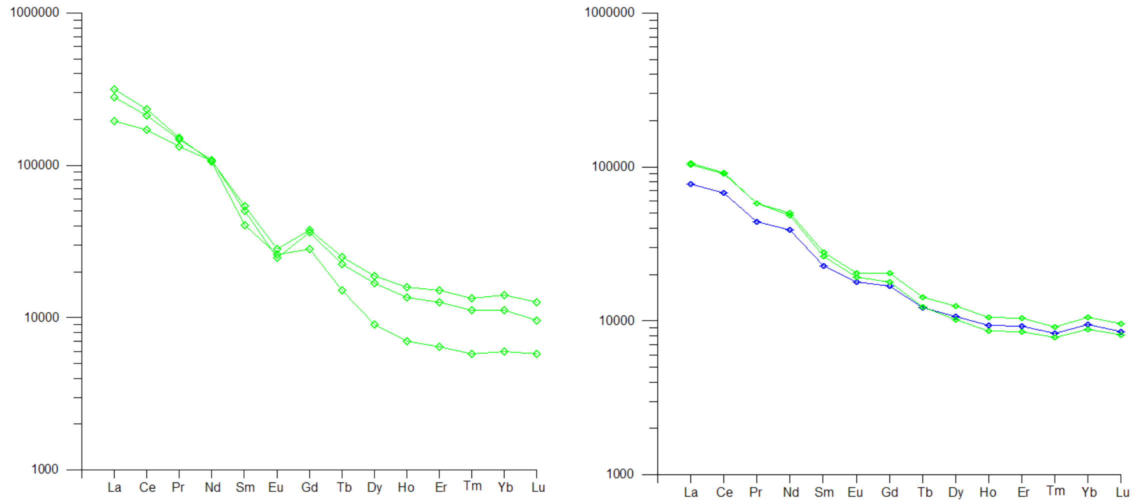

(a) (b)

Figure 4.20: Chondrite-normalized REE patterns for the Gaarseep Granodiorite (a) and Kuams River Formation (b) which are associated with the Blockwerf Migmatite. (Green = granodiorite/dacite, blue = andesite)

The Gaarseep Granodiorite rocks which intrude the Blockwerf Migmatite have the same composition (granodiorite), however, show rather large variations in concentrations, slope and the size of the Eu anomaly. One of these samples also shows an elevated La/Yb ratio (Figure 4.20a), the single most important feature which distinguishes the Blockwerf Migmatite geochemically. The volcanics of the Kuams River Formation show a systematic increase in slope in the range from andesite to dacite, suggesting a fractional crystallization model for their development.

Multi-element diagrams in which the REE are not represented, do not distinguish the Blockwerf Migmatite from the rest of the batholith (4.1.4 Multi-element diagrams, Figure

4.7). The fact that immobile trace elements such as Ba, Nb, Ti, Zr and Hf do not distinguish the Blockwerf Migmatite migmatitic rocks from the rest of the batholith, illustrates that the processes leading to their development were similar, i.e., subduction-related. The steep slopes (high La/Yb ratios), large variations in overall concentrations and the presence of positive Eu anomalies in the Blockwerf Migmatite REE patterns, distinguish them from the other batholith rocks. These features suggest that the Blockwerf Migmatite owes its characteristic nature to primary differences in the source (which is hornblende-dominated), and not to later magmatic processes which acted during its evolution. It can therefore be concluded that the mafic enclaves to which the Blockwerf Migmatite owes its characteristic nature, represents xenoliths of its source, and not of the volcanics which it intrudes. This, along with field evidence indicating the presence of hybrid rocks, suggests a magma mixing model for the origin of the Blockwerf Migmatite.

Note that many of the rock types in the Blockwerf Migmatite are adakitic in nature, bearing evidence as to the origin of adakite and TTG in the Vioolsdrif Batholith (see 4.3.4 TTG and adakite in the Richtersveld Subprovince). The single most distinguishing feature of the Blockwerf Migmatite is the elevated La/Yb ratios. According to Haschke *et al.* (2006), REE fractionation is an indicator as to the depth of magma generation. The La/Yb, La/Sm as well as Sm/Yb ratios relate to the mantle domain in which melting occurs with the following serving as a rough guide:

a) depths of 30-35 km; source dominated by gabbroic compositions (clinopyroxene-bearing); La/Yb<20, La/Sm<4, Sm/Yb<3,
b) depths of approximately 40 km; amphibolitic source; La/Yb>20-30, La/Sm>4, Sm/Yb=3-5 (indicate MREE retention by amphibole),
c) depths>45-50 km; eclogite (garnet-bearing) source; La/Yb>30, Sm/Yb>5 (indicate HREE retention by garnet).

In Figure 4.21, values of the La/Yb ratio are contoured across the batholith and a cross section is constructed to show the anomalous crustal thickness underlying the Blockwerf

Migmatite during its development, relative to the rest of the batholith. The crustal thickness during the development of the Vioolsdrif Batholith is also compared with that of higher La/Yb ratios. The typical modern Andean arc has crustal thicknesses within the eclogite zone (up to 70 km crustal thickness). It is therefore clear that the Vioolsdrif Batholith developed on and in a relatively thin crust above the subduction zone.

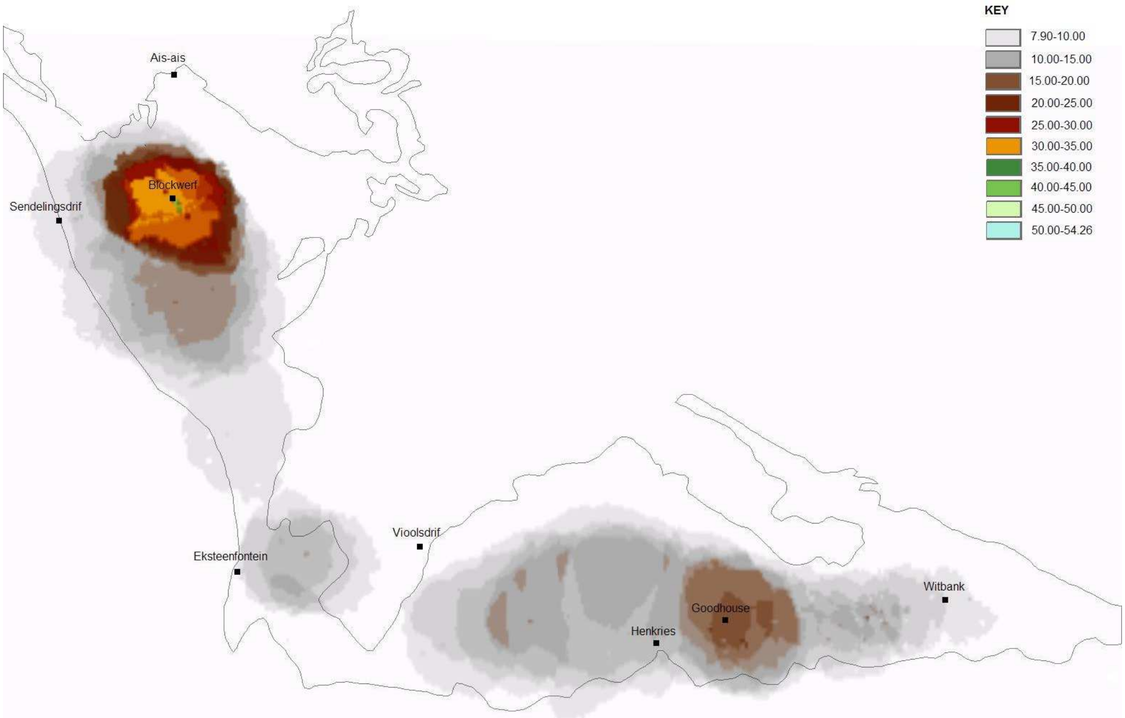

Figure 4.21(a): Distribution of La/Yb values in diorites, tonalites, granodiorites, andesites and dacites across the Vioolsdrif Batholith. To minimize the effects of fractional crystallization, samples of similar composition were used (tonalite-granodiorite for the Vioolsdrif Suite and dacites for the Orange River Group). An interpolation method of kriging was used as executed by the ArcGIS software computer program.

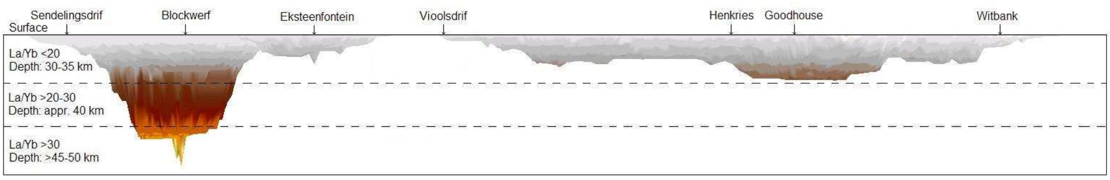

(b): A cross section to show inferred crustal thicknesses.

The Blockwerf Migmatite represents a more or less circular REE fractionation anomaly in the batholith. This suggests the Blockwerf Migmatite as being representative of a volcanic centre and supports the theory of Ritter (1980), envisaging a volcanic centre in the northeast of the Richtersveld area. The thickening of the crust underneath the unit may be explained by a process of mafic underplating.

If the Blockwerf Migmatite does represent a volcanic centre, any volcanics which originated from it will also bear the high La/Yb ratio signature. Figure 4.22 shows a plot of the La/Yb ratios vs. La for migmatites from the unit, the Gaarseep granodiorites associated with it, and all the Orange River Group samples for which REE analyses are available.

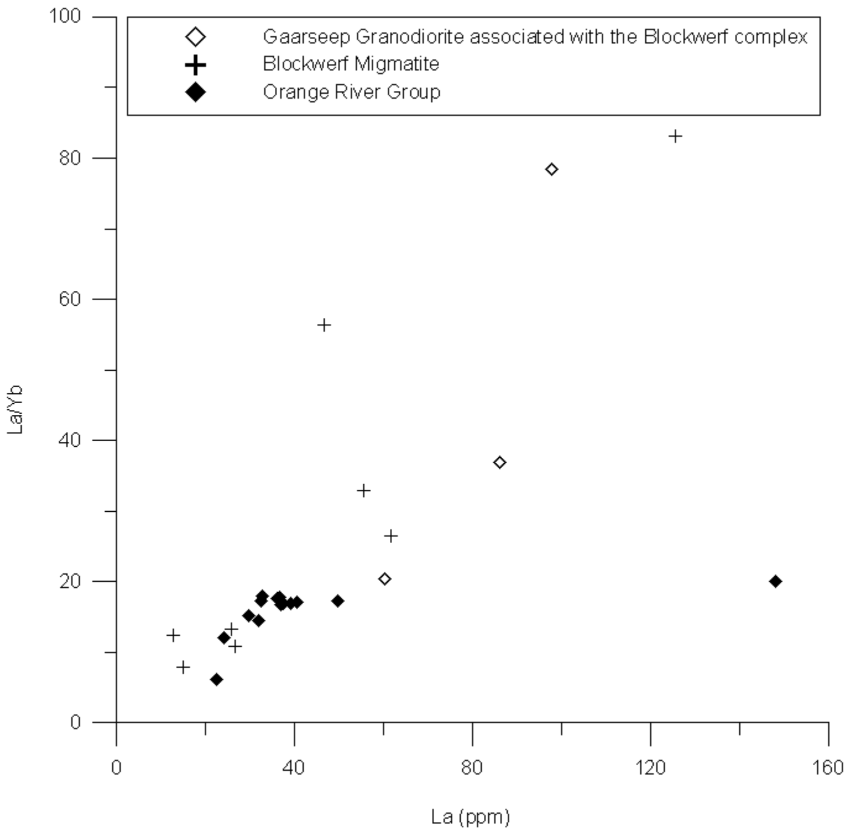

Figure 4.22: La vs. La/Yb for the Blockwerf Migmatite, the Gaarseep Granodiorite which intrudes it and all the samples from the De Hoop Subgroup for which REE analyses are available.

None of the samples from the Orange River Group, for which REE analyses are available, match the high La/Yb values displayed by the Blockwerf Migmatite. This means that, if the Blockwerf Migmatite does indeed represent a volcanic centre, it was not the source for any of the volcanic formations currently preserved within the batholith. However, the current REE analyses which are available for the Orange River Group are not sufficient to be considered representative of the group as a whole. Also apparent from Figure 4.22, is the fact that the granodiorites from the Gaarseep Granodiorite, although not included in the Blockwerf Migmatite and clearly intrusive into it, display some of the highest La/Yb ratios. This is to be expected if the theory of mafic underplating is accepted and they were generated above the same area.

4.2.6 Ramansdrif Subsuite

Geochemically, the granites of the Ramansdrif Subsuite correlate closely with the granites of the Goodhouse Subsuite, as well as the rhyolites of the Orange River Group, on Harker diagrams for all elements analysed (e.g., Figure 4.4) as well as multi-element diagrams (Figure 4.7). However, REE patterns show the Ramansdrif Subsuite granites to be lower in overall concentrations than the granites of the Goodhouse Subsuite, as well as its slope being flatter (Figure 4.11). This precludes the possibility that the Ramansdrif Subsuite represents the final stage of the Vioolsdrif Suite in a continuous fractional crystallization process.

The Ramansdrif Subsuite postdates the Goodhouse Subsuite by approximately 170 m.y. and initial $^{87}Sr/^{86}Sr$ ratios for the Ramansdrif Subsuite (Reid, 1977) suggests an origin through melting of pre-existing crust. The close correlation of the Ramansdrif Subsuite granites with the granites of the Goodhouse Subsuite on variation diagrams as mentioned above, suggests that the Ramansdrif granites could have been derived through partial melting of the granodiorites and tonalites of the Goodhouse Subsuite. This was also suggested by Reid (1977) after major and trace element modelling. Cornell *et al*. (2007) mentioned that the Ramansdrif Subsuite might actually not be genetically linked to the Goodhouse Subsuite but rather represents a magmatic event of its own, limited in extent and producing only felsic magmatism.

4.3 THE ORIGINAL TECTONIC ENVIRONMENT

The original extent of the Vioolsdrif Batholith is not known and subsequent deformation processes further obliterated much of the physical evidence related to the original tectonic environment. In modern convergent plate margins, the most distinctive feature is the magmatic arc – a linearly orientated feature, parallel to the subduction trench and associated with eruptive volcanic centers. Other characteristic features include turbiditic trench deposits, accretionary wedge deposits and diagnostic fore- and backarc assemblages. In the Vioolsdrif Batholith, most of these features, which are located at surface, have been eroded. The only significant sedimentary unit is the Rosyntjieberg Formation, which was interpreted by Ritter (1980) as a marine deposit, indicating a marine ingression towards the end of the volcanic cycle. He also inferred the presence of a volcanic centre in the northwest of the Richtersveld area, based on the distribution of the volcanic deposits. This is supported by the current study in the recognition of the Blockwerf Migmatite as a possible volcanic centre (4.2.7 Blockwerf Migmatite). However, the current configuration of these features in relation to their original settings is difficult, if not impossible, to assess, due to subsequent deformation.

In Figure 4.23, the Vioolsdrif Batholith is geometrically compared to Mesozoic-Tertiary batholiths in the Andean and North American arcs.

Based on a comparison with the Mesozoic-Tertiary batholiths, the preserved part of the Vioolsdrif Batholith represents but a fraction of the original one. Individual plutons in the Mesozoic-Tertiary batholiths have various orientations but collectively and on a regional scale, the batholiths' axes are parallel to the subduction trench. It is not possible to determine the arc axis of the Vioolsdrif Batholith on physical evidence.

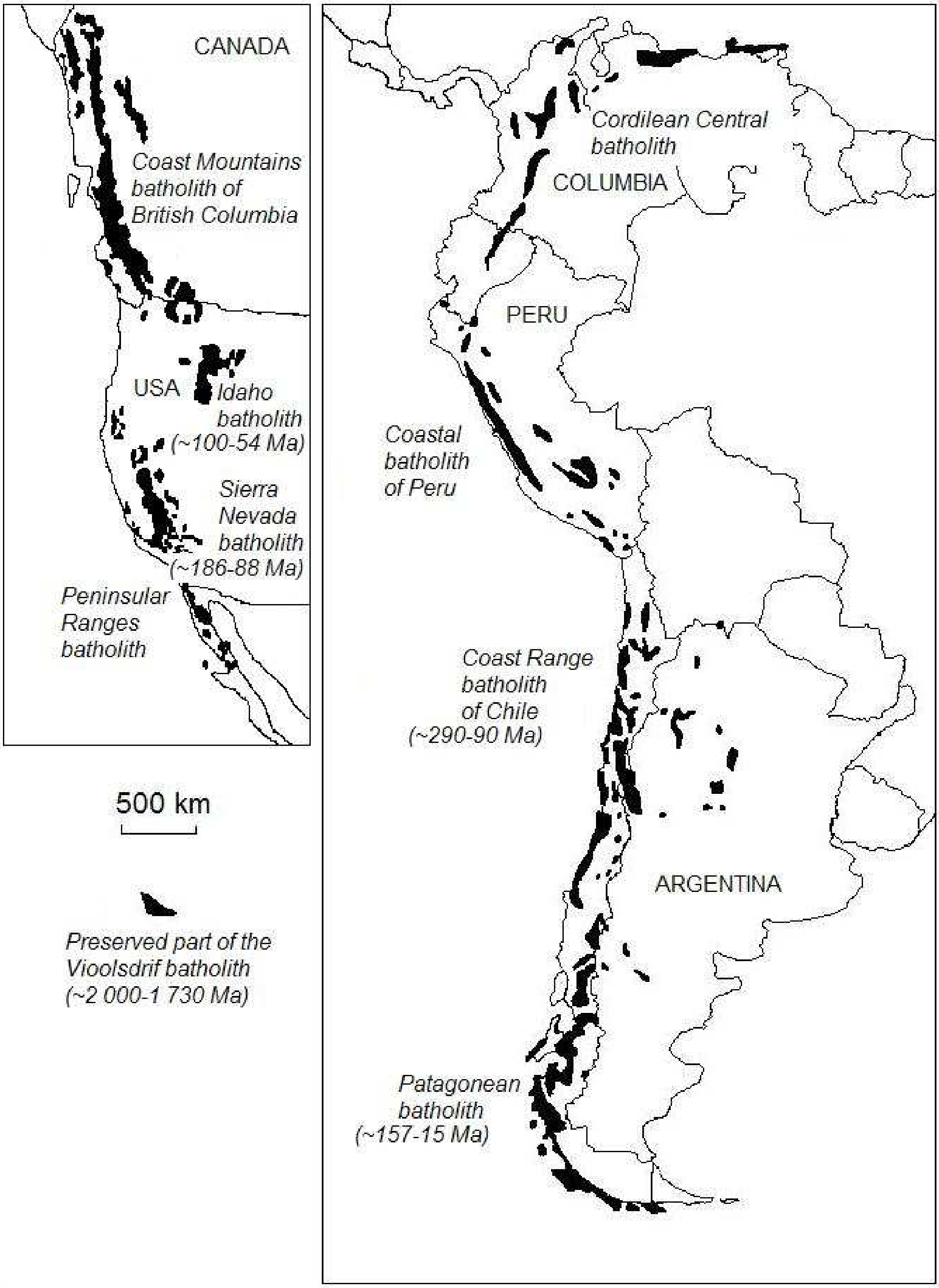

Figure 4.23: Comparison of scale between the Vioolsdrif Batholith and its Mesozoic-Tertiary counterparts.

Radiometric data indicate the Mesozoic-Tertiary batholiths to have developed in a time span of up to 200 m.y. (e.g. the Coast Range batholith of Chile; Parada *et al*., 1999). Some developed in as little as about 50 m.y. (e.g. the Idaho batholith; King *et al*., 2007). The preserved Vioolsdrif Batholith retains evidence of about 270 Ma if the Ramansdrif Subsuite is included. Note however, that the time span with which the Ramansdrif Subsuite postdates the main intrusion (Goodhouse Subsuite; 170 m.y.), is sufficient for an entire batholith to form. Still however, the preserved part of the Vioolsdrif Batholith retains evidence on a major span of its evolutionary history.

There are currently no alternative theories to that of modern-day subduction processes that can explain the tectono-magmatic evolution of the Vioolsdrif Batholith. Referring to the modern configuration Polat *et al*. (2011) state that, fundamentally, continental crust cannot grow, supercontinents cannot form, and arcs cannot generate melts over millions of years without subduction, collision, subduction of water, and slab dehydration or melting. Currently, convergent plate margins are the only tectonic settings where magmatic processes produce granitic bodies of batholithic extent and widespread felsic and andesitic magmas can only be produced in a plate tectonic regime (Condie, 2005b).

Based on various studies (e.g., Patchett, 1989; Hamilton, 1998; Condie, 2005a; Castillo, 2006), it seems likely that the tectonic crust-forming processes which operated on the earth during geological time, underwent dramatic changes during the Late Archean-Early Proterozoic. The formation of the Vioolsdrif Batholith coincides with the late stages of this period. Studies show that about half of the current crust on the earth was produced during the Archean and that it had a TTG composition (Patchett, 1989; Condie, 2005a; Castillo, 2006). Modern crust-forming processes produce precious little crust of that composition and also much less volumes of crust. According to Hamilton (1998), evidence of modern plate tectonic processes, such as obvious continental truncations, rifted margin assemblages and sutures, are only recognized from about 2.0 Ga.

Frost *et al*. (2001) introduced the modified alkali-lime index (MALI) as Na_2O+K_2O-CaO and delineated the fields occupied by the most common granite types of the world. In

Figure 4.24, the Vioolsdrif Batholith units are plotted on this diagram showing the fields for Mesozoic Cordilleran batholiths, Archean tonalitic gneisses and peraluminous leucogranites

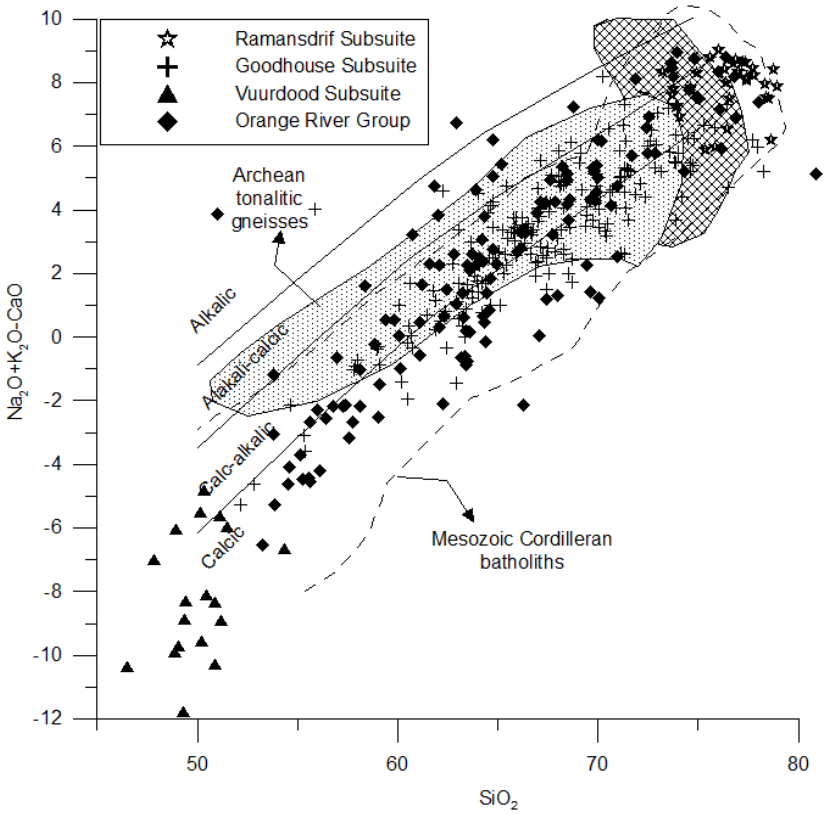

Figure 4.24: Units of the Vioolsdrif Batholith plotted on the SiO_2 vs. MALI diagram of Frost *et al.* (2001) with the fields for Mesozoic Cordilleran batholiths (broken line), Archean tonalitic gneisses (dotted surface) and peraluminous leucogranites (grated surface) indicated.

The Vioolsdrif Batholith coincides well with the field defined for Mesozoic Cordilleran batholiths. The Ramansdrif Subsuite plots in both the field defined for Mesozoic Cordilleran batholiths and peraluminous leucogranites.

The amount of iron enrichment relative to magnesium defines two distinct rock suites and Miyashiro (1974) showed that these two suites could be distinguished on a plot of FeO/(FeO+MgO) vs. SiO_2. The former ratio is commonly referred to as the Fe-number and numerous workers have shown that this plot of Fe-number vs. SiO_2 distinguishes between granites from two different tectonic settings, i.e., anorogenic and arc-related

(Petro *et al.*, 1979; Anderson, 1983; Maniar and Piccoli, 1989; Frost and Lindsley, 1991; Frost and Frost 1997). Frost *et al.* (2001) defined these fields and added those for Archean TTG and peraluminous gneisses, on a FeO(T)/FeO(T)+MgO vs. SiO_2 diagram. In Figure 4.25, the Vioolsdrif Batholith units are plotted on this diagram.

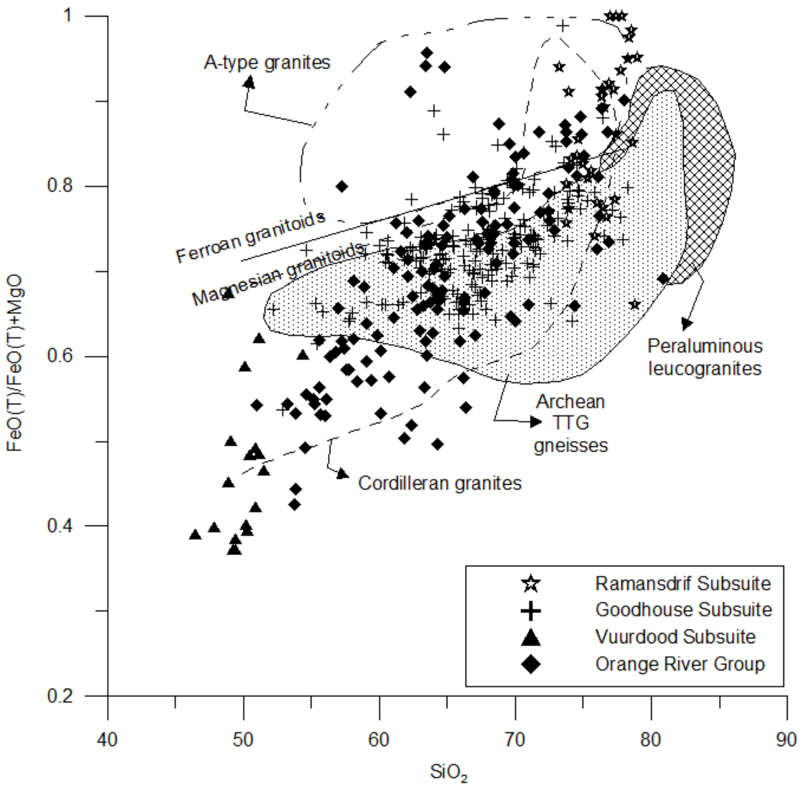

Figure 4.25: The Vioolsdrif Batholith plotted on the SiO_2 vs. Fe-number diagram of Frost *et al.* (2001).

Again, the Vioolsdrif Batholith shows a close affinity to the field for Cordilleran batholiths. The Ramansdrif Subsuite is not distinctly associated with any of the fields.

There is a rather wide variety of discrimination diagrams available on which data is compared with the fields defined by modern tectonic environments. These diagrams seldom provide unequivocal confirmation of a former tectonic environment and at best they can be used to suggest an affiliation for a suite as a whole, and not for single samples (Rollinson, 1993). For the current study, the Vioolsdrif Batholith has been plotted on a variety of discrimination diagrams including Ti-Zr-Y, Ti vs. Zr (normal scale), Ti vs. Zr (log scale) and Ti-Zr-Sr of Pearce and Cann (1973), Zr/Y vs. Zr of Pearce and Norry (1979), Cr vs. Y of Pearce (1982), Zr/Y vs. Zr of Pearce (1983), TiO_2-MnO-P_2O_5 of Mullen (1983) for basaltic compositions, and Nb vs. Y and Rb vs. Y+Nb of Pearce *et al*. (1984) for granitic compositions. All these diagrams identify a volcanic arc setting for the whole of the batholith. Figure 4.26 shows only two of these discrimination diagrams as examples for basaltic and granitic compositions in the batholith.

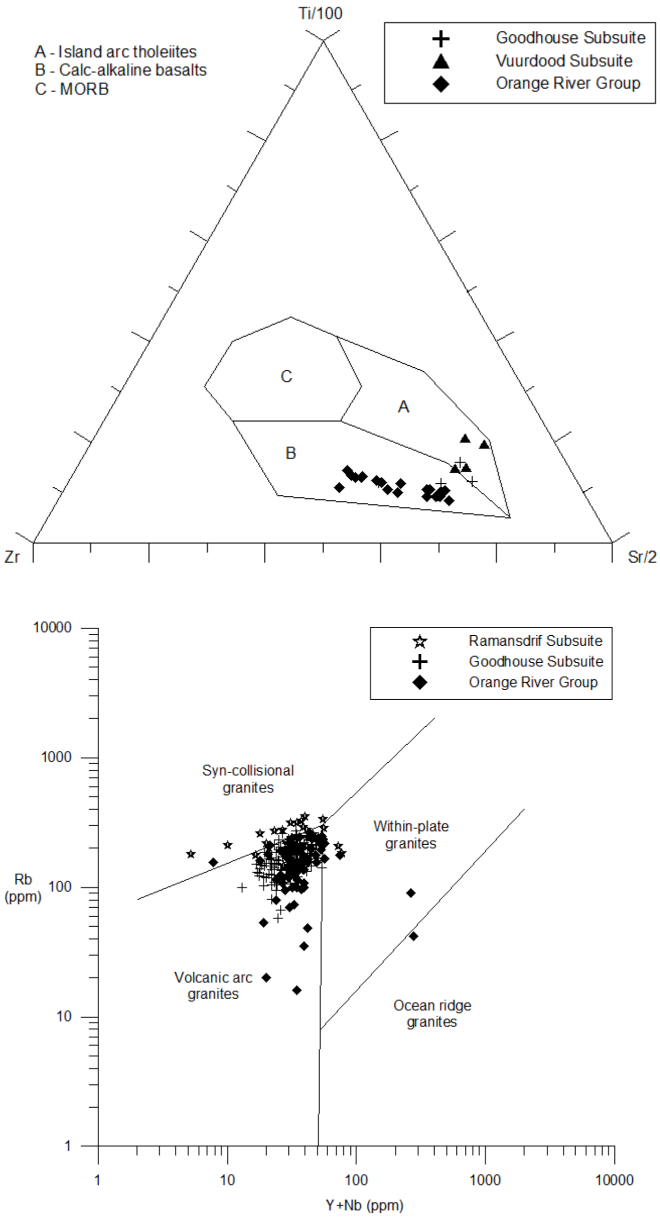

Figure 4.26: The units of the Vioolsdrif Batholith plotted on the Ti-Zr-Sr discrimination diagram of Pearce and Cann (1973) for basaltic rocks and the Rb-Y+Nb discrimination diagram of Pearce *et al*. (1984) for granitic rocks.

The Vuurdood Subsuite is identified as originating in an island arc environment, confirming its genetic relationship with the rest of the suite (e.g., Figure 4.26). This island arc origin for the Vuurdood Subsuite is confirmed and better illustrated by the log-transformed immobile trace element diagram of Agrawal *et al*. (2008), which distinguishes it more clearly from MORB and basalts originating in other tectonic settings (Figure 4.27).

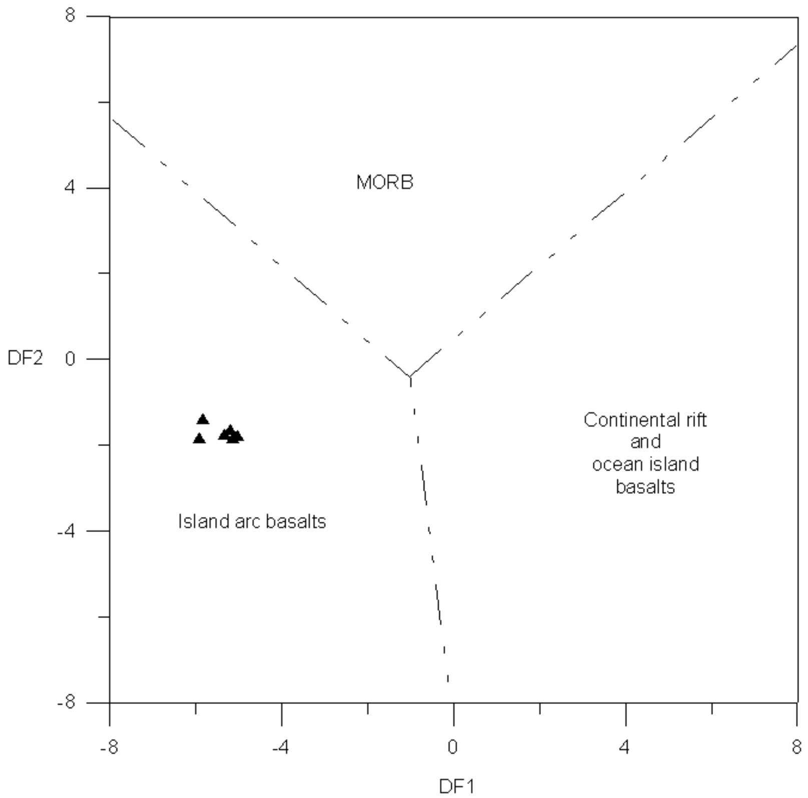

Figure 4.27: The Vuurdood Subsuite on a DF1-DF2 log-transformed immobile trace element tectonic discrimination diagram of Agrawal *et al*. (2008). [DF1 = 0.3518 * Log(La/Th) + 0.6013 * Log(Sm/Th) - 1.3450 * Log(Yb/Th) + 2.1056 * Log(Nb/Th) - 5.4763; and DF2 = -0.3050 * Log(La/Th) - 1.1801 * Log(Sm/Th) + 1.6189 * Log(Yb/Th) + 1.2260 * Log(Nb/Th) - 0.9944].

Ross and Bédard (2009) also defined fields for tholeiitic and calcalkaline basalts with the transitional field between them, on a diagram of Zr vs. Y. In Figure 4.28, the Vuurdood Subsuite is plotted, coinciding with the transitional field.

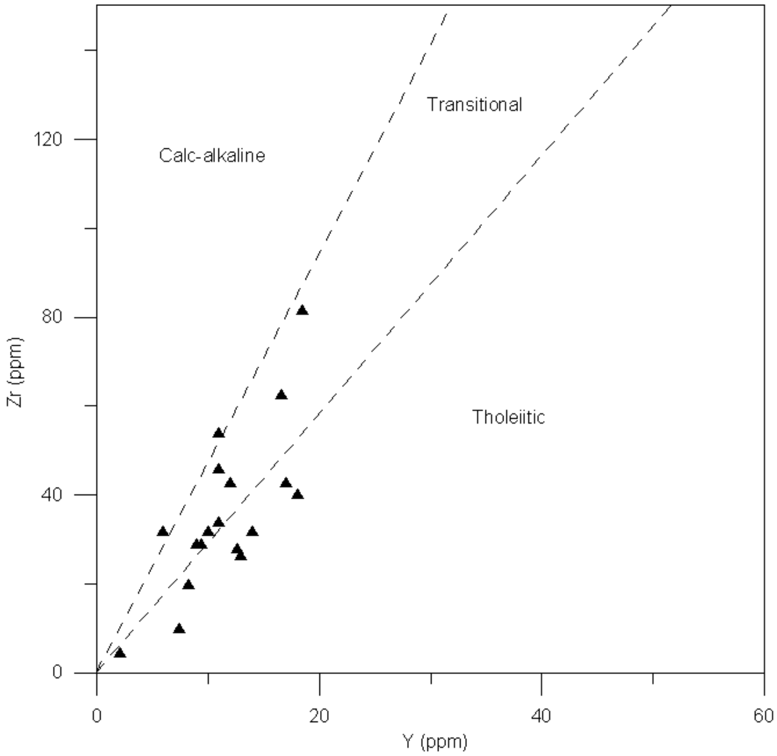

Figure 4.28: The Vuurdood Subsuite on a Y-Zr discrimination diagram (after Ross and Bédard, 2009).

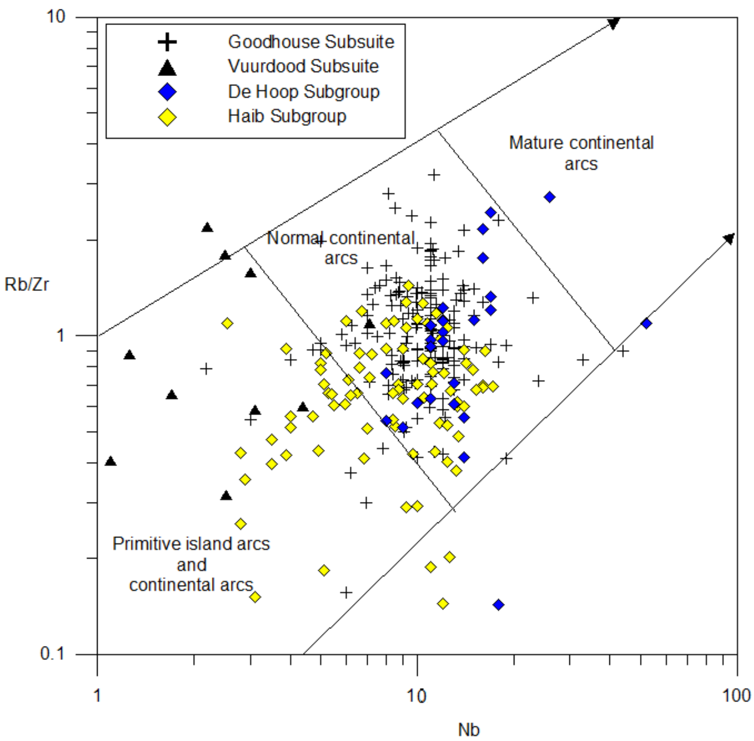

Figure 4.29: Plots of the various units of the Vioolsdrif Batholith on a Nb vs. Rb/Zr diagram indicating arc maturity after Brown *et al*. (1984).

Miyashiro (1974) showed that most arc systems have an older outer, and younger inner arc which is coupled with an increase in arc maturity with the gradual development of overlying continental crust. According to Brown *et al*. (1984), the maturity of a volcanic arc may be exhibited in the Nb contents and Rb/Zr ratio. Figure 4.29 shows a plot of the various units of the Vioolsdrif Batholith on a Nb vs. Rb/Zr diagram.

The Vuurdood Subsuite plots mostly in the field for primitive island and continental arcs. The Haib Subgroup shows a transition from this field into the field for normal continental arcs while the De Hoop Subgroup, along with most of the Goodhouse Subsuite, plots entirely in the latter field. This is in agreement with earlier evidence showing a gradational genetic relationship between the Vuurdood Subsuite and Haib Subgroup. It suggests a gradual development of the batholith from a primitive island arc to a normal continental arc starting with the Vuurdood Subsuite, through the Haib Subgroup to the rest of the batholith. The largest part of the batholith formed in the latter environment.

Certain lines of evidence strongly argue against the comparison of the Vioolsdrif Batholith with modern tectonic environments. Modern equivalents (e.g., the Andean arc), demand the presence of a thick overlying continental crust. This is the only way in which the average felsic composition and calcalkaline character can be accounted for in terms of modern theories. A survey of modern subduction arcs (Miyashiro, 1974) shows that the ratio of tholeiite:calcalkaline rocks in a batholith relates to crustal thickness with 0% calcalkaline rocks indicating crustal thicknesses of between 12-15 km, 10% of 15 km, 50% of 18-30 km and 60-95% of 30-70 km. The absence of basaltic volcanics and a basement to the Orange River Group in the Vioolsdrif Batholith may be explained in terms of deep erosion. However, the prevailing crustal thickness during its development may be inferred from the La/Yb ratios (Haschke *et al*., 2006). This was considered during the investigation of the Blockwerf Migmatite (4.2.5 Blockwerf Migmatite) and Figure 4.21 shows that only a small part of this uint matches such crustal thicknesses as is observed for modern arcs. In the Andean arc, crustal thicknesses vary between 30-70 km, the thickest being in the Central Volcanic Zone. The volcanic rocks also show abundant evidence of crustal contamination. No evidence of crustal contamination can be found in the Orange River Group with all elements correlating well with the concentrations in their intrusive counterparts. Therefore it can be inferred that the major part of the batholith developed in a tectonic terrane of which the crustal thickness cannot be compared to modern equivalents.

If the La/Yb ratios are considered in relation to age, no indication can be found of a gradually thickening overlying crust. La/Yb ratios in the Orange River Group (the oldest among the units) are between 15-20, while that in the youngest granites (from the Gaarseep in the Richtersveld area, intruding the Rosyntjieberg Formation) resembles that of the oldest units. La/Yb ratios in the Khoromus Tonalite (the oldest unit in the Goodhouse Subsuite) are more or less similar to that of the youngest granites in the Gaarseep (Richtersveld area).

4.4 TTG AND ADAKITE IN THE RICHTERSVELD SUBPROVINCE

The recognition (or non-recognition) of a tonalite-trondhjemite-granodiorite (TTG) rock association and adakites in granitic batholiths has become an important topic especially since the work of Barker (1979). TTG suites dominate the earth's Archean crust and their geochemical similarities to modern adakites has been taken by many as an indication that similar tectonomagmatic processes to the modern ones have been active throughout earth's history (Drummond and Defant, 1990; Martin, 1999; Martin *et al*., 2005; Van Tonder and Mouri, 2010). According to Condie (2005a), the fact that similar types of granitoids are recorded from the earliest times, suggest that similar processes of their origin to the present ones were already operational on the early earth (the oldest accretionary orogens recorded date back to 4.0 and 3.9 Ga namely the Acasta and Amitsoq TTG gneisses in northwest Canada and Greenland). As such, Archean processes have been studied at the hand of those acting on the earth today.

Modern adakite was first identified by Kay (1978) from the Adak Island in the western section of the Aleutian arc volcanic chain and the term was defined by Defant and Drummond (1990) who showed that their geochemical character suggested an origin by partial melting of hydrated mafic source rocks containing garnet. Many observations favour the derivation of adakitic magmas from partial melting of the subducting oceanic slab in volcanic arc tectonic settings. However, although the original definition of adakite referred specifically to rock generated from the melting of slab basalt, later studies have shown that adakite magma may be produced in tectonic settings which are unrelated to subduction in both arc and non-arc settings (Castillo, 2006). Furthermore, while Archean TTG is compositionally similar to modern adakite, it is not so to modern TTG and according to Condie (2005a), studies have shown that TTG and adakite are not the same and have different origins.

Nowhere on earth today are adakitic magmas being produced in volumes comparable to those in the Archean. For the generation of such large volumes of TTG as found in the Archean crust, slab melting is not the most effective mechanism, unless a higher geothermal gradient acted in the Archean (Castillo, 2006). In the Archean, higher mantle geotherms may have resulted in subducting slabs reaching partial melting temperatures at shallower dephts before dehydration rendered the slab infusible (Richard and Kerrich, 2007). Alternative models for the generation of adakitic magma include fractional crystallization of basaltic melts (Arth and Hanson, 1975), partial melting of mantle rocks (Moorbath, 1975) and partial melting of pre-existing tonalites (Johnson and Wyllie, 1988). Kay *et al*. (1999) proposed a model of crustal thickening in the Central Volcanic Zone of the Andes and melting of the lower crust to explain the origin of TTG magmas in that area. Richard and Kerrich (2007) state that key adakitic geochemical signatures, such as low Y and Yb concentrations and high Sr/Y and La/Yb ratios, can be generated in normal asthenosphere-derived tholeiitic to calcalkaline arc magmas by common upper plate crustal interaction and crystal fractionation processes and do not require slab melting. Common upper plate magmatic processes such as melting-assimilation-storage-homogenization (MASH) and assimilation-fractional-crystallization (AFC) affecting normal arc magmas can be demonstrated to explain the distinctive compositions of most adakite-like arc rocks.

The Archean crust (presently representing approximately 15% of the total continental crust) is dominated by tonalites and trondhjemites (low-K granitoids) which are characterized by sharply stoping REE patterns indicating the presence of garnet in the source residual phase (Sobolev, 1991). During the late Archean, TTG compositions started to change (Rollinson, 2005) and by about 2.5 Ga, K-rich granites and granodiorites started to appear and the crust became mainly granodioritic (Sobolev, 1991). This, according to Sm/Nd isotope evidence, coincided with a major period of continental crust formation (about 60% of the present bulk). During post-Proterozoic times, the earth's granitoids have become more acidic and richer in K (representing approximately 25% of the current total continental crust). The genesis of the Vioolsdrif Batholith therefore coincides with the era which followed relatively shortly after the change of the earth's crust bulk composition from TTG-dominated towards K-rich, granodioritic-dominated. On the modern earth, calcalkaline magmatism such as that represented by the Vioolsdrif Batholith, is typical of continental margin subduction tectonism of which the Andean chain represents the type area. Adakite magmatism is currently volumetrically minor compared to normal granitoids (as opposed to the Archean), not only worldwide but also in the localities where they occur (Castillo, 2006).

Archean TTG are typified by high Na_2O (>4%) and low K_2O (<3%). The CaO of Archean TGG is also lower than Cordilleran TTG which causes their modified alkali lime index (MALI; Frost *et* al., 2001) to be higher. As such, the Na_2O vs. K_2O and K_2O vs. MALI classification diagrams of Frost *et* al. (*op cit.*) can distinguish Archean TTG suites and Mesozoic Cordilleran batholiths. In Figures 4.30 and 4.31, the Goodhouse Subsuite and Orange River Group are plotted on these diagrams.

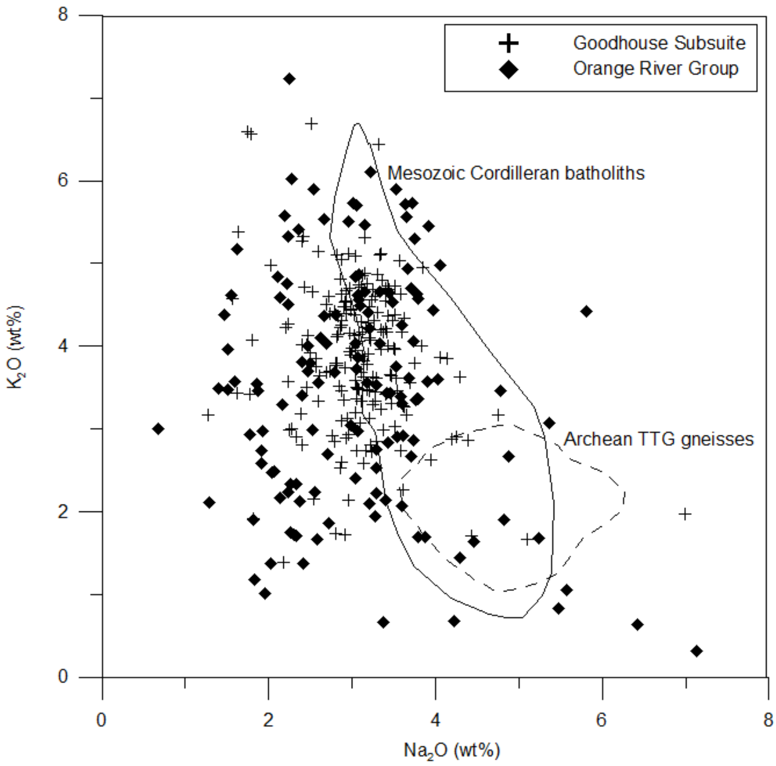

Figure 4.30: A Na_2O vs. K_2O plot for the Orange River Group and Goodhouse Subsuite after Frost *et al*. (2001).

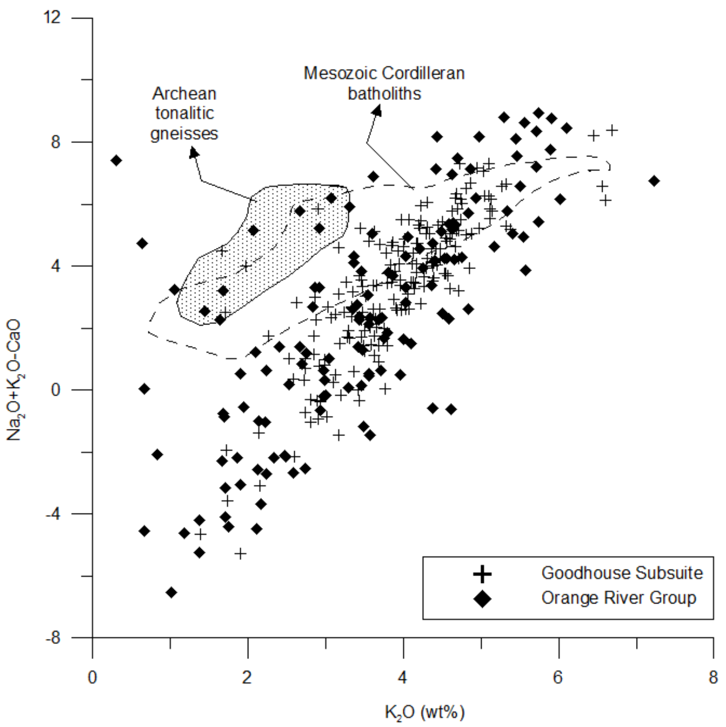

Figure 4.31: The Goodhouse Subsuite and Orange River Group on a K_2O vs. MALI diagram after Frost *et al*. (2001).

On both diagrams, the Vioolsdrif Batholith rocks show a closer affinity with Mesozoic Cordilleran batholiths than with Archean TTG. Note however that the Vioolsdrif Batholith does not coincide entirely with the field defined by the Cordilleran batholiths on either of the two diagrams. Especially the Na_2O content of the Vioolsdrif Batholith is on average lower than that of the Cordilleran batholiths.

In recent years, TTG suites have been further subdivided following the recognition of sanukitoid (a high-Mg, -Ni and -Cr type TTG; Smithies and Champion, 2000) as well as the Closepet-type granite, the latter differing from sanukitoid in having higher K_2O:Na_2O ratios and being relatively enriched in Ti, Nb and Zr (Van Tonder and Mouri, 2010). As such, the MgO, Mg#, Cr, Ni and K_2O contents distinguish sanukitoid and Closepet-type granite from TTG (Martin *et al*., 2005). Sanukitoids are also strongly enriched in LREE, Ba, Sr and P (Rollinson, 2005).

Recognizing TTG and adakite in a granitic batholith may be a matter of chance since, in the field, their physical appearance much resemble normal granitoids. Their distinction is entirely based on their unique geochemical properties. The sampling distribution on the Vioolsdrif Batholith for the current study is thought to include all the compositional variations. Unfortunately, the lack of REE analyses for the Haib Subgroup represents a significant limitation to the study since the La/Yb ratio is a critical factor in the recognition of adakitic rocks. This ratio bears on the single most distinguishing characteristic of adakitic rocks namely a depletion in HREE, indicating the involvement of garnet and/or amphibole in the source. High Sr contents and Sr/Y ratios are the second prerequisite for distinguishing adakitic magmas, the former indicating the presence of plagioclase in the melt and/or its absence in the source, the latter again referring to the presence of garnet and/or amphibole in the source since Y behaves similar to the REE in its compatibility. The behavior of plagioclase may also be displayed in the absence of an Eu anomaly. Early Archean TTG typically do not show a negative Eu anomaly in their REE patterns while post-2.5 Ga TTG do (Condie, 2005a). The behavior of the HREE, Y and Sr therefore represent the most unique characteristics distinguishing adakitic magmas from normal granitoids and the two almost universally used diagnostic tools to identify adakite are the Sr/Y vs. Y and La/Yb vs. La diagrams (Castillo, 2006). Most adakitic rocks also have relatively high Al_2O_3 contents, indicating high-pressure melting of garnet-containing source rocks (eclogite) or amphibolite.

The presence of a primitive component (high MgO, Ni and Cr) in sanukitoids indicates the involvement of a peridotitic mantle in the generation of the melt. Since the absence of such features suggests that the peridotitic mantle wedge was not involved in the generation of the magmas, the conclusion may be drawn that normal TTG magmas originate from melting in the lower crust above the mantle wedge, while sanukitoid magmas originate from melting in the subducting slab beneath the mantle wedge. This model demands the presence of a thick continental crust for the generation of normal TTG magmas (high La/Yb ratios indicates melting in the amphibole-garnet stability parts of the mantle). Characteristics such as depletion in Nb, Ta and Ti are also very common to adakites worldwide, however, in the light of studies showing that adakites are not limited to subduction zone settings, these cannot be considered prerequisites for identifying adakites in a particular suite. After consideration of parameters set in Defant and Kepezhinskas (2001), Condie (2005a), Rollinson (2005) and Castillo (2006), the following criteria were selected for recognition of adakitic and TTG rocks in the Vioolsdrif Batholith:

a) SiO_2 > 56 wt%
b) Al_2O_3 > 15 wt% at 70% SiO_2
c) Sr > 300 ppm
d) Y < 20 ppm
e) Sr/Y > 20
f) Yb < 1.9 ppm
g) La/Yb > 20

These parameters require derivation by hydrous partial melting of mafic rocks (garnetiferous or amphibolite) at high pressure. The La/Yb and Sr/Y ratios considered to typify adakite and TTG differ significantly in literature between >40 and >20. A ratio of

>40 applies strictly to adakite and early Archean TTG, while that of >20 also takes into consideration post-2.5 Ga and later calcalkaline suites, which also have overall lower Al_2O_3 values. Condie (2005a) states that Archean high-Al TTG and adakites both have steep REE patterns while most post-Archean TTG belong to the calcalkaline suite and often show a fractional crystallization sequence extending from diorite (or gabbro) to granite. These rocks typically have very low La/Yb ratios and exhibit a large range of Yb values. These observations are applicable to the Vioolsdrif Batholith.

From an inspection of the analyses for the Vioolsdrif Batholith, a number of samples can be identified as adakitic. They are listed in Table 4.

Table 4: A list of samples from the Vioolsdrif Batholith which have adakitic compositions.

Nr.	**Unit**	**Rock type**	**SiO_2 (wt%)**	**Al_2O_3 (wt%)**	**Sr (ppm)**	**Y (ppm)**	**Yb (ppm)**	**Sr/Y**	**La/Yb**	**Al_2O_3 at SiO_2 = 70%**
CHM95	Blockwerf Migmatite	Migmatitic tonalite	64.89	15.38	468	16	1.6	29.25	32.86	13.12
CHM100	Blockwerf Migmatite	Migmatitic tonalite	62.61	17.77	446	8	0.8	55.75	56.43	14.19
CHM101	Gaarseep Granodiorite (intruding the Blockwerf Migmatite)	Granodiorite	67.50	15.69	309	12	1.2	25.75	78.4	14.45
CHM166	Gaarseep Granodiorite	Tonalite	64.30	16.34	556	16	1.6	34.75	26.89	13.75
CHM56	Xaminxaip River Granodiorite	Granodiorite	69.75	14.96	387	12	1.5	32.25	23.11	14.84
CHM76	Xaminxaip River granodiorite	Granodiorite	70.49	14.44	338	13	1.5	26	22.31	14.68
CHM192	Gaarseep Granodiorite	Granodiorite	70.42	14.68	402	12	1.2	33.5	30.32	14.89
CHM78	Gaarseep Granodiorite	Granodiorite	69.86	14.57	349	10	1.7	34.9	24.21	14.50
CHM98	Blockwerf Migmatite	Granodiorite	63.87	16.05	535	20	1.5	26.75	83.09	13.29

In accordance with the batholith's calcalkaline nature, Al_2O_3 contents are relatively low as are the La/Yb ratios. A number of samples which closely comply to the set parameters were excluded from this list (some only because their adakitic nature could not be confirmed by available REE analyses) but the samples in Table 4 are sufficient to indicate the overall representation of adakitic rock types in the Vioolsdrif Batholith as a whole. Volume-wise they represent but a small fraction of the batholith. They do not represent a single magmatic event and do not show intrusive contact relationships with their host rocks. Rather, they represent compositional varieties within the calcalkaline granitoids. The Blockwerf Migmatite is clearly distinguished as a unique unit, containing a high concentration of adakitic rocks. However, not even this unit is entirely adakitic in composition. The only samples from the batholith of which the La/Yb ratios comply to the >40 value characteristic of type-adakites, are from this unit.

When the adakitic rocks of the Vioolsdrif Batholith are plotted on the $La_{(n)}$ vs. $La/Yb_{(n)}$ and Y vs. Sr/Y diagrams (Castillo, 2006), only a few (consistently from the Blockwerf Migmatite) comply with type examples (Figure 4.32). These figures primarily indicate the absence of garnet in the source for most samples, however, an amphibolitic source may be deduced. The relatively low Sr/Y ratios furthermore indicate the influence of plagioclase fractionation during the batholith's evolution, leading to low Sr values, and is again related to its calcalkaline character.

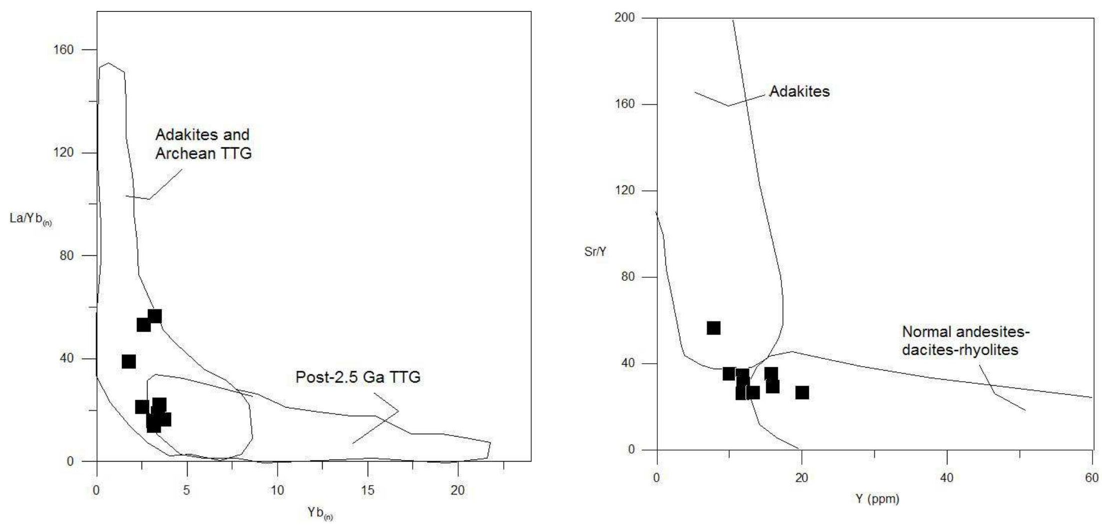

(a) (b)

Figure 4.32: Adakitic rocks of the Vioolsdrif Batholith plotted on the $Yb_{(n)}$ vs. $La/Yb_{(n)}$ (a) and Y vs. Sr/Y (b) diagrams of Castillo (2006).

While the composition of adakites does correspond to that of Archean TTG, they do not correspond to modern TTG. Post-2.5 Ga TGG have higher K_2O:Na_2O ratios than

Archean TTG and the two can be distinguished on a plot of K_2O vs. Na_2O (Figure 4.30). According to Castillo (2006), they may also be distinguished on a plot of $CaO+Na_2O$ vs. Sr (Figure 4.33). On both these diagrams, the Vioolsdrif Batholith shows similarities to modern TTG suites.

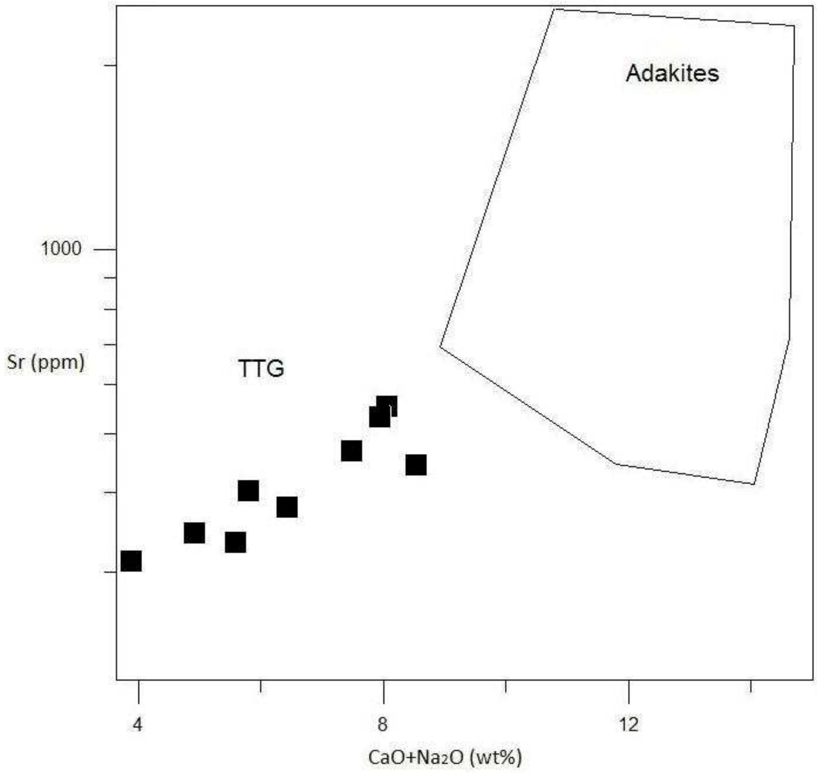

Figure 4.33: Plots of Vioolsdrif adakitic rocks on a $CaO+Na_2O$ vs. Sr diagram after Castillo (2006).

The presence or absence of a primitive component, implying the involvement of peridotitic mantle in the generation of the magmas, may be displayed on a variety of diagrams taking into account variations in MgO (or Mg#), TiO_2, Cr and Ni. Figure 4.34(a) shows the adakitic rocks of the Vioolsdrif Batholith on a diagram of SiO_2 vs. Mg# according to which normal TTG magmas are considered products of melting in the lower crust, while adakitic magmas are considered products of melting of a subducting slab (Condie, 2005a). Figure 4.34(b) shows the Vioolsdrif Batholith adakitic rocks plotted on a diagram of Cr vs. Ni, which indicates the presence of a primitive component.

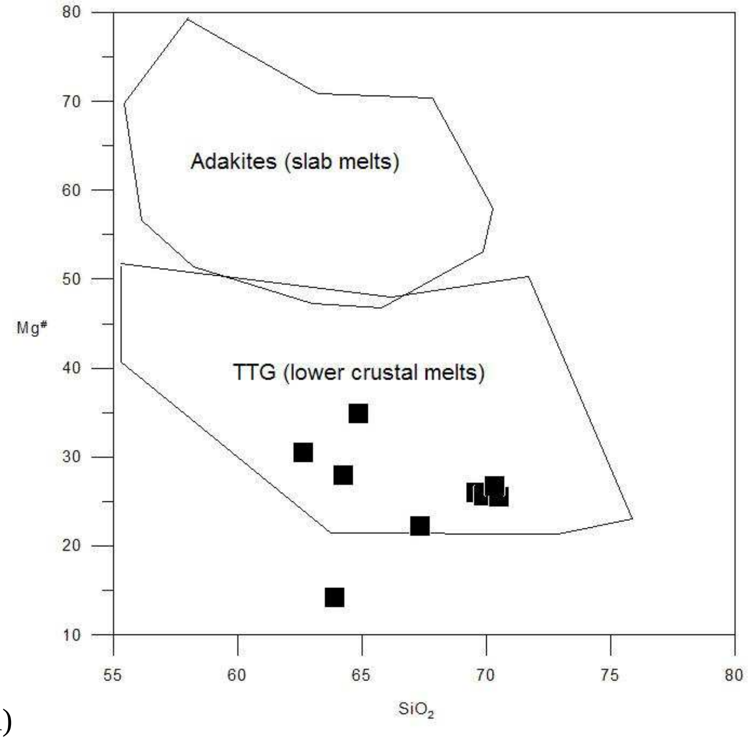

(a)

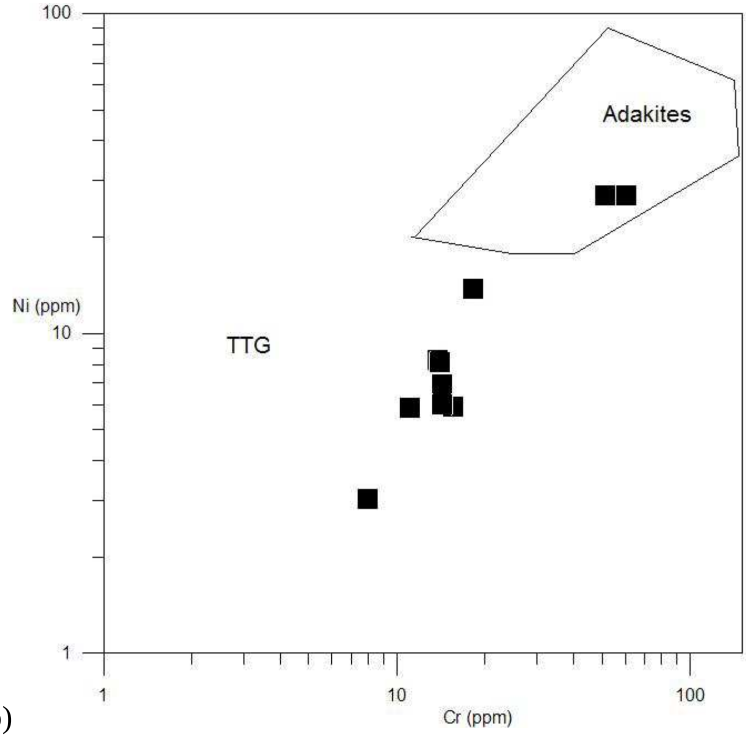

(b)

Figure 4.34: The Vioolsdrif Batholith adakitic rocks plotted on diagrams of SiO_2 vs. Mg# (a) and Cr vs. Ni (b). Both diagrams are after Condie (2005a).

Some conclusions can be drawn from the study concerning the recognition of adakitic and TTG rocks in the Vioolsdrif Batholith.

a) The fact that adakitic rocks in the batholith did not intrude as unique intrusive events (showing intrusive contact relationships with country rock) but merely represent compositional varieties within the calcalkaline granitoids, strongly argues in favour of a magma mixing model involving the mixing of primary adakitic magmas with non-adakitic magmas. This is supported by the inferred magma mixing model for the development of the Blockwerf Migmatite (4.2.5 Blockwerf Migmatite), in which the adakitic rocks occur most frequently.

b) High La/Yb ratios are commonly related to a thick overlying crust (Planck and Langmuir, 1988; Mantle and Collins, 2008) as has been amply shown for the Andean margin (Kay *et al*., 1999, Hashcke *et al*., 2002, Hildreth and Moorbath, 1988). La/Yb ratios for the Vioolsdrif Suite suggest that the evolution of the batholith was not associated with a thick overlying crust. Therefore, the anomalously high La/Yb ratios (compared to the rest of the batholith) for the Blockwerf Migmatite imply a very uneven crustal base for the batholith. This can be achieved by a process such as mafic underplating.

c) If modern adakite and Archean TTG share similar genetic processes then, if anything, it shows that processes of crust formation in the Archean cannot be compared to those on the modern earth. In the Archean these processes produced vast volumes of magmas while on the modern earth, they produce relatively little. The fact that the changing bulk composition in the earth's crust from TTG in the Archean to granodiorite-granitic after 2.5 Ga coincided with a major period of continental crust formation, surely cannot be considered coincidental. It implies major (and rather abrupt) changes in crust formation processes from the Archean to present. For the early Archean, processes involving large-scale melting of deeper parts of the mantle (not necessarily involving any overlying crust) are implied. The fact that Archean TTG on average have higher contents of fluid-mobile elements like Ba, K and Rb than adakites (Condie, 2005a), attests to higher rates of metasomatism in the upper mantle, which are today commonly thought to be active in the mantle wedge overlying the subducting plate.

5. CONCLUSIONS

5.1 SUBDIVISIONS

The proposed subdivision of the Vioolsdrif Batholith in South Africa and within the currently accepted boundaries is shown on the map at the back of this thesis. It largely follows the subdivisions from previous studies. The major and trace element evidence presented in this study, along with isotope and radiometric evidence from previous studies, indicate that the whole batholith formed from a common source during the Orange River orogeny which started around 2.0 Ga.

This study presents geochemical evidence for the subdivision of the Orange River Group into the Haib and De Hoop Subgroups, a subdivision which was previously based entirely on field evidence. It has been shown that the Haib Subgroup shows a genetic relationship with the Vuurdood Subsuite, the latter of which may be interpreted as remnants of the primary, mantle-derived magmas. The De Hoop Subgroup does not show this genetic relationship with the Vuurdood Subsuite.

Since the two subgroups of the Orange River Group occupy two distinct geographical areas – the Haib and Richtersveld areas, separated by an area of no outcrop (cover by younger strata) – the implication of this subdivision is that the two geographical areas may represent two significantly different parts of the batholith. In the Haib area, not only the Haib Subgroup but also the Goodhouse Subsuite, is on average more mafic than the Richtersveld part of the batholith. Both the Vuurdood Subsuite and Khoromus Tonalite, the most mafic members of the Vioolsdrif Suite, are limited to the Haib area and do not occur in the Richtersveld. The Vuurdood Subsuite comprises mafic-ultramafic bodies, which can be expected to be limited to the lower parts of the crust, since such magmas would not be able to rise to higher crustal levels through normal magmatic processes, due to their high densities. The Haib Subgroup contains virtually no interlayered metasediments. In the Haib area, contact relationships between the volcanic group and the plutonic suite suggest intrusion at the root zone of the volcanic pile. In the

Richtersveld, on the other hand, intrusive relationships between the volcanics and the plutonic rocks are mostly concordant. The De Hoop Subgroup contains a relatively high proportion of interlayered metasediments and the Rosyntjieberg Formation represents a rather thick, mature metasedimentary unit, overlying the volcanics. The Kook River Formation, an entirely porphyrytic unit, and the Xaminxaip River Granodiorite have both been considered to represent subvolcanic units (Ritter, 1980). These observations suggest that the Richtersveld may represent an area in which the upper part of the batholith has been preserved, while the Haib area represents a deeper crustal part of the batholith. Furthermore, tectonic environment discrimination diagrams suggest that the Haib Subgroup was formed in a primitive arc environment, while the De Hoop Subgroup was formed in a normal continental arc environment. This suggests that the Haib area represent the initial stages, while the Richtersveld area represents the later stages, in the batholith's evolution.

The subdivision of the De Hoop Subgroup according to the scheme of Ritter (1980) may be controversial since it is largely based on a theory envisaging development from a volcanic centre in the northeast of the Richtersveld. This study identifies the Blockwerf Migmatite as a possible volcanic centre. However, none of the volcanic rocks of the De Hoop Subgroup which were analyzed for REE in this study bears the unique La/Yb signatures of the Blockwerf Migmatite. This means that the De Hoop Subgroup as it is currently exposed, probably did not originate from this unit. However, the geochemical variations within the subgroup presented in this study do not motivate for any alternative subdivision scheme.

Based on its clear association with the rest of the batholith on variation diagrams, the Vuurdood Subsuite is considered here as remnants of the primary source magmas. Multi-element diagrams show that this subsuite was subjected to the same magmatic processes as the rest of the batholith while initial isotope signatures and REE patterns show that it shares a similar source. Some of the ultramafic rocks in the subsuite are considered to represent cumulate material which formed in shallow crustal magma chambers during fractional crystallization.

The Goodhouse Subsuite is subdivided into four units. The Khoromus Tonalite, based on contact relationships and radiometric evidence, is the oldest unit in the subsuite. It is the most mafic unit in the subsuite and shows limited gradation from the Vuurdood Subsuite on classification and variation diagrams. Field and petrographic evidence of possible magma mixing processes are to be found in this unit.

The Xaminxaip River Granodiorite also shows intrusive relationships with the Gaarseep Granodiorite, showing the latter to be intrusive into the former. The Xaminxaip River Granodiorite and Khoromus Tonalite are not found in contact with each other but a single zircon age for the Xaminxaip River Granodiorite shows it to be of similar age as the Gaarseep Granodiorite. Therefore, the Xaminxaip River Granodiorite is placed chronologically between the Khoromus Tonalite and the Gaarseep Granodiorite. The Xaminxaip River Granodiorite is thought to represent a subvolcanic unit, in agreement with Ritter (1980).

The development of migmatite in places in the Xaminxaip River Granodiorite can be explained in terms of locally existing high grade metamorphic conditions in shallower parts of the crust during orogenic processes (as described by Mehnert, 1968), together with the simultaneous intrusion of the Gaarseep Granodiorite on regional scale (in agreement with De villiers and Söhnge, 1959). According to Mehnert (*op cit.*), much evidence suggest that migmatites, as currently exposed at surface, did not form at the base of the crust or at depths of 15-20 km, as should be assumed from experimental data if a normal geothermal gradient of 30-40°C/km is postulated. Rather it has to be assumed that the metamorphic conditions necessary for their partial melting was dragged upwards into relatively shallow depths by orogenic processes. The geothermal gradient may reach 5-150°C/km in orogenic belts, whereby all the metamorphic zones can occur side by side within a rather small area, including those of partial or complete melting, at about 4-10 km depths.

The Gaarseep Granodiorite is the main phase of the currently exposed Vioolsdrif Batholith and spans the entire compositional range represented by the other units (except the ultramafic rocks of the Vuurdood Subsuite) as well as their geographical distribution. It is the only unit which occur in both the Haib and Richtersveld areas but is on average more mafic in the Haib area than in the Richtersveld.

The Hoogoor Granite is the only unit considered in this study which is located outside the batholith type area and bears the pervasive foliation and metamorphism of the Namaqua orogeny. Its inclusion in the batholith may indeed remain controversial but based on the available radiometric and geochemical evidence, it is considered here as part of the Goodhouse Subsuite. All of its major and trace element variations coincide with similar compositions in the rest of the batholith. Currently available radiometric data supports its contemporaneous development with the granodioritic rocks of the Gaarseep Granodiorite (~1.89 Ga; Moen and Toogood, 2007).

The Ramansdrif Subsuite postdates the main intrusion by about 300 m.y. (e.g., Cornell *et al*., 2007). It is regarded here as the product of partial crustal melting of the older phases of the Vioolsdrif Batholith during the final stages of the Orange River orogeny. Within the Ramansdrif Subsuite, the further subdivision into the Ghaams and Sout Granites can be justified on three criteria: texturally the Sout Granite is consistently coarser grained than the Ghaams Granite; petrographically the Sout Granite is microcline-dominated with abundant exsolution textures while the Ghaams Granite is orthoclase-dominated with only minor development of exsolution textures; geochemically the Ghaams Granite is on average less felsic than the Sout Granite. Petrographically and geochemically all the occurrences of the Ramansdrif Subsuite which are located within the Hoogoor Granite, can be correlated with the Ghaams granite.

5.2 MAGMATIC PROCESSES AND TECTONIC ENVIRONMENT

All the evidence relate the Vioolsdrif Batholith to modern continental margin subduction zone tectonic settings. The initial stages of its development, represented by the

Vuurdood Subsuite and part of the Haib Subgroup, may be comparable to a primitive continental arc setting. The absence of basaltic compositions in the volcanic succession argue against an intra-ocean island arc setting. There is also no evidence to be found that any of the volcanic units were deposited under water. In fact, the characteristics of the volcanic rocks call for deposition on a continental crust. The bulk chemical composition of the batholith furthermore demands the presence of an overlying continental crust, in terms of modern tectono-magmatic theories. Leake (1983), among others, states that granite liquids cannot be derived as primary melts from either mantle peridotite or subducted oceanic crust. Atherton and Tarney (1979) state that, over the past few years, evidence have amassed for mixed mantle-crust origin for many granitic rocks. In the Vioolsdrif Batholith, the earliest phases have rhyolitic compositions.

In the Vioolsdrif Batholith, no evidence can be found of pre-existing crust and isotope data argue against it. Modern continental margin volcanic arcs are underlain by thick continental crust and the volcanic rocks show clear evidence of crustal contamination. For the Vioolsdrif Batholith, La/Yb ratios indicate that the crustal thickness during its development cannot be compared to modern examples, except in a few samples of the Blockwerf Migmatite. The Orange River Group also shows no evidence of crustal contamination in relation to the Vioolsdrif Suite. This may be interpreted as further evidence that tectonomagmatic processes during the Archean-Proterozoic transition period, may not be comparable to modern examples. This is supported by studies like that of Hamilton (1998) as well as various studies dealing with TTG and adakite. With the onset of formation at about 2.0 Ga, the Vioolsdrif Batholith falls within a geological time era when crust formation processes are considered to have been similar to those observed today (e.g., Hamilton, *op cit.*). However, the above observations call for the need of alternative theories to those based on uniformitarianism to explain crust formation processes in the Archean and Proterozoic.

A thin continental crust must have been present in the area where the Vioolsdrif Batholith developed. Overall low La/Yb ratios bear evidence that the crust could not have been thicker than 20 km (except under the Blockwerf Migmatite). The fact that the Vioolsdrif

Batholith does not show isotope signatures suggesting a pre-existing crust may be explained by two factors. Firstly, the fact that the crust was thin means that only a small volume of it was recycled. Secondly, the pre-existing crust must have been a primary crust which did not undergo previous recycling episodes, so that its isotope ratios were not significantly raised. The age of this pre-existing crust might have been 2.7 Ga, as indicated by a single inherited zircon (Nordin, 2009). Furthermore, it was noted before that the Vioolsdrif Batholith does not coincide perfectly with fields defined for Mesozoic (Cordilleran) batholiths on the Na_2O vs. K_2O and MALI vs. K_2O diagrams of Frost *et al*. (2001; Figures 4.30 and 4.31). This may also relate to the fact that the crust associated with the development of the Vioolsdrif Batholith was much thinner than that associated with the development of the Mesozoic-Tertiary batholiths.

In the light of all the evidence, the following evolutionary model is suggested for the Vioolsdrif Batholith and summarized in Figure 5.1:

Stage 1 (Figure 5.1a): Initial dehydration and partial melting processes in the subduction zone ced vertical heat flow and accumulation of melt at the base of the original crust. This led to limited crustal melting, producing felsic magmas which rose through the overlying crust and erupted at surface. These are represented by the Tsams Formation.

Stage 2 (Figure 5.1b): At this stage, the mantle was MORB-like in composition but with lower overall trace element concentrations than the modern MORB. In the mantle wedge, olivine-tholeiitic magmas were produced by partial melting' in accordance with modern subduction zone processes (e.g., Condie, 2005b). These magmas rose to shallow magma chambers (3-6 km depth) where they underwent fractional crystallization to produce tholeiitic and more evolved magmas. These phases are represented by the Vuurdood Subsuite. During the residence time of the magmas in the magma chambers and fractional crystallization, cumulates comprising pyroxene and olivine were also formed. With progressive subduction, volcanism predominated and the Haib Subgroup was deposited at surface. Within the crust, the first phases of the plutonic suite were formed.

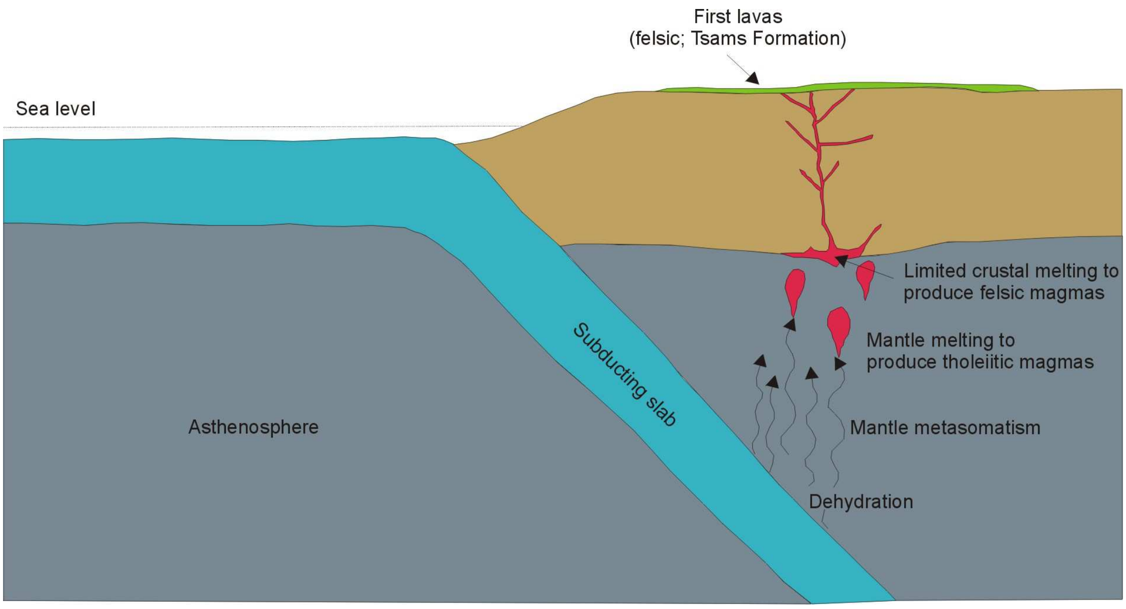

Figure 5.1(a): Initial stages of the evolution of the Vioolsdrif Suite. Vertical heat transfer and build-up of magma at the base of the crust produce limited felsic magmas which erupt at surface through vents and fissures, forming the Tsams Formation.

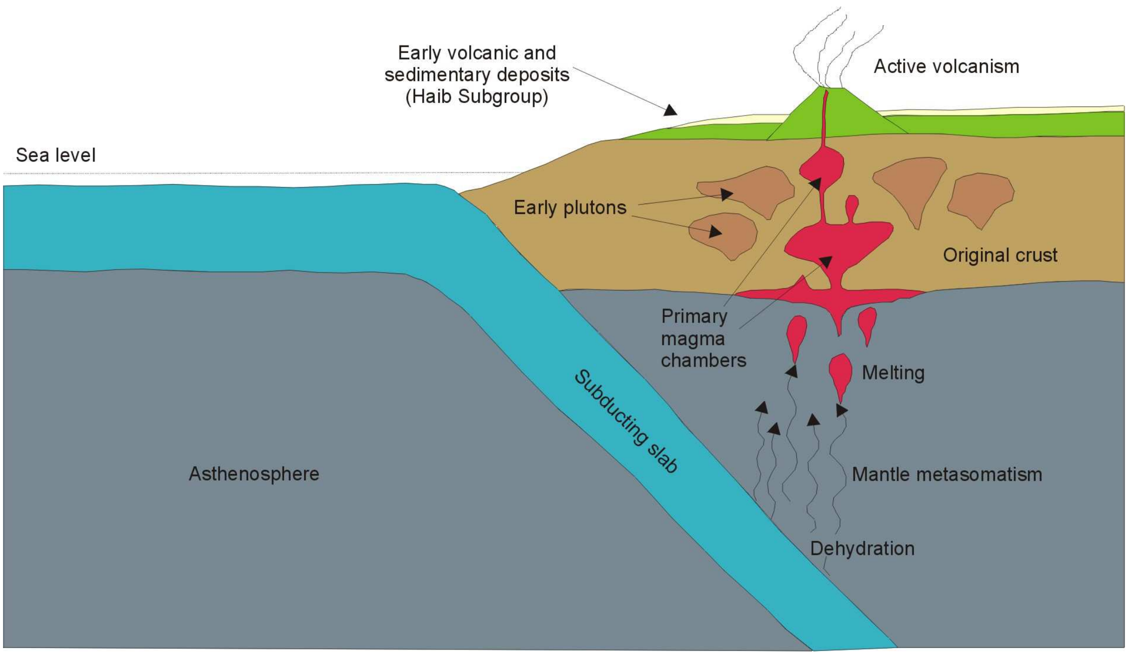

Figure 5.1(b): Early stages (primitive arc environment). Formation of intra-crustal magma chambers and early plutons; eruption of basaltic-andesitic lava (Nous Formation) produced by fractional crystallization in the magma chambers; limited deposition of sedimentary strata at surface.

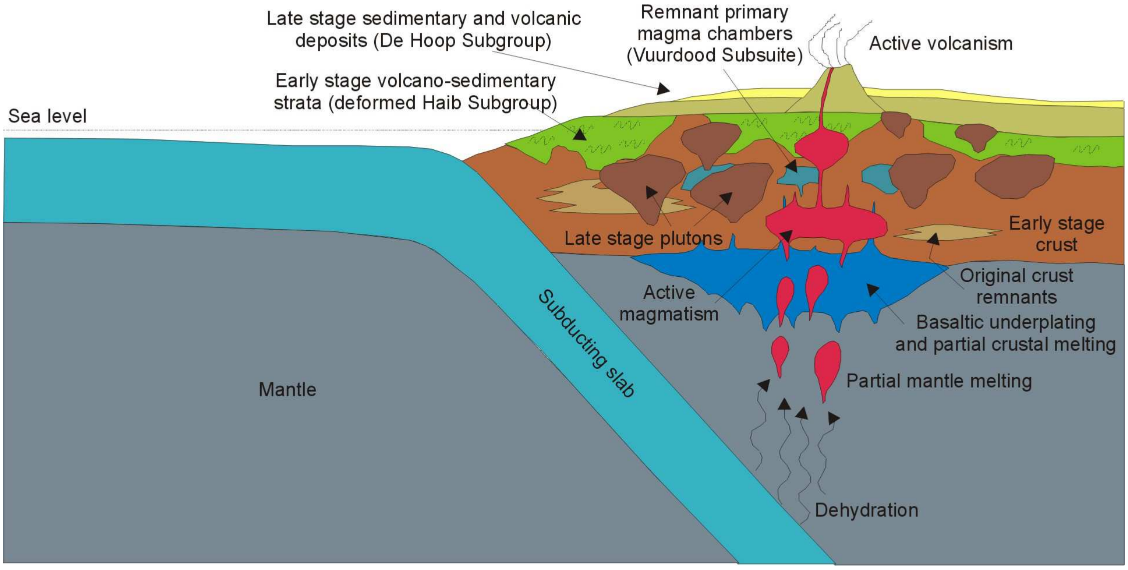

Figure 5.1(c): Late stages (normal arc environment). Extensive partial melting in the mantle lead to basaltic underplating in parts along the arc axis. The rest of the crust remain relatively thin due to continuous reworking by subduction. Early magma chambers and plutons crystallize within the crust (Vuurdood Subsuite and early stages of the Goodhouse Subsuite). Remnants of the original crust may be preserved while the rest of the crust is completely reworked into younger, more felsic crust. Partial melting of the crust results in magma mixing processes between mantle and crustal melts. Younger plutons intrude older units, including the root zone of the older volcanic units. At surface, more felsic lavas and sedimentary deposits are formed (De Hoop Subgroup).

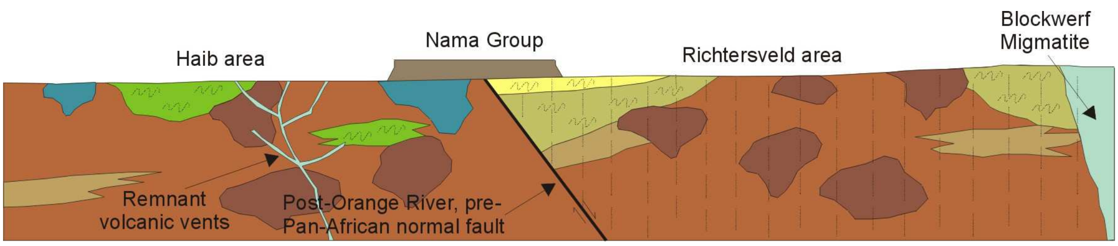

Figure 5.1(d): Post-Orange River orogeny. Tectonic deformation, probably the initial stages of the Pan-African orogeny, produces a normal fault between the Haib and Richtersveld areas, juxtapositioning a deeper part of the crust along a surface to near-surface part. Subsequent erosion and the deposition of the Nama Group lead to the concealment of the boundary.

Stage 3 (Figure 5.1c): Partial melting and recycling of newly formed crust became increasingly important and eventually predominated, producing mainly felsic magmas. During these later stages, magma mixing and contamination played a key role in the determination of final magma compositions. The De Hoop Subgroup is the surface representative of these stages. The various units of the Goodhouse Subsuite were produced at different stages throughout this evolutionary history.

Stage 4 (Figure 5.1d): After closure of the Orange River orogeny, probably during the initial stages of the Pan-african orogeny, the Richtersveld area was thrown down relative to the Haib area along a normal fault. This resulted in the juxtapositioning of a deeper part of the crust (exposed in the Haib area) to a surface to near-surface part of the crust (exposed in the Richtersveld). Subsequent erosion and the deposition of the Nama Group followed, concealing the Post-Orange River normal fault.

The progressive development of a calcalkaline nature from more primitive magmas in modern arcs, relates to the thickness of the overlying crust with the magmas becoming progressively more potassic as well as alkalic, away from the arc towards the continent (e.g., Miyashiro, 1974). For the Vioolsdrif Batholith, the remnant trend of an arc axis could not be established during the current study. However, there is an increase in the calcalkaline nature and K_2O contents from the Vuurdood Subsuite, through the Haib Subgroup to the rest of the batholith. This feature of modern continental arcs is often attributed to an increase in thickness of the overlying crust, but may be related to any process leading to the enrichment of K_2O including fractional crystallization, magma mixing with more felsic magmas, assimilation of continental crust, or the metasomatic process in the mantle wedge. It may also be related to the source composition. At least a portion of this variation is likely to be contributed by a mantle-derived component because it is also observed in island arc lavas, where a continental contribution is lacking (Dickenson, 1975).

No progressive increase in crustal thickening from older to younger units in the Vioolsdrif Batholith can be observed in the La/Yb ratios, as can be for the Andean arc (e.g., Haschke *et al*., 2006). This attests to continuous recycling of newly formed crust throughout its development. The model of recycling of the same material during the evolution of the batholith is also supported by the nature of fragments in agglomerates, pebbles in conglomerates and xenoliths in lava and granitoids, which resemble material from the same batholith throughout (e.g., Figures 2.3, 2.5 and 2.6).

The nature of the Ramansdrif Subsuite has not been settled. Initial isotope ratios indicate that it is the product of partial melting of continental crust (Reid, 1977). The fact that its geochemical variation patterns coincide closely with the Vioolsdrif Batholith, as well as its close spatial association with thise batholith, implies that the Goodhouse Subsuite acted as the source for the Ramansdrif Subsuite magmas. Radiometric ages indicate it to be post-Goodhouse Subsuite but there is no structural evidence of a major orogenic event at this time. On classification diagrams of Frost *et al*. (2001), the Ramansdrif Subsuite shows similarity to both peraluminous leucogranites and cordilleran batholiths (Figures 4.26 and 4.27). On the discrimination diagrams for granites of Pearce *et al*. (1984), it plots mostly in the field for volcanic arc granites (Figure 4.28). The latter observation speaks in favour of the idea that the Ramansdrif Subsuite was derived from the Goodhouse Subsuite, which has been shown to have originated in that environment. The peraluminous leucogranites of Frost *et al*. (2001), tend to be associated with overthickened orogens and are usually produced by small degrees of melting that is typically ascribed to a stage of crustal rebound, without any direct mantle contribution. La/Yb ratios argue against the Vioolsdrif Batholith being associated with an overthickened orogen. It is therefore suggested that the Ramansdrif Subsuite represents an event during which the Vioolsdrif Batholith underwent partial melting to produce felsic magmas. The orogenic event leading to this partial melting has not been identified.

5.3 THE RICHTERSVELD SUBPROVINCE IN ITS REGIONAL SETTING

There is currently general consensus that the Namaqua Metamorphic Province comprises a number of unique tectono-stratigraphic terranes which were amalgamated during the 1.3-1.0 Ga Namaqua orogeny (e.g., Stowe *et al*., 1984; Joubert, 1986; Thomas *et al*., 1994), although the exact configuration and identification of the terrane boundaries is still controversial (e.g., Colliston *et al*., 1992; Cornell and Pettersson, 2007). In this tectonic framework, the Vioolsdrif Batholith is considered to represent a relict Eburnian province surrounded by the Kibaran Namaqua mobile belt, bounded between two tectonic boundaries, viz., the Lower Fish River and Groothoek thrusts (e.g., Blignault *et al*., 1983).

Based on the tectono-magmatic model for the Vioolsdrif Batholith presented above, it is tempting to envisage the regional tectonic evolution of the area in terms of a tectonic model in which two continents, separated by an ocean, approach and eventually collide. In this model, the Vioolsdrif Batholith represents the subduction stage during closing of the ocean, while the Namaqua Metamorphic Province represents the collisional stage. However, such a model is contradicted by the age gap between the end of the Orange River orogeny (1.73 Ga, Ramansdrif Subsuite) and the onset of the Namaqua orogeny (1.3 Ga, Little Namaqualand Suite). Furthermore, the Ramansdrif magmatic event might be considered unrelated to the Vioolsdrif magmatism and Cornell *et al*. (2007) in fact suggest that the Ramansdrif leucogranites be excluded from the Vioolsdrif Suite. This would indicate an even older age for the end of the Orange River orogeny and would be indicated by the youngest ages of the Goodhouse Subsuite, which is currently around 1.8 Ga (e.g., Reid, 1977).

The inability to identify Archean continental crust associated with the Vioolsdrif Batholith and a basement to the Orange River Group, may suggest the complete recycling of such crust during the Orange River orogeny. Currently, the only evidence of such components in the Vioolsdrif Batholith is in a single inherited zircon core of 2.7 Ga (Nordin, 2009). Other inherited zircon cores to date coincide with the earlier stages of the batholith (U-Pb, LA-ICPMS ages of 1.9 and 2.0 Ga in the Xaminxaip River Granodiorite; see Appendix 2). At a number of localities, xenoliths are found in the volcanics of the Orange River Group but none of these have as yet been dated. Based on evidence indicating rapid recycling of newly formed material throughout the batholith, these xenoliths most likely represent recycled material of earlier phases. Reid (1977) dated a xenolith of granodiorite at 1.73 Ma but this suggests resetting during the Ramansdrif magmatic event.

If current models for the tectonic setting of the Vioolsdrif Batholith is accepted then there is no point in searching for basement to the Orange River Group outside the Richtersveld Subprovince, since all evidence related to the batholith would be bounded between the Lower Fish River and Groothoek thrusts. If it is not accepted, a number of units may qualify for such a position. The model of terrane accretion currently reigns popular and alternative models are few. However, much evidence exist to suggest that the Vioolsdrif Batholith might not be isolated from the Namaqua Metamorphic Province by the proposed terrane boundaries. Ward (1977) describes the boundary with the "Bushmanland Subprovince" as fault bounded in part, but "elsewhere the Vioolsdrif igneous assemblage both rests on and intrudes the grey gneisses characteristic of the south" (i.e., the Gladkop Suite, which extends as far south as Springbok in Namaqualand). Marais *et al*. (2001) and Minnaar *et al*. (2011) also present evidence that the Gladkop Suite is intruded by the Vioolsdrif Suite. Radiometric ages of 1.8 Ga for the Gladkop Suite also contradicts the idea that the Richtersveld Subprovince is unique in its early-Proterozoic age. Isotopic data and model ages show extensive reworking of Vioolsdrif-age crust in the rest of the Namaqua Province during the Namaqua orogeny (e.g., Barton, 1983; Reid, 1981).

Furthermore, it seems likely that the Orange River Group grades from a volcanic-dominated unit in its type area, to a sedimentary-dominated unit eastwards. In the east, the pervasive foliation and metamorphism of the Namaqua orogeny have rendered correlation among stratigraphic units controversial but various studies imply the possible correlation of the Orange River Group with Namaqua Metamorphic Province supracrustal units. Moen and Toogood (2007) considered the Orange River and Droëboom Groups lateral equivalents, while possible correlations between the Orange River and Bushmanland Groups are suggested in all of Colliston (1990), Agenbacht (2007), Bertrand (1975) and Moen and Toogood (2007). In all of these findings, the Steinkopf Gneiss of the Gladkop Suite is implied as basement to the Orange River Group. In Bushmanland, the "Achap Gneiss" has been considered the basement to the Bushmanland Group by Moore (1977) and Watkeys (1986). Bailie *et al*. (2007) also state that combined earlier works have suggested that the "Achap" and "Hoogoor" Gneisses (the latter does not refer to the Hoogoor Granite) are older than the Bushmanland Group and acted as the basement and provenance to the metasediments and source of the mineralization (at Black Mountain and Gamsberg mines). Radiometric data contradicts the idea of a correlation between the Orange River and Bushmanland Groups with the inferred ages of deposition for Bushmanland formations ranging between 1.5-1.2 Ga (e.g., Bailie *et al.*, 2007). However, the 2.0 Ga ages for the Haib Subgroup are representative of the early stages of Orange River Group evolution. Inferred depositional ages of post-1.76 Ga for the Rosyntjieberg metasediments, imply that Orange River Group deposition continued even after Ramansdrif magmatism, suggesting a possible continuation into Bushmanland deposition, which precedes the Namaqua orogeny.

6. ACKNOWLEDGEMENTS

Dave Cornell and Valby von Schrijndel of the Gothenburg University are warmly thanked for U-Pb (LA-ICPMS) age determinations on zircons from two samples.

The author wishes to thank Prof. A.E. Schoch, not only for acting as supervisor but also for his invaluable input and positive guidance throughout the execution of this study.

REFERENCES

Agenbacht, A.L.D., 2007. The geology of the Pofadder area. Explanation, 2918 Pofadder (1:250 000), Council for Geoscience, 89 p.

Agrawal, S., Guevara, M., Verma, S.P., 2008. Tectonic discrimination of basic and ultrabasic volcanic rocks through log-transformed ratios of immobile trace elements. International Geology Review 50, 1057-1079.

Allsopp H.L., Köstlin E.O., Welke H.J., Kröner A. and Blignault H.J., 1979. Rb-Sr and U-Pb geochronology of late Precambrian-early Palaeozoic igneous activity in the Richtersveld (South Africa) and southern South West Africa. Transactions, Geological Society of South Africa, 82, 185 - 204.

Anderson, J.L. 1983. Proterozoic anorogenic granite plutonism of North America. In: L.G. Mederis, C.W. Byers, D.M. Mickelson and W.C. Shanks (editors) Proterozoic Geology, Selected Papers from an International Proterozoic Symposium. Memoir, Geological Society of America, 161, 133-154.

Arth, J.G. and Hanson, G.N. 1975. Geochemistry and origin of the early Precambrian crust of northern Minnesota. Geochimica et Cosmochimica Acta, 39, 325-362.

Atherton, M.P. and Tarney, J. 1979. Origin of granite batholiths: geochemical evidence. Shiva Publishing, 148 p.

Bailie, R.H., Armstrong, R.A. and Reid, D.L. 2007. The Bushmanland Group supracrustal succession, Aggeneys, Bushmanland, South Africa: Provenance, age of deposition and metamorphism. Journal of Geology, 110(1), 59 - 86.

Barker, F. 1979. trondhjemites, dacites and related rocks. Elsevier, New York.

Barton, E.S. 1983. Reconnaissance isotopic investigations in the Namaqua mobile belt and implications for Proterozoic crustal evolution – Namaqualand Geotraverse. In: B.J.V. Botha (editor) Namaqualand Metamorphic Complex. Special Publication, Geological Society of South Africa, 10, 45-66.

Bertrand, J.M. 1975. Granitoids and deformation sequence in the Goodhouse - Henkries area: A new interpretation of the relationship between rocks of the Vioolsdrif - Goodhouse area and the Namaqualand and Bushmanland gneisses. Annual Report, Precambrian Research Unit, University of Cape Town, 13, 61 - 70.

Beukes, G.J. 1973. 'n Geologiese ondersoek van die gebied suid van Warmbad, Suidwes-Afrika, met spesiale verwysing na die metamorf-magmatiese assosiasies van die Voorkambriese gesteentes. D.Sc. Thesis, University of the Orange Free state, Bloemfontein, 333 p.

Blignault, H.J. 1974. Aspects of the Richtersveld Province. In: A. Kröner (editor) Contributes to the Precambrian geology of Southern Africa. Bulletin, Precambrian Research Unit, University of Cape Town, 15, 49 – 56

Blignault, H.J. 1977. Structural-metamorphic imprint on part of the Namaqua mobile belt in South West Africa. Bulletin, Precambrian Research Unit, University of Cape Town, 23, 197 p.

Blignault, H.J., Jackson, M.P.A., Beukes, G.J. and Toogood, D.J. 1974. The Namaqua tectonic province in South West Africa. In: A. Kröner (Editor) Contributions to the Precambrian geology of southern Africa. Bulletin, Precambrian Research Unit, University of Cape Town, 15, 29 – 48.

Blignault, H.J., Van Aswegen, G., Van der Merwe, S.W. and Colliston, W.P. 1983. The Namaqualand geotraverse and environs: part of the Proterozoic Namaqua mobile belt.

In: B.J.V. Botha (editor) Namaqualand Metamorphic Complex. Special Publication, Geological Society of South Africa, 10, 1-29.

Bowen, N.L. 1928. The evolution of the igneous rocks. Princeton University Press.

Bowles, M. 1988. Tungsten mineralisation in the Namaqualand - Bushmanland region, Northwestern Cape, South Africa. Memoir, Geological Survey of South Africa, 74, 75 p.

Boynton, W.V. 1984. Geochemistry of the rare earth elements: meteorite studies. In: P. Henderson (editor) Rare earth element geochemistry. Elsevier, 63-114.

Brown, G.C., Thorpe, R.S. and Webb, P.C. 1984. The geochemical characteristics of granitoids in contrasting arcs and comments on magma source. Journal of the Geological Society of London, 141, 413-426.

Buddington, A.F. 1959. Granite emplacement with special reference to North America. Bulletin, Geological Society of America, 70, 671-747.

Castillo, P.R. 2006. An overview of adakite petrogenesis. Chinese Science Bulletin, 51, 257-268.

Coetzee, C.B. 1941. The petrology of the Goodhouse-Pella area, Namaqualand, South Africa. Transactions of the Geological Society of South Africa, 44, 167 – 206.

Colliston, W.P. 1990. A stratigraphic and structural investigation of part of the Namaqua mobile belt between Dabenoris and Steyerkraal, South Africa. Ph.D. thesis, University of the Orange Free state, Bloemfontein, 260 p.

Colliston, W.P. and Schoch, A.E. 2006. The distribution and diagnostic features of deformed plutonic rocks in two terranes of the Namaqua mobile belt along the Orange (Gariep) River, South Africa. South African Journal of Geology, 109, 369-392.

Colliston, W.P., Praekelt, H.E. and Schoch, A.E. 1992. The western margin of the Proterozoic Namaqua-Natal mobile belt in the nortwestern Cape Province. Field guide book for excursion 6A, 24th Geocongress, Geological Society of South Africa.

Condie, K.C. 2005a. TTGs and adakites: are they both slab melts? Lithos, 80, 33-44.

Condie, K.C. 2005b. Earth as an evolving planetary system. Elsevier Academic Press, 447 p.

Cornell, D.H. and Pettersson, A. 2007. Ion probe zircon dating of metasediments from the Areachap and Kakamas Terrane, Namaqua-Natal Province and the stratigraphic integrity of the Areachap Group. South African Journal of Geology, 110, 169 - 178.

Cornell, D.H., Thomas, R.J., Moen, H.F.G., Reid, D.L., Moore, J.M. and Gibson, R.L. 2007. The Namaqua-Natal Province. In: The Geology of South Africa, M.R. Johnson, C.R. Anhauesser and R.J. Thomas (editors), 325 – 379.

Cox, K.G., Bell, J.D. and Pankhurst, R.J. 1979. The interpretation of igneous rocks. George, Allen and Unwin, London.

De la Roche, H., Leterrier, J., Grande Claude, P. and Marchal, M., 1980. A classification of volcanic and plutonic rocks using R1-R2 diagrams and major element analyses – its relationship and current nomenclature. Chemical Geology, 29, 183 – 210.

De Villiers, J. and Burger, A.J. 1967. Note on the minimum age of certain granites from the Richtersveld area. Annals, Geological Survey of South Africa, 6, pp. 83 - 84.

De Villiers, J. and Söhnge, P.G. 1959. The geology of the Richtersveld. Memoir, Geological Survey of South Africa, 48, 266 p.

Defant, M.J. and Drummond, M.S. 1990. Derivation of some modern arc magmas by melting of young subducted lithosphere. Nature, 347, 662-665.

Defant, M.J. and Kepenzhinskas, P. 2001. Evidence suggests slab melting in arc magmas. Eos, 82, 62-70.

Dhuime, B, Bosch, D, Bodinier, J.-L., Garrido, C.J., Bruguier, O., Hussain, S.S. and Dawood, H. 2007. Multistage evolution of the Jijal ultramafic–mafic complex (Kohistan, N Pakistan): Implications for building the roots of island arcs. Earth and Planetary Science Letters 261, 179–200.

Dickenson, W.R. 1975. Potash-depth (K-*h*) relations in continental margins and intra-oceanic magmatic arcs. Geology, 3, 53-56.

Drummond, M.S. and Defant, M.J. 1990. A model for trondhjemite-tonalite-dacite genesis and crustal growth via slab melting: Archaean to modern comparisons. Journal of Geophysical Research, 95, 21503-21521.

Frost, C.D. and Frost, B.R. 1997. High-K, iron-enriched rapakivi-type granites: the tholeiite connection. Geology, 25, pp. 647-650.

Frost, B.R. and Linsley, D.H. 1991. The occurrence of Fe-Ti oxides in igneous rocks. In: D.H. Lindsley (editor) Oxide Minerals: Petrologic and Magnetic Significance. Reviews in Mineralogy, 25, 433-486.

Frost, B.R., Barnes, C.G., Collins, W.J., Arculus, R.J., Ellis, D.J. and Frost, C.D. 2001. A geochemical classification for granitic rocks. Journal of Petrology, 42, 2033-2048.

Germs, G.J.B. 1972. The stratigraphy and palaeontology of the lower Nama Group, South West Africa. Bulletin, Precambrian Research Unit, University of Cape Town, 12, 250 p.

Gevers, T.W. 1941. Correlation of the pre-Cape formations in the western Cape Province: Discussion, Proceedings of the Geological Society of South Africa, 43, p. 17 – 30.

Gevers, T.W., Partridge, F.C. and Joubert, G.K. 1937. The pegmatite area south of the Orange River in Namaqualand. Memoir, Geological Survey of South Africa, 31, 172 p.

Gresse, P.G. and Germs, G.J.B., 1993. The Nama foreland basin: sedimentation, major unconformity-bounded sequences and multisided active margin advance. Precambrian Research, 63, p. 247 – 272

Griffin, W.L., O'Reilly, S.Y., Afonso, J.C. and Begg, G.C. 2009. The composition and evolution of lithospheric mantle: a re-evaluation and its tectonic implications. Journal of Petrology, 50, 1185-1204.

Hamilton, W.B. 1998. Archean deformation and magmatism: no plate tectonics. Geocongress, Geological Society of South Africa, p. 26-28.

Hartnady, C.J.H., Joubert, P. and Stowe, C.W. 1985. Proterozoic crustal evolution in southwestern Africa. Episodes, 8, 236 - 244.

Haschke, M., Günther, A., Melnick, D, Echtler, H., Reutter, K-J, Scheuber, E and Oncken, O. 2006. Central and southern Andean tectonic evolution inferred from arc magmatism. In: The Central and Southern Andes, Springer Verlag, p. 189-202.

Haschke, M., Siebel, W., Günther, A. and Scheuber, E. 2002. Repeated crustal thickening and recycling during the Andean orogeny in north Chili (21°-26°S). Journal of Geophysical Research, 107, 1-17.

Hildreth, W. and Moorbath, S. 1988. Crustal contributions to arc magmatism in the Andes of central Chile. Contributions to Mineralogy and Petrology, 98, 455-489.

Irvine, T.N. and Baragar, W.R.A. 1971. A guide to the chemical classification of the common volcanic rocks. Canadian Journal of Earth Sciences, 8, 523-548.

Jensen, L.S. 1976. A new cation plot for classifying subalkalic volcanic rocks. Paper, Ontario Division of Mines, 66.

Johnson, A.D. and Wyllie, P.J. 1988. Constraints on the origin of Archaean trondhjemites based on phase relationships of Nuk Gneiss with H_2O at 15kbar. Contributions to Mineralogy and Petrology, 100, pp. 35-46.

Joubert, P. 1986. Namaqualand - A model of Proterozoic accretion? Transactions of the Geological Society of South Africa 89, 79-96.

Joubert, P., Hartnady, C.J.H. and Von Veh, M.W. 1986. The geology of the Alexander Bay area. Explanation, sheet 2816 (1:250 000), Geological Survey of South Africa, 22 p.

Kaur, P.K., Chaundhri, N., Kröner, A and Hofmann, A.W. 2009. Record of 1.82 Ga Andean-type continental arc magmatism in NE Rajasthan, India: Insights from zircon and Sm-Nd ages, combined with Nd-Sr isotope geochemistry. Gondwana Research, 16, 56-71.

Kay, R.W. 1978. Aleutian magnesian andesites: melts from subducted Pacific Ocean crust. Journal of Volcanology and Geothermal Research, 4, 117-132.

Kay, S.M. 2005. Tertiary to recent evolution of Andean arc and back-arc magmas between 36°S and 38°S and evidence for Miocene shallowing of the Nazca plate under the Neuquén basin. In: 6th International Symposium on Andean Geodynamics, Barcelona, 420-423.

Kay, S.M. and Mpodozis, C. 2002. Magmatism as a probe to the Neogene shallowing of the Nazca plate beneath the modern Chilean flat-slab. Journal of South American Earth Sciences, 15, 39-57.

Kay, S.M., Mpodozis, C. and Coira, A.B. 1999. Neogene magmatism, tectonism and mineral deposits of the central Andes. In: B.J. Skinner (editor) Geology and Ore Deposits of the Central Andes. Special Publication, Society of Economic Geology, 7, 27-59.

King, E.M., Beard, B.L. and Valley, J.W. 2007. Strontium and oxygen isotope evidence for strike/slip movement of accreted terranes in the Idaho Batholith. Lithos, 96, 387-401.

Kostitsyn, Y, A., Volkov, V.N. and Zhuravlev, D.Z. 2007. Trace elements and evolution of granite melt as exemplified by the Raumid Pluton, Southern Pamirs. Geochemistry International, 45, 971-982.

Kröner, A. and Blignault, H.J. 1976. Towards a definition of some tectonic and igneous provinces in western South Africa and southern South West Africa. Transactions, Geological Society of South Africa, 79, 232 – 238.

Kröner, A., Barton, E.S., Burger, A.J., Allsopp, H.L. and Bertrand, J.M. 1983. The ages of the Goodhouse Granite and grey gneisses from the marginal zone of the Richtersveld Province and their bearing on the timing of tectonic events in the Namaqualand mobile belt. In: B.J.V. Botha (editor) Namaqualand Metamorphic Complex. Special Publication, Geological Society of South Africa, 10, 123 - 130.

Le Maitre, R.W. 1976. The geochemical variability of some common igneous rocks. Journal of Petrology, 17, 589-637.

Le Maitre, R.W., Bateman, P., Dudek, A., Keller, J., Lameyre Le Bas, M.J., Sabine, P.A., Schmid, R., Sorensen, H., Streckeisen, A., Woolley, A.R. and Zanettin, B. 1989. A classification of igneous rocks and glossary of terms. Blackwell, Oxford, 193 p.

Leake, B.E. 1983. Ultrametamorphism, migmatites, melting and granitoid formation. In: M.P. Atherton and C.D. Gribble (editors) Migmatites, Melting and Metamorphism. Proceedings of the Geochemical Group of the Mineralogical Society, Shiva Publishing, 2-9.

Maniar, P.D. and Piccoli, P.M. 1989. Tectonic discrimination of granitoids. Bulletin, Geological Society of America, 101, pp. 635-643.

Mantle, G.W. and Collins, W.J. 2008. Quantifying crustal thickness variations in evolving orogens: correlation between arc basalt composition and Moho depth. Geology, 36, 87-90.

Marais, J.A.H., Agenbacht, A.L.D., Prinsloo, M. and Basson, W.A. 2001. Geology of the Springbok area. Explanation, sheet 2916 Springbok (1 : 250 000), Council for Geoscience, 103 p.

Martin, H. 1999. Adakitic magmas: modern analogues of Archean granitoids. Lithos, 46, 411-429.

Martin, H., Smithies, R.H., Rapp, R., Moyen, J.-F. and Champion, D. 2005. An overview of adakite, tonalite-trondhjemite-granodiorite (TTG), and sanukitoid: relationships and some implications for crustal evolution. Lithos, 79, 1-24.

Mehnert, K.R. 1968. Migmatites and the origin of granitic rocks. Elsevier Publishing Company, Amsterdam, 393 p.

Middlemost, E.A.K. 1965. Ultramafic rocks of the south-eastern Richtersveld. Transactions, Geological Society of South Africa, 68, 53 - 60.

Miller, R.McG. 2008. The geology of Namibia. Handbook, Geological Survey of Namibia, 3 volumes.

Minnaar, H., Botha, P.M.W. and Roberts, D. 2011. The geology of the Alexander Bay area. Explanation, sheet 2816 Alexander Bay (1 : 250 000), Council for Geoscience, 178 p.

Minnitt, R.C.A. 1979. The geological setting of porphyry-type copper mineralization in the Haib River area, South West Africa. Ph.D. thesis (unpubl.), University of the Witwatersrand, Johannesburg, 366 p.

Miyashiro, A. 1974. Volcanic rocks series in island arcs and active continental margins. American Journal of Sciences, 274, 321-355.

Moen, H.F.G. and Toogood, D.J. 2007. The geology of the Onseepkans area. Explanation, sheet 2818 Onseepkans (1 : 250 000), Council for Geoscience, 101 p.

Moorbath, S. 1975. Evolution of Precambrian crust from strontium evidence. Nature, 254, pp. 395-398.

Moore, J.M. 1977. The geology of Namiesberg, Northern Cape. Bulletin, Precambrian Research Unit, University of Cape Town, 20, 69 p.

Mullen, E.D. 1983. $MnO/TiO_2/P_2O_5$: a minor element discriminant for basaltic rocks of oceanic environments and its implications for petrogenesis. Earth and Planetary Science Letters, 62, 53-62.

Nordin, F. 2009. U-Pb dating, Lu-Hf isotopic analyses and geothermobarometry of rocks in the Grünau Terrane and Richtersveld Subprovince, Namaqua Sector, southern Africa. M.Sc. thesis (unpublished), Göteborgs Universitet, 54 p.

Parada, M.A., Nyström, J.O. and Levi, B. 1999. Multiple sources for the Coastal Batholith of central Chile (31-34°S): geochemical and Sr-Nd isotopic evidence and tectonic implications. Lithos, 46, 505-521.

Patchett, P.J. 1989. Radiogenic isotope geochemistry of rare earth elements. In: P.H. Ribbe (editor), Geochemistry and Mineralogy of Rare Earth Elements. Reviews in Mineralogy, 21, 348 p.

Pearce, J.A. 1982. Trace element characteristics of lavas from destructive plate boundaries. In: R.S. Thorpe (editor) Andesites. Wiley, Chichester, 525-548.

Pearce, J.A. 1983. Role in the sub-continental lithosphere in magma genesis at active continental margins. In: C.J. Hawkesworth and M.J. Norry (editors) Continental Basalts and Mantle Xenoliths. Shiva, Nantwich, 230-249.

Pearce, J.A. and Cann, J.R. 1973. Tectonic setting of basic volcanic rocks determined using trace element analyses. Earth and Planetary Science Letters, 19, 290-300.

Pearce, J.A. and Norry, M.J. 1979. Petrogenetic implications of Ti, Zr, Y and Nb variations in volcanic rocks. Contributions to Mineralogy and Petrology, 69, 33-47.

Pearce, J.A. and Parkinson, I.J. 1993. Trace element models for mantle melting: application to volcanic arc petrogenesis. In: H.M. Prichard, T. Alabaster, N.B.W. Harris and C.R. Neary (editors) Magmatic processes and plate tectonics. Special Publication, Geological Society, 76, 373-403.

Pearce, J.A. and Peate, D.W. 1995. Tectonic implications of the composition of volcanic arc magmas. Annual Review, Earth and Planetary Science, 23, 251–285.

Pearce, J.A., Lippard, S.J. and Roberts, S. 1984. Characteristics and tectonic significance of supra subduction zone ophiolites. In: B.P. Kokelaar and M.R. Howells (editors) Marginal Basin Geology. Special Publication, Geological Society of London, 16, 77-94.

Perugini, D. and Poli, G. 2004. Analysis and numerical simulation of chaotic advection and chemical diffusion during magma mixing: petrological implications. Lithos, 78, 43-66.

Perugini, D., Poli, G. and Gatta, G.D. 2002. Analysis and simulation of magma mixing processes in 3D. Lithos, 65, 313-330.

Petro, W.L., Vogel, T.A. and Wilband, J.T. 1979. Major-element chemistry of plutonic rock suites from compressional and extensional plate boundaries. Chemical Geology, 26, pp. 217-235.

Piper, J.D.A. 2000. The Neoproterozoic Supercontinent: Rodinia or Palaeopangea? Earth and Planetary Science letters, 176, 131 - 146.

Planck, T and Langmuir, C.H. 1988. An evaluation of the global variations in the major element chemistry of arc basalts. Earth and Planetary Science Letters, 90, 349-370.

Polat, A., Appel, P.W.U. and Fryer, B.J. 2011. An overview of the geochemistry of Eoarchean to Mesoarchean ultramafic to mafic volcanic rocks, SW Greenland: Implications for mantle depletion and petrogenetic processes at subduction zones in the early Earth. Gondwana Research, 4-67.

Prinsloo, M.C. 1987. Notas oor die geologie van blaaie 2917BA, BB, BC en BD. Report, Council for Geoscience (unpublished).

Reid, D.L. 1974. Preliminary report on petrologic studies of volcanic and intrusive rocks in the Vioolsdrif region, lower Orange River. In: A. Kröner (editor) Contributions to the Precambrian geology of southern Africa. Bulletin, Precambrian Research Unit, University of Cape Town, 15, 57-68.

Reid, D.L. 1975. Geochronology of the Haib-Vioolsdrif igneous Province. Annual Report, Precambrian Research Unit, University of Cape Town, 13, 49 - 60.

Reid, D.L. 1977. Geochemistry of Precambrian igneous rocks in the lower Orange River region. Bulletin (P.hD. thesis), Precambrian Research Unit, University of Cape Town, 22, 397 p.

Reid, D.L. 1979. Total rock Rb-Sr and U-Th-Pb isotopic study of Precambrian metavolcanic rocks in the Lower Orange River region. Earth and Planetary Science Letters, 42, 368-378.

Reid D.L. 1981. Sm-Nd ages from the Namaqua and Richtersveld Provinces. Abstracts, Geocongress (1981), Pretoria, Geological Society of South Africa, 173 - 174.

Reid, D.L. 1982. Age relationships within the Vioolsdrif Batholith, lower Orange River region II. A two stage emplacement history and the extent of Kibaran overprinting. Transactions, Geological Society of South Africa, 85, 105 - 110.

Reid, D.L. 1997. Sm-Nd age and REE geochemistry of Proterozoic arc-related igneous rocks in the Richtersveld Subprovince, Namaqua Mobile Belt, Southern Africa. Journal of African Earth Sciences, 24(4), 621 – 633.

Richard, J.P. and Kerrich, R. 2007. Adakite-like rocks: their diverse origins and questionable role in metallogenesis. Economic Geology, 102, 537-576.

Ritter U. 1980. The Precambrian evolution of the eastern Richtersveld. Bulletin, Precambrian Research Unit, University of Cape Town, 26, 276 p.

Ritter U. 1983. The Mid-proterozoic magmatic and tectonothermal evolution of the Richtersveld. In: B.J.V. Botha (editor) Namaqualand Metamorphic Complex. Special Publication, Geological Society of South Africa, 10, 111 - 122.

Rogers, A.W. 1911. The Kheis Series. Transactions, Geological Society of South Africa, 13, 93 – 104.

Rogers A.W. 1916. The nature of the copper deposits of Little Namaqualand. Proceedings, Geological Society of South Africa, 19, 21 - 35.

Rollinson, H.R. 1993. Using geochemical data: evaluation, presentation, interpretation. Longman Group UK, 352 p.

Rollinson, H.R. 2005. Geodynamic controls on adakite, TTG and sanukitoid genesis: implications for models of crust formation. Editorial column, Special Issue, Lithos, 79, p. ix-xii.

Ross, P.S., Bédard, J.H. 2009. Magmatic affinity of modern and ancient subalkaline volcanic rocks determined from trace element discrimination diagrams. Canadian Journal of Earth Sciences, 46, 823-839.

SACS (South African Committee for Stratigraphy). 1980. Stratigraphy of South Africa, part 1 (compiler LE Kent), Lithostratigraphy of the Republic of South Africa, South West Africa/Namibia and the Republics of Bophuthatswana, Transkei and Venda. Handbook, Geological Survey of South Africa, 8, 690 p.

Smithies, R.H. and Champion, D.C. 2000. The Archean high-Mg diorite suite: links to tonalite-trondhjemite-granodiorite magmatism and implications for early Archaean crustal growth. Journal of Petrology, 41, 1653-1671.

Sobolev, R. 1991. Rare earth minerals in conception of granite genesis. In: B. Siribumrungsukha, S. Arrykul, P. Sanguansai, T. Pungrassanni, L. Sikong and K. Kooptarnoud (editors), Proceedings of the International Conference on Rare Earth Minerals and Minerals for Electronic Uses, Faculty of Engineering, Prince of Songkla University, Thailand, 662 p.

Stowe, C.W., Hartnady, C.J.H. and Joubert, P. 1984. Proterozoic tectonic provinces of Southern Africa. Precambrian Research, 25, 229 - 231.

Streckeisen, A. 1976. To each plutonic rock its proper name. Earth Science Reviews, 12, 1-33.

Strydom, D., Colliston, W.P., Praekelt, H.E., Schoch, A.E., Van Aswegen, G., Pretorius, J.J., Beukes, G.J., De Villiers, B., Watkeys, M.K. and Botes, F.J. 1987. The tectonic units of parts of Namaqualand, Bushmanland and southern South West Africa/Namibia. Map (1:250 000), Bushmanland Research Project, Department of Geology, University of the Orange Free State, one sheet.

Thomas, R.J., Agenbacht, A.L.D., Cornell, D.H. & Moore, J.M. 1994. The Kibaran of southern Africa: tectonic evolution and metallogeny. Ore Geology Review, 9, 131-160.

Thompson, R.N. 1982. British Tertiary volcanic province. Scottish Journal of Geology, 18, 49-107.

Van der Merwe, S.W. 1986. The structural development of part of the Namaqua Mobile Belt in an area between Springbok and Vioolsdrif, South Africa. Ph.D. thesis, University of the Orange Free State, Bloemfontein, 373 p.

Van der Merwe, S.W. and Botha, B.J.V. 1989. The Groothoek thrust belt in western Namaqualand: an example of a mid-crustal structure. South African Journal of Geology, 92, 156 - 166.

Van Tonder, D.M. and Mouri, H. 2010. Petrology and geochemistry of the granitoid rocks of the Johannesburg Dome, Central Kaapvaal Craton, South Africa. South African Journal of Geology, 113, 257-285.

Von Backström, J.W. 1953. Geological map 2817D Vioolsdrif, 2818C Goodhouse, 2818D Dabenoris, 2819C Onseepkans (1:125 000), Geological Survey of South Africa, one sheet.

Von Backström, J.W. and De Villiers, J. 1972. The geology along the Orange River Valley between Onseepkans and the Richtersveld. Explanation, sheets 2817D (Vioolsdrif), 2818C (Goodhouse), 2818D (Dabenoris) and 2819C (Onseepkans), Geological Survey of South Africa, 101 p.

Von Veh, M.W., 1993. The stratigraphy and structural evolution of the late Proterozoic Gariep belt in the Sendelingsdrif – Annisfontein area, orthwestern Cape Province. Bulletin, Precambrian Research Unit, University of Cape Town, 174 p.

Ward, J.H.W. 1977. The geology of the area south of Vioolsdrif, Cape Province. Internal Report, Atomic Energy Board, PEL-257, 48 p.

Watkeys, M.K. 1986. The Achab Gneiss: a "floor" in Bushmanland or a flaw in Namaqualand? Transactions, Geological Society of South Africa, 89, 103 - 116.

Wyllie, P.J. 1983. Experimental and thermal constraints on the deep-seated parentage of some granitoid magmas in subduction zones. In: M.P. Atherton and C.D. Gribble (editors) Migmatites, Melting and Metamorphism. Shiva, Nantwich, UK.

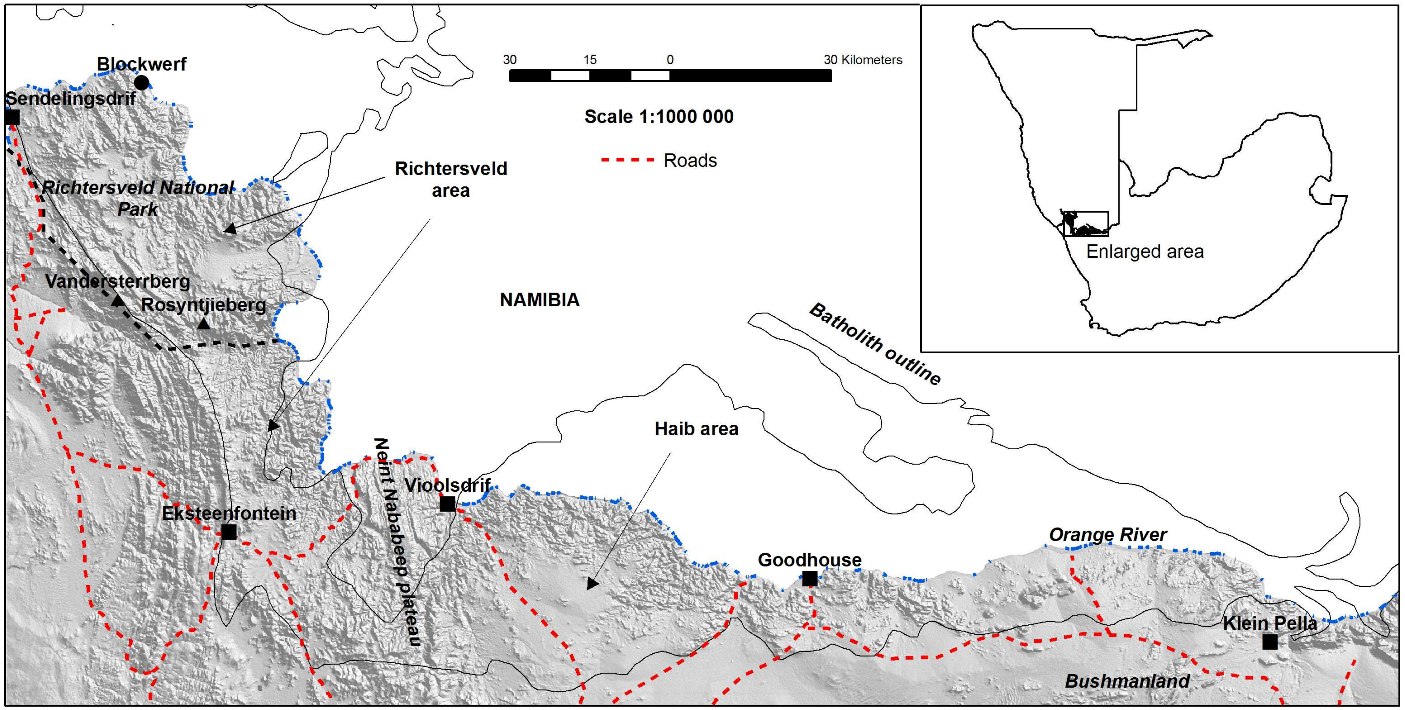

Figure 1.1: Location of the study area. The extent of the batholith is shown on a topographic background (DEM) of the study area, which includes only the South African part of the batholith.

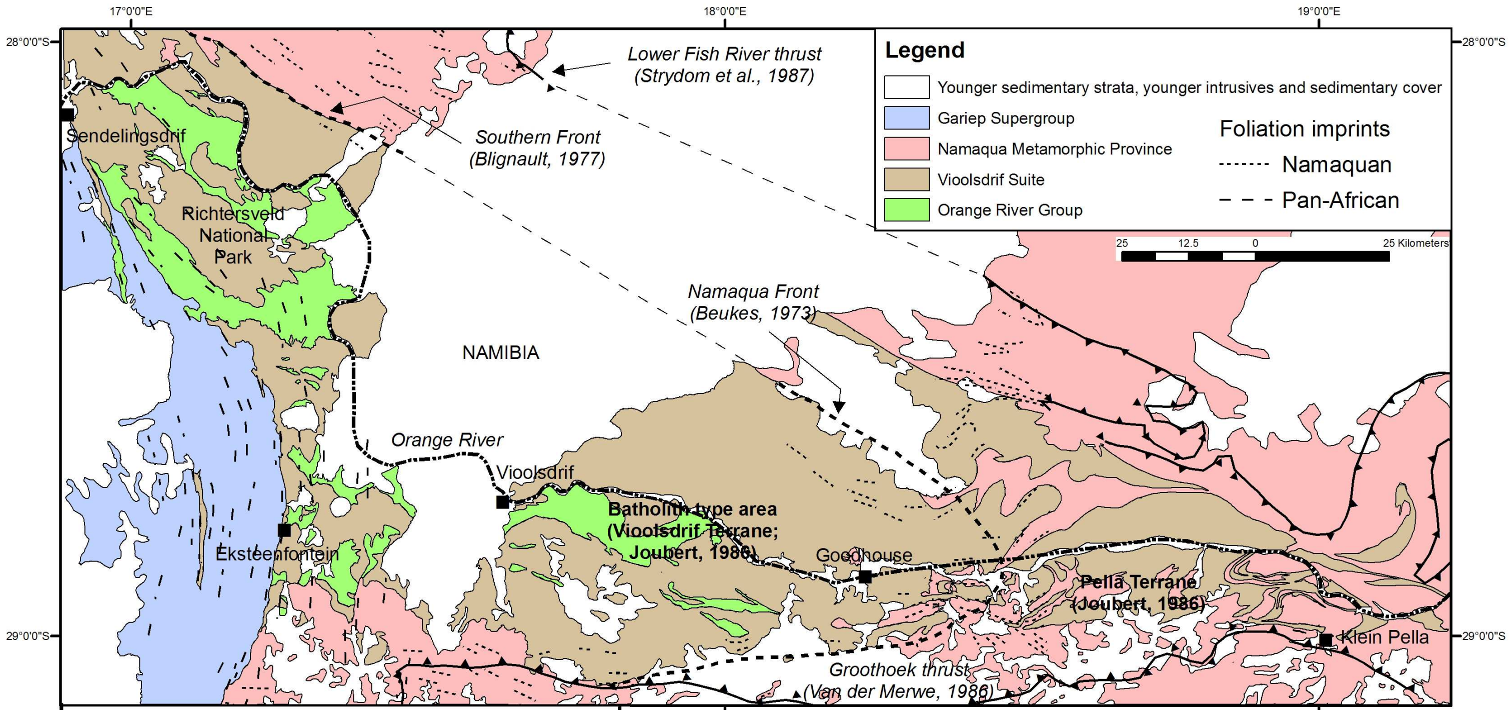

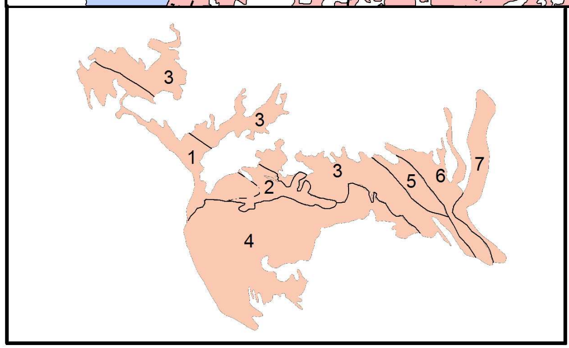

Figure 2.1: Extent of the Vioolsdrif Suite and Orange River Group as displayed in most current literature.

Insert: Tectonic subdivision of the Namaqua Metamorphic Province according to various previous investigators.
1 - Vioolsdrif Terrane (Joubert, 1986)
2 - Pella Terrane (Joubert, 1986)
3 - Aus Terrane (Joubert, 1986)
4 - Bushmanland Terrane (Cornell and Petterson, 2007)
5 - Areachap Terrane (Cornell and Petterson, 2007)
6 - Kaaien Terrane (Cornell and Petterson, 2007)
7 - Kheis Terrane (Cornell and Petterson, 2007)

APPENDIX 1

ANALYSES, SAMPLE LOCALITIES, DATA TREATMENT AND PROCESSING

1. DATA PROCESSING

Sample classification was done using the total alkali-silica (TAS) diagram of Le Maitre *et al*. (1989) for the volcanic rocks, and the R1-R2 diagram of De La Roche *et al*. (1980) for the plutonic rocks. In the thesis, data from Reid (1977) and Ritter (1980) are also used and data as to their localities, descriptions and analyses are to be found in those studies. Samples collected during the current study were analysed at the laboratory of the Council for Geoscience in Silverton. REE were analysed by ICPMS (results in ppb) while all other elements were analysed by XRF (results in ppm).

All results were recalculated to 100% volatile and Cr_2O_3 free. Wherever Cr is used in this study, the total ppm values from trace element analyses are used. Total iron contents received from the laboratory were calculated to FeO and Fe_2O_3 following the equations of Le Maitre (1976)[1], i.e.:

$Ox = 0.93 – 0.0042SiO_2 – 0.022(Na_2O + K_2O)$ for volcanic rocks

$Ox = 0.88 – 0.0016SiO_2 – 0.027(Na_2O + K_2O)$ for plutonic rocks

Then

$$Ox = FeO/Fe_2O_3T$$

Thus

$$FeO = Ox(Fe_2O_3T)$$

And

$$Fe_2O_3 = Fe_2O_3T – FeO$$

2. ANALYSES AND SAMPLE LOCALITIES

The analyses and localities of samples collected for the current study are given in the next table. A sample locality map is provided.

[1] Le Maitre, R.W. 1976. Some problems of the projections of chemical data into mineralogical classifications. Contributions to Mineralogy and Petrology, 56, 181-189.

Abreviations:

UNIT

VD = Vuurdood Subsuite

KH = Khoromus Tonalite

BW = Blockwerf migmatite Complex

XX = Xaminxaip River Granodiorite

GSh = Gaarseep Granodiorite in the Haib area

GSr = Gaarseep granodiorite in the Richtersveld

GSr(bw) = Gaarseep granodiorite in the Richtersveld intruding the Blockwerf migmatite Complex

HO = Hoogoor Granite

GH = Ghaams Granite

ST = Sout Granite

NO = Nous Formation

WV = Windvlakte Formation

PR = Paradys River Formation

AR = Abiekwa River Formation

KR = Kook River Formation

KU = Kuams River Formation

ROCK TYPE

PY = Pyroxenite

Ol-G = Olivine gabbro

G = Gabbro

GN = Gabbro norite

D = Diorite

SD = Syenodiorite

T = Tonalite

QzMO = Quartz monzonite

GD = Granodiorite

MGR = Monzogranite

SGR = Syenogranite

AGR = Alkali granite

BA = Basaltic andesite

A = Andesite

TA = Trachyandesite

D = Dacite

RH = Rhyolite

<u>Legend to localities map (Figure 1)</u>

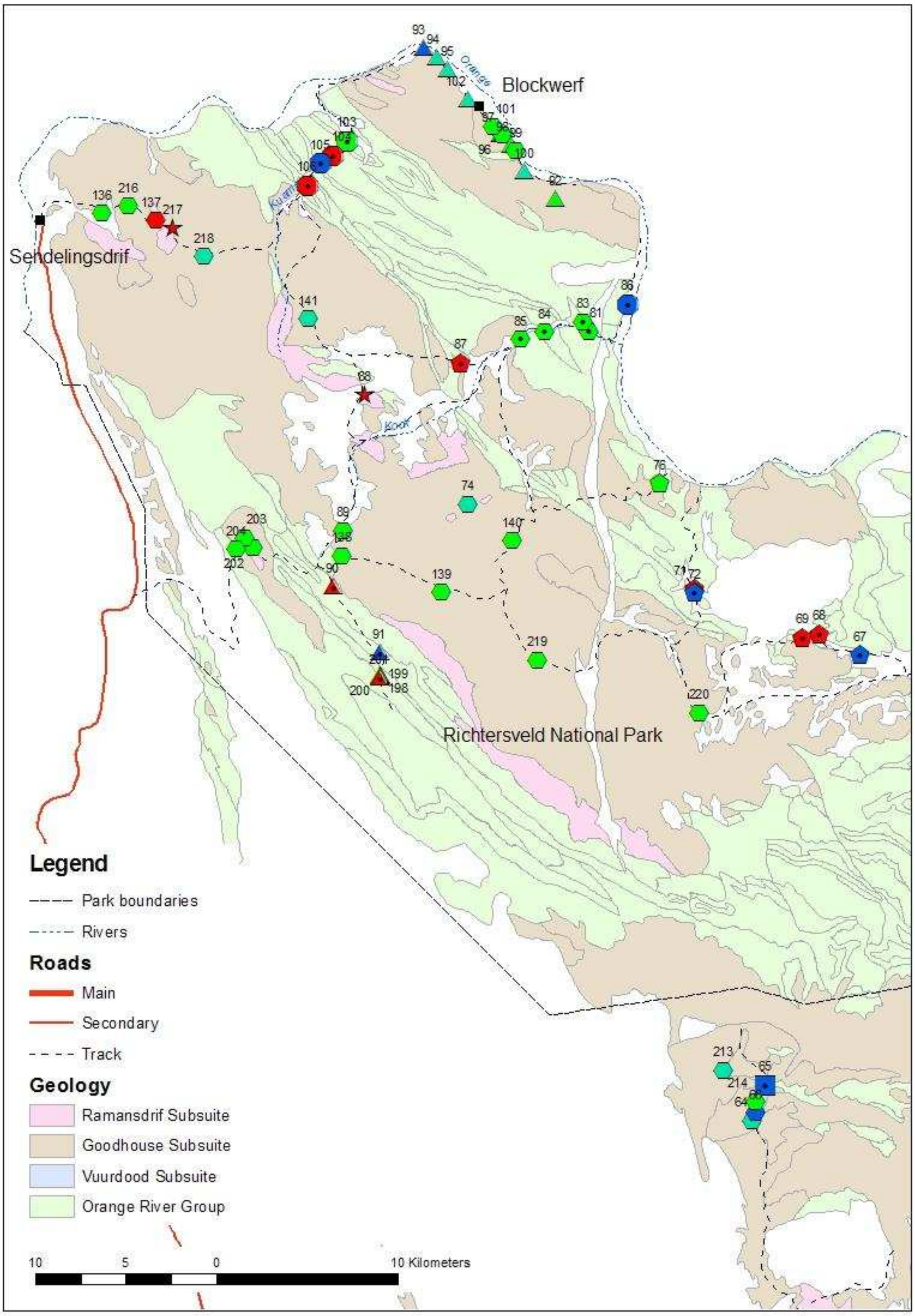

Figure 1: Sample localities.

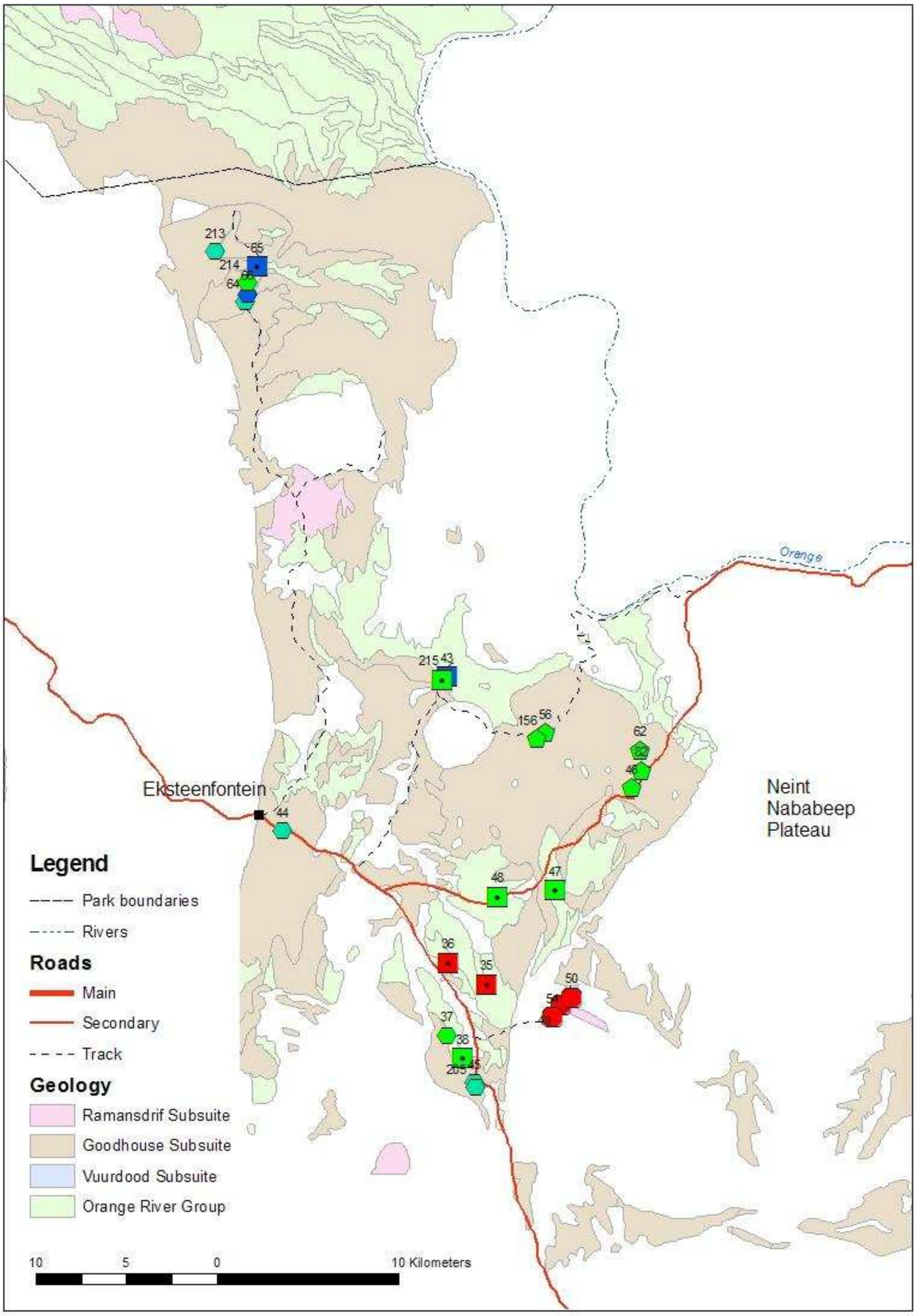

Figure 1 (continue).

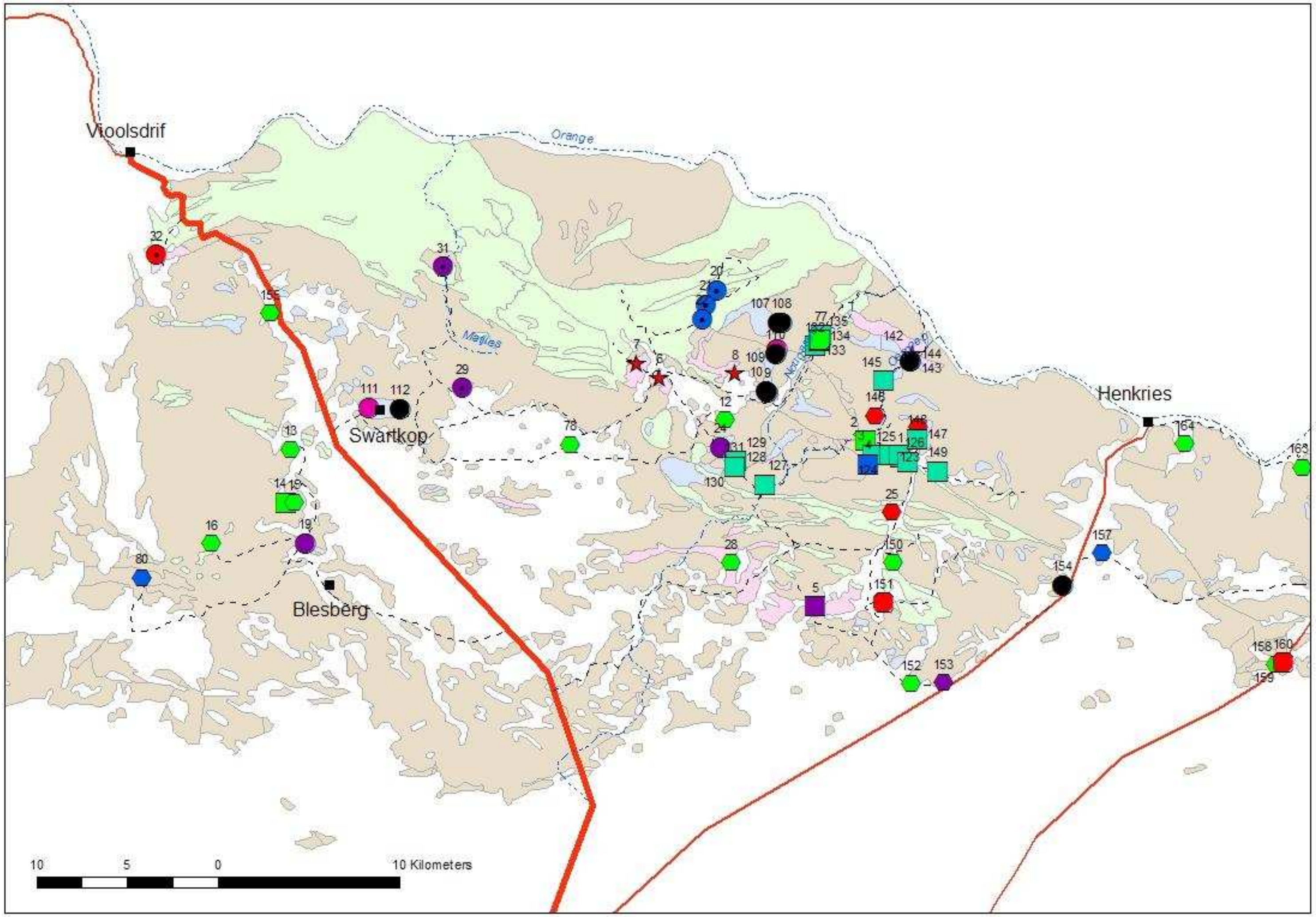

Figure 1 (Continue).

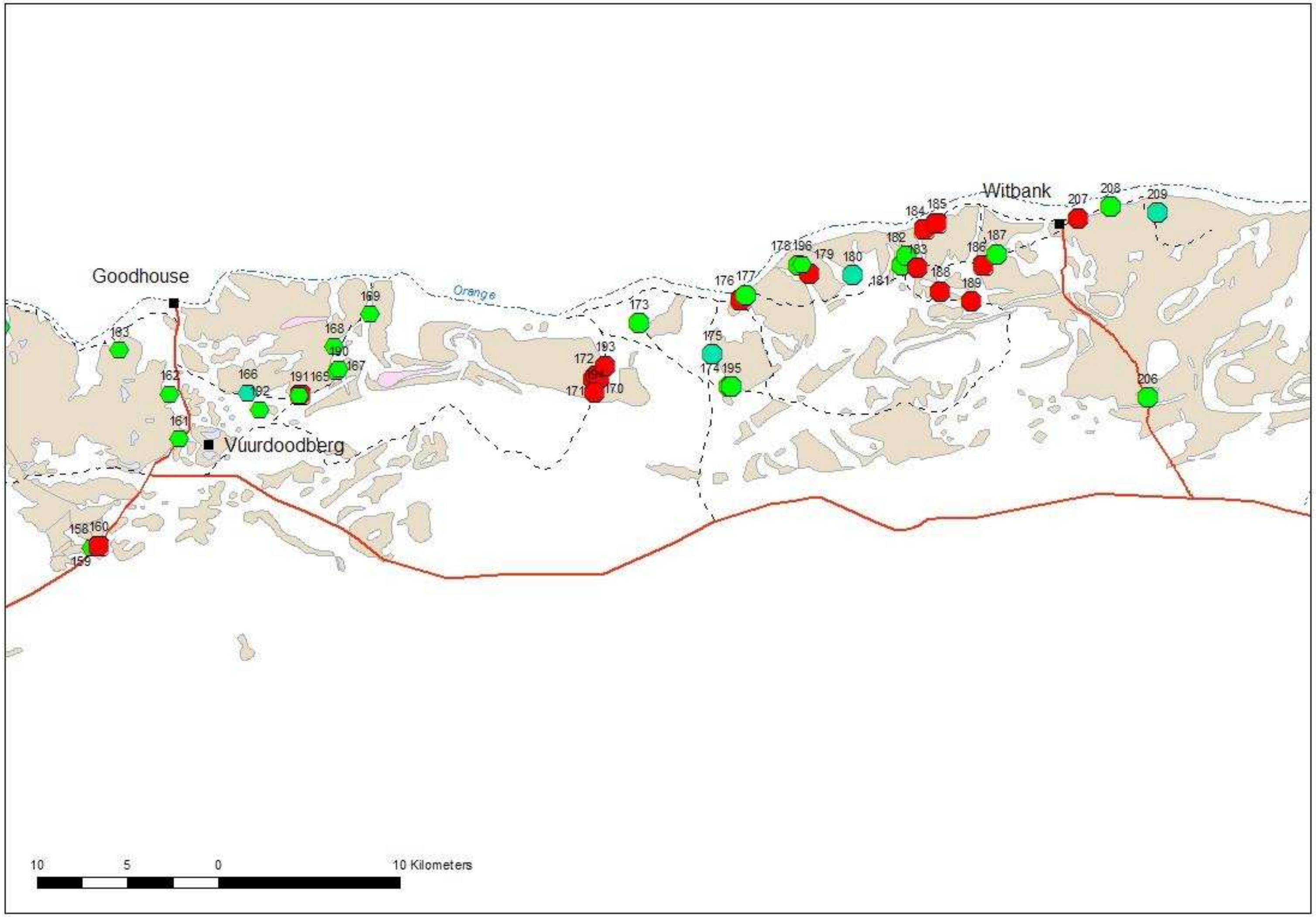
Goodhouse
Vuurdoodberg
Witbank
Orange
158
159
160
161
162
163
165
166
167
168
169
170
171
172
173
174
175
176
177
178
179
180
181
182
183
184
185
186
187
188
189
190
191
192
193
194
195
196
206
207
208
209
10
5
0
10 Kilometers

CHM	9	143	144	10	107	24	108	19	110	112	154	109	111	5	4	123	1	3	77	124
LONG	17.94330	18.01460	18.01460	17.94290	17.94860	17.92030	17.95044	17.71440	17.94760	17.76100	18.09000	17.94810	17.74600	17.96710	17.99350	18.00412	18.00940	17.99610	17.97000	18.00410
LAT	-28.88460	-28.86910	-28.86910	-28.88430	-28.85030	-28.91230	-28.85000	-28.95980	-28.86560	-28.89310	-28.98080	-28.86300	-28.89230	-28.99090	-28.92020	-28.91540	-28.91680	-28.91560	-28.85630	-28.91540
UNIT	VD	VD	VD	VD	VD	VD	VD	VD	VD	VD	VD	VD	VD	KH	KH	KH	KH	KH	KH	KH
ROCKTYPE	PY	PY	PY	Ol-G	Ol-G	Ol-G	Ol-G	G	G	G	G	GN	GN	G	D	D	T	T	T	T
SiO_2	49.02	51.80	49.83	47.98	47.91	49.10	47.93	49.92	48.67	48.55	47.15	50.51	50.72	51.30	60.38	59.61	61.71	61.46	66.39	62.01
TiO_2	0.37	0.37	0.35	0.24	0.45	0.74	1.12	0.97	0.35	0.27	0.38	0.44	0.49	0.94	0.74	0.71	0.70	0.71	0.50	0.58
Al_2O_3	6.88	4.95	8.90	17.72	18.54	16.34	16.41	15.50	10.38	16.54	16.86	13.97	16.13	18.08	17.63	17.43	17.12	17.39	16.51	17.74
Fe_2O_3(T)	11.36	8.45	7.95	7.86	7.48	10.82	12.56	11.81	10.18	6.60	8.78	9.25	8.48	9.78	5.96	5.68	5.67	5.58	2.88	4.23
MnO	0.20	0.17	0.16	0.13	0.11	0.15	0.14	0.20	0.19	0.12	0.13	0.17	0.15	0.15	0.11	0.11	0.11	0.11	0.07	0.08
MgO	19.16	15.43	13.79	9.54	7.46	7.59	6.05	7.18	16.24	11.07	13.22	10.63	8.98	5.15	2.45	2.31	2.25	2.24	0.83	1.49
CaO	10.17	16.01	16.16	12.19	12.58	9.21	9.77	8.58	10.61	13.48	9.44	9.46	11.48	8.84	6.11	6.32	5.54	5.68	3.84	5.74
Na_2O	1.30	0.63	0.81	1.84	1.94	2.25	2.48	1.64	1.31	1.61	2.07	2.24	2.26	1.78	2.91	3.00	2.92	2.85	3.48	3.00
K_2O	0.64	0.42	0.32	0.61	1.15	1.58	1.38	1.44	0.56	0.26	0.48	1.38	0.38	1.88	2.87	3.15	3.11	3.08	4.33	3.31
P_2O_5	0.09	0.02	0.08	0.06	0.08	0.12	0.12	0.40	0.08	0.03	0.07	0.07	0.07	0.47	0.25	0.23	0.23	0.24	0.10	0.17
Cr_2O_3	0.16	0.09	0.04	0.02	0.02	0.02	0.01	0.04	0.18	0.13	0.01	0.07	0.03	0.02	0.00	0.00	0.00	0.00	0.00	0.00
LOI	0.79	1.36	1.51	1.84	2.02	1.97	1.68	1.97	0.81	1.14	1.17	1.63	0.42	1.86	0.70	0.90	0.69	0.83	0.52	1.12
TOTAL	100.13	99.72	99.89	100.04	99.75	99.91	99.66	99.64	99.55	99.80	99.77	99.82	99.60	100.25	100.12	99.45	100.03	100.17	99.45	99.47
H_2O	0.05	0.21	0.17	0.12	0.09	0.08	0.16	0.02	0.11	0.13	0.12	0.15	0.14	0.08	0.10	0.07	0.07	0.10	0.06	0.05
Ba	242.00	65.00	67.00	162.00	209.00	398.00	345.00	311.00	192.00	59.00	162.00	320.00	149.00	463.00	821.00	901.00	892.00	875.00	1164.00	1014.00
Ce	<10	14.00	17.00	<10	21.00	12.00	34.00	34.00	10.00	<10	<10	16.00	<10	37.00	63.00	52.00	68.00	62.00	69.00	48.00
Co	83.00	54.00	53.00	54.00	37.00	44.00	42.00	35.00	64.00	40.00	59.00	45.00	40.00	25.00	18.00	9.60	15.00	9.00	<5	6.20
Cr	946.00	765.00	343.00	162.00	216.00	130.00	91.00	244.00	1991.00	1514.00	86.00	782.00	260.00	101.00	21.00	22.00	22.00	21.00	15.00	19.00
Cu	32.00	20.00	5.90	24.00	74.00	242.00	255.00	136.00	57.00	41.00	55.00	129.00	100.00	130.00	70.00	57.00	81.00	55.00	26.00	36.00
Hf	<5	<3	<3	<5	<3	<5	3.00	<5	<3	<3	<3	<3	<3	<5	8.00	4.50	7.00	6.00	5.00	5.40
Nb	<2	3.20	2.40	<2	2.20	<2	3.00	<2	1.70	7.10	3.10	2.50	1.10	<2	4.00	10.00	5.00	5.00	33.00	12.00
Ni	420.00	134.00	121.00	136.00	101.00	100.00	56.00	86.00	425.00	265.00	592.00	227.00	173.00	45.00	12.00	14.00	12.00	11.00	<5	9.20
Pb	<5	2.30	2.60	5.00	7.00	6.00	8.60	9.00	6.20	3.10	2.40	7.90	2.60	11.00	18.00	17.00	21.00	19.00	27.00	22.00
Rb	21.00	11.00	7.60	23.00	64.00	93.00	68.00	64.00	21.00	11.00	17.00	61.00	13.00	137.00	116.00	128.00	134.00	142.00	162.00	137.00
Sr	159.00	109.00	237.00	640.00	687.00	408.00	479.00	366.00	269.00	207.00	275.00	351.00	294.00	469.00	558.00	537.00	525.00	528.00	428.00	504.00
Th	<5	<3	<3	<5	3.40	<5	<3	<5	<3	<3	<3	<3	<3	<5	8.00	11.00	10.00	9.00	14.00	13.00
U	<3	<2	<2	<3	2.00	<3	<2	<3	<2	<2	<2	<2	2.30	<3	<3	4.10	<3	<3	7.00	4.40
V	138.00	167.00	159.00	91.00	152.00	283.00	422.00	251.00	130.00	122.00	92.00	178.00	151.00	226.00	111.00	98.00	102.00	103.00	42.00	66.00
Y	11.00	10.00	10.00	6.00	9.40	11.00	12.00	17.00	10.00	7.40	9.00	11.00	14.00	16.00	21.00	21.00	21.00	21.00	21.00	20.00
Zn	69.00	50.00	49.00	48.00	46.00	72.00	77.00	105.00	66.00	37.00	55.00	62.00	55.00	87.00	64.00	65.00	63.00	62.00	38.00	54.00
Zr	46.00	30.00	24.00	32.00	29.00	54.00	43.00	43.00	32.00	10.00	29.00	34.00	32.00	65.00	138.00	141.00	148.00	150.00	192.00	148.00
La	9133	6619	5459	6583	8430	12493	13163	23066	6579	1708	6759	8893	4819			35173			43075	41787
Ce	19990	15223	12399	13308	17673	26498	27164	47594	14254	3512	13599	17871	10630			70606			86360	81591
Pr	2754	2192	1880	1758	2416	3447	3699	5962	1977	591	1784	2513	1528			8802			10594	9965
Nd	12235	10232	9343	7295	10605	14754	15694	24412	8609	2606	7419	10647	7311			34336			39535	38894
Sm	2879	2462	2571	1618	2378	3090	3259	4837	2000	802	1507	2312	2008			6218			6996	6850
Eu	741	709	747	550	804	915	1014	1320	581	363	534	760	674			1565			1655	1718
Gd	2578	2410	2346	1374	2077	2689	2874	4146	1732	983	1603	2031	2043			5140			5661	5751
Tb	262	369	362	131	206	287	360	553	143	125	215	211	273			731			850	848
Dy	2484	2482	2615	1312	2090	2508	2768	3564	1866	1408	1740	2146	2777			4462			4784	4979
Ho	472	491	500	243	391	511	528	726	369	308	374	433	560			841			965	960
Er	1367	1287	1376	726	1106	1399	1468	1979	1074	938	1102	1252	1673			2434			2798	2738
Tm	180	178	188	106	151	191	213	278	152	133	161	182	231			344			393	392
Yb	1302	1241	1323	718	1120	1438	1558	2095	1121	946	1159	1323	1725			2544			2893	2777
Lu	204	162	184	103	158	200	228	299	161	140	170	198	263			370			438	404

CHM	125	126	127	128	129	130	131	132	133	134	145	148	149	2	14	135	96	93	94	95
LONG	18.00871	18.01308	17.94223	17.92787	17.92790	17.92749	17.92750	17.96730	17.96730	17.96930	18.00130	18.01810	18.02800	17.99240	17.70490	17.96960	17.12180	17.08380	17.08990	17.09530
LAT	-28.91586	-28.91905	-28.93036	-28.91873	-28.91870	-28.92152	-28.92150	-28.86150	-28.86150	-28.85920	-28.87870	-28.90780	-28.92370	-28.90870	-28.93920	-28.85870	-28.07870	-28.03580	-28.04080	-28.04690
UNIT	KH	KH	KH	KH	KH	KH	KH	KH	KH	KH	KH	KH	KH	KH	KH	KH	BW	BW	BW	BW
ROCKTYPE	T	T	T	T	T	T	T	T	T	T	T	T	T	GD	GD	GD	D	SD	T	T
SiO_2	63.35	61.94	65.08	62.84	62.11	62.39	62.67	62.95	62.63	62.79	66.05	64.78	62.56	66.75	66.14	70.27	60.73	55.42	62.01	64.89
TiO_2	0.51	0.58	0.69	0.69	0.70	0.72	0.72	0.60	0.61	0.61	0.69	0.70	0.77	0.67	0.50	0.36	0.64	0.67	0.63	0.45
Al_2O_3	17.71	17.77	16.06	16.30	16.59	16.43	16.34	16.78	16.91	16.98	15.24	15.55	15.86	15.28	14.53	15.05	16.00	19.70	16.60	15.38
Fe_2O_3(T)	3.51	4.12	4.17	4.74	4.89	5.01	4.88	4.43	4.66	4.57	4.25	4.50	5.52	4.03	5.08	2.25	6.17	6.05	5.40	4.19
MnO	0.07	0.08	0.09	0.09	0.09	0.09	0.09	0.09	0.10	0.09	0.08	0.08	0.10	0.08	0.10	0.06	0.12	0.10	0.09	0.07
MgO	1.22	1.53	1.20	1.69	1.81	1.89	1.83	1.57	1.69	1.65	1.43	1.66	2.20	1.10	2.61	0.59	3.17	3.22	2.60	2.26
CaO	5.23	5.56	4.34	5.08	4.91	5.38	5.28	5.04	5.04	5.23	3.89	4.49	5.14	3.42	3.80	2.22	5.55	4.92	3.69	3.75
Na_2O	3.49	3.09	2.96	2.76	2.85	2.65	3.07	3.19	3.02	3.01	3.49	3.50	3.58	3.07	2.71	3.36	3.54	6.94	3.40	3.70
K_2O	3.41	3.57	3.92	3.72	3.66	3.62	3.64	3.57	3.43	3.45	3.93	3.58	3.25	4.25	3.67	4.65	2.71	1.96	3.60	3.74
P_2O_5	0.14	0.17	0.19	0.22	0.23	0.24	0.23	0.18	0.19	0.20	0.21	0.24	0.28	0.18	0.12	0.07	0.21	0.24	0.34	0.17
Cr_2O_3	0.00	0.00	0.00	0.00	0.00	0.00	0.00	0.00	0.00	0.00	0.00	0.00	0.00	0.00	0.00	0.00	0.00	0.00	0.00	0.00
LOI	0.69	1.01	0.76	1.34	1.42	0.94	0.78	0.95	1.21	0.84	0.67	0.88	0.60	1.05	0.92	0.63	0.85	1.07	1.27	1.07
TOTAL	99.34	99.42	99.44	99.47	99.25	99.37	99.52	99.36	99.48	99.41	99.94	99.97	99.85	99.88	100.20	99.51	99.69	100.29	99.63	99.68
H_2O	0.08	0.11	0.20	0.05	0.10	0.13	0.06	0.21	0.12	0.10	0.18	0.18	0.14	0.14	0.14	0.16	0.14	0.08	0.12	0.10
Ba	954.00	1028.00	1095.00	1025.00	1014.00	1087.00	1063.00	1032.00	1011.00	990.00	1053.00	986.00	889.00	1053.00	716.00	1162.00	888.00	364.00	741.00	996.00
Ce	51.00	53.00	65.00	62.00	59.00	49.00	53.00	56.00	59.00	58.00	70.00	65.00	52.00	79.00	64.00	68.00	49.00	93.00	26.00	97.00
Co	4.80	5.80	4.80	8.70	8.40	7.50	7.70	6.30	7.60	7.20	10.00	11.00	15.00	6.00	5.00	1.70	12.00	20.00	10.00	8.00
Cr	13.00	14.00	9.40	31.00	37.00	33.00	34.00	18.00	18.00	19.00	36.00	32.00	62.00	9.00	80.00	7.20	53.00	84.00	39.00	51.00
Cu	27.00	40.00	45.00	52.00	52.00	45.00	48.00	40.00	38.00	40.00	57.00	61.00	36.00	44.00	54.00	13.00	14.00	<5	30.00	12.00
Hf	<3	<3	4.30	4.90	4.20	4.00	5.20	3.30	4.30	3.10	3.10	3.20	3.80	6.00	<5	4.40	<5	7.00	<5	<5
Nb	12.00	11.00	12.00	12.00	12.00	12.00	11.00	11.00	11.00	11.00	12.00	13.00	10.00	11.00	7.00	13.00	10.00	12.00	18.00	10.00
Ni	7.40	8.90	6.60	14.00	16.00	17.00	16.00	9.50	10.00	11.00	10.00	13.00	21.00	<5	27.00	4.80	25.00	40.00	15.00	27.00
Pb	22.00	21.00	20.00	20.00	17.00	19.00	17.00	20.00	19.00	15.00	20.00	20.00	16.00	27.00	24.00	24.00	18.00	21.00	22.00	25.00
Rb	152.00	162.00	154.00	148.00	141.00	130.00	134.00	147.00	135.00	136.00	157.00	143.00	148.00	183.00	161.00	177.00	98.00	73.00	173.00	120.00
Sr	506.00	511.00	371.00	394.00	442.00	417.00	403.00	450.00	473.00	455.00	358.00	375.00	408.00	338.00	268.00	286.00	534.00	417.00	363.00	468.00
Th	14.00	12.00	11.00	12.00	12.00	7.80	5.70	12.00	12.00	12.00	9.80	17.00	6.60	19.00	12.00	14.00	<5	22.00	5.00	19.00
U	5.50	4.60	2.90	4.10	4.10	2.70	2.60	4.00	4.10	4.00	<2	4.20	<2	3.00	<3	3.10	<2	6.00	3.00	3.00
V	55.00	62.00	67.00	86.00	93.00	92.00	93.00	74.00	80.00	74.00	83.00	90.00	117.00	65.00	92.00	24.00	135.00	108.00	93.00	78.00
Y	21.00	22.00	24.00	25.00	24.00	23.00	23.00	22.00	22.00	22.00	25.00	26.00	23.00	32.00	26.00	26.00	18.00	22.00	27.00	16.00
Zn	45.00	52.00	49.00	56.00	57.00	56.00	54.00	55.00	58.00	54.00	53.00	56.00	62.00	48.00	51.00	32.00	68.00	68.00	61.00	48.00
Zr	151.00	154.00	186.00	175.00	172.00	165.00	164.00	164.00	163.00	159.00	186.00	177.00	164.00	201.00	139.00	192.00	135.00	172.00	75.00	110.00
La	36748	43951	40617	46149	37541	39350	42070	51285	44781	46552	48705	45999	35679		38244	45494	25682	61539	15050	55475
Ce	72233	86974	80702	91253	74921	77051	81916	99612	87826	89739	95019	92139	69912		75206	89856	54989	119860	31866	110363
Pr	8874	10650	10023	11488	9397	9527	10088	11883	10613	10898	11630	11235	8847		9085	10968	6477	12296	3709	11508
Nd	33871	41758	39229	44809	36987	37706	39900	45753	40507	41673	43971	42760	34707		34450	40381	27298	45373	15545	41068
Sm	6101	7541	7174	8250	6646	6847	7331	8030	7222	7278	7880	7663	6293		6437	7054	4948	7318	3804	5832
Eu	1550	1777	1766	1962	1681	1836	1938	1997	1814	1932	1889	1782	1681		1336	1445	1422	1621	1208	1616
Gd	4986	6078	5836	6917	5673	5986	6390	6589	6009	6304	6683	6525	5434		5559	5941	4789	7000	4216	5720
Tb	701	890	866	1067	837	889	931	1005	891	906	1001	994	795		798	871	638	850	840	632
Dy	4252	5282	5093	5957	5057	5120	5341	5597	5121	5147	5678	5463	4603		4782	5172	3418	4370	5630	3181
Ho	848	1044	981	1184	968	996	1045	1068	966	997	1095	1079	891		964	991	664	813	1102	598
Er	2449	3020	2785	3328	2747	2835	2939	3142	2854	2811	3250	3071	2436		2731	2827	1957	2366	2998	1730
Tm	338	415	378	470	387	401	426	447	416	401	465	463	355		389	430	268	343	330	249
Yb	2544	3073	2917	3626	2896	2885	3036	3255	3063	2983	3281	3276	2655		2945	3064	1931	2325	1905	1688
Lu	369	429	414	503	421	429	453	484	449	433	494	490	374		434	464	289	335	271	250

CHM	100	102	92	98	46	56	62	76	82	156	153	80	157	66	45	166	12	13	15	16
LONG	17.13360	17.10550	17.14920	17.12700	17.43890	17.39600	17.44320	17.20110	17.44330	17.39160	18.03080	17.63310	18.10960	17.24830	17.36080	18.27310	17.92280	17.70710	17.70880	17.66770
LAT	-28.09710	-28.06130	-28.11100	-28.08410	-28.80950	-28.78190	-28.79070	-28.25220	-28.80090	-28.78510	-29.02890	-28.97680	-28.96470	-28.56450	-28.95590	-28.94290	-28.89840	-28.91320	-28.93950	-28.96000
UNIT	BW	BW	BW	BW	XX	XX	XX	XX	XX	XX	GSh	GSh	GSh	GSh	GSh	GSh	GSh	GSh	GSh	GSh
ROCKTYPE	T	T	GD	GD	GD	GD	GD	GD	GD	GD	G	D	D	SD	T	T	GD	GD	GD	GD
SiO_2	62.61	66.43	67.90	63.87	71.90	69.75	65.73	70.49	72.51	71.80	54.75	59.83	59.80	51.90	61.37	64.30	67.88	67.65	73.42	65.77
TiO_2	0.56	0.35	0.32	0.56	0.37	0.37	0.53	0.36	0.29	0.28	0.77	0.97	0.64	1.97	1.01	0.55	0.47	0.53	0.22	0.71
Al_2O_3	17.77	15.84	15.96	16.05	14.12	14.96	15.50	14.44	13.33	14.16	17.06	16.95	15.90	16.73	16.23	16.34	14.99	14.58	13.46	14.87
Fe_2O_3(T)	4.07	3.58	3.06	7.21	2.34	2.95	4.19	2.82	2.56	2.55	8.16	6.62	7.36	10.90	6.50	5.22	3.54	4.02	2.22	4.91
MnO	0.07	0.08	0.06	0.09	0.04	0.06	0.12	0.07	0.07	0.05	0.15	0.13	0.12	0.17	0.12	0.09	0.07	0.08	0.05	0.08
MgO	1.77	1.56	1.04	1.16	0.73	1.02	1.60	0.98	0.92	0.83	5.11	2.56	3.79	2.46	2.47	2.03	1.37	1.32	0.65	1.77
CaO	4.19	3.29	2.96	3.60	1.80	3.29	3.67	2.41	2.41	2.52	8.03	5.55	6.45	5.16	5.29	4.86	2.89	2.96	1.96	3.65
Na_2O	4.31	4.11	3.80	4.37	1.61	3.15	3.86	3.17	1.53	3.15	2.77	3.19	2.94	5.10	1.59	3.15	3.60	3.20	3.48	2.99
K_2O	2.82	3.82	3.98	1.69	5.29	3.45	2.57	4.25	4.49	3.75	1.72	2.69	2.12	2.91	3.38	2.72	4.31	4.51	3.96	4.09
P_2O_5	0.14	0.13	0.15	0.05	0.06	0.11	0.16	0.10	0.07	0.10	0.37	0.32	0.20	0.60	0.31	0.19	0.17	0.18	0.06	0.23
Cr_2O_3	0.00	0.00	0.00	0.00	0.00	0.00	0.00	0.00	0.00	0.00	0.02	0.00	0.00	0.00	0.00	0.00	0.00	0.00	0.00	0.02
LOI	1.02	0.89	0.66	0.90	1.03	0.85	1.35	1.02	0.89	1.13	1.02	1.15	0.81	1.56	1.41	0.78	0.54	0.79	0.42	0.95
TOTAL	99.32	100.08	99.89	99.57	99.30	99.97	99.26	100.12	99.07	100.31	99.92	99.96	100.11	99.46	99.66	100.22	99.84	99.81	99.91	100.03
H_2O	0.13	0.13	0.09	0.17	0.06	0.10	0.14	0.04	0.13	0.14	0.14	0.17	0.40	0.10	0.07	0.19	0.08	0.09	0.15	0.11
Ba	706.00	983.00	1127.00	365.00	1033.00	910.00	479.00	1310.00	609.00	795.00	438.00	1083.00	426.00	1168.00	1323.00	1399.00	811.00	832.00	702.00	1109.00
Ce	65.00	41.00	19.00	210.00	90.00	36.00	46.00	60.00	61.00	64.00	48.00	73.00	59.00	133.00	60.00	70.00	55.00	75.00	45.00	64.00
Co	8.00	<5	<5	11.00	8.00	<5	<5	11.00	<5	6.80	26.00	9.00	22.00	23.00	12.00	14.00	<5	8.00	<5	9.00
Cr	8.00	22.00	<5	62.00	17.00	15.00	11.00	14.00	18.00	17.00	187.00	87.00	46.00	14.00	50.00	18.00	39.00	35.00	10.00	78.00
Cu	<5	<5	<5	6.00	23.00	51.00	108.00	98.00	9.00	77.00	105.00	85.00	52.00	13.00	84.00	100.00	65.00	68.00	168.00	82.00
Hf	<5	<5	<5	14.00	6.00	5.00	<5	<5	<5	<3	3.60	<5	<3	13.00	5.00	<3	<5	<5	<5	<5
Nb	11.00	8.00	8.00	6.00	9.00	9.00	23.00	9.00	10.00	9.70	5.80	24.00	11.00	39.00	13.00	8.10	10.00	7.00	5.00	6.00
Ni	<5	14.00	<5	27.00	10.00	6.00	8.00	6.00	8.00	6.40	59.00	29.00	30.00	11.00	23.00	14.00	14.00	12.00	6.00	17.00
Pb	16.00	21.00	19.00	35.00	34.00	22.00	16.00	19.00	28.00	35.00	12.00	23.00	9.50	14.00	22.00	12.00	26.00	27.00	32.00	23.00
Rb	102.00	135.00	118.00	67.00	159.00	126.00	165.00	124.00	153.00	151.00	71.00	119.00	84.00	85.00	128.00	95.00	179.00	204.00	167.00	164.00
Sr	446.00	471.00	410.00	535.00	225.00	387.00	368.00	338.00	179.00	379.00	538.00	475.00	447.00	348.00	465.00	556.00	300.00	292.00	278.00	343.00
Th	31.00	6.00	<5	57.00	27.00	7.00	7.00	7.00	18.00	11.00	4.80	10.00	3.20	8.00	10.00	6.90	13.00	14.00	11.00	8.00
U	<2	2.00	2.00	<2	4.00	<2	<2	3.00	5.00	2.60	2.30	4.00	<2	<2	3.00	<2	<3	<3	<3	<3
V	58.00	61.00	41.00	90.00	33.00	54.00	81.00	47.00	40.00	45.00	187.00	136.00	163.00	102.00	122.00	112.00	79.00	69.00	33.00	95.00
Y	8.00	21.00	12.00	20.00	34.00	12.00	21.00	13.00	10.00	15.00	17.00	25.00	23.00	72.00	25.00	16.00	20.00	19.00	16.00	18.00
Zn	45.00	39.00	32.00	63.00	20.00	47.00	59.00	47.00	27.00	47.00	80.00	81.00	72.00	138.00	77.00	68.00	33.00	43.00	28.00	53.00
Zr	108.00	81.00	79.00	428.00	218.00	140.00	125.00	151.00	81.00	128.00	70.00	165.00	102.00	600.00	189.00	136.00	156.00	151.00	84.00	175.00
La	46724	26606	12812	125556	69812	35129	35539	34373	32979	29233	26199	41143	25433	65142	44375	44804	33772	51206	28109	48947
Ce	83655	55003	23856	219964	132131	69500	70749	66427	66009	58315	52241	84199	58368	140632	88679	83604	67439	93286	51382	94104
Pr	8206	6452	2527	21376	15854	8612	8787	7599	7560	7020	6691	10942	7997	19270	11277	9771	7953	10184	6179	11150
Nd	29869	26604	9162	75451	56367	33293	33554	27764	26941	26058	27561	43153	32510	81531	45028	36900	29452	34403	22303	42293
Sm	4070	5461	1666	10249	9953	5781	6321	4542	4148	4524	5251	8093	6072	16691	8088	6135	5262	5261	4183	7408
Eu	1426	1521	1178	2079	1596	1303	1060	1019	921	994	1633	2109	1232	4436	2029	1425	1134	1184	797	1863
Gd	3965	5217	1551	10189	8366	4647	5093	3554	3197	3605	4676	6580	5184	15051	6998	5000	4426	4597	3476	6183
Tb	399	761	256	1023	1316	586	803	411	284	448	678	1040	799	2839	987	606	573	541	401	894
Dy	1753	4613	1787	4368	7251	3398	4750	2622	2188	2798	4133	5830	4428	14993	5595	3344	3716	3736	3027	5141
Ho	316	909	385	772	1478	615	845	518	408	533	776	1161	883	2989	1099	621	732	759	598	1016
Er	882	2689	1253	1780	4407	1531	2349	1467	1188	1609	2237	3248	2514	8730	2985	1677	2223	2373	1793	2847
Tm	120	379	166	213	608	204	308	210	182	253	328	450	373	1199	411	227	307	359	264	383
Yb	828	2451	1028	1511	4705	1520	2280	1541	1444	1902	2286	3221	2636	8761	3163	1666	2317	2794	2031	2815
Lu	129	361	149	237	700	248	306	227	219	290	324	471	367	1281	456	225	348	425	295	401

CHM	28	78	150	152	155	158	159	161	162	163	164	167	168	169	190	191	192	196	25	146
LONG	17.92560	17.84600	18.00630	18.01520	17.69660	18.19590	18.19960	18.23910	18.23460	18.20940	18.15060	18.31730	18.31630	18.33400	18.31830	18.29850	18.27940	18.54850	18.00540	17.99710
LAT	-28.96940	-28.91070	-28.96940	-29.02940	-28.84560	-29.01990	-29.01870	-28.96600	-28.94350	-28.92200	-28.91050	-28.93220	-28.92010	-28.90390	-28.93150	-28.94410	-28.95130	-28.87920	-28.94450	-28.89630
UNIT	GSh	GSh	GSh	GSh	GSh	GSh	GSh	GSh	GSh	GSh	GSh	GSh	GSh	GSh	GSh	GSh	GSh	GSh	GSh	GSh
ROCKTYPE	GD	GD	GD	GD	GD	GD	GD	GD	GD	GD	GD	GD	GD	GD	GD	GD	GD	GD	MGR	MGR
SiO_2	71.63	69.86	66.14	70.30	68.76	67.16	66.71	66.98	74.64	74.01	69.12	74.56	70.52	69.67	73.98	70.76	70.42	69.29	72.47	74.57
TiO_2	0.25	0.34	0.48	0.31	0.37	0.48	0.43	0.51	0.22	0.19	0.56	0.23	0.36	0.44	0.23	0.30	0.33	0.48	0.40	0.18
Al_2O_3	14.20	14.57	14.57	13.72	14.22	14.60	14.97	14.63	13.39	13.51	14.01	13.41	14.61	14.37	13.47	14.51	14.68	14.48	13.96	12.82
Fe_2O_3(T)	2.65	3.02	4.66	3.44	3.75	4.67	4.51	4.98	1.87	2.00	4.62	1.97	3.88	3.63	2.09	2.94	3.11	3.63	2.55	1.91
MnO	0.06	0.10	0.08	0.07	0.07	0.08	0.09	0.10	0.04	0.03	0.07	0.06	0.07	0.08	0.06	0.08	0.06	0.07	0.05	0.05
MgO	0.80	1.05	2.15	1.41	1.70	2.36	2.20	2.41	0.48	0.52	1.11	0.51	1.27	1.28	0.56	1.04	1.12	1.25	0.44	0.56
CaO	2.43	3.19	3.75	2.90	3.00	3.62	3.80	4.05	1.93	1.94	3.03	1.78	3.08	2.93	1.75	2.80	3.25	2.54	1.64	1.66
Na_2O	3.67	1.76	2.85	3.01	2.71	2.20	2.47	2.37	3.17	2.59	2.97	2.68	2.91	3.12	2.00	2.21	2.57	3.10	3.35	2.86
K_2O	3.54	3.99	4.22	3.92	4.35	4.20	3.89	3.16	4.23	5.14	3.87	4.50	3.36	3.81	4.93	4.22	3.30	4.14	4.79	5.03
P_2O_5	0.09	0.09	0.13	0.09	0.10	0.13	0.12	0.12	0.06	0.07	0.21	0.08	0.13	0.15	0.07	0.11	0.12	0.15	0.07	0.05
Cr_2O_3	0.00	0.00	0.00	0.00	0.00	0.00	0.00	0.00	0.00	0.00	0.00	0.00	0.00	0.00	0.00	0.00	0.00	0.00	0.00	0.00
LOI	0.38	1.02	1.00	0.73	0.96	1.06	1.00	0.88	0.32	0.25	0.77	0.57	0.74	0.85	0.49	0.62	0.49	0.37	0.39	0.35
TOTAL	99.70	98.99	100.04	99.90	99.98	100.58	100.17	100.19	100.36	100.25	100.34	100.34	100.94	100.31	99.63	99.60	99.45	99.50	100.12	100.05
H_2O	0.08	0.19	0.18	0.13	0.14	0.35	0.27	0.07	0.26	0.36	0.26	0.09	0.15	0.35	0.06	0.10	0.08	0.06	0.06	0.19
Ba	767.00	1199.00	825.00	573.00	746.00	695.00	747.00	696.00	1084.00	1481.00	1202.00	1125.00	894.00	929.00	1000.00	770.00	1098.00	699.00	1148.00	740.00
Ce	58.00	63.00	56.00	62.00	58.00	56.00	58.00	51.00	62.00	59.00	41.00	78.00	50.00	43.00	63.00	61.00	66.00	110.00	131.00	79.00
Co	<5	8.00	14.00	9.60	13.00	16.00	15.00	15.00	4.50	5.10	10.00	4.80	10.00	10.00	3.60	6.80	7.20	8.40	<5	5.40
Cr	15.00	14.00	45.00	31.00	44.00	62.00	46.00	59.00	13.00	13.00	23.00	16.00	12.00	20.00	5.60	8.50	14.00	16.00	62.00	21.00
Cu	9.00	25.00	35.00	12.00	40.00	27.00	96.00	54.00	20.00	14.00	43.00	7.90	83.00	161.00	26.00	35.00	64.00	4.00	<5	8.70
Hf	9.00	6.00	4.40	<3	3.40	3.50	<3	<3	4.30	3.80	3.90	4.10	<3	<3	<3	3.80	<3	6.20	13.00	3.90
Nb	10.00	44.00	11.00	11.00	11.00	11.00	11.00	11.00	9.20	8.30	8.30	11.00	8.90	8.80	9.30	11.00	7.10	13.00	13.00	11.00
Ni	9.00	8.00	24.00	15.00	21.00	27.00	25.00	25.00	3.80	5.20	8.60	4.60	8.70	7.10	5.10	7.60	6.80	11.00	5.00	6.80
Pb	29.00	25.00	23.00	31.00	23.00	20.00	19.00	18.00	26.00	31.00	22.00	26.00	18.00	23.00	31.00	29.00	22.00	25.00	30.00	36.00
Rb	152.00	142.00	206.00	188.00	208.00	215.00	207.00	151.00	140.00	186.00	150.00	185.00	138.00	146.00	190.00	193.00	120.00	185.00	178.00	224.00
Sr	391.00	349.00	312.00	250.00	284.00	336.00	322.00	282.00	261.00	288.00	311.00	238.00	379.00	413.00	234.00	258.00	402.00	252.00	261.00	173.00
Th	11.00	13.00	19.00	21.00	18.00	12.00	17.00	7.00	9.60	16.00	6.90	14.00	8.10	9.30	11.00	15.00	10.00	25.00	22.00	26.00
U	<3	7.00	4.40	7.10	5.30	5.10	4.70	<2	<2	<2	3.10	2.90	<2	2.70	<2	3.10	<2	3.60	<3	4.10
V	34.00	47.00	95.00	55.00	79.00	105.00	96.00	89.00	29.00	30.00	76.00	27.00	77.00	73.00	15.00	45.00	43.00	49.00	23.00	25.00
Y	14.00	10.00	21.00	17.00	19.00	19.00	20.00	22.00	20.00	11.00	15.00	20.00	13.00	13.00	17.00	22.00	12.00	24.00	29.00	18.00
Zn	42.00	37.00	51.00	39.00	44.00	51.00	56.00	62.00	25.00	25.00	66.00	38.00	49.00	53.00	31.00	45.00	45.00	38.00	50.00	29.00
Zr	112.00	159.00	124.00	106.00	113.00	124.00	111.00	130.00	147.00	149.00	184.00	163.00	111.00	106.00	143.00	147.00	167.00	174.00	240.00	115.00
La	33717	42392	45056	42808	41922	33343	33352	28726	48787	39101	28033	43695	27753	24448	38746	37375	37294	60207		51035
Ce	66386	80662	88864	78119	79895	64164	65545	57303	97551	78486	53277	84775	53975	49234	80006	79253	71375	121300		98141
Pr	7812	9321	10526	9026	9368	7779	7880	7031	11766	9583	6640	9926	6460	6070	8477	8677	7521	12399		11024
Nd	29125	32933	39159	31708	33862	29284	29913	27053	44280	35352	26232	36555	24639	23730	32456	33437	28913	45104		38136
Sm	5159	5037	6827	4976	5728	5200	5752	5348	8040	5788	4715	6284	4268	4318	5485	6466	4408	7165		6009
Eu	1016	1203	1372	962	1167	1126	1114	1238	1566	1335	1307	1234	980	1040	1344	1187	1264	1294		902
Gd	3985	3990	5975	4168	4982	4551	4685	4845	6848	4512	3990	4990	3566	3426	4991	6460	4203	6799		4998
Tb	486	415	887	573	675	628	689	779	1086	510	535	625	430	449	678	982	507	896		687
Dy	3235	2583	5090	3329	4088	3793	4093	4475	6163	2485	3260	3459	2625	2711	3496	5082	2451	4952		3500
Ho	629	499	1052	644	806	746	785	867	1275	435	616	698	503	530	654	918	464	1000		680
Er	1838	1427	3219	1909	2299	2109	2286	2516	3647	1154	1706	1938	1495	1363	1790	2270	1241	2906		1871
Tm	265	212	509	296	352	309	343	359	550	176	240	291	206	207	274	317	184	452		277
Yb	2052	1751	4003	2253	2618	2459	2417	2528	3989	1373	1904	2187	1608	1535	1950	2049	1230	3117		1917
Lu	303	254	646	343	385	346	358	376	577	229	289	324	227	232	298	289	195	473		292

CHM	147	205	44	218	64	74	141	213	37	89	97	99	101	136	138	139	140	202	203	204
LONG	18.01880	17.36120	17.26560	16.97473	17.24690	17.10560	17.02630	17.23258	17.34710	17.04390	17.12290	17.12970	17.11840	16.92410	17.04340	17.09240	17.12790	16.99890	16.99500	16.99060
LAT	-28.90220	-28.95810	-28.83080	-28.13970	-28.56840	-28.26260	-28.17070	-28.54349	-28.93230	-28.27560	-28.07950	-28.08740	-28.07540	-28.11810	-28.28810	-28.30640	-28.28080	-28.28390	-28.27930	-28.28500
UNIT	GSh	GSr	GSr	GSr	GSr	GSr	GSr	GSr	GSr	GSr	GSr(bw)	GSr(bw)	GSr	GSr	GSr	GSr	GSr	GSr	GSr	GSr
ROCKTYPE	MGR	T	T	T	T	T	T	QzMO	GD	GD	GD	GD	GD	GD	GD	GD	GD	GD	GD	GD
SiO_2	75.04	62.64	62.19	63.62	61.47	64.93	63.35	61.77	64.50	65.99	69.69	66.07	67.50	70.44	71.04	67.47	67.70	66.82	67.21	67.49
TiO_2	0.10	0.88	0.89	0.61	0.66	0.69	0.57	0.84	0.82	0.65	0.41	0.61	0.45	0.35	0.41	0.58	0.46	0.45	0.45	0.41
Al_2O_3	13.26	15.46	16.34	16.26	15.55	15.37	16.25	16.69	15.62	14.67	14.77	15.19	15.69	14.15	13.87	14.52	14.82	14.47	14.12	14.44
Fe_2O_3(T)	1.23	5.78	5.98	5.58	6.75	4.93	4.94	6.10	5.40	4.47	3.02	4.00	3.27	3.20	2.75	4.45	4.27	4.56	4.40	4.34
MnO	0.04	0.10	0.11	0.11	0.12	0.10	0.10	0.09	0.10	0.08	0.03	0.06	0.03	0.07	0.07	0.09	0.08	0.09	0.07	0.09
MgO	0.34	2.10	2.16	2.24	2.84	1.84	1.75	2.28	1.59	1.58	0.77	1.17	0.93	1.05	0.98	1.49	1.46	2.02	1.99	1.85
CaO	1.50	4.53	5.07	4.87	5.77	4.00	4.75	3.30	4.28	3.44	1.76	2.85	2.17	2.79	2.38	3.69	3.51	4.20	3.66	3.77
Na_2O	3.30	3.19	1.74	2.74	1.24	3.05	4.15	4.71	2.54	3.33	1.76	3.28	1.71	3.42	3.37	3.62	3.27	2.58	2.41	2.37
K_2O	4.85	3.23	3.35	2.89	3.10	4.03	2.85	3.15	3.71	4.11	6.48	5.03	6.49	3.99	4.18	3.15	3.59	3.61	3.96	3.98
P_2O_5	0.05	0.26	0.29	0.18	0.15	0.23	0.18	0.27	0.24	0.19	0.09	0.17	0.11	0.14	0.11	0.20	0.15	0.13	0.13	0.13
Cr_2O_3	0.00	0.01	0.00	0.00	0.00	0.00	0.00	0.01	0.00	0.00	0.00	0.00	0.00	0.00	0.00	0.00	0.00	0.00	0.00	0.00
LOI	0.48	1.43	1.25	1.21	1.57	1.02	0.79	1.09	1.03	0.85	0.55	0.87	0.67	0.67	0.96	0.97	0.91	1.16	1.67	1.42
TOTAL	100.19	99.59	99.36	100.31	99.21	100.18	99.69	100.29	99.85	99.37	99.34	99.29	99.02	100.26	100.12	100.22	100.22	100.08	100.08	100.27
H_2O	0.18	0.08	0.06	0.20	0.10	0.02	0.19	0.25	0.10	0.06	0.11	0.06	0.10	0.24	0.25	0.23	0.22	0.06	0.06	0.07
Ba	730.00	1174.00	1329.00	992.00	737.00	1263.00	816.00	1969.00	1225.00	1036.00	1304.00	1686.00	1618.00	984.00	878.00	1091.00	992.00	766.00	896.00	924.00
Ce	59.00	38.00	57.00	43.00	55.00	62.00	50.00	25.00	68.00	78.00	176.00	134.00	156.00	62.00	62.00	54.00	64.00	51.00	52.00	49.00
Co	4.10	14.00	14.00	16.00	21.00	10.00	12.00	20.00	<5	8.00	6.00	6.00	<5	8.80	7.60	12.00	11.00	15.00	14.00	13.00
Cr	17.00	49.00	44.00	28.00	39.00	31.00	19.00	56.00	46.00	20.00	10.00	15.00	11.00	17.00	27.00	37.00	18.00	32.00	42.00	26.00
Cu	21.00	71.00	77.00	24.00	103.00	44.00	27.00	137.00	46.00	35.00	29.00	44.00	45.00	23.00	7.80	11.00	29.00	24.00	147.00	18.00
Hf	<3	3.60	<5	4.90	<5	<5	3.00	7.60	<5	6.00	8.00	11.00	9.00	<3	3.60	3.10	3.20	3.50	4.10	4.50
Nb	8.10	11.00	11.00	8.90	10.00	10.00	9.80	10.00	13.00	14.00	12.00	19.00	10.00	9.90	11.00	12.00	11.00	11.00	10.00	8.60
Ni	3.80	23.00	19.00	12.00	31.00	20.00	7.70	27.00	20.00	14.00	6.00	8.00	6.00	7.20	11.00	16.00	10.00	17.00	17.00	13.00
Pb	35.00	19.00	20.00	13.00	22.00	24.00	14.00	21.00	23.00	20.00	20.00	27.00	22.00	16.00	21.00	19.00	14.00	20.00	24.00	15.00
Rb	195.00	127.00	120.00	110.00	132.00	148.00	106.00	114.00	147.00	133.00	195.00	169.00	168.00	187.00	163.00	108.00	144.00	156.00	172.00	161.00
Sr	208.00	456.00	385.00	432.00	333.00	336.00	447.00	297.00	375.00	282.00	253.00	320.00	309.00	345.00	209.00	326.00	331.00	336.00	305.00	326.00
Th	16.00	7.30	7.00	6.50	12.00	9.00	9.10	6.20	10.00	17.00	16.00	10.00	12.00	11.00	13.00	13.00	14.00	15.00	14.00	13.00
U	<2	2.70	<2	2.70	3.00	4.00	2.80	<2	<3	5.00	2.00	2.00	3.00	2.80	<2	2.50	3.60	3.70	3.90	2.80
V	10.00	111.00	107.00	99.00	129.00	89.00	81.00	119.00	96.00	76.00	42.00	63.00	48.00	56.00	41.00	93.00	74.00	94.00	88.00	84.00
Y	17.00	21.00	24.00	19.00	20.00	19.00	21.00	24.00	32.00	27.00	25.00	32.00	12.00	14.00	21.00	22.00	19.00	19.00	20.00	16.00
Zn	20.00	68.00	69.00	64.00	79.00	65.00	60.00	63.00	69.00	44.00	25.00	49.00	29.00	40.00	41.00	60.00	45.00	47.00	57.00	39.00
Zr	70.00	168.00	173.00	132.00	120.00	177.00	149.00	275.00	207.00	182.00	306.00	411.00	305.00	138.00	157.00	184.00	133.00	112.00	143.00	106.00
La	39156	26059	43687	20230	33678	38906	37348	30107		46529	86175	60154	97761	33029	53347	53268	44103	31457	26306	31975
Ce	77260	53825	88657	42580	67422	74751	74069	61668		93903	171987	138305	189620	65806	99218	105695	82035	61731	54635	64821
Pr	9135	7110	11303	5405	8262	9038	9137	8241		11514	18094	16267	18494	7114	11771	12551	9392	7522	6957	6876
Nd	33451	28374	45755	21250	31611	34515	35794	33447		43929	64728	63995	63466	25045	42654	46870	33371	27800	26835	24779
Sm	6234	5650	8739	3914	5829	6157	6425	6332		7759	9785	10456	7872	4019	7387	7953	5509	4931	5001	4110
Eu	1108	1665	2177	1059	1269	1520	1547	1863		1436	1810	2082	1906	923	1364	1687	1145	1108	1009	1003
Gd	5075	4937	7162	3407	4784	5029	5394	5509		6101	9445	9732	7315	3422	6352	6631	4621	4192	4083	3688
Tb	687	836	1116	696	672	731	771	860		943	1070	1179	719	408	926	974	611	770	764	708
Dy	3696	4214	6207	2812	4234	4334	4494	4665		5329	5397	6063	2891	2495	5574	5491	3590	3486	3547	2919
Ho	686	811	1180	552	832	887	857	875		1097	978	1142	502	495	1063	1060	708	692	688	570
Er	1981	2234	3256	1588	2491	2438	2532	2324		3116	2631	3179	1349	1469	3089	3084	2091	2053	1954	1704
Tm	312	349	419	257	346	338	373	363		426	363	435	187	214	438	453	303	348	322	273
Yb	2408	2355	3135	1637	2567	2526	2742	2273		3281	2331	2938	1247	1677	3245	3359	2353	2237	2016	1837
Lu	363	337	426	254	376	377	399	330		473	309	404	185	247	457	486	337	343	311	265

CHM	214	216	219	220	137	175	180	209	173	174	177	178	181	182	187	195	197	206	208	170
LONG	17.24848	16.93747	17.13988	17.22077	16.95070	18.50390	18.57360	18.72450	18.46710	18.51230	18.52040	18.54670	18.59770	18.59990	18.64510	18.51300	19.00010	18.72000	18.70160	18.44470
LAT	-28.55896	-28.11473	-28.33985	-28.36600	-28.12170	-28.92360	-28.88430	-28.85350	-28.90830	-28.93980	-28.89420	-28.87930	-28.87940	-28.87480	-28.87380	-28.93970	-28.92810	-28.94520	-28.85040	-28.93600
UNIT	GSr	GSr	GSr	GSr	GSr	HO	HO	HO	HO	HO	HO	HO	HO	HO	HO	HO	HO	HO	HO	HO
ROCKTYPE	GD	GD	GD	GD	MGR	T	T	T	GD	GD	GD	GD	GD	GD	GD	GD	GD	GD	GD	MGR
SiO_2	68.19	71.23	69.19	70.40	73.51	63.80	64.34	64.81	68.08	70.23	71.15	73.91	71.73	66.52	72.90	69.40	76.02	71.58	67.15	70.18
TiO_2	0.49	0.26	0.52	0.44	0.20	0.94	0.60	0.64	0.61	0.37	0.33	0.35	0.37	0.54	0.28	0.38	0.36	0.37	0.44	0.27
Al_2O_3	15.22	14.34	14.23	14.05	13.25	15.78	14.97	15.43	14.22	14.47	14.41	13.32	14.27	15.06	13.99	14.92	13.34	14.05	14.90	15.78
Fe_2O_3(T)	3.99	2.95	3.58	3.63	2.04	5.86	5.77	5.13	4.41	3.41	2.72	2.49	2.87	5.01	2.35	3.59	1.06	2.89	4.37	1.83
MnO	0.08	0.07	0.07	0.06	0.05	0.11	0.13	0.09	0.08	0.07	0.04	0.05	0.06	0.10	0.06	0.07	0.05	0.07	0.08	0.03
MgO	1.61	1.03	1.27	1.14	0.56	2.29	3.11	2.04	1.31	1.27	1.14	0.70	1.11	2.16	0.82	1.31	0.37	1.10	1.85	0.45
CaO	3.87	2.85	2.93	2.65	1.78	4.08	4.34	4.43	3.15	3.10	2.64	1.80	2.41	3.80	2.12	2.94	1.73	2.33	4.06	1.56
Na_2O	2.77	2.81	2.85	2.78	3.43	3.57	2.83	3.19	4.05	3.19	2.82	3.22	2.97	3.08	2.98	2.55	2.71	3.27	3.33	3.31
K_2O	2.83	4.11	4.27	4.41	4.66	2.25	2.50	3.90	3.86	3.45	4.35	4.07	3.93	3.05	4.45	3.82	3.68	4.31	3.23	6.44
P_2O_5	0.16	0.12	0.16	0.16	0.06	0.37	0.19	0.26	0.21	0.13	0.13	0.10	0.11	0.15	0.10	0.11	0.06	0.11	0.19	0.08
Cr_2O_3	0.00	0.00	0.00	0.00	0.00	0.00	0.00	0.00	0.00	0.00	0.00	0.00	0.00	0.00	0.00	0.00	0.00	0.00	0.00	0.00
LOI	1.18	0.74	0.53	0.65	0.45	1.13	1.19	0.23	0.16	0.56	0.37	0.41	0.52	0.56	0.32	0.57	0.27	0.33	0.41	0.26
TOTAL	100.38	100.50	99.59	100.39	99.99	100.20	99.98	100.16	100.13	100.24	100.09	100.41	100.35	100.02	100.37	99.68	99.65	100.42	100.00	100.19
H_2O	0.15	0.27	0.24	0.21	0.20	0.12	0.07	0.06	0.26	0.05	0.26	0.08	0.07	0.42	0.13	0.11	0.04	0.10	0.06	0.33
Ba	1239.00	843.00	895.00	806.00	614.00	565.00	1196.00	1239.00	977.00	888.00	841.00	732.00	921.00	892.00	1141.00	722.00	779.00	864.00	998.00	1064.00
Ce	56.00	58.00	50.00	73.00	55.00	59.00	52.00	74.00	68.00	74.00	91.00	95.00	89.00	58.00	102.00	76.00	47.00	85.00	66.00	79.00
Co	13.00	7.90	11.00	8.80	5.70	15.00	18.00	13.00	9.30	9.30	8.40	6.70	7.40	14.00	6.60	10.00	1.70	7.90	11.00	4.70
Cr	44.00	8.30	54.00	47.00	12.00	44.00	66.00	41.00	23.00	37.00	16.00	19.00	24.00	23.00	31.00	22.00	10.00	31.00	45.00	9.80
Cu	125.00	24.00	38.00	43.00	13.00	23.00	50.00	68.00	27.00	3.40	753.00	<2	<2	3.60	4.00	134.00	<2	61.00	9.80	6.90
Hf	4.00	3.30	4.50	3.20	<3	3.80	<3	4.00	4.30	4.60	<3	4.40	<3	3.20	3.40	4.40	5.90	3.50	3.90	3.90
Nb	8.40	8.70	14.00	13.00	11.00	13.00	8.00	11.00	11.00	11.00	12.00	14.00	9.90	9.00	13.00	10.00	9.10	12.00	9.10	14.00
Ni	11.00	6.70	17.00	15.00	4.70	21.00	28.00	18.00	9.90	10.00	8.70	7.60	11.00	13.00	8.30	12.00	2.60	11.00	14.00	5.70
Pb	19.00	19.00	26.00	25.00	24.00	16.00	21.00	20.00	21.00	22.00	25.00	23.00	22.00	16.00	21.00	28.00	13.00	20.00	17.00	27.00
Rb	105.00	163.00	157.00	178.00	215.00	177.00	104.00	132.00	130.00	164.00	181.00	181.00	171.00	137.00	163.00	188.00	137.00	200.00	110.00	274.00
Sr	364.00	337.00	265.00	239.00	221.00	313.00	557.00	480.00	275.00	328.00	271.00	213.00	268.00	353.00	345.00	304.00	115.00	252.00	500.00	247.00
Th	6.70	15.00	10.00	14.00	19.00	4.60	9.80	12.00	17.00	17.00	22.00	25.00	19.00	11.00	23.00	17.00	14.00	19.00	12.00	32.00
U	2.40	4.20	3.30	4.00	4.40	2.10	2.60	2.80	3.40	2.70	<2	5.10	2.20	2.70	2.80	2.30	2.00	3.20	<2	3.70
V	87.00	52.00	73.00	73.00	29.00	114.00	137.00	97.00	69.00	66.00	48.00	37.00	47.00	103.00	33.00	66.00	12.00	46.00	79.00	25.00
Y	16.00	13.00	23.00	21.00	12.00	22.00	14.00	20.00	20.00	19.00	18.00	22.00	17.00	17.00	29.00	17.00	20.00	24.00	14.00	20.00
Zn	56.00	36.00	53.00	50.00	23.00	77.00	95.00	57.00	48.00	37.00	26.00	33.00	35.00	53.00	36.00	38.00	11.00	37.00	46.00	14.00
Zr	138.00	119.00	162.00	149.00	95.00	194.00	114.00	162.00	174.00	134.00	130.00	141.00	134.00	121.00	149.00	133.00	166.00	132.00	136.00	197.00
La	29225	27918	32990	38506	36044	34529	26759	39699	44913	38008	47850	48320	49261	30311	51928	40445	39475	34995	23189	54550
Ce	57940	53512	66744	71814	61380	66459	53521	78816	80839	73518	92675	91054	88022	58122	92846	84210	77804	69193	49644	99117
Pr	7463	6153	8004	8532	6647	8084	6494	9972	9184	8730	10948	10143	9949	6917	10274	8937	8023	8624	5824	10797
Nd	29133	21853	29866	30825	22520	31758	24829	37693	33336	32067	40494	34268	34670	26265	35579	33700	29479	32157	21935	37104
Sm	5387	3671	5009	5147	3286	5724	4286	6850	5444	5688	6961	5636	5170	4489	5978	5754	4817	5631	3941	5618
Eu	1296	864	1086	1181	668	1555	1089	1583	1359	1096	1168	899	1095	1071	1063	1253	1106	1093	912	1007
Gd	4490	3135	4314	4305	2800	5308	3550	5389	4817	4613	5391	4635	4553	3778	5480	5246	4773	4843	3084	4642
Tb	772	681	757	784	315	707	496	820	615	594	679	604	566	652	846	698	732	805	668	581
Dy	3519	2455	3649	3585	2036	4342	2776	4348	3678	3678	3738	3837	3286	3216	5381	3676	4295	4293	2337	3483
Ho	661	482	710	710	404	841	547	829	731	730	701	784	672	641	1133	692	901	811	443	724
Er	1785	1362	2084	2178	1299	2315	1514	2342	2120	2082	1796	2427	1872	1848	3324	1823	2664	2612	1274	2199
Tm	280	238	336	342	211	312	227	379	328	321	259	376	267	278	528	257	409	415	207	329
Yb	1809	1638	2272	2431	1643	2199	1555	2418	2387	2423	1796	2851	1991	2037	3752	1696	2948	2823	1377	2601
Lu	265	248	361	366	266	291	230	377	386	327	245	421	305	300	499	258	472	435	197	379

CHM	171	172	179	183	188	189	193	194	207	160	165	49	54	151	186	176	184	185	50	217
LONG	18.44620	18.44760	18.55200	18.60570	18.61670	18.63210	18.45050	18.44520	18.68520	18.19960	18.29950	17.40390	17.39950	18.00140	18.63850	18.51770	18.60940	18.61490	17.40880	16.95914
LAT	-28.93410	-28.93540	-28.88340	-28.88080	-28.89230	-28.89750	-28.92920	-28.94280	-28.85620	-29.01870	-28.94400	-28.91680	-28.92320	-28.98890	-28.87950	-28.89670	-28.86170	-28.85860	-28.91310	-28.12543
UNIT	HO	HO	HO	HO	HO	HO	HO	HO	HO	GH	GH	GH	GH	GH	GH	GH	GH	GH	GH	ST
ROCKTYPE	MGR	MGR	MGR	MGR	MGR	MGR	MGR	MGR	MGR	MGR	MGR	SGR	SGR	SGR	SGR	SGR	AGR	AGR	AGR	MGR
SiO_2	71.36	71.16	73.09	76.04	71.25	77.11	77.52	73.98	77.99	75.52	75.35	73.96	73.16	76.27	78.67	78.49	78.41	78.95	75.05	76.64
TiO_2	0.50	0.44	0.37	0.30	0.39	0.23	0.14	0.18	0.15	0.12	0.16	0.09	0.18	0.05	0.06	0.11	0.14	0.10	0.10	0.07
Al_2O_3	13.92	14.47	13.45	12.57	14.11	11.74	12.03	13.57	11.83	13.83	13.19	14.13	13.79	13.31	11.90	11.77	11.87	11.50	13.69	12.87
Fe_2O_3(T)	3.07	2.65	2.88	1.95	3.72	1.48	1.15	1.60	1.15	1.40	1.57	0.90	1.73	0.75	0.60	0.79	1.15	0.79	0.94	1.20
MnO	0.06	0.05	0.05	0.04	0.07	0.04	0.02	0.04	0.04	0.07	0.04	0.10	0.03	0.04	0.01	0.01	0.01	0.01	0.03	0.03
MgO	0.73	0.68	0.75	0.51	1.29	0.46	0.41	0.34	0.29	0.49	0.37	0.19	0.34	0.09	0.01	0.02	0.06	0.04	0.21	0.35
CaO	1.99	1.82	1.73	1.10	0.82	0.99	1.12	1.66	1.49	1.05	1.71	0.47	0.58	0.73	0.73	0.71	0.25	0.37	0.23	1.23
Na_2O	3.42	3.15	3.49	2.41	3.04	2.51	2.85	2.80	3.27	2.38	2.78	3.64	3.62	3.41	2.25	2.33	2.38	2.48	3.54	2.91
K_2O	4.73	5.31	4.32	5.28	5.09	4.63	4.20	5.07	3.43	4.61	4.81	5.03	4.57	4.79	5.98	5.92	5.84	5.76	5.44	4.90
P_2O_5	0.15	0.13	0.11	0.06	0.12	0.05	0.03	0.05	0.05	0.14	0.05	0.19	0.13	0.19	0.01	0.01	0.05	0.01	0.05	0.05
Cr_2O_3	0.00	0.00	0.00	0.00	0.00	0.00	0.00	0.00	0.00	0.00	0.00	0.00	0.00	0.00	0.00	0.00	0.00	0.00	0.00	0.00
LOI	0.31	0.35	0.38	0.17	0.35	0.67	0.17	0.27	0.07	0.66	0.45	0.84	1.20	0.61	0.17	0.26	0.31	0.36	0.57	0.36
TOTAL	100.23	100.20	100.62	100.41	100.24	99.90	99.67	99.55	99.75	100.28	100.48	99.54	99.35	100.24	100.35	100.41	100.46	100.36	99.86	100.61
H_2O	0.26	0.09	0.04	0.26	0.08	0.07	0.04	0.31	0.08	0.11	0.34	0.16	0.09	0.20	0.08	0.09	0.16	0.04	0.10	0.18
Ba	1073.00	1224.00	781.00	626.00	955.00	340.00	589.00	1095.00	766.00	411.00	806.00	83.00	481.00	157.00	249.00	53.00	915.00	64.00	425.00	401.00
Ce	115.00	133.00	90.00	82.00	53.00	71.00	46.00	68.00	50.00	27.00	39.00	<5	83.00	<10	14.00	57.00	34.00	41.00	13.00	53.00
Co	6.10	6.10	7.10	4.30	8.00	4.50	1.80	2.80	2.50	4.70	4.80	<5	5.00	2.30	1.90	2.50	2.90	2.20	6.00	3.30
Cr	16.00	15.00	22.00	16.00	27.00	15.00	<3	3.50	13.00	15.00	12.00	55.00	16.00	14.00	7.70	8.50	9.60	11.00	33.00	24.00
Cu	39.00	73.00	3.40	16.00	6.70	2.20	45.00	<2	33.00	32.00	21.00	9.00	8.00	5.80	101.00	130.00	38.00	2.40	19.00	21.00
Hf	5.70	4.60	5.20	<3	4.50	3.50	3.60	3.00	<3	<3	3.10	<5	<5	<3	<3	<3	<3	<3	<5	<3
Nb	19.00	18.00	15.00	11.00	16.00	14.00	11.00	12.00	11.00	9.20	13.00	24.00	14.00	14.00	3.10	10.00	15.00	13.00	6.00	11.00
Ni	6.50	6.70	8.40	4.90	12.00	5.20	4.10	3.50	<2	6.30	4.00	<5	<5	2.90	<2	2.30	2.50	2.20	<5	3.30
Pb	21.00	25.00	22.00	30.00	8.80	26.00	12.00	27.00	17.00	36.00	33.00	31.00	47.00	40.00	30.00	35.00	29.00	24.00	36.00	35.00
Rb	225.00	211.00	201.00	211.00	192.00	219.00	160.00	221.00	124.00	227.00	208.00	353.00	239.00	313.00	181.00	218.00	198.00	271.00	261.00	201.00
Sr	228.00	227.00	220.00	147.00	116.00	98.00	141.00	194.00	152.00	129.00	216.00	36.00	136.00	57.00	131.00	68.00	94.00	27.00	120.00	129.00
Th	23.00	21.00	27.00	22.00	16.00	31.00	18.00	13.00	17.00	9.50	25.00	6.00	51.00	6.90	18.00	24.00	14.00	38.00	12.00	14.00
U	4.60	3.30	4.50	2.40	4.20	5.60	2.40	3.70	<2	<2	4.20	4.00	5.00	4.00	<2	<2	4.60	3.90	4.00	2.30
V	39.00	35.00	44.00	21.00	50.00	17.00	29.00	20.00	12.00	20.00	20.00	10.00	19.00	3.00	4.50	4.40	15.00	4.80	17.00	21.00
Y	29.00	31.00	23.00	21.00	14.00	23.00	14.00	18.00	12.00	24.00	28.00	16.00	29.00	17.00	2.10	9.90	13.00	10.00	12.00	10.00
Zn	43.00	42.00	36.00	25.00	38.00	23.00	10.00	18.00	12.00	35.00	26.00	14.00	24.00	18.00	6.10	7.00	13.00	6.20	11.00	14.00
Zr	241.00	254.00	143.00	142.00	150.00	102.00	118.00	159.00	93.00	62.00	104.00	27.00	150.00	40.00	58.00	70.00	84.00	65.00	66.00	71.00
La	62121	73875	43506	44721	42171	46945	45040	56730	33985	23087	21564	8156	58739	7869	14641	27679	30376	25242	16775	29313
Ce	125295	137169	85793	85826	82791	89283	91083	116352	74929	44641	44060	16869	108193	16178	22401	54996	52971	43375	34751	66338
Pr	14654	15818	10029	9941	9459	10091	9428	11916	6653	5090	5626	2126	11480	1897	2586	6324	5685	4372	4094	5814
Nd	52604	55526	35047	34854	33175	34959	33844	41488	21894	18224	22609	7610	37814	6770	7828	22202	19195	13501	15109	19056
Sm	8951	8984	5772	6247	5094	6031	5735	6219	3533	3903	5145	2394	6797	1799	920	3899	3108	2049	3103	2906
Eu	1528	1393	985	953	1015	750	859	1091	589	869	991	332	859	376	325	489	696	344	577	540
Gd	7195	7337	4863	5047	4393	5221	5317	5878	2959	3585	4747	2393	5845	1868	870	3082	2684	1914	2437	2520
Tb	972	962	672	792	699	808	670	767	648	660	832	461	874	434	64	385	355	319	239	631
Dy	5639	5713	4188	4410	3052	4863	3444	3934	2203	5039	5327	4017	5414	3313	368	2184	2359	1822	2250	2094
Ho	1123	1144	864	830	589	983	648	751	440	1088	1078	815	1035	663	67	410	492	387	444	431
Er	3046	3267	2609	2146	1680	2948	1789	2029	1290	3458	3036	2582	3115	2102	209	1024	1434	1240	1214	1375
Tm	465	474	395	299	269	449	269	295	216	579	430	421	426	348	34	144	244	213	198	249
Yb	3412	3468	3012	1918	1915	3286	1926	2079	1373	4528	2829	3440	3240	2656	308	980	1877	1577	1402	1870
Lu	501	488	425	251	279	494	294	316	202	670	371	486	458	367	50	147	285	241	209	306

CHM	6	88	7	8	142	29	31	20	22	21	32	65	43	215	38	47	48	35	36	91
LONG	17.89010	17.05440	17.87850	17.92720	18.01540	17.79210	17.78280	17.91820	17.91140	17.91300	17.64020	17.25330	17.34720	17.34493	17.35490	17.40080	17.37190	17.36670	17.34780	17.06140
LAT	-28.87740	-28.20800	-28.87030	-28.87520	-28.86570	-28.88240	-28.82240	-28.83390	-28.84820	-28.84100	-28.81620	-28.55060	-28.75400	-28.75550	-28.94320	-28.86010	-28.86330	-28.90680	-28.89600	-28.33570
UNIT	ST	ST	ST	ST	ST	NO	NO	NO	NO	NO	NO	WV	WV	WV	WV	WV	WV	WV	WV	PR
ROCKTYPE	SGR	SGR	AGR	AGR	AGR	BA	BA	A	A	TA	RH	A	TA	TA	D	D	D	RH	RH	TA
SiO_2	76.24	77.61	76.46	77.04	77.87	55.11	52.98	57.11	62.40	59.97	69.52	61.30	55.58	63.83	68.88	66.13	67.69	70.91	74.65	60.40
TiO_2	0.19	0.18	0.15	0.11	0.13	0.76	0.69	0.73	0.65	0.76	0.65	0.46	1.14	0.40	0.66	0.76	0.62	0.40	0.32	0.64
Al_2O_3	12.49	11.69	12.35	11.89	11.84	15.64	14.10	17.36	15.01	15.28	14.52	19.55	19.29	16.70	14.43	15.47	15.46	14.19	12.95	16.35
Fe_2O_3(T)	1.49	1.26	1.27	1.27	0.88	9.23	9.50	7.51	6.18	5.99	3.31	2.35	6.10	6.37	3.27	4.44	3.14	2.86	1.73	6.01
MnO	0.05	0.05	0.05	0.02	0.02	0.15	0.15	0.12	0.10	0.09	0.09	0.05	0.17	0.19	0.08	0.07	0.07	0.06	0.06	0.10
MgO	0.14	0.22	0.12	0.12	0.06	5.70	7.62	3.39	3.62	2.04	0.79	0.23	1.53	0.41	0.65	1.68	0.83	0.45	0.28	2.41
CaO	0.63	0.77	0.44	0.34	0.46	8.36	7.90	6.42	4.97	4.26	2.68	8.26	3.02	2.21	2.69	3.59	3.39	2.14	1.07	4.51
Na_2O	3.14	1.85	3.75	3.07	3.35	2.24	2.26	3.23	2.96	4.62	3.32	5.39	5.65	5.29	2.32	1.47	3.15	3.00	3.14	3.37
K_2O	5.46	5.04	5.40	5.91	5.57	1.74	1.66	2.18	3.02	3.35	4.65	0.82	4.29	3.03	5.32	3.38	4.36	4.78	5.45	3.34
P_2O_5	0.02	0.02	0.01	0.01	0.02	0.20	0.20	0.24	0.21	0.35	0.14	0.09	0.39	0.11	0.12	0.26	0.15	0.09	0.04	0.18
Cr_2O_3	0.00	0.00	0.00	0.00	0.00	0.02	0.04	0.00	0.02	0.00	0.00	0.03	0.00	0.00	0.00	0.00	0.00	0.00	0.00	0.00
LOI	0.20	0.31	0.16	0.15	0.08	0.74	1.67	1.67	0.91	2.80	0.45	1.25	3.05	2.17	0.90	2.20	1.13	0.83	0.57	2.00
TOTAL	100.05	98.99	100.16	99.94	100.27	99.88	98.77	99.95	100.05	99.50	100.11	99.78	100.20	100.71	99.33	99.45	100.00	99.71	100.27	99.32
H_2O	0.09	0.08	0.13	0.14	0.19	0.07	0.15	0.02	0.05	0.04	0.15	0.09	0.02	0.24	0.11	0.12	0.05	0.05	0.08	0.11
Ba	499.00	263.00	360.00	192.00	217.00	567.00	900.00	937.00	771.00	1024.00	683.00	556.00	1191.00	317.00	1163.00	1280.00	1134.00	877.00	1019.00	955.00
Ce	116.00	51.00	66.00	59.00	60.00	46.00	63.00	53.00	51.00	73.00	28.00	95.00	269.00	271.00	86.00	68.00	61.00	96.00	111.00	56.00
Co	5.00	<5	<5	<5	1.80	24.00	19.00	19.00	21.00	12.00	39.00	<5	<5	3.90	<5	11.00	<5	<5	<5	7.00
Cr	<5	7.00	7.00	6.00	16.00	83.00	197.00	35.00	138.00	26.00	255.00	178.00	5.00	<3	16.00	41.00	31.00	23.00	15.00	22.00
Cu	13.00	8.00	22.00	21.00	3.70	68.00	56.00	57.00	30.00	197.00	12.00	<5	<5	7.30	<5	44.00	37.00	<5	5.00	63.00
Hf	5.00	<5	<5	<5	<3	<5	9.00	6.00	<5	6.00	7.00	10.00	14.00	21.00	<5	6.00	5.00	<5	<5	<5
Nb	14.00	55.00	14.00	3.00	5.60	7.00	10.00	<2	5.00	9.00	4.00	18.00	196.00	197.00	13.00	11.00	13.00	12.00	17.00	11.00
Ni	<5	<5	<5	<5	<2	33.00	40.00	8.00	42.00	<5	73.00	<5	<5	3.20	<5	14.00	<5	10.00	<5	13.00
Pb	35.00	49.00	40.00	34.00	29.00	13.00	17.00	16.00	18.00	17.00	11.00	14.00	12.00	11.00	29.00	20.00	28.00	31.00	40.00	20.00
Rb	245.00	209.00	275.00	210.00	178.00	61.00	114.00	80.00	124.00	116.00	53.00	25.00	154.00	90.00	152.00	128.00	156.00	198.00	243.00	152.00
Sr	69.00	68.00	52.00	38.00	37.00	449.00	365.00	625.00	347.00	445.00	387.00	719.00	604.00	131.00	320.00	331.00	337.00	229.00	150.00	386.00
Th	22.00	27.00	23.00	15.00	13.00	6.00	10.00	<5	6.00	9.00	<5	29.00	19.00	21.00	12.00	12.00	14.00	18.00	31.00	10.00
U	4.00	8.00	3.00	<3	<2	<3	<3	<3	<3	<3	<3	6.00	4.00	3.50	<3	<2	4.00	4.00	3.00	3.00
V	10.00	14.00	10.00	9.00	5.30	201.00	134.00	183.00	143.00	180.00	182.00	45.00	15.00	<3	38.00	87.00	46.00	40.00	19.00	122.00
Y	37.00	17.00	27.00	7.00	11.00	18.00	21.00	17.00	19.00	20.00	15.00	37.00	31.00	69.00	25.00	23.00	29.00	33.00	19.00	19.00
Zn	31.00	41.00	23.00	10.00	22.00	83.00	73.00	72.00	55.00	61.00	84.00	<5	98.00	162.00	54.00	52.00	45.00	45.00	37.00	73.00
Zr	140.00	86.00	109.00	90.00	91.00	119.00	161.00	136.00	158.00	182.00	103.00	174.00	649.00	1111.00	249.00	202.00	219.00	176.00	202.00	141.00
La		35105	17427	25520	40493									148187						
Ce		69516	66915	60481	69354									291868						
Pr		7331	6223	5828	7646									36631						
Nd		23599	23631	20819	24851									134495						
Sm		3737	5408	3590	3182									22546						
Eu		434	586	498	841									2208						
Gd		3078	4587	2750	2752									17920						
Tb		350	763	153	304									1729						
Dy		2865	5148	1758	2111									14963						
Ho		627	1026	327	435									2715						
Er		2106	3098	996	1386									7673						
Tm		353	466	156	211									1215						
Yb		3018	3513	1319	1455									7395						
Lu		461	500	229	190									1091						

CHM	198	199	200	90	201	67	72	68	69	71	87	81	83	85	84	86	105	103	104	106
LONG	17.06170	17.06170	17.06170	17.03830	17.06180	17.30010	17.21830	17.28010	17.27190	17.21820	17.10230	17.16550	17.16250	17.13190	17.14350	17.18480	17.03270	17.04540	17.03830	17.02590
LAT	-28.34710	-28.34730	-28.34750	-28.30300	-28.34830	-28.33730	-28.30630	-28.32680	-28.32850	-28.30440	-28.19240	-28.17670	-28.17220	-28.18080	-28.17710	-28.16310	-28.09320	-28.08220	-28.08930	-28.10430
UNIT	PR	PR	PR	PR	PR	AR	AR	AR	AR	AR	AR	KR	KR	KR	KR	KU	KU	KU	KU	KU
ROCKTYPE	D	D	D	RH	RH	A	A	RH	RH	RH	RH	TA	TA	TA	D	A	A	D	RH	RH
SiO_2	69.32	68.98	69.21	76.05	69.30	63.19	60.08	76.04	71.41	76.52	74.48	66.11	65.96	66.81	63.51	62.47	62.01	63.42	71.40	76.24
TiO_2	0.40	0.33	0.40	0.15	0.43	0.62	0.73	0.16	0.37	0.15	0.26	0.46	0.46	0.47	0.62	0.75	0.63	0.60	0.37	0.21
Al_2O_3	15.67	15.57	15.42	12.93	14.89	15.37	16.52	13.42	14.03	12.80	13.29	16.18	16.49	16.41	15.29	15.71	15.37	15.16	14.63	13.26
Fe_2O_3(T)	2.92	2.74	3.17	1.14	2.87	5.76	7.00	1.08	2.11	1.24	1.53	2.89	3.12	2.94	5.34	6.79	6.16	5.25	2.24	1.28
MnO	0.06	0.09	0.11	0.04	0.07	0.11	0.11	0.17	0.04	0.03	0.09	0.08	0.07	0.08	0.10	0.11	0.10	0.08	0.06	0.09
MgO	0.66	0.68	0.56	0.18	0.71	2.81	2.94	0.39	0.67	0.15	0.30	1.03	0.73	1.07	2.66	2.92	2.86	2.55	0.59	0.30
CaO	2.48	2.81	3.03	0.21	2.12	4.90	5.68	0.39	1.45	0.24	0.92	3.70	3.88	3.57	4.43	5.30	5.06	4.91	1.73	0.81
Na_2O	3.05	3.16	3.32	3.93	2.25	1.48	3.22	3.64	3.72	3.75	3.68	3.43	3.55	3.12	3.37	1.75	1.82	3.65	4.80	3.09
K_2O	4.59	4.16	4.01	4.39	5.94	3.89	1.91	3.57	4.56	5.31	4.67	4.46	4.19	4.62	3.39	2.90	3.38	2.63	2.63	4.88
P_2O_5	0.15	0.12	0.19	0.02	0.16	0.15	0.16	0.05	0.06	0.02	0.05	0.11	0.12	0.11	0.14	0.18	0.16	0.19	0.07	0.04
Cr_2O_3	0.00	0.00	0.00	0.00	0.00	0.02	0.02	0.02	0.02	0.02	0.00	0.00	0.00	0.00	0.00	0.00	0.00	0.00	0.00	0.00
LOI	1.31	1.61	1.09	0.47	1.18	1.21	4.50	0.87	1.05	0.23	0.66	0.73	1.04	0.86	0.98	0.65	1.89	1.16	1.23	0.55
TOTAL	100.59	100.24	100.52	99.49	99.91	99.50	99.85	99.77	99.48	100.44	99.93	99.18	99.61	100.07	99.83	99.52	99.44	99.59	99.76	100.76
H_2O	0.08	0.08	0.07	0.08	0.08	0.09	0.08	0.02	0.04	0.06	0.10	0.12	0.07	0.04	0.08	0.08	0.14	0.15	0.13	0.14
Ba	1156.00	1182.00	1053.00	586.00	1482.00	834.00	657.00	191.00	1167.00	94.00	855.00	1069.00	1114.00	1145.00	607.00	898.00	873.00	879.00	1024.00	737.00
Ce	60.00	63.00	66.00	57.00	61.00	64.00	29.00	5.00	89.00	59.00	67.00	69.00	79.00	86.00	67.00	55.00	52.00	48.00	69.00	50.00
Co	5.10	5.10	6.30	<5	5.00	19.00	20.00	10.00	7.00	5.00	<5	6.00	5.00	5.00	14.00	14.00	12.00	17.00	7.00	<5
Cr	6.50	6.90	9.10	<5	8.10	204.00	62.00	72.00	24.00	39.00	<5	7.00	8.00	8.00	56.00	36.00	28.00	24.00	<5	<5
Cu	6.90	4.70	5.00	<5	5.50	90.00	61.00	10.00	501.00	5.00	5.00	13.00	13.00	18.00	71.00	11.00	51.00	85.00	14.00	<5
Hf	3.20	4.40	5.00	<5	5.70	<5	<5	<5	6.00	<5	5.00	6.00	6.00	<5	<5	<5	<5	7.00	7.00	<5
Nb	12.00	12.00	11.00	16.00	12.00	11.00	8.00	26.00	14.00	17.00	17.00	52.00	12.00	15.00	11.00	10.00	8.00	9.00	14.00	16.00
Ni	3.20	2.90	3.50	<5	8.70	29.00	21.00	<5	<5	<5	<5	6.00	5.00	<5	27.00	16.00	20.00	22.00	<5	<5
Pb	16.00	13.00	17.00	26.00	17.00	25.00	12.00	44.00	26.00	21.00	25.00	26.00	28.00	36.00	27.00	18.00	18.00	19.00	18.00	33.00
Rb	221.00	207.00	187.00	178.00	239.00	159.00	64.00	167.00	113.00	259.00	155.00	177.00	153.00	181.00	146.00	97.00	125.00	79.00	100.00	195.00
Sr	372.00	320.00	442.00	92.00	280.00	337.00	373.00	93.00	164.00	28.00	153.00	386.00	420.00	362.00	329.00	376.00	379.00	555.00	195.00	149.00
Th	14.00	15.00	13.00	17.00	15.00	15.00	6.00	11.00	28.00	22.00	15.00	16.00	17.00	16.00	15.00	9.00	13.00	13.00	21.00	14.00
U	4.20	6.40	4.00	5.00	4.60	2.00	2.00	6.00	6.00	6.00	5.00	8.00	4.00	5.00	5.00	2.00	3.00	4.00	6.00	4.00
V	36.00	34.00	41.00	15.00	41.00	113.00	141.00	16.00	38.00	11.00	16.00	46.00	49.00	48.00	108.00	138.00	128.00	110.00	29.00	13.00
Y	19.00	19.00	19.00	32.00	20.00	21.00	20.00	31.00	21.00	27.00	32.00	22.00	21.00	23.00	21.00	18.00	18.00	15.00	25.00	37.00
Zn	40.00	35.00	45.00	18.00	39.00	64.00	72.00	30.00	43.00	15.00	29.00	46.00	38.00	65.00	70.00	75.00	66.00	60.00	36.00	29.00
Zr	199.00	201.00	203.00	82.00	195.00	164.00	118.00	61.00	204.00	106.00	117.00	162.00	159.00	161.00	158.00	158.00	163.00	153.00	240.00	111.00
La	37445	40563	36924		39170							32358	36536	36094	29585	23977	31991	32853	49651	22341
Ce	73306	78967	73061		81216							71986	80945	79909	66682	54549	73212	74159	102006	60052
Pr	8979	9534	8841		9359							6905	7783	7665	6332	5391	7084	7047	10757	6018
Nd	33404	34965	33228		35390							28621	32225	31157	26586	23397	30052	29189	40910	24469
Sm	5901	6072	5738		6311							4988	5622	5541	4818	4446	5424	5097	6843	5295
Eu	1455	1480	1459		1570							1480	1638	1539	1190	1313	1495	1409	1664	1312
Gd	4634	4734	4661		5045							4873	5376	5100	4640	4353	5257	4623	7055	5751
Tb	775	785	785		807							625	644	663	583	576	671	586	885	906
Dy	3710	3770	3663		3850							3437	3730	3753	3433	3432	4020	3277	4967	5735
Ho	698	764	688		761							654	684	718	641	666	757	619	961	1190
Er	2087	2105	1993		2208							1825	1952	2044	1902	1929	2188	1779	2783	3605
Tm	330	369	330		358							256	275	281	267	269	295	252	415	525
Yb	2211	2368	2203		2323							1872	2049	2059	1940	1981	2212	1839	2879	3661
Lu	333	355	332		347							263	281	283	260	272	309	261	430	526

APPENDIX 2

NEW GEOCHRON DATA

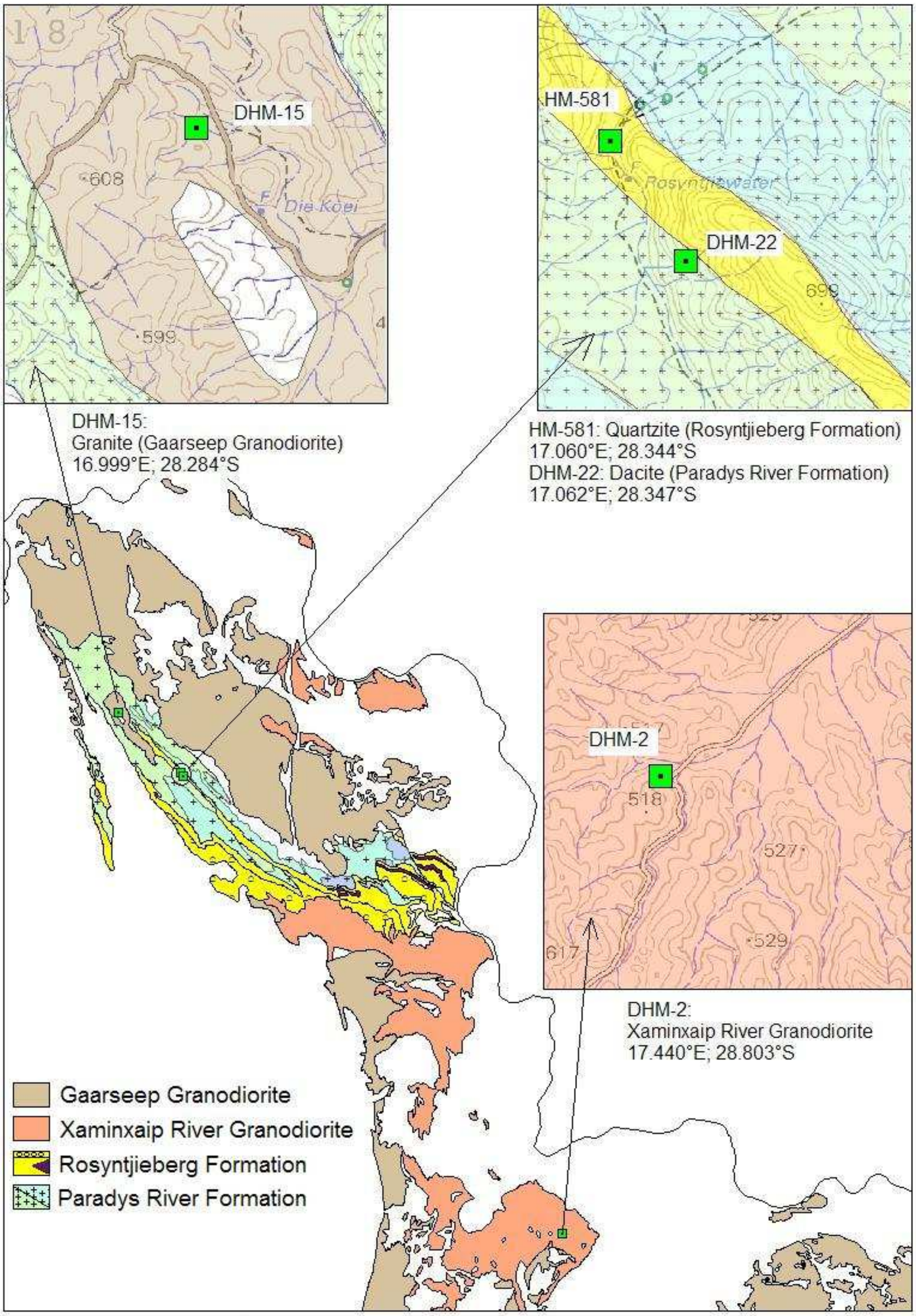

DHM-15
608
Die Koei
599
DHM-15:
Granite (Gaarseep Granodiorite)
16.999°E; 28.284°S
HM-581
Rosyntjiewater
DHM-22
699
HM-581: Quartzite (Rosyntjieberg Formation)
17.060°E; 28.344°S
DHM-22: Dacite (Paradys River Formation)
17.062°E; 28.347°S
DHM-2
518
527
529
617
DHM-2:
Xaminxaip River Granodiorite
17.440°E; 28.803°S
Gaarseep Granodiorite
Xaminxaip River Granodiorite
Rosyntjieberg Formation
Paradys River Formation

			Ratios							Ages					
Sample	U (ppm)	Pb (ppm)	$^{207}Pb/^{206}Pb$	±σ	$^{207}Pb/^{235}U$	±σ	$^{206}Pb/^{238}U$	±σ	ρ	$^{207}Pb/^{206}Pb$	±σ	$^{207}Pb/^{235}U$	±σ	$^{206}Pb/^{238}U$	±σ
n3642-2	363	154	0.11199	0.50	5.33519	1.09	0.3455	0.96	0.88768	1831.9	9.0	1874.5	9.3	1913.2	16.0
n3642-5	186	78	0.11093	1.29	4.36462	1.61	0.2854	0.96	0.59479	1814.6	23.3	1705.7	13.4	1618.4	13.7
n3642-8	208	95	0.11344	0.47	5.31179	1.07	0.3396	0.96	0.89577	1855.2	8.6	1870.8	9.2	1884.8	15.6
n3642-9	200	83	0.11482	0.50	5.42490	1.13	0.3427	1.01	0.89380	1877.1	9.1	1888.8	9.7	1899.4	16.6
n3642-11	491	220	0.11557	0.38	5.49672	1.12	0.3450	1.05	0.94111	1888.8	6.8	1900.1	9.6	1910.5	17.4
n3642-27	117	48	0.11177	0.95	5.29292	1.41	0.3435	1.04	0.73827	1828.4	17.1	1867.7	12.1	1903.3	17.2
n3642-29	202	90	0.11178	0.59	5.25074	1.13	0.3407	0.97	0.85482	1828.5	10.6	1860.9	9.7	1890.0	15.9
n3642-30	301	158	0.11027	0.45	4.96646	1.06	0.3266	0.96	0.90617	1803.9	8.1	1813.6	9.0	1822.1	15.2
n3642-35	267	129	0.10994	0.49	5.06553	1.20	0.3342	1.10	0.91190	1798.4	9.0	1830.4	10.3	1858.5	17.7
n3642-36	322	141	0.11289	0.38	5.17169	1.10	0.3323	1.04	0.93905	1846.4	6.9	1848.0	9.4	1849.3	16.7
n3642-38	262	120	0.11165	0.48	5.16264	1.07	0.3354	0.96	0.89241	1826.5	8.7	1846.5	9.2	1864.3	15.5
n3642-39	363	101	0.10826	3.12	3.35599	3.38	0.2248	1.31	0.38741	1770.4	55.9	1494.2	26.8	1307.3	15.5
n3642-41	325	125	0.10732	0.81	3.90963	1.40	0.2642	1.14	0.81464	1754.4	14.7	1615.7	11.4	1511.4	15.3
n3642-48	296	142	0.11122	0.68	5.05577	1.18	0.3297	0.96	0.81465	1819.4	12.3	1828.7	10.0	1836.9	15.3
n3642-67	131	52	0.11093	0.86	5.05571	1.35	0.3305	1.05	0.77491	1814.7	15.5	1828.7	11.5	1841.0	16.8
n3642-65	83	37	0.11232	1.21	5.07118	1.74	0.3275	1.24	0.71541	1837.2	21.8	1831.3	14.8	1826.1	19.8
n3642-77	269	134	0.11302	0.48	5.14338	1.09	0.3301	0.98	0.89915	1848.5	8.6	1843.3	9.3	1838.7	15.7
n3642-78	92	45	0.12698	0.65	6.78687	1.16	0.3876	0.96	0.82946	2056.6	11.4	2084.0	10.3	2111.9	17.4
n3642-76	458	215	0.11338	0.46	5.12469	1.06	0.3278	0.96	0.90240	1854.3	8.3	1840.2	9.1	1827.8	15.3
n3642-84	39	18	0.11358	1.36	5.30729	1.68	0.3389	0.98	0.58461	1857.4	24.4	1870.0	14.5	1881.4	16.1
n3642-90	430	181	0.11452	0.52	5.16357	1.13	0.3270	1.00	0.88529	1872.3	9.4	1846.6	9.6	1823.9	15.9
n3642-103	197	85	0.11245	0.69	5.03603	1.18	0.3248	0.96	0.81406	1839.4	12.4	1825.4	10.1	1813.2	15.2
n3642-97	331	176	0.11196	0.40	5.44457	1.09	0.3527	1.02	0.93178	1831.4	7.2	1891.9	9.4	1947.5	17.1
n3642-100	275	151	0.11098	0.45	5.34578	1.06	0.3493	0.96	0.90570	1815.6	8.1	1876.2	9.1	1931.4	16.0
n3642-110	83	38	0.11299	1.06	5.41226	1.45	0.3474	0.99	0.68018	1848.1	19.1	1886.8	12.5	1922.2	16.4
n3642-95	252	132	0.11484	0.69	5.24215	1.18	0.3311	0.96	0.81283	1877.4	12.3	1859.5	10.1	1843.5	15.4
n3642-107	1490	560	0.10767	0.27	4.62882	1.03	0.3118	0.99	0.96359	1760.4	5.0	1754.5	8.6	1749.5	15.2
n3642-114	99	44	0.11176	0.76	5.35387	1.25	0.3474	0.99	0.79163	1828.2	13.8	1877.5	10.7	1922.4	16.4
n3642-113	242	113	0.11165	0.62	5.04075	1.14	0.3274	0.96	0.83901	1826.5	11.2	1826.2	9.7	1825.9	15.3
n3642-128	270	125	0.11334	0.45	5.35036	1.06	0.3424	0.96	0.90669	1853.6	8.0	1876.9	9.1	1898.1	15.8
n3642-133	730	309	0.11233	0.31	5.13435	1.01	0.3315	0.96	0.95055	1837.5	5.6	1841.8	8.6	1845.6	15.4
n3642-140	707	348	0.11756	0.25	5.69602	1.06	0.3514	1.04	0.97289	1919.4	4.4	1930.8	9.2	1941.3	17.4
n3642-143	84	37	0.11608	0.74	5.49791	1.21	0.3435	0.96	0.78932	1896.8	13.3	1900.3	10.5	1903.5	15.8
n3642-1	306	79	0.10599	3.89	2.78664	4.03	0.1907	1.06	0.26226	1731.6	69.7	1352.0	30.6	1125.1	10.9
n3642-4	744	222	0.10752	0.54	3.79063	1.12	0.2557	0.98	0.87632	1757.8	9.8	1590.8	9.0	1467.8	12.9
n3642-6	1229	144	0.09821	7.39	1.30603	7.48	0.0964	1.20	0.15985	1590.4	132.0	848.4	44.0	593.6	6.8
n3642-147	51	24	0.11108	2.01	5.24043	2.28	0.3421	1.08	0.47394	1817.2	36.0	1859.2	19.6	1897.0	17.8
n3642-107	2112	672	0.10506	0.24	3.84717	1.01	0.2656	0.98	0.97189	1715.3	4.3	1602.7	8.1	1518.4	13.2
n3642-102	448	162	0.11004	0.68	4.32178	1.19	0.2849	0.98	0.82282	1800.0	12.3	1697.5	9.9	1615.8	14.1
n3642-44	115	51	0.10996	0.87	4.81028	1.26	0.3173	0.91	0.72057	1798.8	15.8	1786.7	10.6	1776.4	14.1
n3642-54	285	126	0.11185	0.76	4.78028	1.36	0.3100	1.13	0.83088	1829.7	13.7	1781.4	11.5	1740.5	17.3
n3642-80	1819	365	0.08900	5.49	1.76502	5.60	0.1438	1.09	0.19505	1404.1	101.6	1032.7	36.9	866.3	8.9

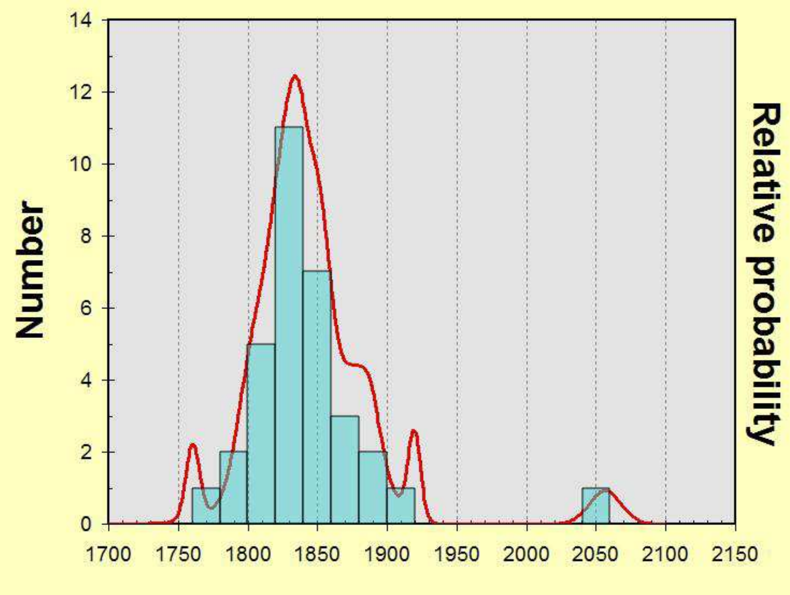

HM-581: Quartzite; Rosyntjieberg Formation

SPOT_NAME	U (ppm)	Pb (ppm)	Ratios $^{207}Pb/^{206}Pb$	±2σ	$^{207}Pb/^{235}U$	±2σ	$^{206}Pb/^{238}U$	±2σ	ρ	Ages $^{207}Pb/^{235}U$	±2σ	$^{206}Pb/^{238}U$	±2σ	$^{207}Pb/^{206}Pb$	±2σ	Conc %
Zircon_Sample-163	244	84	0.116	0.002	5.48	0.14	0.343	0.007	0.78	1898	23	1903	34	1893	30	101
Zircon_Sample-164	264	90	0.114	0.004	5.39	0.36	0.342	0.020	0.86	1884	58	1897	96	1869	62	101
Zircon_Sample-165	248	78	0.115	0.004	4.94	0.23	0.313	0.011	0.75	1810	40	1754	55	1874	56	94
Zircon_Sample-166	223	73	0.116	0.003	5.21	0.26	0.327	0.014	0.86	1855	42	1824	68	1889	45	97
Zircon_Sample-167	523	161	0.114	0.003	4.82	0.19	0.307	0.008	0.70	1788	33	1728	42	1859	50	93
Zircon_Sample-168	255	86	0.115	0.004	5.35	0.32	0.338	0.017	0.84	1876	51	1879	81	1873	58	100
Zircon_Sample-169	297	98	0.115	0.004	5.22	0.23	0.330	0.010	0.69	1855	37	1839	49	1874	57	98
Zircon_Sample-170	151	47	0.115	0.004	5.00	0.33	0.315	0.018	0.88	1820	55	1763	89	1885	55	94
Zircon_Sample-171	146	48	0.115	0.002	5.17	0.20	0.327	0.011	0.85	1847	32	1823	51	1875	36	97
Zircon_Sample-172	148	49	0.115	0.003	5.25	0.17	0.331	0.007	0.67	1861	28	1845	35	1879	44	98
Zircon_Sample-176	170	53	0.116	0.003	4.99	0.21	0.312	0.011	0.86	1817	36	1750	56	1895	39	92
Zircon_Sample-177	165	54	0.116	0.004	5.23	0.27	0.327	0.012	0.75	1857	44	1824	61	1896	61	96
Zircon_Sample-178	200	68	0.116	0.003	5.44	0.28	0.339	0.015	0.87	1890	45	1880	74	1902	46	99
Zircon_Sample-179	136	44	0.114	0.003	5.11	0.27	0.325	0.015	0.90	1839	44	1814	74	1866	41	97
Zircon_Sample-180	120	38	0.117	0.003	5.08	0.22	0.316	0.011	0.82	1834	36	1771	54	1905	44	93
Zircon_Sample-181	284	93	0.115	0.002	5.15	0.24	0.326	0.014	0.91	1844	39	1817	67	1875	34	97
Zircon_Sample-182	347	116	0.114	0.004	5.29	0.30	0.336	0.016	0.83	1868	49	1868	78	1867	58	100
Zircon_Sample-183	176	58	0.116	0.003	5.22	0.22	0.326	0.011	0.84	1856	35	1820	55	1897	41	96
Zircon_Sample-184	233	76	0.116	0.003	5.25	0.25	0.328	0.013	0.85	1861	40	1828	63	1899	45	96
Zircon_Sample-185	314	105	0.115	0.002	5.29	0.20	0.333	0.010	0.83	1868	32	1852	50	1886	37	98
Zircon_Sample-192	193	64	0.115	0.003	5.21	0.19	0.329	0.008	0.68	1854	32	1835	41	1876	49	98
Zircon_Sample-193	230	77	0.116	0.003	5.37	0.22	0.336	0.009	0.68	1880	34	1865	44	1895	53	98
Zircon_Sample-194	339	106	0.115	0.003	5.00	0.28	0.314	0.015	0.89	1819	47	1762	76	1884	45	94
Zircon_Sample-195	196	63	0.116	0.004	5.10	0.35	0.320	0.020	0.89	1836	59	1788	97	1890	57	95
Zircon_Sample-196	496	149	0.114	0.004	4.71	0.26	0.300	0.013	0.80	1769	46	1693	66	1859	60	91
Zircon_Sample-197	249	78	0.114	0.002	4.94	0.12	0.314	0.005	0.66	1808	21	1759	25	1866	34	94
Zircon_Sample-198	234	75	0.116	0.002	5.07	0.23	0.318	0.013	0.93	1831	39	1780	66	1888	31	94
Zircon_Sample-199	204	68	0.115	0.003	5.28	0.28	0.332	0.016	0.87	1866	46	1849	76	1885	47	98
Zircon_Sample-200	366	118	0.115	0.003	5.10	0.21	0.322	0.011	0.81	1836	35	1800	52	1877	43	96
Zircon_Sample-201	258	82	0.113	0.002	4.93	0.26	0.316	0.016	0.94	1807	45	1769	77	1851	34	96
Zircon_Sample-205	300	98	0.115	0.003	5.19	0.24	0.327	0.012	0.79	1851	39	1823	58	1882	51	97
Zircon_Sample-206	146	48	0.116	0.005	5.27	0.35	0.329	0.017	0.80	1864	57	1835	84	1898	72	97
Zircon_Sample-207	266	87	0.115	0.002	5.23	0.13	0.328	0.007	0.81	1857	21	1830	33	1887	26	97
Zircon_Sample-208	185	57	0.117	0.003	4.96	0.18	0.309	0.009	0.80	1812	30	1734	43	1903	39	91
Zircon_Sample-209	368	118	0.115	0.002	5.07	0.29	0.320	0.017	0.94	1831	49	1788	84	1881	35	95
Zircon_Sample-210	301	103	0.116	0.003	5.46	0.33	0.342	0.019	0.93	1895	52	1898	92	1891	40	100
Zircon_Sample-211	367	115	0.115	0.003	4.97	0.28	0.313	0.016	0.91	1815	48	1756	79	1883	41	93
Zircon_Sample-212	355	120	0.115	0.002	5.36	0.29	0.338	0.017	0.92	1879	47	1875	82	1883	38	100
Zircon_Sample-213	261	80	0.115	0.003	4.85	0.31	0.306	0.019	0.94	1794	55	1722	92	1878	41	92
Zircon_Sample-214	211	67	0.115	0.003	5.05	0.24	0.318	0.012	0.77	1827	40	1779	57	1882	54	95
Zircon_Sample-218	248	83	0.116	0.005	5.31	0.32	0.333	0.015	0.74	1870	52	1851	72	1892	74	98
Zircon_Sample-219	210	70	0.114	0.002	5.27	0.23	0.335	0.014	0.95	1864	37	1862	67	1866	25	100
Zircon_Sample-220	154	46	0.114	0.002	4.72	0.18	0.299	0.010	0.85	1771	31	1687	47	1871	36	90
Zircon_Sample-221	609	201	0.113	0.003	5.13	0.21	0.330	0.010	0.75	1841	34	1836	48	1846	49	99
Zircon_Sample-222	296	72	0.113	0.002	3.79	0.37	0.243	0.023	0.98	1591	78	1400	120	1855	33	75
Zircon_Sample-223	430	130	0.114	0.004	4.74	0.22	0.302	0.011	0.75	1774	40	1699	53	1864	56	91
Zircon_Sample-224	253	85	0.115	0.004	5.32	0.29	0.337	0.015	0.82	1872	46	1872	72	1872	56	100
Zircon_Sample-225	359	119	0.114	0.003	5.20	0.29	0.331	0.016	0.87	1853	47	1843	77	1864	49	99
Zircon_Sample-226	229	79	0.115	0.002	5.47	0.28	0.345	0.016	0.93	1895	44	1911	79	1879	34	102
Zircon_Sample-227	325	102	0.115	0.002	4.95	0.21	0.313	0.012	0.90	1811	36	1754	58	1877	34	93
Zircon_Sample-231	509	172	0.113	0.004	5.27	0.27	0.339	0.013	0.76	1863	44	1880	63	1845	61	102
Zircon_Sample-232	228	70	0.116	0.002	4.88	0.32	0.306	0.019	0.95	1799	55	1721	94	1891	36	91
Zircon_Sample-233	302	102	0.115	0.003	5.34	0.30	0.337	0.016	0.86	1876	49	1870	79	1882	52	99
Zircon_Sample-234	155	50	0.116	0.004	5.11	0.34	0.319	0.019	0.89	1837	57	1785	93	1896	55	94
Zircon_Sample-235	414	145	0.116	0.003	5.61	0.27	0.351	0.014	0.85	1917	41	1940	67	1893	46	103

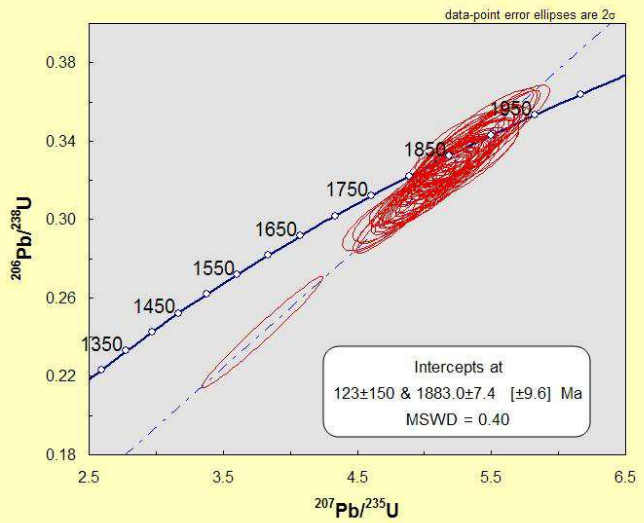

DHM-22: Dacite; Paradys River Formation

			Ratios							Ages						Concord.
Analysis	U [ppm]	Pb [ppm]	$^{207}Pb/^{235}U$	2 σ	$^{206}Pb/^{238}U$	2 σ	rho	$^{207}Pb/^{206}Pb$	2 σ	$^{207}Pb/^{235}U$	2 σ	$^{206}Pb/^{238}U$	2 σ	$^{207}Pb/^{206}Pb$	2 σ	%
Zircon_Sample_007	241	82	5.44	0.21	0.340	0.008	0.63	0.116	0.002	1890	75	1887	41	1894	27	100
Zircon_Sample_008	139	48	5.48	0.25	0.342	0.009	0.60	0.116	0.002	1897	85	1897	44	1897	32	100
Zircon_Sample_009	204	70	5.53	0.23	0.344	0.009	0.62	0.117	0.002	1905	78	1905	42	1906	29	100
Zircon_Sample_010	140	48	5.50	0.25	0.343	0.009	0.60	0.116	0.002	1901	86	1901	45	1900	32	100
Zircon_Sample_011	175	55	5.14	0.27	0.315	0.010	0.58	0.119	0.003	1843	97	1763	47	1935	38	91
Zircon_Sample_012	153	52	5.44	0.23	0.340	0.009	0.61	0.116	0.002	1892	82	1889	43	1895	30	100
Zircon_Sample_013	149	51	5.52	0.30	0.342	0.011	0.58	0.117	0.003	1903	103	1898	51	1909	39	99
Zircon_Sample_014	207	72	5.54	0.31	0.345	0.011	0.57	0.116	0.003	1907	107	1912	53	1900	41	101
Zircon_Sample_015	235	80	5.43	0.22	0.339	0.009	0.62	0.116	0.002	1889	77	1883	41	1896	29	99
Zircon_Sample_016	281	71	4.08	0.18	0.253	0.007	0.60	0.117	0.002	1650	74	1455	35	1909	32	76
Zircon_Sample_020	235	67	4.58	0.20	0.285	0.007	0.61	0.116	0.002	1746	75	1618	37	1902	31	85
Zircon_Sample_021	223	67	4.79	0.20	0.300	0.008	0.61	0.116	0.002	1783	76	1690	38	1894	30	89
Zircon_Sample_022	262	83	5.08	0.21	0.319	0.008	0.62	0.116	0.002	1833	75	1783	39	1890	29	94
Zircon_Sample_023	216	60	4.47	0.20	0.277	0.007	0.60	0.117	0.002	1726	78	1575	38	1914	32	82
Zircon_Sample_024	863	138	2.55	0.10	0.160	0.004	0.62	0.116	0.002	1286	52	955	22	1893	28	50
Zircon_Sample_025	277	91	5.23	0.22	0.329	0.008	0.61	0.115	0.002	1858	77	1833	40	1886	29	97
Zircon_Sample_026	179	56	4.99	0.22	0.311	0.008	0.60	0.116	0.002	1817	81	1746	41	1900	32	92
Zircon_Sample_027	447	133	4.67	0.19	0.297	0.007	0.62	0.114	0.002	1762	70	1679	36	1863	28	90
Zircon_Sample_028	263	71	4.26	0.19	0.269	0.007	0.60	0.115	0.002	1685	74	1535	36	1877	31	82
Zircon_Sample_029	179	61	5.46	0.27	0.342	0.010	0.58	0.116	0.002	1894	93	1894	47	1895	35	100
Zircon_Sample_033	252	80	5.04	0.22	0.320	0.008	0.60	0.114	0.002	1826	79	1788	40	1870	31	96
Zircon_Sample_034	449	108	3.82	0.16	0.240	0.006	0.60	0.116	0.002	1597	67	1384	31	1891	30	73
Zircon_Sample_035	247	82	5.31	0.23	0.332	0.009	0.60	0.116	0.002	1870	82	1848	42	1895	31	97

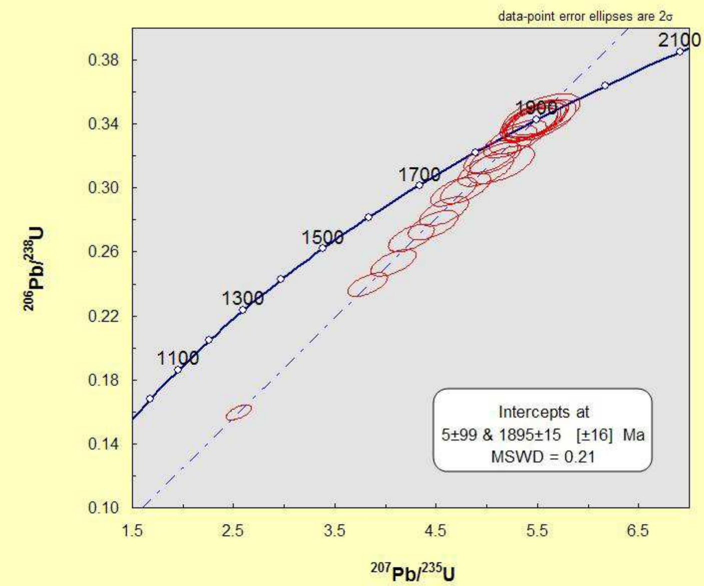

DHM-15: Granodiorite; Gaarseep Granodiorite

	U	Pb	ratios							Ages						
sample	[ppm]	[ppm]	$^{207}Pb/^{206}Pb$	1σ%	$^{207}Pb/^{235}U$	1σ%	$^{206}Pb/^{238}U$	1σ%	rho	$^{207}Pb/^{206}Pb$	2σ%	$^{207}Pb/^{235}U$	2σ%	$^{206}Pb/^{238}U$	2σ%	concord.
25_01DHM-2_10-25-50	106	34	0.116160	0.65	5.496117	1.17	0.34316	0.97	0.83	1898	23	1900	20	1902	32	100
26_02DHM-2_10-25-50	71	23	0.116690	0.65	5.600556	1.29	0.34809	1.11	0.86	1906	24	1916	22	1925	37	101
29_03DHM-2_10-35-50	136	42	0.115916	0.63	5.483229	1.19	0.34308	1.00	0.85	1894	23	1898	21	1901	33	100
30_04DHM-2_10-35-50	366	117	0.115958	0.64	5.560673	1.04	0.34780	0.82	0.79	1895	23	1910	18	1924	27	102
33_05DHM-2_10-35-50	363	115	0.115207	0.63	5.511168	1.07	0.34695	0.87	0.81	1883	23	1902	19	1920	29	102
34_06DHM-2_10-25-50	864	211	0.116127	0.66	4.210905	1.34	0.26299	1.17	0.87	1897	24	1676	22	1505	31	79
35_07DHM-2_10-25-50	160	51	0.116413	0.64	5.594824	1.13	0.34856	0.93	0.82	1902	23	1915	20	1928	31	101
38_08DHM-2_10-25-50	121	38	0.115694	0.65	5.431748	1.23	0.34051	1.05	0.85	1891	23	1890	21	1889	34	100
39_09DHM-2_10-25-50	202	63	0.115506	0.64	5.356971	1.16	0.33637	0.97	0.84	1888	23	1878	20	1869	32	99
40_10DHM-2_10-25-50	428	134	0.115475	0.48	5.388731	1.06	0.33845	0.95	0.89	1887	17	1883	18	1879	31	100
45_11DHM-2_10-35-50	124	40	0.115435	0.49	5.533551	0.99	0.34767	0.86	0.87	1887	18	1906	17	1923	29	102
46_12DHM-2_10-25-50	199	63	0.115550	0.56	5.411619	1.20	0.33967	1.06	0.88	1888	20	1887	21	1885	35	100
48_13DHM-2_10-35-50	167	54	0.115594	0.48	5.574667	1.11	0.34977	1.00	0.90	1889	17	1912	19	1933	33	102
49_14DHM-2_10-35-50	137	43	0.115832	0.48	5.582846	1.18	0.34956	1.08	0.91	1893	17	1913	21	1933	36	102
50_15DHM-2_10-15-50	878	185	0.132988	1.79	4.036090	3.45	0.22011	2.94	0.85	2138	63	1641	57	1282	69	60
54_16DHM-2_10-35-50	111	35	0.115746	0.49	5.552026	1.18	0.34789	1.07	0.91	1892	18	1909	20	1925	36	102
55_17DHM-2_10-25-50	779	264	0.127519	0.48	6.395141	1.10	0.36373	0.99	0.90	2064	17	2032	19	2000	34	97
56_18DHM-2_10-20-50	108	34	0.116063	0.54	5.532822	1.13	0.34574	0.99	0.88	1896	20	1906	20	1914	33	101
58_19DHM-2_10-25-50	368	113	0.124664	0.49	6.169604	1.14	0.35893	1.03	0.90	2024	17	2000	20	1977	35	98
59_20DHM-2_10-25-50	552	137	0.111669	0.51	4.244874	1.23	0.27570	1.12	0.91	1827	19	1683	20	1570	31	86
60_21DHM-2_10-25-50	163	51	0.116035	0.48	5.532349	1.20	0.34580	1.10	0.92	1896	17	1906	21	1914	36	101

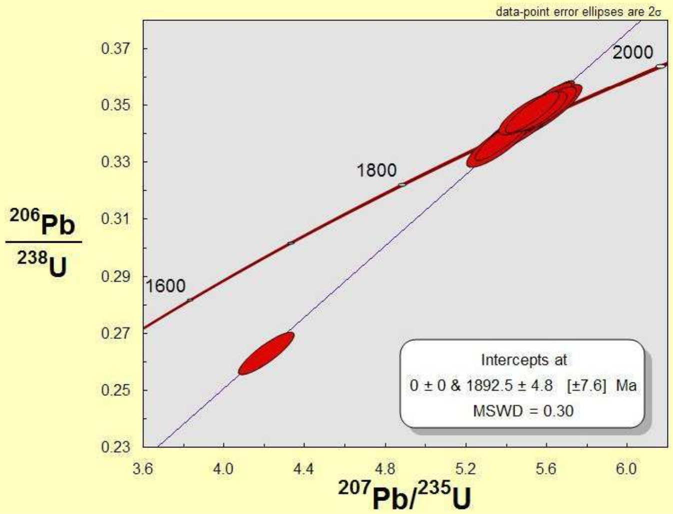

DHM-2: Granodiorite, Xaminxaip River Granodiorite